Studies on Synthesis and Structures of Liquid Crystalline Helical Polymers Based on Their Main-Chain Stiffness

主鎖の剛直性に由来する液晶性らせん高分子の
合成と構造に関する研究

Kanji Nagai

永井　寛嗣

2009

Studies on Synthesis and Structures of Liquid Crystalline Helical Polymers Based on Their Main-Chain Stiffness

主鎖の剛直性に由来する液晶性らせん高分子の合成と構造に関する研究

Table of Contents

General Introduction

Naturally occurring biological macromolecules, such as proteins and nucleic acids, are optically active and take a unique one-handed helical structure. In 1951, Pauling proposed an 18 unit / 5 turn (18/5) helix for poly(L-glutamic acid) esters based on fiber X-ray diffraction (XRD) measurements.[1] In 1953, Watson and Crick discovered the right-handed double helical structure for DNA (10/1 helix) on the basis of its fiber XRD analysis.[2] After the discovery of these biological helical structures, remarkable progress has been made in molecular biology, and their sophisticated functions have been elucidated on a molecular level.[3]

The history of synthetic helical polymers also extends back to the 1950s when Natta found highly isotactic polypropylene prepared by the Ziegler-Natta catalyst which possesses a mixture of 3/1 right- and left-handed helices in the crystalline state on the basis of its XRD measurements.[4] Since Natta's discovery, a number of stereoregular vinyl polymers have been prepared and their helical structures in the crystalline state have been revealed.[5] However, their helical conformations are not stable in solution and instantly randomize once dissolved. Therefore, the helical polymers stable in solution have been considered to be difficult to synthesize at that time.

Since the 1970s, however, significant progress has been made in synthetic helical polymers. In 1974, Nolte and Drenth et al. successfully resolved poly(*t*-butyl isocyanide) (**1**) into enantiomeric right- and left-handed helices by chiral chromatography (Figure 1).[6] Later, Okamoto et al. synthesized the first helical vinyl polymer (**2**) by the helix-sense-selective polymerization of an achiral monomer, triphenylmethyl methacrylate (TrMA), using chiral anionic initiators in 1979, which produced a single-handed, fully isotactic helical polymer with a large optical rotation.[7] These findings clearly proved that helical polymers stable in solution can be artificially synthesized. In addition, the one-handed helical **2** was found to show a remarkable chiral recognition for a variety of racemic compounds, thus providing a

practically useful chiral stationary phase (CSP) for high-performance liquid chromatography (HPLC).[8] This was an important milestone in the field of synthetic helical polymers, through which many optically active polymers[9] and oligomers (foldamers)[10] have been prepared for use as CSPs in HPLC as well as to develop novel chiral materials, such as enantioselective catalysts, chemical sensors, and liquid crystals.[8-10]

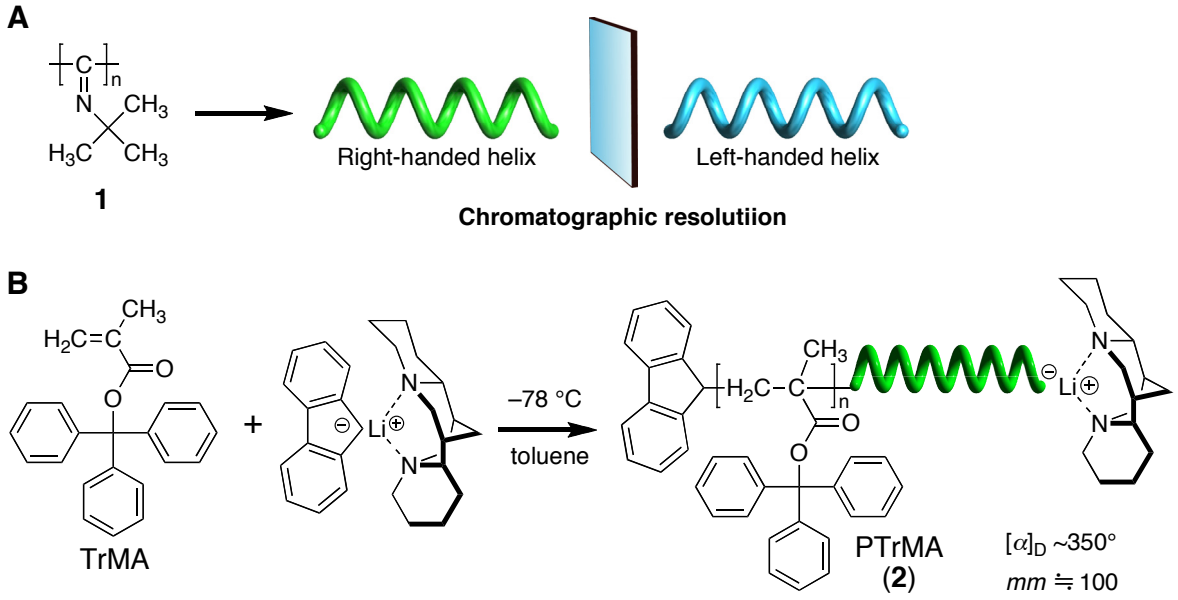

Figure 1. Schematic illustrations of (A) chromatographic resolution of **1** and (B) helix-sense-selective polymerization of TrMA.

The synthetic helical polymers, whose helical conformations are stable and can exhibit an optical activity mainly due to the helicity of the polymer backbones like PTrMA (**2**), can be classified as stable (static) helical polymers (Figure 2). Polyisocyanides (**3**),[6,9b,f,11] poly(triarylmethyl methacrylate)s (**4**),[7,8,9a,e,12] polychloral (**5**),[13] poly(2,3-quinoxaline)s (**6**),[14] and polyguanidines (**7**)[15] belong to this category. They have a rigid helix with a sufficiently high helix inversion barrier. Therefore, optically active helical polymers with an excess of a one helical sense can be prepared by the polymerization of the corresponding optically active monomers or by the helix-sense-selective polymerization of achiral or prochiral monomers with chiral catalysts or initiators. These polymers have bulky substituents on the side chains,

so that a one-handed helical conformation is formed and retained in solution by steric hindrance during the polymerization under kinetic control.

Besides these helical polymers being stable in solution, Green et al. discovered an alternative unique helical polymer, that is, a dynamic helical polymer in the late 1980s (Figure 2). They found that rod-like polyisocyanates (**8**),[9c,d,16] which have no stereogenic centers, consist of interconvertible left- and right-handed helical segments separated by helical reversals that can readily move along the polymer backbones. Since the helix inversion barriers of dynamic helical polyisocyanates are very low, small chiral bias can be cooperatively transformed into a main-chain conformational change with a large amplification through covalent or noncovalent bonding, resulting in the formation of an excess preferred-handed helical conformation. Therefore, optically active polyisocyanates with a controlled helical sense can be prepared by the copolymerization of achiral monomers with a small amount of optically active monomers or by the copolymerization of a mixture of enantiomers with a small enantiomeric excess (ee) under thermodynamic control. These highly cooperative chiral amplification phenomena are called the "sergeants and soldiers effect" and "majority rule", respectively. Polysilanes (**9**)[9g,17] and polyacetylenes (**10**)[9i-l,18] are now recognized as a class of dynamic helical polymers.

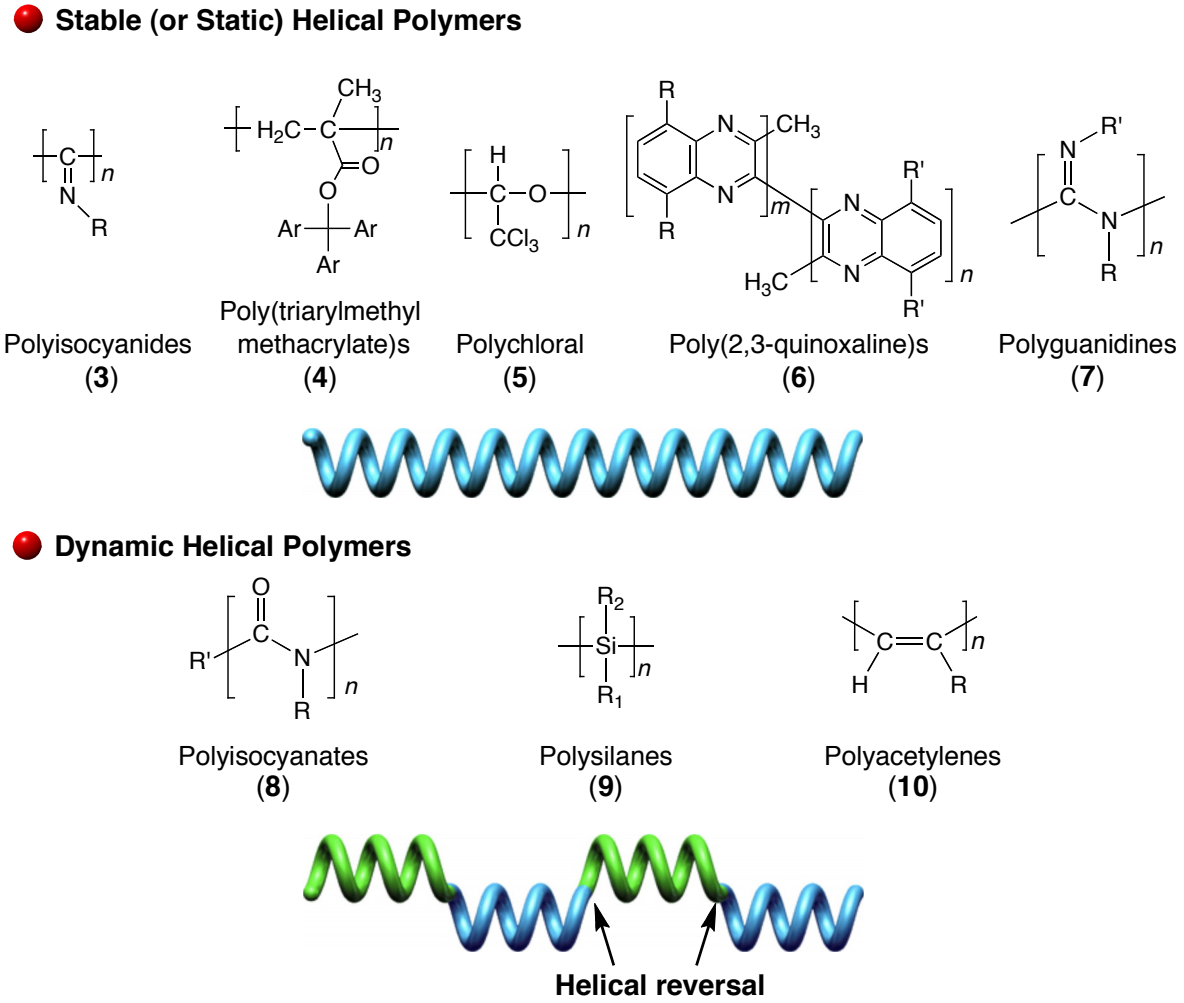

Figure 2. Structures of typical synthetic helical polymers.

Macromolecular helicity with an excess single-handed helical sense can also be induced in optically inactive, dynamically racemic helical polymers through noncovalent bonding interactions. In 1995, Yashima et al. found that an optically inactive, *cis-transoidal* poly((4-carboxyphenyl)acetylene) (**11**) changed its dynamically racemic helical structure to a preferred-handed helix upon complexation with optically active amines in dimethyl sulfoxide (DMSO), resulting in the appearance of a characteristic induced circular dichroism (ICD) in the long wavelength region of the π-conjugated polymer backbone (300–500 nm) (Figure 3).[19] The induced Cotton effect signs corresponding to the helical sense of **11** can be used to predict the absolute configurations of chiral amines.[20] Taking advantage of this helicity induction concept, a variety of poly(phenylacetylene)s with various functional groups as the

pendant groups, such as boronate (**12**),[21] phosphonate (**13a**–**13c**)[22] and sulfonate (**14**) residues,[23] amino (**15**),[24] and bulky crown ether (**16a**, **16b**)[25] groups, have been designed and synthesized. These functional poly(phenylacetylene)s also respond to the chirality of sugars, chiral amines, acids, and ammoniums, and their complexes exhibit characteristic ICDs due to the predominantly one-handed helix formation.

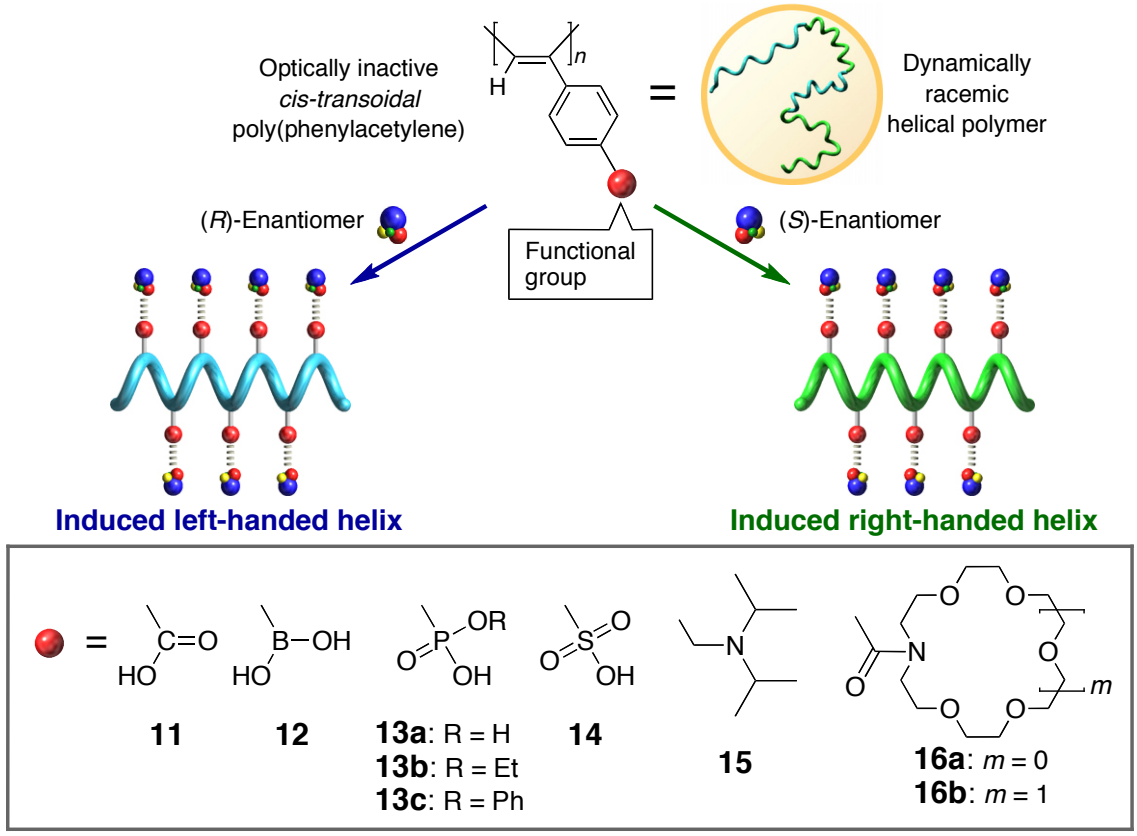

Figure 3. Schematic illustration of the formation of a one-handed helical structure of dynamically racemic helical poly(phenylacetylene)s upon complexation with chiral compounds.

Beside the static and dynamic helical polymers, certain helical polymers exhibit both static and dynamic features depending on the structures of the monomer units. Yashima et al. recently found that an optically inactive poly(4-carboxyphenyl isocyanide) (**17**–**H**) changed its structure into the prevailing one-handed helical conformation upon complexation with chiral amines in DMSO[26] and water,[27] and the complexes showed characteristic ICDs in the UV-visible region of the polymer backbone (Figure 4). Interestingly, the helical **17**–**H** with an excess helical sense induced in water and aqueous organic solutions containing more than 50 vol% water was found to be automatically maintained, namely "*memorized*", after complete removal of the optically active amine (***h*-17b**–**H**).[27,28] This is an unprecedented example of the synthesis of a static helical polymer after polymerization through specific noncovalent chiral interactions, and further modifications of the pendant groups to esters and amide residues were possible without loss of the macromolecular helicity memory.[29] In contrast, the induced helical **17**–**H** in DMSO and DMSO–water mixtures containing less than 30 vol% water cannot maintain the helicity after removing the chiral amines (**17a**–**H**).[28] The helix formation of **17**–**H** is considered to be accompanied by a configurational isomerization around the C=N double bonds (*syn–anti* isomerization) into one single configuration upon complexation with the chiral amine, which may force the polymer backbone to take an excess of one helical sense as revealed by the various spectroscopic measurements, such as the absorption, circular dichroism (CD), IR, vibrational CD (VCD), and NMR spectroscopies.[30] As described above, polyisocyanides are believed to belong to a static helical polymer when they have a bulky side group. However, the results imply that poly(phenyl isocyanide)s with less bulky side groups have a dynamic helical characteristic as well as a static one, being different from the other static and dynamic helical polymers.

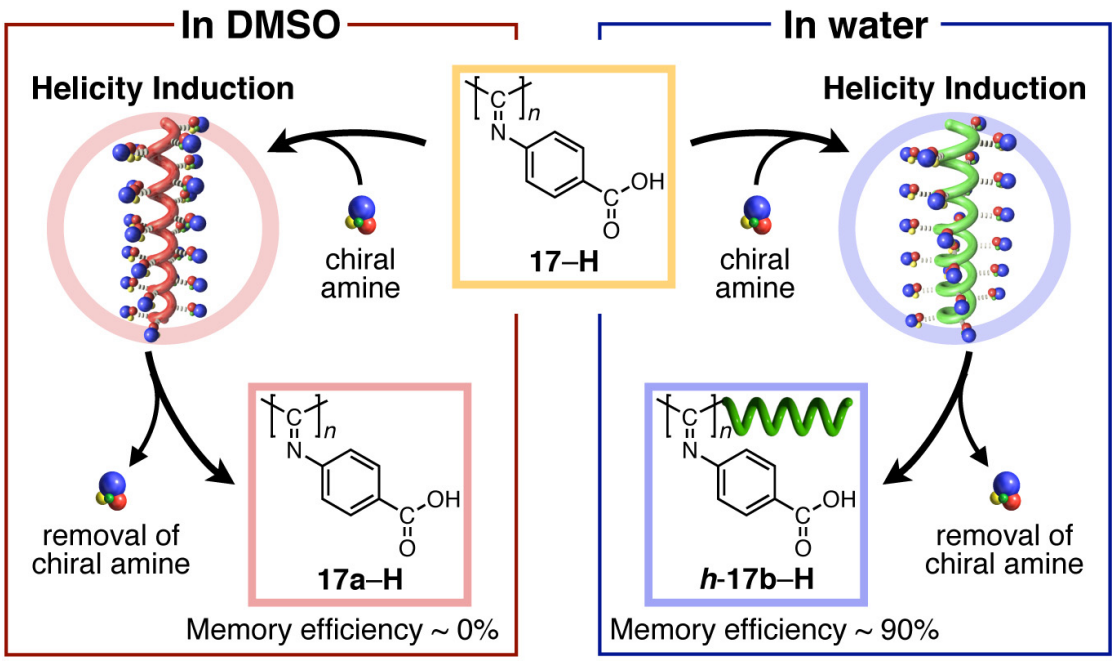

Figure 4. Schematic illustration of helicity induction in **17–H** in DMSO and water with chiral amines. The macromolecular helicity induced in water is memorized after complete removal of the chiral amines (***h*-17b–H**), whereas that induced in DMSO cannot be memorized (**17a–H**).

Although numerous synthetic helical polymers have been prepared, their exact helical structures including helical pitch and handedness (right- or left-handed helix) remain unclear. The detailed structural determinations of helical polymers are essential to understand the relationships between their helical structures and functions, and also to develop new helical polymers with sophisticated functions. Figure 5 shows the general methods for the structural analyses of helical polymers.

Spectroscopic analysis	Microscopic observation
· NMR spectra	· Scanning electron microscopy (SEM)
· Absorption spectra	· Transmission electron microscopy (TEM)
· CD spectra	· Atomic force microscopy (AFM)
· Optical rotation	· Scanning tunneling microscopy (STM)
· IR spectra	
· Vibrational CD (VCD) spectra	

Diffraction method	Computer calculation
· X-ray diffraction (XRD)	· Molecular mechanics (MM) calculation
· Neutron diffraction	· Molecular orbital (MO) calculation
· Electron diffraction	· Molecular dynamics (MD) calculation

Figure 5. General methods for structural analyses of helical polymers.

Evidence for a preferred-handed helix formation of synthetic helical polymers is usually obtained by CD or optical rotation measurements. VCD is now recognized as a facile method to investigate the chiroptical properties of certain small molecules and biological polymers. NMR, absorption, and IR can also provide structural information including the conformation, configuration, and/or molecular ordering of helical polymers, particularly in solution.

XRD, neutron diffraction, and electron diffraction methods are also useful to get information about ordered polymer structures, particularly in the solid state. Among them, XRD is the most convenient and widely used technique for elucidating the structures of helical polymers as demonstrated for polypeptides and DNA. In fact, based on the XRD measurements of oriented films or fibers derived from a few synthetic helical polymers, their helical structures were elucidated. However, due to the limited number of diffractions and difficulty in obtaining crystalline samples from synthetic helical polymers, the XRD method may not provide unambiguous helical structural information, and in particular, the helical sense.

Microscopic observations of the helical structures of helical polymers using scanning electron microscopy (SEM) and transmission electron microscopy (TEM) are potentially

attractive, but still difficult due to poor resolution. The direct observation of helical structures by scanning probe microscopy (SPM), such as scanning tunneling microscopy (STM) and atomic force microscopy (AFM), is one of the most promising methods to determine the helical structures, in particular, helical aggregates prepared from small molecules, and have been extensively studied. However, SPM observations of helical polymers at the molecular level are still challenging even for a large biological polymer such as the double-stranded helix of DNA; high resolution images showing the right-handed double-stranded helix (helical pitch = 3.4 nm) by AFM[31] and STM[32] are quite rare, indicating that it is likely more difficult to observe the helical structures of synthetic helical polymers with a smaller helical pitch than that of DNA. However, Yashima et al. recently found that rigid-rod helical poly(phenylacetylene)s and poly(phenyl isocyanide)s showing a cholesteric or smectic liquid crystalline (LC) phase self-assembled to form two-dimensional crystals with a controlled helical conformation on solid substrates upon exposure to solvent vapors, which revealed their helical structures including the helical pitch and handedness as visualized by high resolution AFM.[91,33]

The recent striking progress in computer performance has made it possible to predict the structures and dynamic behaviors of helical polymers by means of molecular mechanics (MM), molecular orbital (MO), and molecular dynamics (MD) calculations. However, these computer methods are not straightforward, and may not provide unambiguous helical structural information. A brief overview of the helical structures of synthetic helical polymers determined by various methods is now described.

As mentioned earlier, the helical structures of biomacromolecules, such as polypeptides (18/5 helix)[1] and DMA (10/1 helix),[2] were determined using the fiber XRD technique. In the same way, the helical structures of poly(*n*-butyl isocyanate) (**18**)[34] and poly(di-*n*-pentylsilane) (**19**)[35] have been determined to be an 8/3 helix and 7/3 helix, respectively, by XRD measurements of their oriented films (Figure 6). The 7/3 helical structure of polysilanes were further supported by XRD measurements of analogous helical poly(*n*-alkylsilane)s (**20a** and **20b**)[36] and poly(*n*-decyl-(*S*)-2-methylbutylsilane) (**21**).[37]

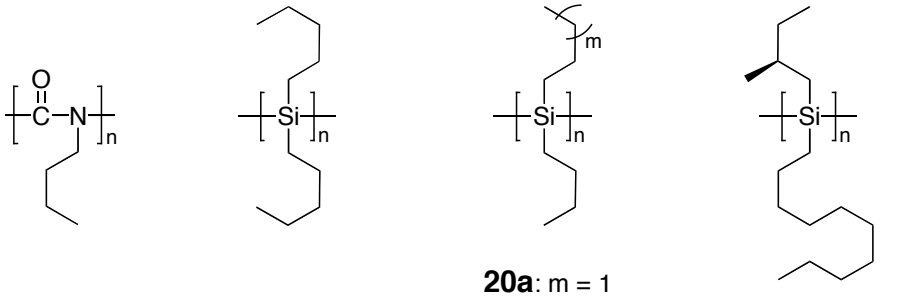

18
8/3 helix (1969)

19
7/3 helix (1987)

20a: m = 1
20b: m = 2
7/3 helix (1989, 1993)

21
7/3 helix (2001)

Figure 6. Synthetic helical polymers whose helical structures were determined by XRD measurements of the oriented films.

The structural elucidation of helical polymers by XRD on a molecular level is, in general, a laborious task, particularly for helical polymers bearing a complex repeating unit and those being insoluble in common solvents after polymerization. However, when the corresponding uniform oligomers can be isolated and crystallized for the single-crystal X-ray analysis, convincing evidence of their helical structures could be obtained (Figure 7).

Isotactic polychloral (**5**) prepared by the helix-sense-selective polymerization of chloral with optically active initiators was believed to possess a 4/1 helical conformation and showed a high optical activity in films ($[\alpha]_D$ +4000°).[13] Because the polymer is totally insoluble in solvents, further structural explorations in solutions were hampered. Ute et al. prepared and isolated isotactic enantiomerically pure uniform oligomers bearing different end groups (**22**) by size-exclusion chromatography (SEC) from the oligomerization products and subsequent optical resolution into enantiomers by chiral HPLC. They found that the (–)-pentamer with the (*R*,*R*,*R*,*R*,*R*) main-chain configuration adopted a right-handed 4/1 helical conformation by an X-ray crystallographic determination.[38] Ute et al. also determined the helical structure of the dodecamer of *n*-butyl isocyanate (**23**) to be approximately an 8/3 helix.[39] This helical structure resembles the corresponding helical structure of polyisocyanate **18** determined by the fiber XRD method.[34]

Poly(2,3-quinoxaline)s (**6**) are considered to possess a one-handed helical conformation as supported by their intense Cotton effect intensities.[14] The helical structure and handedness were determined by the X-ray crystallographic analysis of an active pentamer of a diastereomerically pure oligo(2,3-quinoxaline) (**24**) to be a right-handed 5/2 helix in the solid state.[40] A helical structure of an analogous uniform oligomer, a hexamer of oligo(quinoline) (**25**), was also determined to be a 5/2 helix.[41] Yokozawa et al. prepared a series of uniform *N*-methyl substituted oligo(*p*-benzamide) (**26**) by a step-growth oligomerization technique and determined their helical structure by a single-X-ray crystallographic analysis to be a 3/1 helix;[42] this helical structure is consistent with that proposed for the corresponding optically active *N*-alkyl substituted poly(*p*-benzamide)s based on their observed and calculated CD spectra.[42]

Thus, the X-ray crystallographic analysis of uniform oligomers is certainly a powerful method to unambiguously determine the helical structures including helical pitch and handedness as well, if single crystals of uniform oligomers with an optical activity like **22** and **24** are available.

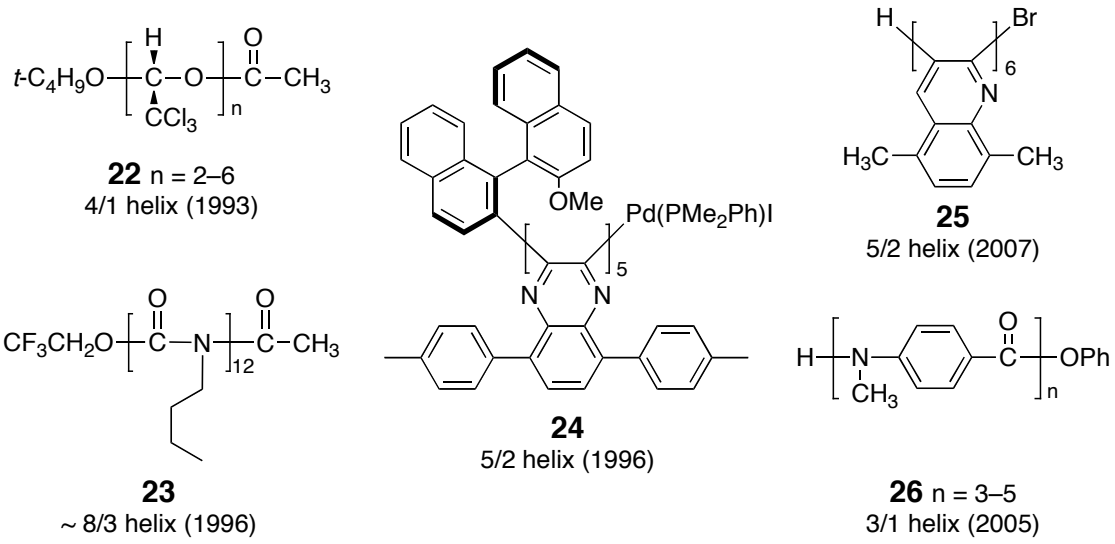

Figure 7. Synthetic uniform helical oligomers whose helical structures were determined by single-crystal X-ray crystallographic analyses.

The nonempirical exciton-coupled CD method developed by Nakanishi and Harada, that is a practically useful method for determining the absolute configuration of a variety of chiral small molecules,[43] is often used for predicting the predominant helical sense of synthetic helical polymers, although the method, when applied to helical polymers, may involve more or less uncertainty (Figure 8). Achiral chromophores, such as porphyrin and diazo dye residues, were covalently introduced as the pendant groups in the optically active polyisocyanide **27**[44] and poly(*N*-propargylamide) **28**[45] and polyisocyanide **29**,[46] respectively, and their helical senses were proposed on the basis of the signs of the split exciton-coupled Cotton effects.

Theoretical calculations of the electric CD and subsequent comparison with the observed CD may suggest a possible helical sense of certain helical polymers, although calculating the electric CD involves difficulty in resolving the contributions from individual electronic transitions from the main-chain and side-chain chromophores. Nevertheless, the preferred-handed helical sense of the optically active **1** isolated by chromatographic resolution was predicted by calculating the CD in the imino chromophore region by Drenth and Nolte.[47] Yokozawa and Kobayashi et al. performed an exciton model analysis of the absorption and CD spectra of the *N*-alkylated optically active poly(*p*-benzamide) (**30**) based on the crystal structure of the corresponding uniform oligomers (**26**) and proposed a right-handed helical structure (*P*-helix) for **30** in solution.[42] The helix-senses of a series of poly(*N*-butynylamide)s having various optically active side chains (**31a–d**) were also postulated by comparison of the observed CD spectra with the simulated ones.[48] Kaneko et al. helix-sense selectively polymerized a phenylacetylene bearing achiral galvinoxyl pendants in the presence of optically active amines and its helical sense of the resulting helical polymer (**32**) was determined to be a *P*-helix when (*R*)-1-phenylethylamine was used as the cocatalyst.[49]

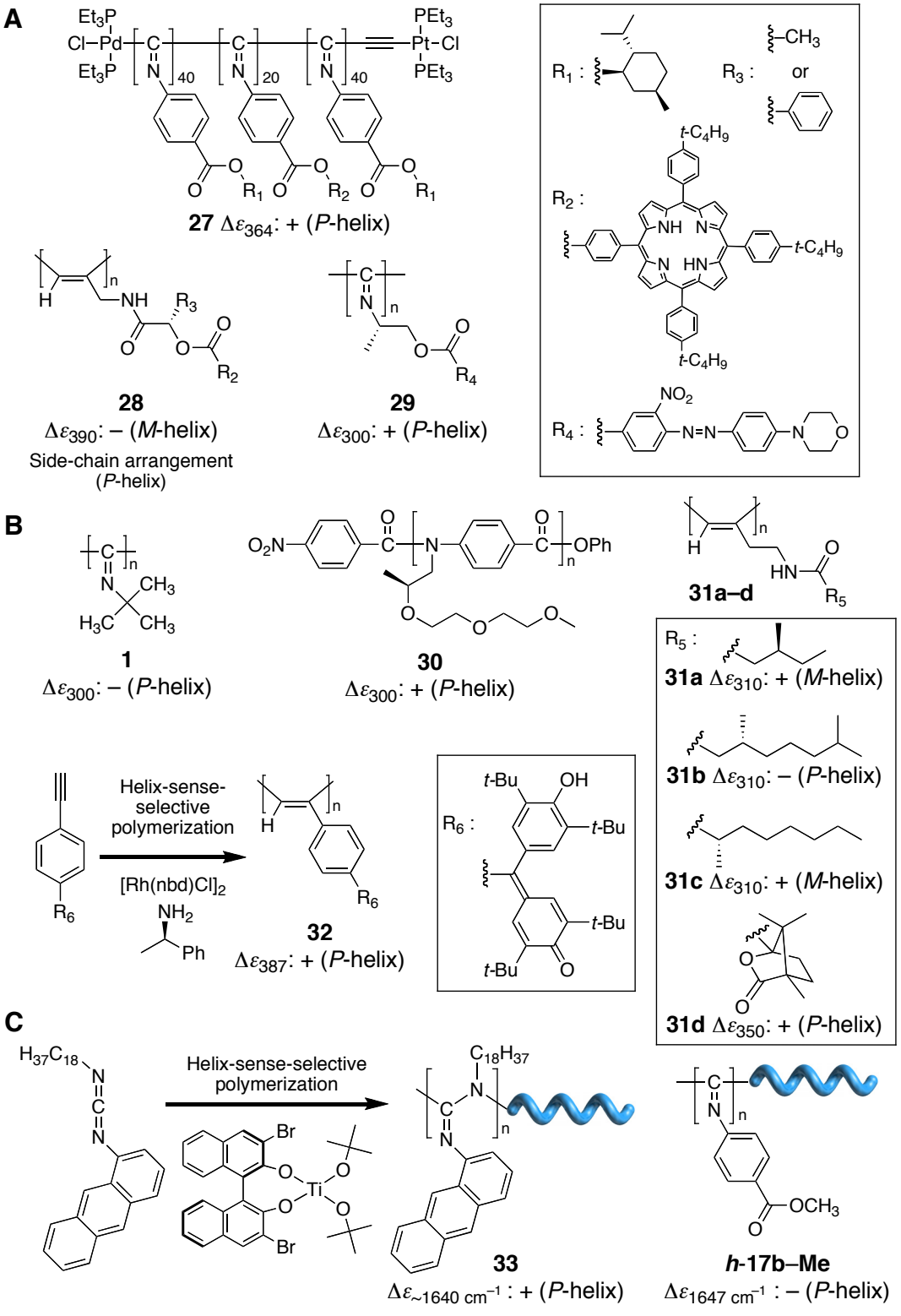

Figure 8. Synthetic helical polymers whose helical senses were determined by the exciton-coupled CD method (A), theoretical calculation of the CD spectra (B), and DFT calculations coupled with VCD measurements (C). The signs of the observed CD and VCD spectra and

the determined helical senses are also shown. *P*-helix and *M*-helix represent the right- and left-handed helical main-chain structures, respectively.

In sharp contrast to the electric CD, VCD has significant advantages not only for its sensitivity to chiral non-chromophoric molecules, but also for the reliable theoretical calculations of its spectrum using the density functional theory (DFT) available in the Gaussian program. Taking advantage of the available DFT calculation method, the helical structure of a model polymer of the optically active polyguanidine (**33**) prepared by the helix-sense-selective polymerization of the corresponding achiral carbodiimide with a chiral titanium complex was calculated to simulate its VCD spectrum, which was further used to determine the helix-sense of **33** by comparison with the experimental VCD spectrum.[15d] In a similar way, preferred-handed helical structures and their helical senses of polyisocyanide with macromolecular helicity memory (***h*-17b–Me**)[30] and optically active syndiotactic poly(methyl methacrylate) (st-PMMA)[50] have been determined.

As previously described, a very few helical structures of synthetic helical polymers (**18**–**21**) were elucidated by an XRD analysis. This may be due to the difficulty in obtaining oriented films suitable for the XRD measurements. As anticipated, when helical polymers are rigid-rod that form a lyotropic or thermotropic LC phase based on their main-chain stiffness, uniaxially oriented films with a regular helical structure over a long distance may be prepared by physical shearing or under electric- and magnetic-fields, thus providing useful structural information available to define the main-chain helical structures by XRD. In fact, the helical structure of **21** was determined by the XRD analysis of the oriented film prepared from its thermotropic LC state in the melt to be a 7/3 helix.

Since the pioneering research by Aharoni and Millich et al. in the 1970s on the LC formations of polyisocyanates[51] and polyisocyanides,[11b,52] various LC helical polymers based on their main-chain stiffness, such as polyisocyanides (**34**–**43**), polyguanidines (**44**–**47**), poly(quinoxaline)s (**48**), polymethacrylamide (**49**), polysilanes (**20**–**21** and **50**–**53**),

polyisocyanates (**18** and **54**–**58**), and polyacetylenes (**15**-**HCl**, **59**, and **60**), have been synthesized as summarized in Figure 9.

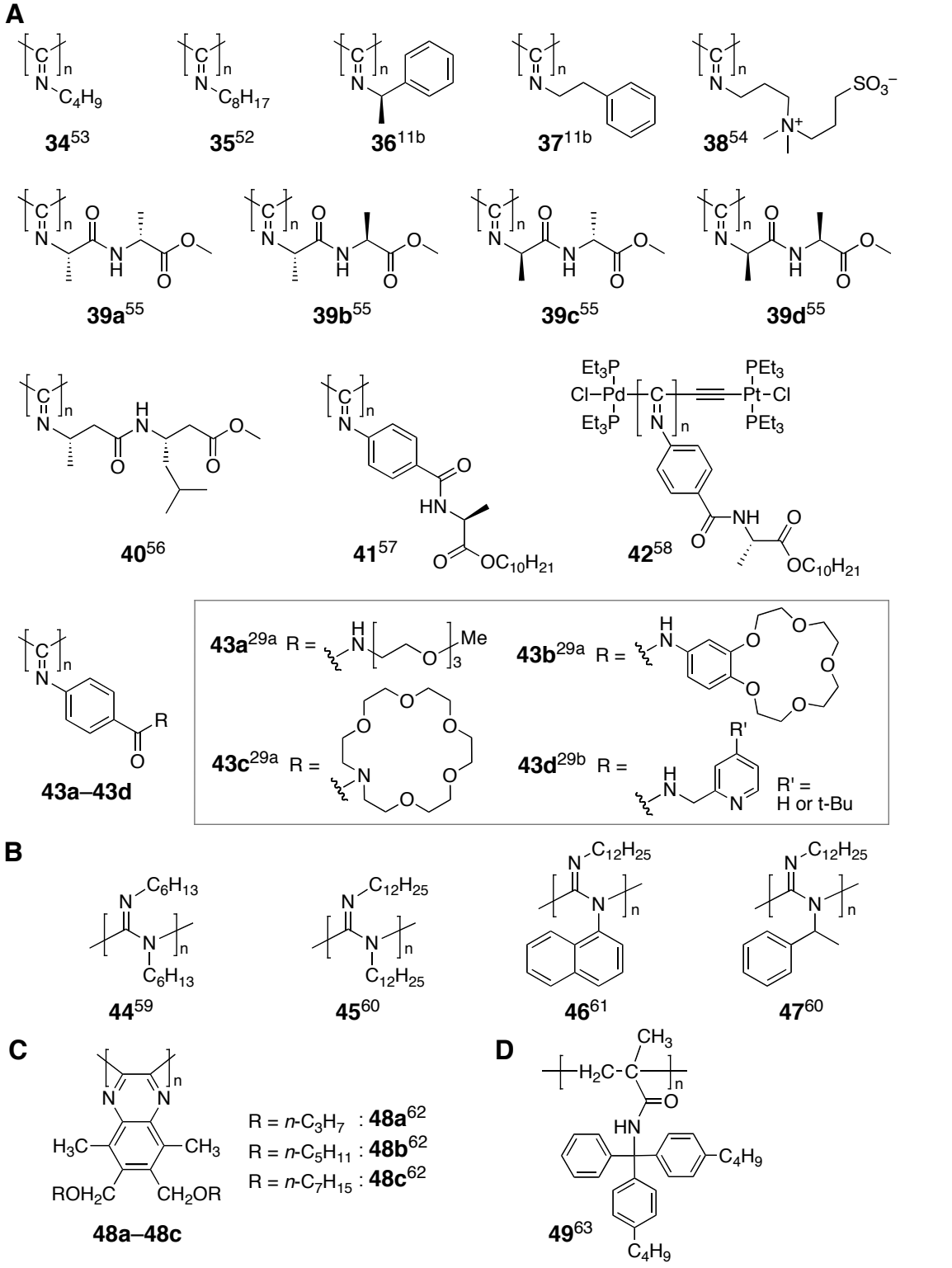

(Figure 9 continued)

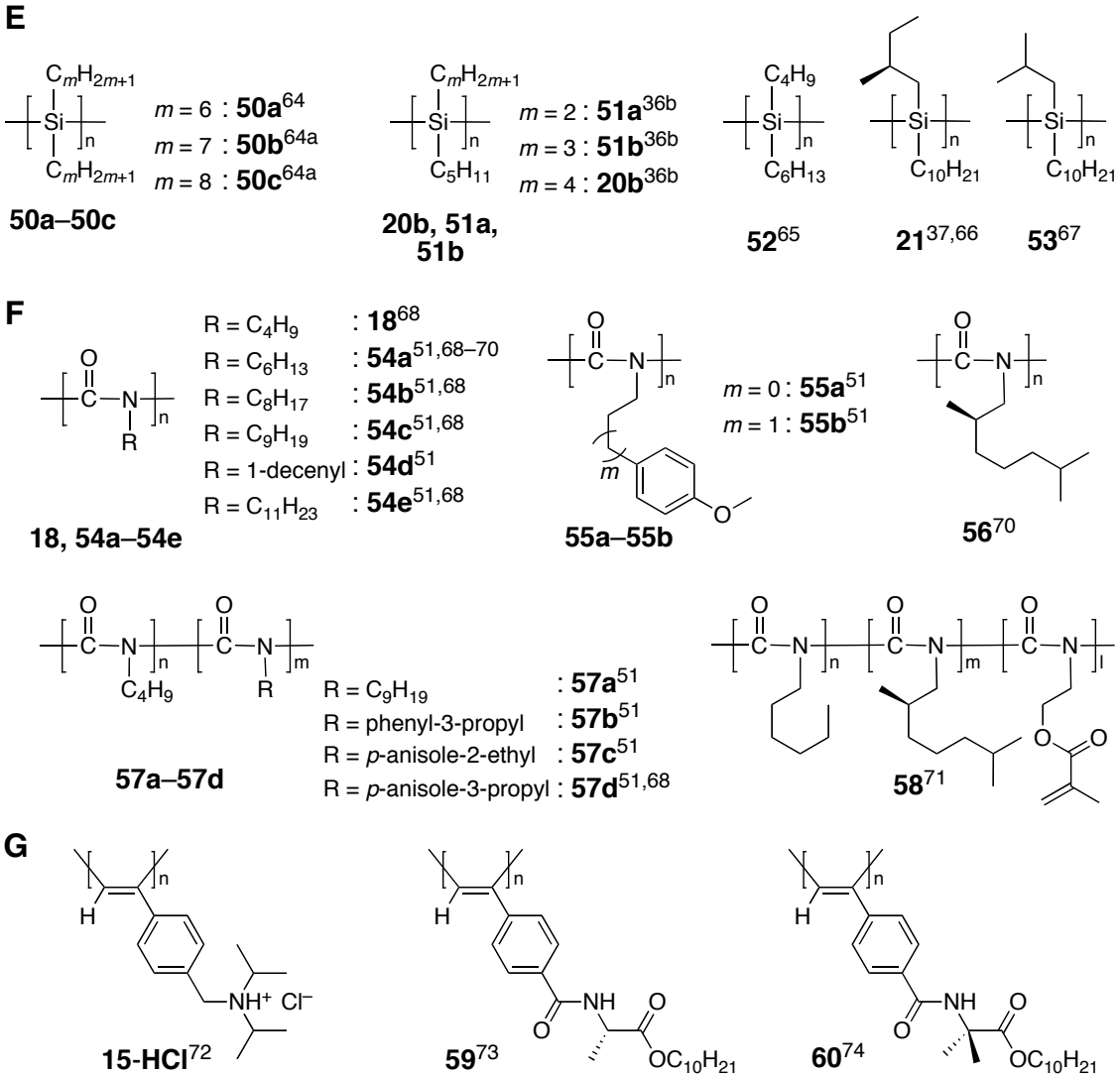

Figure 9. Structures of LC helical polymers due to the main-chain stiffness in concentrated solution or in a melt: polyisocyanides (A), polyguanidines (B), poly(quinoxaline)s (C), polymethacrylamide (D), polysilanes (E), polyisocyanates (F), and polyacetylenes (G).

Interestingly, these prepared LC polymers belong to either static (**34**–**49**) or dynamic (**18**, **20**, **21**, and **50**–**60**) helical polymers (Figure 2). The LC formation of polymers requires a main-chain stiffness in order to self-assemble in a close parallel packing of the polymer chains in a concentrated solution or in a melt. The persistence length (q) is a useful measure to evaluate the stiffness of the LC polymers, and can be estimated on the basis of the wormlike chain model[75] when the molecular-weight dependent changes in the radius of gyration, intrinsic viscosity, or sedimentation coefficient are available. The q values can also be obtained by measuring the isotropic-LC phase boundary concentrations of particular LC polymers in solution in conjunction with the scaled particle theory.[76] The minimum q value required for lyotropic LC formation is considered between 1–6 nm.[77] It should be noted that a number of LC helical polymers have been prepared as shown in Figure 9, but only a limited number of q values have been determined for helical polymers.

Table 1 summarizes the reported q values for synthetic helical polymers prepared so far, thus showing lyotropic and/or thermotropic LC phases. An optically active helical poly(phenylacetylene) bearing an L-alanine residue with a long alkyl chain as the pendants (**59**) has an exceptionally long q value of ca. 130 nm in nonpolar solvents, such as CCl_4 and toluene. This q value is the highest among all synthetic helical polymers reported so far and even stiffer than the double-helical DNA (< 60 nm),[78] but not comparable to those of biological, multi-stranded helical polymers, such as the triple-stranded helical collagen (160–180 nm)[79] and schizophyllan (150–200 nm).[80] Interestingly, **59** showed a dramatic decrease in its q value to 19–43 nm in polar solvents, such as tetrahydrofuran (THF) and chloroform. This significant change in the main-chain stiffness is accompanied by inversion of the helix-sense of the polymer main-chain, resulting from the "on and off" fashion of the intramolecular hydrogen bonding networks between the pendant amide residues in nonpolar and polar solvents.[73b] As expected, **59** formed cholesteric LC phases with an opposite twist-sense to each other in polar and nonpolar solvents. An optically active poly(phenyl isocyanide) (**41**) bearing the same L-alanine-based pendant groups like **59** was also prepared with a nickel

catalyst. In contrast to **59**, the helix-sense (right- or left-handed helix) of **41** can be controlled by the polymerization solvent and temperature governed by intermolecular hydrogen-bonding occurring between the pendant residues of the growing chain end and monomers during the propagation reaction (Figure 10). The resulting diastereomeric **41** formed lyotropic cholesteric LC phases with opposite twist senses in concentrated chloroform solutions due to their main-chain stiffness arising from the intramolecular hydrogen-bonding between the pendant amide groups.[57]

Table 1. Persistence Length (q) Values of Liquid Crystalline Synthetic Helical Polymers

polymer		solvent	q (nm)	method[a]	temp.	LC phase[b]	ref
polyisocyanides	**36**	$CHCl_3$	3.2	LS	[c]	[c]	81
	38	0.05 M $LiClO_4$ aq.	5.7	V	25 °C	N	54
	39a	$CHCl_3$, TCE	76	A	[c]	Ch	82
polyguanidine	**47**	THF	42	SEC-LS	25 °C	N	83
polysilanes	**50a**	THF	2.7	LS, V	25 °C	T	84
	21	isooctane	70	LS, V, C	25 °C	T, Ch, Sm	85
polyisocyanates	**54a**	toluene	37–38	V, C	25 °C	N	86
		CH_2Cl_2	18–21	V, C	20 °C	N	86
		hexane	42	LS, V, S	25 °C	N	87
		1-chlorobutane	35	V	25 °C	N	88
	56	hexane	56	LS, V	25 °C	Ch	89
		$CHCl_3$	34	LS, V	25 °C	Ch	89
polyacetylenes	**59**	CCl_4	134.5	SEC-LS	25 °C	Ch	73b
		toluene	126.3	SEC-LS	25 °C	[c]	73b
		$CHCl_3$	42.9	SEC-LS	25 °C	Ch	73b
		THF	19.2	SEC-LS	25 °C	[c]	73b
	60	toluene	89.6	SEC-LS	25 °C	N	74

[a] Method for evaluation the q values: LS = light scattering, V = viscosity, A = atomic force microscopy, SEC-LS = size exclusion chromatography equipped with light scattering detector, C = phase boundary concentration, S = sedimentation equilibrium. [b] Liquid crystalline (LC) phase: N = nematic, Ch = cholesteric, T = thermotropic, Sm = smectic. [c] Not available.

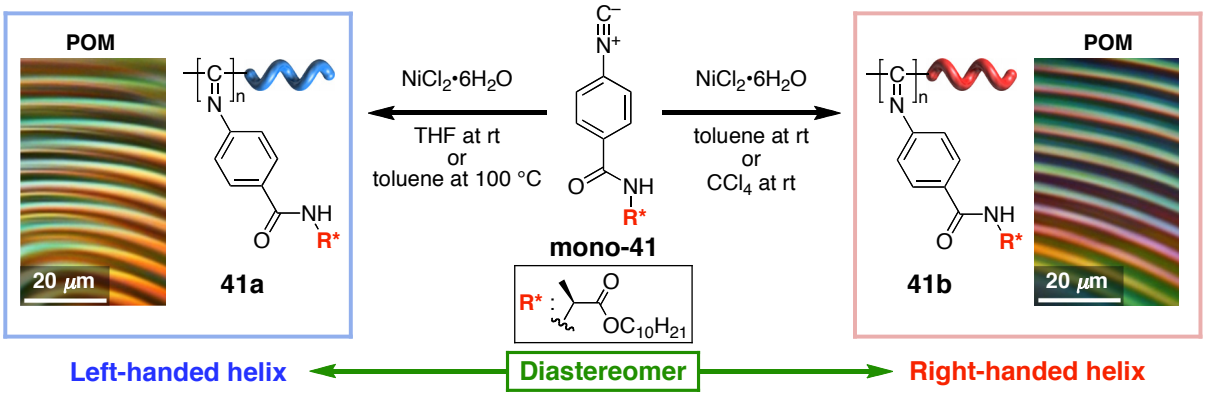

Figure 10. Schematic illustration of helix-sense controlled polymerization of **mono-41**. The helix-sense can be controlled by the solvent polarity and temperature during the polymerization, resulting in the formation of diastereomeric helical polyisocyanides. Polarized optical micrographs (POM) of cholesteric LC phases of **41a** and **41b** in 15 wt % chloroform solution are also shown.

The optically inactive poly(*n*-hexyl isocyanate) (**54a**) is one of the most extensively studied dynamic helical polymers and formed a lyotropic nematic LC phase, which further converted to the cholesteric counterpart by doping with small chiral molecules or optically active polyisocyanates in organic solvents.[70] Green et al. discovered the amplification of the helix-sense excess in the LC state rather than in a dilute solution due to the reduction in population of the energetically unfavorable, kinked helical reversals in the LC state. This is called the "bad neighbors" rule.[69a]

The synthetic helical polymers prepared so far often exhibited lyotropic LC phases in organic solvents or in a melt, and the synthetic helical polymers showing lyotropic LC phases in water are quite rare,[29a,90] in spite of their potential for a wide range of applications including biomimetic composite materials and electric-field responsive materials.

Recently, Yashima et al. reported that a positively charged polyacetylene, the hydrochloride of **15** (**15**-**HCl**) formed a lyotropic nematic LC phase in concentrated water solution. As expected, the nematic LC phase converted to the cholesteric counterpart by doping with a tiny amount of optically active acids (Figure 11). This is the first example of

LC polyacetylenes based on the main-chain stiffness.[72] However, detailed investigations of the structures and chiroptical properties of **15**-**HCl** have not yet been conducted. In addition, although a large number of stereoregular polyacetylenes bearing aliphatic and aromatic pendants have been synthesized with much interest, their exact helical structures have not been determined. The fact that **15**-**HCl** is a rigid-rod LC polyacetylene suggests that its helical structure can be determined by measuring the XRD of the oriented film prepared from the LC state.

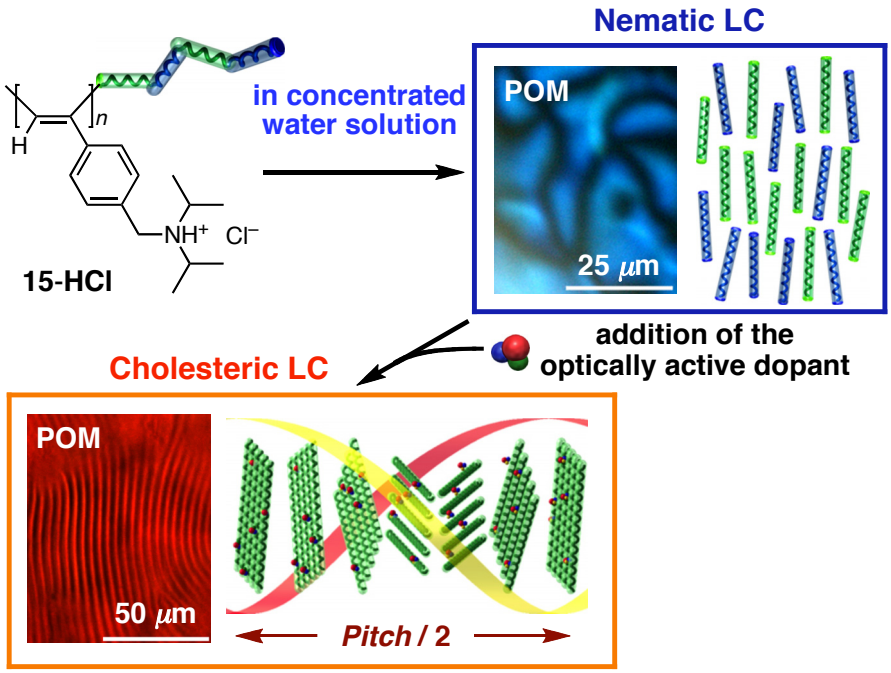

Figure 11. Schematic illustration of nematic LC formation of **15**-**HCl** in concentrated water solution. The nematic LC phase was converted to the cholesteric counterpart by doping with optically active acids.

On the basis of this information, the author studied the following six areas concerning the synthesis and structures of LC helical polymers based on their main-chain stiffness.

(1) Helicity induction and chiral amplification in a poly(phenylacetylene) bearing *N*,*N*-diisopropylaminomethyl groups with chiral acids in water
(2) Hierarchical amplification of macromolecular helicity in a lyotropic liquid crystalline charged poly(phenylacetylene) by nonracemic dopants in water and its helical structure
(3) Temperature induced chiroptical changes in a helical poly(phenylacetylene) bearing *N*,*N*-diisopropylaminomethyl groups complexed with chiral acids in water
(4) Mechanism of helicity induction and memory of the macromolecular helicity in poly(phenyl isocyanide) derivatives based on their structural analyses
(5) Anomalous stiff backbones of helical poly(phenyl isocyanide) derivatives
(6) Helical structure of liquid crystalline poly(*N*-((4-butylphenyl)diphenylmethyl) methacrylamide)

These studies will be described in the following six chapters.

In chapter 1, the helicity induction on **15**-**HCl** in the presence of various chiral acids including aromatic and aliphatic carboxylic acids, phosphoric and sulfonic acids, and amino acids in water is described (Figure 12). Polyelectrolytes, such as nucleic acids, can efficiently interact with a variety of oppositely charged small molecules in water through electrostatic and/or directed hydrogen bonding interactions. The author anticipated that the chromophoric polyelectrolyte, *cis-transoidal* **15**-**HCl** which possesses positively charged functional groups as the pendants could efficiently interact with a variety of negatively charged chiral nonracemic acids, including important biomolecules, such as amino acids and nucleotides, and form supramolecular assemblies with a controlled helicity through electrostatic and

hydrogen bonding interactions in water. If these specific interactions would occur in water, they could be detected and evaluated using CD spectroscopy with **15**-**HCl** as a sensing probe. In fact, **15**-**HCl**—various chiral acids complexes showed ICDs in the UV-visible region of the polymer backbone. **15**-**HCl** was highly sensitive to the chirality of carboxylic acids and exhibited the same Cotton effect signs if the configurations of the chiral acids were the same. **15**-**HCl** also complexed with biomolecules, such as ribonucleotides, DNA, and amino acids in water and exhibited similar ICDs in their patterns in the UV-visible region. Moreover, **15**-**HCl** showed a positively nonlinear relationship ("majority rule") between the ee of chiral acids and the observed ICD, and can detect a tiny enantiomeric imbalance in the chiral acids in water. These results demonstrate that **15**-**HCl** can be utilized as a chirality sensing probe for chiral acids in water. Furthermore, **15**-**HCl** exhibited intense ICDs in the presence of chiral aromatic alcohols, indicating that **15**-**HCl** can also be used to detect the chirality of chiral neutral molecules through hydrophobic interactions in water. The polyelectrolyte function of **15**-**HCl** accompanied by the hydrophobic pendants may play an important role in the highly chiral detection and amplification in water.

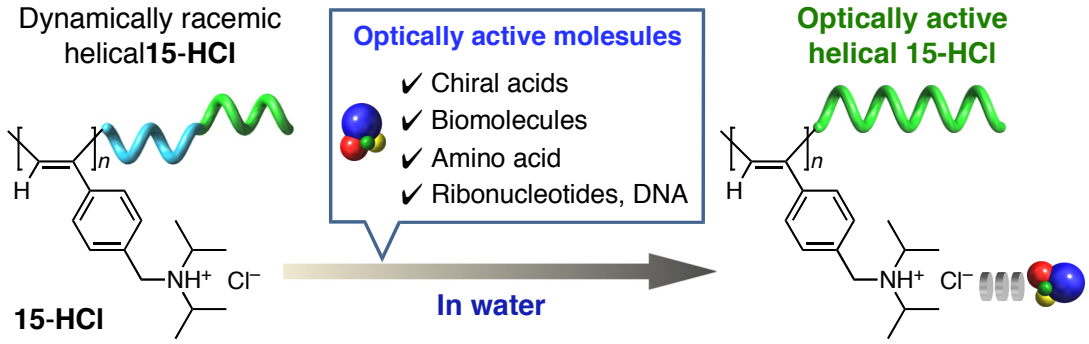

Figure 12. Schematic illustration of a one-handed helicity induction in **15**-**HCl** upon complexation with optically active molecules in water.

Chapter 2 deals with a hierarchical amplification of the macromolecular helicity of **15**-**HCl** induced by nonracemic dopants in the aqueous LC state and its helical structure based on the XRD analysis (Figure 13). As mentioned previously, **15**-**HCl** forms a lyotropic LC phase in concentrated water solution, which further converted to the cholesteric counterpart by doping with a small amount of nonracemic acids. The author anticipated that the helix-sense excess of **15**-**HCl** would be amplified in the cholesteric LC state over that in dilute solution because each helical polymer chain can interact with others, thus leading to a tightening of the cholesteric pitch. Actually, the helical sense of **15**-**HCl** induced by nonracemic dopants in dilute water solution was further amplified in the cholesteric LC state by direct comparison of the helix-sense excess of the polymer backbone in dilute solution with that in the cholesteric LC state. This LC formation of **15**-**HCl** together with high sensitivity to the chirality of the dopants may result from the rigidity of the polymer backbone with relatively bulky pendant groups assisted by its polyelectrolyte function.

The main-chain stiffness of **15**-**HCl** in water before and after the one-handed helicity induction was experimentally evaluated by measuring the q value of the polymer on the basis of the isotropic–LC phase boundary concentrations; the persistence length of optically inactive **15**-**HCl** was estimated to be 26.2 nm and that of the one-handed helical **15**-**HCl** was 28.0 nm. The fact that the optically active and inactive **15**-**HCl**s have similar q values indicates that kinks due to the helical reversal in the polymer chain are too few to contribute to the chain flexibility and the alternative contribution of the torsional fluctuation in the polyacetylene chain may be predominant. Consequently, the dynamically racemic **15**-**HCl** helices likely have a long helical sequence with few helical reversals.

XRD of the oriented films of the nematic and cholesteric LC **15**-**HCl**s exhibited almost the same diffraction pattern, suggesting that both polymers may have the same helical structure in spite of the substantial difference in their helical characteristics; dynamically racemic and one-handed helices in dilute solution, respectively. On the basis of the X-ray analyses, the most plausible helical structure of **15**-**HCl** was proposed to be a 23/10 helix.

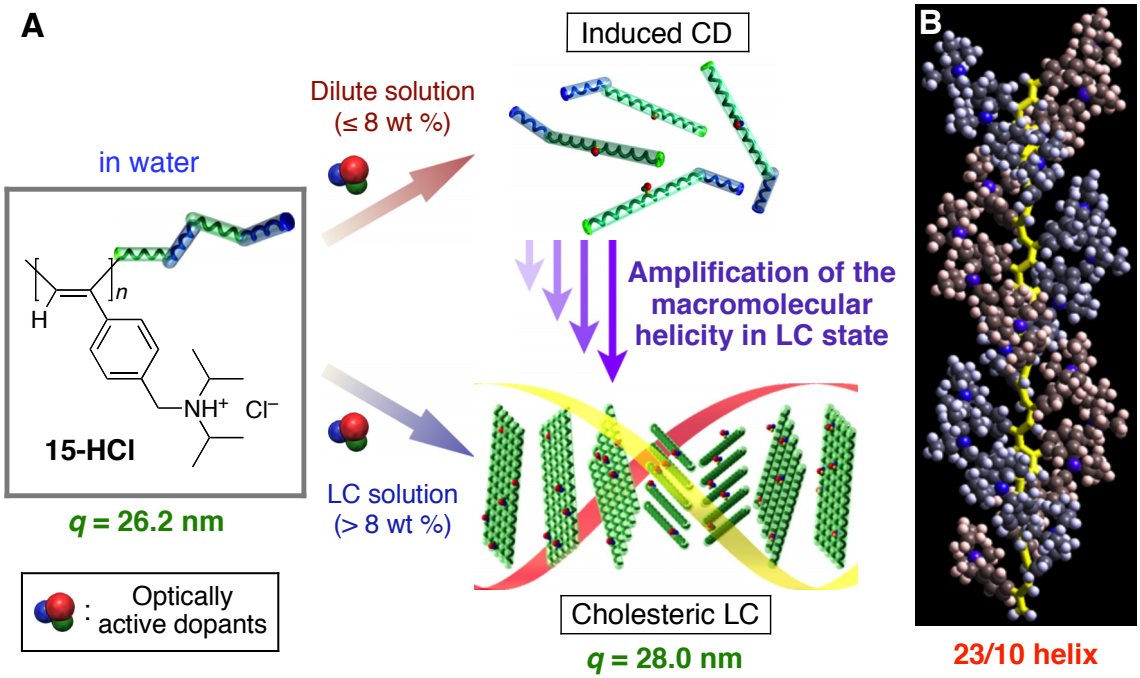

Figure 13. (A) Schematic illustration of the hierarchical amplification process of the macromolecular helicity of **15**-**HCl** mediated by a nonracemic dopant in dilute and concentrated LC water solutions. (B) A plausible 23/10 helical structure of **15** based on the XRD analysis.

In charter 3, the helicity induction and chiral amplification of free **15** in the presence of various chiral acids in water are described (Figure 14). As already mentioned, **15**-**HCl** was highly sensitive to the chirality of chiral acids in water and exhibited intense ICDs in dilute water solution. However, the neutral **15** has a low sensitivity to the chirality of the chiral acids and produces no LC phase in organic solvents. During the course of the author's study, he found that the neutral **15**, which is not soluble in water, became soluble in the presence of excess amounts of free aromatic and aliphatic carboxylic acids, which promoted to investigate the helicity induction and chiral amplification of free **15** with chiral acids in water.

15 was found to be highly sensitive to the chirality of optically active acids in water and could detect a small enantiomeric imbalance of these acids, for example, 0.005% ee of phenyl lactic acid in water. The observed ICD intensity and pattern of **15** complexed with chiral acids were dependent on the temperature and concentration of **15**, accompanied by a significant

change in the absorption spectra, thus showing a clear color change. This remarkable change is probably due to the aggregations of the polymer at high temperature as revealed by dynamic light scattering and AFM observation. Taking advantage of this temperature-induced ICD change, the preferred handed helix sense of **15** was found to be controlled by noncovalent bonding interactions by using structurally different enantiomeric acids.

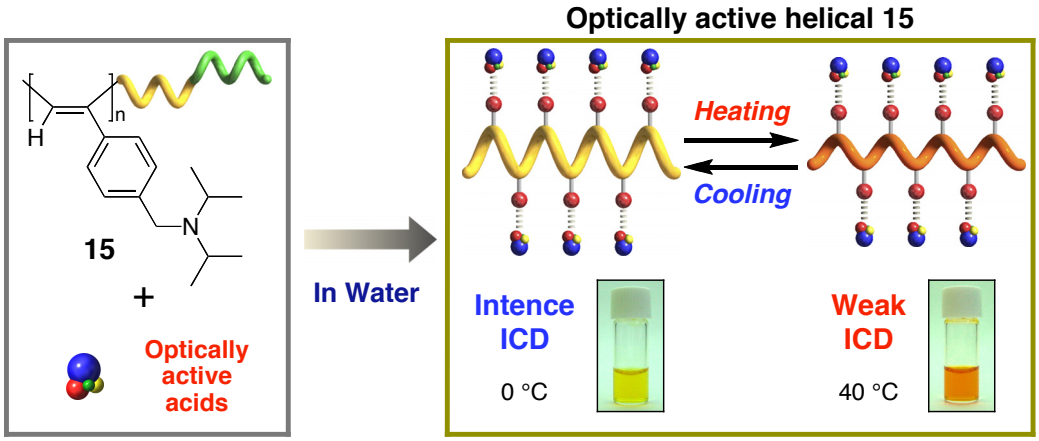

Figure 14. Schematic illustration of helicity induction in **15** in water upon complexation with optically active acids and a possible conformational change of **15**—optically active acid complex accompanied by a visible color change.

Chapter 4 deals with the mechanism of helicity induction and memory of the macromolecular helicity in **17**–**H** based on their structural analyses (Figure 15). As already described, **17**–**H** changed its structure into the prevailing, one-handed helical structure upon complexation with optically active amines in DMSO and water, and the complexes show a characteristic ICD in the polymer backbone region. Moreover, the macromolecular helicity induced in water and aqueous organic solutions containing more than 50 vol% water could be "*memorized*" even after complete removal of the chiral amines (***h*-17b**–**H**), while that induced in DMSO and DMSO–water mixtures containing less than 30 vol% water could not maintain the optical activity after removing the chiral amines (**17a**–**H**). The spectroscopic results such as CD, absorption, IR, VCD, and NMR of **17a**–**H**, ***h*-17b**–**H**, and the original **17**–**H** revealed that the specific configurational isomerization around the C=N double bonds may occur in the

helicity induction process in each solvent. However, the spectroscopic results could not solve the question what different helical structures the polyisocyanide can form in DMSO and water in the presence of chiral amines, respectively. Taking advantage of the liquid crystallinity of the methyl esters of the high-molecular-weight **17**s (**17–Me**, **17a–Me**, and ***h*-17b–Me**) in concentrated chloroform solution, the author prepared their uniaxially oriented films from the LC states and measured the XRD in order to obtain the structural information. On the basis of the XRD analyses, the most plausible helical structure for **17a–Me** was proposed to be an 18/5 helix and that of ***h*-17b–Me** was a 10/3 helix. Moreover, the author measured the persistence lengths of these polymers in order to estimate the main-chain stiffness. The estimated q value of the original **17–Me** was 59 nm, while those of **17a–Me** and ***h*-17b–Me** were 43 and 88 nm, respectively, indicating that these structural changes accompany the significant change in their main-chain stiffness. On the basis of the XRD results together with the spectroscopic analyses and theoretical calculations, the mechanism of the helix induction in **17–H** and subsequent memory of the macromolecular helicity were discussed.

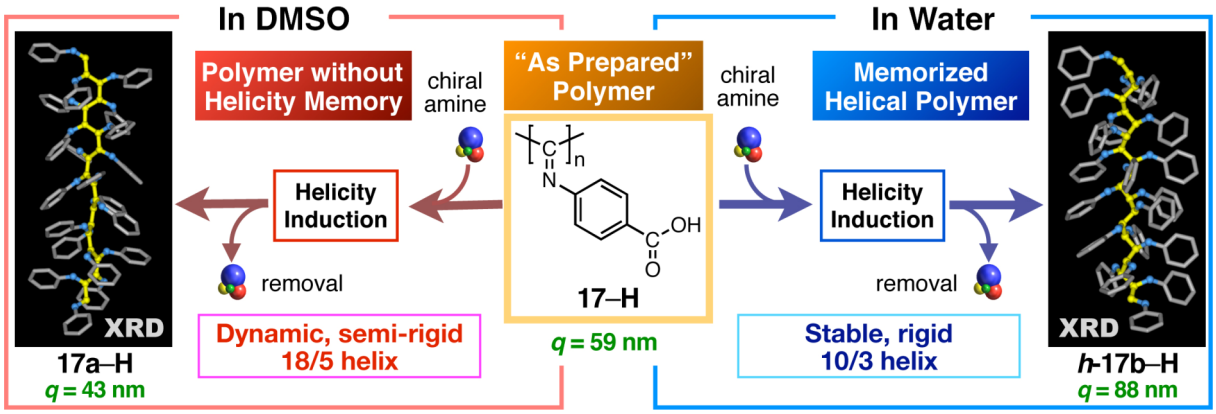

Figure 15. Schematic illustration of helicity induction in **17–H** in DMSO and water with chiral amines and subsequent removal of the chiral amines. The plausible helical structures of **17a–H** and ***h*-17b–H** based on XRD measurements and their persistence length values of **17–H**, **17a–H**, and ***h*-17b–H** are also shown.

Chapter 5 deals with the persistence length measurements of a series of optically active helical poly(phenyl isocyanide)s bearing different optically active functional groups with a long *n*-decyl chain as the pendants (Figure 16). As shown in Figure 10, the helix-sense of **41** could be controlled by the polymerization solvent and temperature governed by intermolecular hydrogen-bonding occurring between the pendant amide residues of the growing chain end and monomers during the propagation reaction. In order to explore the effect of the chiral pendant structure on the chiroptical properties of the polyisocyanide, a series of optically active polyisocyanides bearing different optically active functional groups, such as L-lactic acid (**61**), L-phenylalanine (**62**), and L-alaninol (**63**) residues, with the same *n*-decyl chain as the pendants were prepared in various solvents at different temperatures and chiroptical properties of these polymers were investigated.[91] **41a** formed a cholesteric LC in concentrated solutions, which indicated its rigid rodlike feature of the main-chain. The author measured the persistence lengths of **41a** and **61**–**63** and investigated the effect of the chiral pendant structures on their main-chain stiffness. The persistence lengths of the polymers significantly depended on their chiral pendant structures involving the hydrogen-bonding ability and bulkiness, and **41a** was found to possess an unprecedented long persistence length of 220 nm. This value is the highest among all synthetic helical polymers reported so far and is comparable to those of biological, multi-stranded helical polymers, such as the triple-stranded helical collagen and schizophyllan.

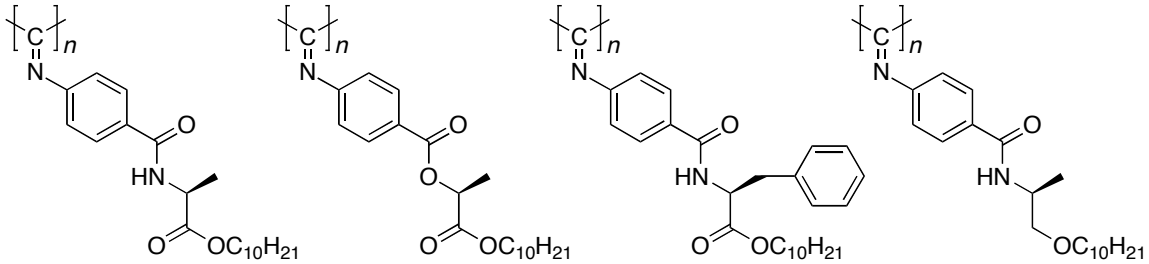

Figure 16. Structures and persistence length values of helical polyisocyanides.

In chapter 6, the structural analysis of LC poly(*N*-((4-butylphenyl)diphenylmethyl) methacrylamide) (**64**) (Figure 17) is described. Okamoto et al. recently found that the radical polymerization of *n*-butyl-substituted *N*-triphenylmethyl methacrylamides in toluene or THF produced the corresponding high-molecular weight polymethacrylamides with a nearly 100% isotacticity being soluble in common organic solvents, such as chloroform. When chiral additives such as (+)-menthol were used as a polymerization solvent, the optically active polymers due to a preferred-handed helicity were obtained (*helical*-**64**).[92] In addition, Okamoto et al. also found that a poly(*n*-butyl-substituted *N*-triphenylmethyl methacrylamide) (**49**) formed an LC phase in concentrated chloroform solution,[63] which promoted the author to investigate the helical structure of analogous poly(*n*-butyl-substituted *N*-triphenylmethyl methacrylamide)s by means of XRD. The author found that **64** and *helical*-**64** exhibited lyotropic LC phases in concentrated chloroform solutions, indicating their rigid-rod helical characteristics as evidenced by the long persistence lengths of 57 nm (**64**) and 53 nm (*helical*-**64**). XRD of the shear-oriented *helical*-**64** and **64** films showed almost the same diffraction pattern, suggesting that both the polymers may have the same helical structure despite the difference in their optical activity. On the basis of the X-ray analyses, the most plausible helical structure for **64** is proposed to be a 4/1 or 6/1 helix. High-resolution AFM observations of the polymers provided more detailed molecular structures including molecular length and helical pitch.

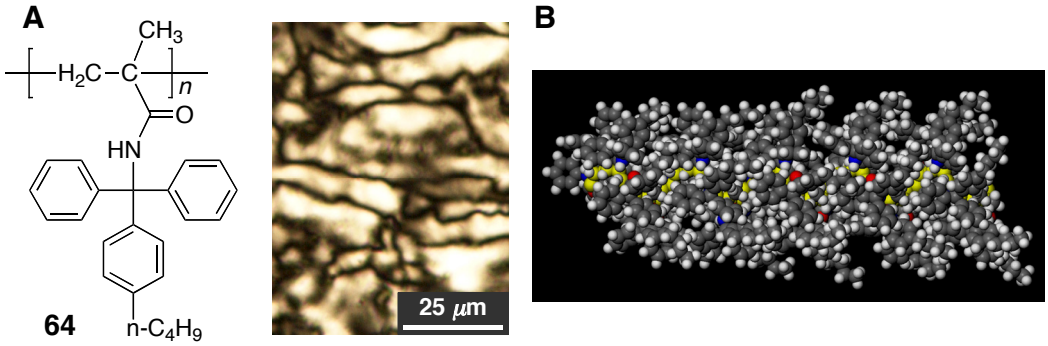

Figure 17. (A) Structure of **64** and polarized optical micrograph of optically inactive **64** in chloroform. (B) A plausible 6/1 helical structure of **64** based on XRD analysis.

References and Notes

(1) Pauling, L.; Corey, R. B. *Proc. Natl. Acad. Sci. U. S. A.* **1951**, *37*, 241–250.

(2) Watson, J. D.; Crick, F. H. C. *Nature* **1953**, *171*, 737–738.

(3) (a) Saenger, W. *Principles of Nucleic Acid Structure*; Springer-Verlag: New York, 1984. (b) Schulz, G. E.; Schirmer, R. H. *Principles of Protein Structure*; Springer-Verlag: New York, 1979.

(4) Natta, G.; Pino, P.; Corradini, P.; Danusso, F.; Mantica, E.; Mazzanti, G.; Moraglio, G. *J. Am. Chem. Soc.* **1955**, *77*, 1708–1710.

(5) Tadokoro, H. *Structure of Crystalline Polymers*; Wiley: New York, 1979.

(6) Nolte, R. J. M.; van Beijnen, A. J. M.; Drenth, W. *J. Am. Chem. Soc.* **1974**, *96*, 5932–5933.

(7) Okamoto, Y.; Suzuki, K.; Ohta, K.; Hatada, K.; Yuki, H. *J. Am. Chem. Soc.* **1979**, *101*, 4763–4765.

(8) (a) Yuki, H.; Okamoto, Y.; Okamoto, I. *J. Am. Chem. Soc.* **1980**, *102*, 6356-6358. (b) Nakano, T. *J. Chromatogr. A* **2001**, *906*, 205–225. (c) Yamamoto, C.; Okamoto, Y. *Bull. Chem. Soc. Jpn.* **2004**, *77*, 227–257.

(9) Reviews: (a) Okamoto, Y.; Nakano, T. *Chem. Rev.* **1994**, *94*, 349–372. (b) Nolte, R. J. M. *Chem. Soc. Rev.* **1994**, 11–19. (c) Green, M. M.; Peterson, N. C.; Sato, T.; Teramoto, A.; Cook, R.; Lifson, S. *Science* **1995**, *268,* 1860–1866. (d) Green, M. M.; Park, J.-W.; Sato, T.; Teramoto, A.; Lifson, S.; Selinger, R. L. B.; Selinger, J. V. *Angew. Chem., Int. Ed.* **1999**, *38*, 3138–3154. (e) Nakano, T.; Okamoto, Y. *Chem. Rev.* **2001**, *101*, 4013–4038. (f) Cornelissen, J. J. L. M.; Rowan, A. E.; Nolte, R. J. M.; Sommerdijk, N. A. J. M. *Chem. Rev.* **2001**, *101*, 4039–4070. (g) Fujiki, M.; Koe, J. R.; Terao, K.; Sato, T.; Teramoto, A.; Watanabe, J. *Polym. J.* **2003**, *35*, 297–344. (h) Reggelin, M.; Doerr, S.; Klussmann, M.; Schultz, M.; Holbach, M. *Proc. Natl. Acad. Sci. U. S. A.* **2004**, *101*, 5461–5466. (i) Yashima, E.; Maeda, K.; Nishimura, T. *Chem. –Eur. J.* **2004**, *10*, 42–51. (j) Maeda, K.; Yashima, E. *Top. Curr. Chem.* **2006**, *265*, 47–88. (k) Yashima, E.;

Maeda, K. *Macromolecules* **2008**, *41*, 3–12. (l) Yashima, E.; Maeda, K.; Furusho, Y. *Acc. Chem. Res.* **2008**, *41*, 1166–1180. (m) Kim, H.-J.; Lim, Y.-B.; Lee, M. *J. Polym. Sci., Part A: Polym. Chem.* **2008**, *46*, 1925–1935.

(10) Reviews: (a) Lehn, J. M. *Supramolecular Chemistry*; VCH: Weinheim, Germany, 1995. (b) Gellman, S. H. *Acc. Chem. Res.* **1998**, *31*, 173–180. (c) Srinivasarao, M. *Curr. Opin. Colloid Interface Sci.* **1999**, *4,* 370–376. (d) Hill, D. J.; Mio, M. J.; Prince, R. B.; Hughes, T. S.; Moore, J. S. *Chem. Rev.* **2001**, *101*, 3893–4011. (e) Cheng, R. P.; Gellman, S. H.; DeGrado, W. F. *Chem. Rev.* **2001**, *101*, 3219–3232. (f) Brunsveld, L.; Folmer, B. J. B.; Meijer, E. W.; Sijbesma, R. P. *Chem. Rev.* **2001**, *101*, 4071–4097. (g) Elemans, J. A. A. W.; Rowan, A. E.; Nolte, R. J. M. *J. Mater. Chem.* **2003**, *13*, 2661–2670. (h) Huc, I. *Eur. J. Org. Chem.* **2004**, 17–29. (i) Seebach, D.; Beck, A. K.; Bierbaum, D. J. *Chem. Biodiv.* **2004**, *1*, 1111–1239. (j) Vriezema, D. M.; Aragonès, M. C.; Elemans, J. A. A. W.; Cornelissen, J. J. L. M.; Rowan, A. E.; Nolte, R. J. M. *Chem. Rev.* **2005**, *105*, 1445–1489. (k) Hoeben, F. J. M.; Jonkheijm, P.; Meijer, E. W.; Schenning, A. P. H. J. *Chem. Rev.* **2005**, *105*, 1491–1546. (l) Lockman, J. W.; Paul, N. M.; Parquette, J. R. *Prog. Polym. Sci.* **2005**, *30*, 423–452. (m) Furusho, Y.; Yashima, E. *Chem. Rec.* **2007**, *7*, 1–11. (n) Palmans, A. R. A.; Meijer, E. W. *Angew. Chem., Int. Ed.* **2007**, *46*, 8948–8968. (o) *Foldamers: Structure, Properties, and Applications*; Hecht, S.; Huc, I., Eds.; Wiley-VCH: Weinheim, 2007. (p) Pijper, D.; Feringa, B. L. *Soft Matter* **2008**, *4*, 1349–1372.

(11) (a) Millich, F. *Chem. Rev.* **1972**, *72*, 101–113. (b) Millich, F. *Adv. Polym. Sci.* **1975**, *19*, 117–141. (c) Drenth, W.; Nolte, R. J. M. *Acc. Chem. Res.* **1979**, *12,* 30–35. (d) Millich, F. *J. Polym. Sci. Macromol. Rev.* **1980**, *15*, 207–253. (e) Takahashi, S.; Onitsuka, K.; Takei, F. *Proc. Japan Acad. Ser. B* **1998**, *74*, 25–30. (f) Hasegawa, T.; Kondoh, S.; Matsuura, K.; Kobayashi, K. *Macromolecules* **1999**, *32*, 6595–6603. (g) Yamada, Y.; Kawai, T.; Abe, J.; Iyoda, T. *J. Polym. Sci., Part A: Polym. Chem.* **2002**, *40*, 399–408.

(h) Amabilino, D. B.; Serrano, J.-L.; Sierra, T.; Veciana, J. *J. Polym. Sci., Part A: Polym. Chem.* **2006**, *44*, 3161–3174.

(12) (a) Okamoto, Y.; Yashima, E. *Prog. Polym. Sci.* **1990**, *15*, 263–298. (b) Nakano, T.; Okamoto, Y.; Hatada, K. *J. Am. Chem. Soc.* **1992**, *114*, 1318–1329.

(13) (a) Corley, L. S.; Vogl, O. *Polym. Bull.* **1980**, *3*, 211–217.(b) Vogl, O.; Jaycox, G. D.; Kratky, C.; Simonsick, W. J.; Hatada, K. *Acc. Chem. Res.* **1992**, *25*, 408–413.

(14) (a) Ito, Y.; Ihara, E.; Murakami, M. *Angew. Chem., Int. Ed.* **1992**, *31*, 1509–1510. (b) Ito, Y.; Ihara, E.; Murakami, M.; Sisido, M. *Macromolecules* **1992**, *25*, 6810–6813. (c) Ito, Y.; Kojima, Y.; Murakami, M. *Tetrahedron Lett.* **1993**, *34*, 8279–8282. (d) Ito, Y.; Miyake, T.; Ohara, T.; Suginome, M. *Macromolecules* **1998**, *31*, 1697–1699. (e) Ito, Y.; Miyake, T.; Hatano, S.; Shima, R.; Ohara, T.; Suginome, M. *J. Am. Chem. Soc.* **1998**, *120*, 11880–11893. (f) Ito, Y.; Miyake, T.; Suginome, M. *Macromolecules* **2000**, *33*, 4034–4038. (g) Suginome, M.; Collet, S.; Ito, Y. *Org. Lett.* **2002**, *4*, 351–354. (h) Suginome, M.; Ito, Y. *Adv. Polym. Sci.* **2004**, *177*, 77–136.

(15) (a) Goodwin, A.; Novak, B. M. *Macromolecules* **1994**, *27*, 5520–5522. (b) Schlitzer, D. S.; Novak, B. M. *J. Am. Chem. Soc.* **1998**, *120*, 2196–2197. (c) Tang, H.-Z.; Lu, Y.; Tian, G.; Capracotta, M. D.; Novak, B. M. *J. Am. Chem. Soc.* **2004**, *126*, 3722-3723. (d) Tang, H.-Z.; Novak, B. M.; He, J.; Polavarapu, P. L. *Angew. Chem., Int. Ed.* **2005**, *44*, 7298–7301. (e) Tang, H.-Z.; Boyle, P. D.; Novak, B. M. *J. Am. Chem. Soc.* **2005**, *127*, 2136–2142. (f) Tang, H.-Z. Garland, E. R.; Novak, B. M.; He, J.; Polavarapu, P. L.; Sun, F. C.; Sheiko, S. S. *Macromolecules* **2007**, *40*, 3575–3580.

(16) (a) Green, M. M.; Andreola, C.; Muñoz, B.; Reidy, M. P.; Zero, K. *J. Am. Chem. Soc.* **1988**, *110*, 4063–4065. (b) Green, M. M.; Reidy, M. P.; Johnson, R. J.; Darling, G.; O'Leary, D. J.; Willson, G. *J. Am. Chem. Soc.* **1989**, *111*, 6452–6454. (c) Lifson, S.; Androla, C.; Peterson, N. C.; Green, M. M. *J. Am. Chem. Soc.* **1989**, *111*, 8850–8858. (d) Okamoto, Y.; Matsuda, M.; Nakano, T.; Yashima, E. *J. Polym. Sci., Part A: Polym. Chem.* **1994**, *32*, 309–315. (e) Maeda, K.; Matsuda, M.; Nakano, T.; Okamoto, Y.

Polym. J. **1995**, *27*, 141–146. (f) Müller, M.; Zentel, R. *Macromolecules* **1996**, *29*, 1609–1617. (g) Maeda, K.; Okamoto, Y. *Macromolecules* **1998**, *31*, 1046–1052. (h) Li, J.; Schuster G. B.; Cheon, K.-S.; Green, M. M.; Selinger, J. V. *J. Am. Chem. Soc.* **2000**, *122*, 2603–2612. (i) Mayer, S.; Zentel, R. *Prog. Polym. Sci.* **2001**, *26*. 1973–2013. (j) Mruk, R.; Zentel, R.; *Macromolecules* **2002**, *35*, 185–192. (k) Yoshiba, K.; Hama, R.; Teramoto, A.; Nakamura, N.; Maeda, K.; Okamoto, Y.; Sato, T. *Macromolecules* **2006**, *39*, 3435–3440. (l) Neth, G. Y.; Samal, S.; Park, S.-Y.; Murthy, C. N.; Lee, J.-S. *Macromolecules* **2006**, *39*, 5965–5966. (m) Pijper, D.; Feringa, B. L. *Angew. Chem., Int. Ed.* **2007**, *46*, 3693–3696.

(17) (a) Fujiki, M. *J. Am. Chem. Soc.* **1994**, *116*, 6017–6018. (b) Fujiki, M. *J. Am. Chem. Soc.* **1994**, *116*, 11976–11981. (c) Fujiki, M. *Appl. Phys. Lett.* **1994**, *65*, 3251–3253. (d) Fujiki, M. *J. Am. Chem. Soc.* **1996**, *118*, 7424–7425. (e) Koe, J. R.; Fujiki, M.; Nakashima, H. *J. Am. Chem. Soc.* **1999**, *121*, 9734–9735. (f) Toyoda, S.; Fujiki, M. *Macromolecules* **2001**, *34*, 640–644. (g) Koe, J. R.; Fujiki, M.; Motonaga, M.; Nakashima, H. *Macromolecules* **2001**, *34*, 1082–1089. (h) Terao, K.; Terao, Y.; Teramoto, A.; Nakamura, N.; Terakawa, I.; Sato, T.; Fujiki, M. *Macromolecule* **2001**, *34*, 2682–2685. (i) Terao, K.; Terao, Y.; Teramoto, A.; Nakamura, N.; Fujiki, M.; Sato, T. *Macromolecule* **2001**, *34*, 6519–6525. (j) Fujiki, M. *Macromol. Rapid. Commun.* **2001**, *22*, 539–563. (k) Sato, T.; Terao, K.; Teramoto, A.; Fujiki, M. *Macromolecule* **2002**, *35*, 2141–2148. (l) Sato, T.; Terao, K.; Teramoto, A.; Fujiki, M. *Macromolecule* **2002**, *35*, 5355–5357. (m) Ohira, A.; Kunitake, M.; Fujiki, M.; Naito, M.; Saxena, A. *Chem. Mater.* **2004**, *16*, 3919–3923. (n) Terao, K.; Mori, Y.; Dobashi, T.; Sato, T.; Teramoto, A.; Fujiki, M. *Langmuir* **2004**, *20*, 306-308. (o) Kim, S.-Y.; Fujiki, M.; Ohira, A.; Kwak, G.; Kawakami, Y. *Macromolecules* **2004**, *37*, 4321–4324. (p) Saxena, A.; Guo, G.; Fujiki, M.; Yang, Y.; Ohira, A.; Okoshi, K.; Naito, M. *Macromolecules* **2004**, *37*, 3081–3083.

(18) (a) Yashima, E.; Okamoto, Y. In *Circular Dichroism: Principles and Applications, 2nd ed*.; Berova, N., Nakanishi, K., Woody, R. W., Eds.; John Wiley & Sons, Inc.: New York, 2000; Chapter 18. (b) Schenning, A. P. H. J.; Fransen, M.; Meijer, E. W. *Macromol Rapid Commun*. **2002**, *23*, 266–270. (c) Yashima, E. *Anal. Sci*. **2002**, *18*, 3–6. (d) Lam, J. W. Y.; Tang, B. Z. *Acc. Chem. Res*. **2005**, *38*, 745–754. (e) Aoki, T.; Kaneko, T.; Teraguchi, M. *Polymer* **2006**, *47*, 4867–4892. (f) Masuda, T. *J. Polym. Sci., Part A: Polym. Chem*. **2007**, *45*, 165–180. (g) Rudick, J. G.; Percec, V. *New J. Chem*. **2007**, *31*, 1083–1096. (h) Rudick, J. G.; Percec, V. *Acc. Chem. Res*. **2008**, *41*, 1641–1652.

(19) Yashima, E.; Matsushima, T.; Okamoto, Y. *J. Am. Chem. Soc*. **1995**, *117*, 11596–11597.

(20) (a) Yashima, E.; Matsushima, T.; Okamoto, Y. *J. Am. Chem. Soc*. **1997**, *119*, 6345–6359. (b) Yashima, E.; Maeda, K.; Okamoto, Y. *Nature* **1999**, *399,* 449–451. (c) Saito, M. A.; Maeda, K.; Onouchi, H.; Yashima, E. *Macromolecules* **2000**, *33,* 4316–4318. (d) Maeda, K.; Morino, K.; Okamoto, Y.; Sato, T.; Yashima, E. *J. Am. Chem. Soc*. **2004**, *126*, 4329–4342. (e) Morino, K.; Watase, N.; Maeda, K.; Yashima, E. *Chem. –Eur. J*. **2004**, *10*, 4703–4707. (f) Hasegawa, T.; Morino, K.; Tanaka, Y.; Katagiri, H.; Furusho, Y.; Yashima, E. *Macromolecules* **2006**, *39*, 482–488.

(21) (a) Yashima, E.; Nimura, T.; Matsushima, T.; Okamoto, Y. *J. Am. Chem. Soc*. **1996**, *118*, 9800–9801. (b) Kawamura, H.; Maeda, K.; Okamoto, Y.; Yashima, E. *Chem. Lett*. **2001**, 58–59.

(22) (a) Onouchi, H.; Maeda, K.; Yashima, E. *J. Am. Chem. Soc*. **2001**, *123*, 7441–7442. (b) Onouchi, H.; Kashiwagi, D.; Hayashi, K.; Maeda, K.; Yashima, E. *Macromolecules* **2004**, *37*, 5495–5503. (c) Nishimura, T.; Tsuchiya, K.; Ohsawa, S.; Maeda, K.; Yashima, E.; Nakamura, Y.; Nishimura, J. *J. Am. Chem. Soc*. **2004**, *126*, 11711–11717. (d) Onouchi, H.; Miyagawa, T.; Furuko, A.; Maeda, K.; Yashima, E. *J. Am. Chem. Soc*. **2005**, *127*, 2960–2965. (e) Miyagawa, T.; Furuko, A.; Maeda, K.; Katagiri, H.; Furusho, Y.; Yashima, E. *J. Am. Chem. Soc*. **2005**, *127*, 5018–5019. (f) Onouchi, H.; Hasegawa,

T.; Kashiwagi, D.; Ishiguro, H.; Maeda, K.; Yashima, E. *Macromolecules* **2005**, *38*, 8625–8633. (g) Onouchi, H.; Hasegawa, T.; Kashiwagi, D.; Ishiguro, H.; Maeda, K.; Yashima, E. *J. Polym. Sci., Part A: Polym. Chem.* **2006**, *44*, 5039–5048.

(23) Hasegawa, T.; Maeda, K.; Ishiguro, H.; Yashima, E. *Polym. J.* **2006**, *38*, 912–919.

(24) (a) Yashima, E.; Maeda, Y.; Okamoto, Y. *Chem. Lett.* **1996**, 955–956. (b) Yashima, E.; Maeda, Y.; Matsushima, T.; Okamoto, Y. *Chirality* **1997**, *9*, 593–600. (c) Maeda, K.; Okada, S.; Yashima, E.; Okamoto, Y. *J. Polym. Sci., Part A: Polym. Chem.* **2001**, *39*, 3180–3189.

(25) (a) Nonokawa, R.; Yashima, E. *J. Am. Chem. Soc.* **2003**, *125*, 1278–1283. (b) Nonokawa, R.; Yashima, E. *J. Polym. Sci., Part A: Polym. Chem.* **2003**, *41*, 1004–1013. (c) Nonokawa, R.; Oobo, M.; Yashima, E. *Macromolecules* **2003**, *36*, 6599–6606. (d) Morino, K.; Oobo, M.; Yashima, E. *Macromolecules* **2005**, *38*, 3461–3468. (e) Miyagawa, T.; Yamamoto, M.; Muraki, R.; Onouchi, H.; Yashima, E. *J. Am. Chem. Soc.* **2007**, *129*, 3676–3682.

(26) Ishikawa, M.; Maeda, K.; Yashima, E. *J. Am. Chem. Soc.* **2002**, *124*, 7448–7458.

(27) Ishikawa, M.; Maeda, K.; Mitsutsuji, Y.; Yashima, E. *J. Am. Chem. Soc.* **2004**, *126*, 732–733.

(28) Hase, Y.; Ishikawa, M.; Muraki, R.; Maeda, K.; Yashima, E. *Macromolecules* **2006**, *39*, 6003–6008.

(29) (a) Hase, Y.; Mitsutsuji, Y.; Ishikawa, M.; Maeda, K.; Okoshi, K.; Yashima, E. *Chem. Asian J.* **2007**, *2*, 755–763. (b) Miyabe, T.; Hase, Y.; Iida, H.; Maeda, K.; Yashima, E. *Chirality* **2009**, *21,* 44–50.

(30) Hase, Y. Ph. D Thesis, Graduate School of Engineering, Nagoya University (2007).

(31) (a) Hansma, H. G.; Laney, D. E.; Bezanilla, M.; Sinsheimer, R. L.; Hansma, P. K. *Biophys. J.* **1995**, *68*, 1672-1677. (b) Maeda, Y.; Matsumoto, T.; Tanaka, H.; Kawai, T. *Jpn. J. Appl. Phys.* **1999**, *38*, L1211–L1212. (c) Maaloum, M. *Eur. Biophys. J.* **2003**, *32*, 585–587.

(32) Tanaka, H.; Hamai, C.; Kanno, T.; Kawai, T. *Surface Science* **1999**, *432*, L611–L616.

(33) Kumaki, J.; Sakurai, S.-i.; Yashima, E. *Chem. Soc. Rev. in press*

(34) Shmueli, U.; Traub, W.; Rosenheck, K. *J. Polym. Sci., Part A-2: Polym. Phys.* **1969**, *7*, 515–524.

(35) Miller, R. D.; Farmer, B. L.; Fleming, W.; Sooriyakumaran, R.; Rabolt, J. *J. Am. Chem. Soc.* **1987**, *109*, 2509–2510.

(36) (a) Schilling, F. C.; Lovinger, A. J.; Zeigler, J. M.; Davis, D. D.; Bovey, F. A. *Macromolecules* **1989**, *22*, 3055–3063. (b) Klemann, B.; West, R.; Koutsky, J. A. *Macromolecules* **1993**, *26*, 1042–1046.

(37) Watanabe, J.; Kamee, H.; Fujiki, M. *Polym. J.* **2001**, *33*, 495–497.

(38) Ute, K.; Hirose, K.; Kashimoto, H.; Nakayama, H.; Hatada, K.; Vogl, O. *Polym. J.* **1993**, *25*, 1175–1186.

(39) Ute, K.; Fukunishi, Y.; Niimi, R.; Iwakura, T.; Hatada, K. *Polym. Prep., Jpn.* **1996**, *45*, 3284–8285.

(40) Ito, Y.; Ohara, T.; Shima, R.; Suginome, M. *J. Am. Chem. Soc.* **1996**, *118*, 9188–9189.

(41) Suginome, M.; Noguchi, H.; Murakami, M. *Chem. Lett.* **2007**, *36*, 1036–1037.

(42) Tanatani, A.; Yokoyama, A.; Azumaya, I.; Takakura, Y.; Mitsui, C.; Shiro, M.; Uchiyama, M.; Muranaka, A.; Kobayashi, N.; Yokozawa, T. *J. Am. Chem. Soc.* **2005**, *127*, 8553–8561.

(43) (a) Harada, N.; Nakanishi, K. *Circular Dichroic Spectroscopy–Exciton Coupling in Organic Stereochemistry*; University Science Book: Mill Valley, CA, 1983. (b) Nakanishi, K.; Berova, N. In *Circular Dichroism–Principles and Applications*; Nakanishi, K., Berova, N., Woody, R. W., Eds.; VCH: New York, 1994; Chapter 13.

(44) Takei, F.; Hayashi, H.; Onitsuka, K.; Kobayashi, N.; Takahashi, S. *Angew. Chem., Int. Ed.* **2001**, *40*, 4092–4094.

(45) Tabei, J.; Shiotsuki, M.; Sanda, F.; Masuda, T. *Macromolecules* **2005**, *38*, 9448–9454.

(46) Cornelissen, J. J. L. M.; Sommerdijk, N. A. J. M.; Nolte, R. J. M. *Macromol. Chem. Phys.* **2002**, *203*, 1625–1630.

(47) Beijnen, A. J. M. V.; Nolte, R. J. M.; Drenth, W.; Hezemans, A. M. F. *Tetrahedron* **1976**, *32*, 2017–2019.

(48) Suzuki, Y.; Tabei, J.; Shiotsuki, M.; Inai, Y.; Sanda, F.; Masuda, T. *Macromolecules* **2008**, *41*, 1086–1093.

(49) Kaneko, T.; Umeda, Y.; Yamamoto, T.; Teraguchi, M.; Aoki, T. *Macromolecules* **2005**, *38*, 9420–9426.

(50) Kawauchi, T.; Kumaki, J.; Kitaura, A.; Okoshi, K.; Kusanagi, H.; Kobayashi, K.; Sugai, T.; Shinohara, H.; Yashima, E. *Angew. Chem., Int. Ed.* **2008**, *47*, 515–519.

(51) Aharoni, S. M. *Macromolecules* **1979**, *12*, 94–103.

(52) Aharoni, S. M. *J. Polym. Sci.: Polym. Phys. Ed.* **1979**, *17*, 683–691.

(53) Aharoni, S. M. *J. Macromol. Sci. –Phys.* **1982**, *B21*, 105–129.

(54) Bieglé, A.; Mathis, A.; Galin, J.-C. *Macromol. Chem. Phys.* **2000**, *201*, 113–125.

(55) (a) Cornelissen, J. J. L. M.; Donners, J. J. J. M.; de Gelder, R.; Graswinckel, W. S.; Metselaar, G. A.; Rowan, A. E.; Sommerdijk, N. A. J. M.; Nolte, R. J. M. *Science* **2001**, *293*, 676–680. (b) Cornelissen, J. J. L. M.; Graswinckel, W. S.; Rowan, A. E.; Sommerdijk, N. A. J. M.; Nolte, R. J. M. *J. Polym Sci., Part A: Polym. Chem.* **2003**, *41*, 1725–1736. (c) Metselaar, G. A.; Wezenberg, S. J.; Cornelissen, J. J. L. M.; Nolte, R. J. M.; Rowan, A. E. *J. Polym. Sci., Part A: Polym. Chem.* **2007**, *45*, 981–988.

(56) Wezenberg, S. J.; Metselaar, G. A.; Rowan, A. E.; Cornelissen, J. J. L. M.; Seebach, D.; Nolte, R. J. M. *Chem. –Eur. J.* **2006**, *12*, 2778–2786.

(57) Kajitani, T.; Okoshi, K.; Sakurai, S.-i.; Kumaki, J.; Yashima, E. *J. Am. Chem. Soc.* **2006**, *128*, 708–709.

(58) Onouchi, H.; Okoshi, K.; Kajitani, T.; Sakurai, S.-i.; Nagai, K.; Kumaki, J.; Onitsuka, K.; Yashima, E. *J. Am. Chem. Soc.* **2008**, *130*, 229–236.

(59) Kim, J.; Novak, B. M.; Waddon, A. J. *Macromolecules* **2004**, *37*, 1660–1662.

(60) Kim, J.; Novak, B. M.; Waddon, A. J. *Macromolecules* **2004**, *37*, 8286–8292.

(61) Tian, G.; Lu, Y.; Novak, B. M. *J. Am. Chem. Soc.* **2004**, *126*, 4082–4083.

(62) Ito, Y.; Ihara, E.; Uesaka, T.; Murakami, M. *Macromolecules* **1992**, *25*, 6711–6713.

(63) Hoshikawa, N.; Yamamoto, C.; Hotta, Y.; Okamoto, Y. *Polym. J.* **2006**, *38*, 1258–1266.

(64) (a) Rabolt, J. F.; Hofer, D.; Miller, R. D.; Fickes, G. N. *Macromolecules* **1986**, *19*, 611–616. (b) Lovinger, A. J.; Schilling, F. C.; Bovey, F. A.; Zeigler, J. M. *Macromolecules* **1986**, *19*, 2657–2660. (c) Weber, P.; Guillon, D.; Skoulios, A.; Miller, R. D. *J. Phys. France* **1989**, *50*, 793–801.

(65) Asuke, T.; West, R. *Macromolecules* **1991**, *24*, 343–344.

(66) (a) Okoshi, K.; Kamee, H.; Suzaki, G.; Tokita, M.; Fujiki, M.; Watanabe, J. *Macromolecules* **2002**, *35*, 4556–4559. (b) Okoshi, K.; Saxena, A.; Naito, M.; Suzaki, G.; Tokita, M.; Watanabe, J.; Fujiki, M. *Liq. Cryst.* **2004**, *31*, 279–283. (c) Okoshi, K.; Saxena, A.; Fujiki, M.; Suzaki, G.; Watanabe, J.; Tokita, M. *Mol. Cryst. Liq. Cryst.* **2004**, *419*, 57–68.

(67) Oka, H.; Suzaki, G.; Edo, S.; Suzuki, A.; Tokita, M.; Watanabe, J. *Macromolecules* **2008**, *41*, 7783–7786.

(68) Aharoni, S. M. *J. Polym. Sci., Polym. Phys. Ed.* **1980**, *18*, 1303–1310.

(69) (a) Green, M. M.; Zanella, S.; Gu, H.; Sato, T.; Gottarelli, G.; Jha, S. K.; Spada, G. P.; Schoevaars, A. M.; Feringa, B.; Teramoto, A. *J. Am. Chem. Soc.* **1998**, *120*, 9810–9817. (b) Tang, K.; Green, M. M.; Cheon, K. S.; Selinger, J. V.; Garetz, B. A. *J. Am. Chem. Soc.* **2003**, *125*, 7313–7323. (c) Pijper, D.; Jongejan, M. G. M.; Meetsma, A.; Feringa, B. L. *J. Am. Chem. Soc.* **2008**, *130*, 4541–4552.

(70) Sato, T.; Sato, Y.; Umemura, Y.; Teramoto, A.; Nagamura, Y.; Wagner, J.; Weng, D.; Okamoto, Y.; Hatada, K.; Green, M. M. *Macromolecules* **1993**, *26*, 4551-4559.

(71) (a) Maxein, G.; Keller, H.; Novak, B. M.; Zentel, R. *Adv. Mater.* **1998**, *10*, 341–345. (b) Maxein, G.; Mayer, S.; Zentel, R. *Macromolecules* **1999**, *32*, 5747–5754.

(72) Maeda, K.; Takeyama, Y.; Sakajiri, K.; Yashima, E. *J. Am. Chem. Soc.* **2004**, *126*, 16284–16285.

(73) (a) Okoshi, K.; Sakajiri, K.; Kumaki, J.; Yashima, E. *Macromolecules* **2005**, *38*, 4061–4064. (b) Okoshi, K.; Sakurai, S.-i.; Ohsawa, S.; Kumaki, J.; Yashima, E. *Angew. Chem., Int. Ed.* **2006**, *45*, 8173–8176. (c) Okoshi, K.; Kajitani, T.; Nagai, K.; Yashima, E. *Macromolecules* **2008**, *41*, 258-261.

(74) Sakurai, S.-i.; Ohsawa, S.; Nagai, K.; Okoshi, K.; Kumaki, J.; Yashima, E. *Angew. Chem., Int. Ed.* **2007**, *46*, 7605–7608.

(75) Yamakawa, H. *Helical Wormlike Chains in Polymer Solutions*; Springer: Berlin, 1997.

(76) (a) Khokhlov, A. R.; Semenov, A. N. *Physica A* **1981**, *108*, 546–556. (b) Khokhlov, A. R.; Semenov, A. N. *Physica A* **1982**, *112*, 605–614.

(77) Sato, T.; Teramoto, A. *Adv. Polym. Sci.* **1996**, *126*, 85–161.

(78) Godfrey, J. E.; Einsenberg, H. *Biophys. Chem.* **1976**, *5*, 301–318.

(79) Saito, T.; Iso, N.; Mizuno, H,; Onda, N.; Yamato, H.; Odashima, H. *Biopolymers* **1982**, *21*, 715–728.

(80) (a) Yanai, T.; Norisuye, T.; Fujita, H. *Macromolecules* **1980**, *13*, 1462–1466. (b) Kashiwagi, Y.; Norisuye, T.; Fujita, H. *Macromolecules* **1981**, *14*, 1220–1225.

(81) Green, M. M.; Gross, R. A.; Schilling, F. C.; Zero, K.; Crosby, C. I. *Macromolecules* **1988**, *21*, 1839–1846.

(82) Samorí, P.; Ecker, C.; Gössl, I.; de Witte, P. A. J.; Cornelissen, J. J. L. M.; Metselaar, G. A.; Otten, M. B. J.; Rowan, A. E.; Nolte, R. J. M.; Rabe, J. P. *Macromolecules* **2002**, *35*, 5290–5294.

(83) Nieh, M.-P.; Goodwin, A. A.; Stewart, J. R.; Novak, B. M.; Hoagland, D. A. *Macromolecules* **1998**, *31*, 3151–3154.

(84) Cotts, P. M.; Ferline, S.; Dagli, G.; Pearson, D. S. *Macromolecules* **1991**, *24*, 6730–6735.

(85) Natsume, T.; Wu, L.; Sato, T.; Terao, K.; Teramoto, A.; Fujiki, M. *Macromolecules* **2001**, *34*, 7899–7904.

(86) (a) Conio, G.; Bianchi, E.; Ciferri, A.; Krigbaum, W. R. *Macromolecules* **1984**, *17*, 856–861. (b) Itou, T.; Chikiri, H.; Teramoto, A.; Aharoni, S. M. *Polym. J.* **1988**, *20*, 143–151.

(87) Murakami, H.; Norisuye, T.; Fujita, H. *Macromolecules* **1980**, *13*, 345–352.

(88) Kuwata, M.; Murakami, H.; Norisuye, T.; Fujita, H. *Macromolecules* **1984**, *17*, 2731–2734.

(89) Gu, H.; Nakamura, Y.; Sato, T.; Teramoto, A.; Green, M. M.; Andreola, C. *Polymer* **1999**, *40*, 849–856.

(90) Bellomo, E. G.; Davidson, P.; Impéror-Clerc, M.; Deming, T. J. *J. Am. Chem. Soc.* **2004**, *126*, 9101–9105.

(91) Kajitani, T.; Okoshi, K.; Yashima, E. *Macromolecules* **2008**, *41*, 1601–1611.

(92) (a) Hoshikawa, N.; Hotta, Y.; Okamoto, Y. *J. Am. Chem. Soc.* **2003**, *125*, 12380–12381. (b) Azam, A. K. M. F.; Kamigaito, M.; Okamoto, Y. *Polym. J.* **2006**, *38*, 1035–1042.

Chapter 1

Helicity Induction and Chiral Amplification in a Poly(phenylacetylene) Bearing *N*,*N*-Diisopropylaminomethyl Groups with Chiral Acids in Water

Abstract: A water soluble, hydrochloride of a stereoregular poly(phenylacetylene) bearing an *N*,*N*-diisopropylaminomethyl group (poly-**1**-HCl) as the pendant was found to form a predominantly one-handed helix upon complexation with various chiral acids including aromatic and aliphatic carboxylic acids, phosphoric and sulfonic acids, and amino acids through noncovalent bonding interactions in water. The complexes exhibited an induced circular dichroism (ICD) in the UV-visible region of the polymer backbone. The Cotton effect signs were the same when chiral carboxylic acids with the same absolute configurations were used. In sharp contrast to the helix induction in the neutral poly-**1** with chiral acids in organic solvents, the charged poly-**1**-HCl is highly sensitive to the chirality of the acids and can detect a small enantiomeric imbalance in the chiral acids in water.

Introduction

Chiral acids including phosphoric and sulfonic acids as well as carboxylic acids and amino acids are the particularly common and important structural units in many natural products and drug molecules,[1] and therefore, the development of convenient and accurate methodologies for the detection and assignments of the chirality of chiral acids and determination of their enantiomeric compositions have attracted significant interest. Various types of chiral[2,3] or achiral[4] host molecules, in particular for chiral carboxylic acids, have been prepared. Chiral host molecules composed of optically active and fluorescent receptor units are often used to sense the chiral carboxylic acids because of the high sensitivity inherent to fluorescence spectroscopy.[2] Circular dichroism (CD) spectroscopy is also a powerful tool for chirality sensing, particularly when a host molecule is achiral, and chromophoric. The noncovalent bonding to a chiral, non-racemic guest provides a characteristic induced CD (ICD) in the absorption region of the achiral receptors; the Cotton effect sign can be used to determine the absolute configuration of the guest molecules.[4,5]

In a series of studies, Yashima and co-workers reported the helicity induction in optically inactive, stereoregular *cis-transoidal* poly(phenylacetylene)s bearing functional groups such as carboxy,[6] phosphonate,[7] boronate,[8] and amino groups,[9] or bulky crown ethers as the pendants,[10] which can change their structures into the prevailing, dynamic one-handed helices upon complexation with specific chiral guests, and their complexes show a characteristic ICD in the UV-visible region of the polymer backbones. The Cotton effect signs corresponding to the helical sense can be used as a novel probe for the chirality assignments of the guest molecules.[11] Helical polyacetylenes are very sensitive to chiral stimuli and exhibit optical activity due to a one-handed helicity of the polymer main chains through a significant amplification of chirality with high cooperativity, which is a unique feature of dynamic helical polyacetylenes.[12,13] For instance, the introduction of bulky crown ethers as the pendants in poly(phenylacetylene)s backbones produced dynamic helical polymers which can respond to the chirality of nearly racemic amino acids and amino

alcohols in organic solvents with high sensitivity without derivatization.[10]

On the other hand, a number of chiral receptor molecules has been prepared for chiral or chirality recognition, but almost all host molecules prepared so far work in organic solvents, and the chiral recognition of charged chiral molecules in water with charged, water soluble chiral hosts remains very difficult.[14] Because small electrolytes completely dissociate into free ions in water by hydration, attractive electrostatic and hydrogen bonding interactions are hindered in water.[15] In sharp contrast, polyelectrolytes, such as nucleic acids, are completely different from small electrolytes; that is, a portion of the counterions are bound to polyelectrolytes with a sufficiently high charge density, and therefore, polyelectrolytes can effectively interact with small charged biomolecules even in water.[16] On the basis of these considerations, Yashima et al. recently found that a charged polyelectrolyte consisting of a chromophoric polyacetylene backbone and benzoic acid or phenylphosphonic acid as the pendant could interact with a variety of charged chiral biomolecules including amines, amino alcohols, amino acids, aminosugars, and peptides in water.[17] The complexes form supramolecular assemblies with a controlled helicity and exhibit a characteristic ICD without derivatization in water. These polyelectrolytes possess negatively charged functional groups as the pendants and can efficiently detect the chirality of positively charged chiral guest molecules.

In the present study, the author investigated the helicity induction and chiral amplification of an optically inactive, positively charged polyacetylene, the hydrochloride of poly(4-(*N*,*N*-diisopropylaminomethyl)phenylacetylene) (poly-**1**-HCl) (Chart 1-1), in water with various chiral acids including phosphoric and sulfonic acids and amino acids as well as carboxylic acids by CD spectroscopy to develop a novel helical polymer capable of sensing chiral acids in water. The neutral poly-**1** was already reported to show an ICD in the UV-visible region due to the helix formation in the presence of chiral carboxylic acids in organic solvents.[9a,b] However, the neutral poly-**1** is not sensitive to the chirality of chiral acids in organic solvents and requires a large excess amount of chiral acids to exhibit a full ICD. Very

recently, Yashima et al. also found that poly-**1**-HCl formed a predominantly one-handed helix induced by a small amount of a chiral acid as the dopant in water, thus showing a characteristic ICD in the UV-visible region. Moreover, the complex was found to form a lyotropic cholesteric liquid crystalline phase in concentrated water solutions and the helix sense excess of the polymer backbone was significantly amplified through interchain interactions in a lyotropic cholesteric state compared to that in a dilute solution.[18] However, a detailed investigation of the helix induction and chiral amplification of poly-**1**-HCl with various chiral acids in dilute water solution have not yet been reported.

Chart 1-1. Structures of Poly-**1**-HCl and Chiral Carboxylates

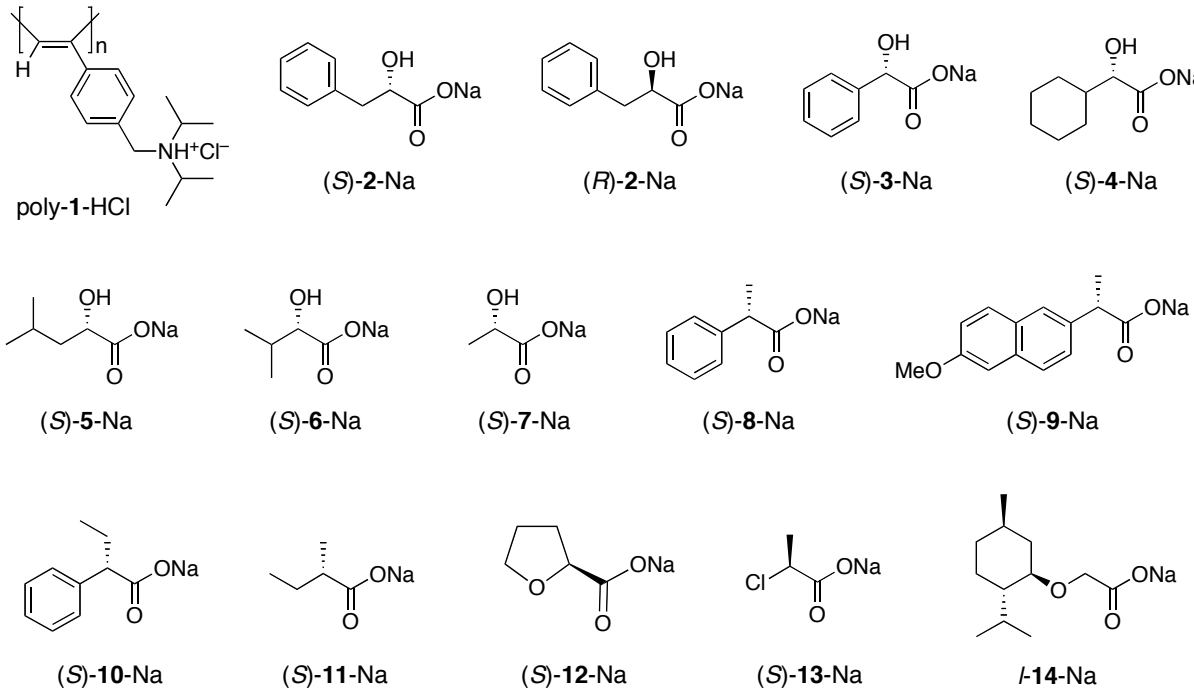

Results and Discussion

CD Studies on Helix Induction of Poly-1-HCl with Chiral Acids in Water. Figure 1-1 shows the typical CD and absorption spectra of poly-**1**-HCl in the presence of the sodium salts of (*R*)- and (*S*)-phenyl lactic acid (**2**-Na) (0.5 equiv to monomer units of poly-**1**-HCl) in water. The complexes showed mirror images of the split-type intense ICDs in the polymer backbone region. A similar helicity induction on optically inactive polymers and oligomers through intermolecular chiral interactions has been reported.[19] The ICD magnitude slightly increased with the decreasing temperature (Table 1-1). These results indicate that poly-**1**-HCl can form a predominantly one-handed helix upon noncovalent complexation with the chiral acids in water. The CD titration experiments using (*S*)-**2**-Na in water (pH 4.9—5.4) at 25 and 0 °C were then carried out. The ICD intensities of the second Cotton ($\Delta\varepsilon_{2nd}$) increased with the increasing concentration of (*S*)-**2**-Na and reached an almost constant value at [(*S*)-**2**-Na]/[poly-**1**-HCl] = 0.3 (Figure 1-2). The CD titration data were then analyzed to estimate the binding constant (*K*). Plots of the $\Delta\varepsilon_{2nd}$ values of poly-**1**-HCl as a function of the concentrations of (*S*)-**2**-Na gave a saturation binding isotherm. The Hill plot analysis of the data resulted in apparent binding constants (*K*s) of 1.9×10^4 and 2.9×10^4 (M^{-1}) at 25 and 0 °C, respectively.[20] Poly-**1**-HCl exhibited apparent ICDs even with 0.001 equiv of (*S*)-**2**-Na (Figure 1-2, inset). A very small chiral bias in the monomeric diisopropylaminomethyl units of poly-**1**-HCl complexed with (*S*)-**2**-Na is significantly amplified to induce the same helix sense on the major free monomeric units. In sharp contrast, the neutral poly-**1** required a large amount of chiral acids (> 500 equiv) to induce a full ICD in organic solvents, such as tetrahydrofuran (THF).[9a,b] A similar and strong chiral amplification was observed for crown ether-bound poly(phenylacetylene)s in organic solvents.[10] However, the neutral polyacetylenes were not sensitive to the chirality in water,[21] suggesting that the polyelectrolyte function of the poly-**1**-HCl is essential for a powerful chirality-sensing probe with a high sensitivity in water.

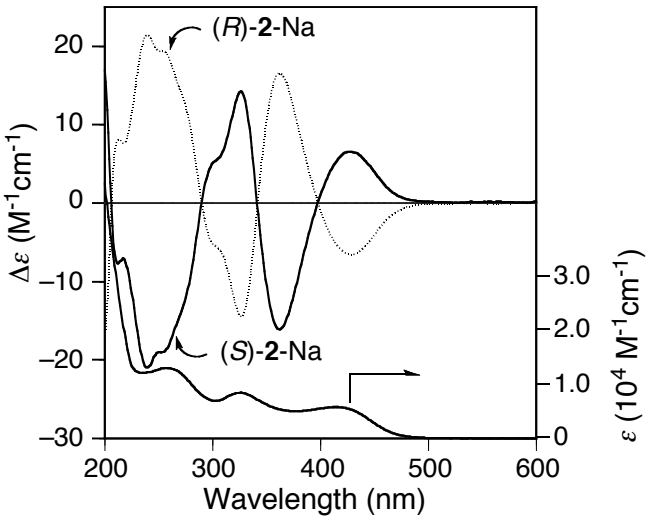

Figure 1-1. CD spectra of poly-**1**-HCl with (*S*)- and (*R*)-**2**-Na in water at room temperature. The absorption spectrum of poly-**1**-HCl with (*S*)-**2**-Na at room temperature is also shown. The concentration of poly-**1**-HCl is 1.0 mg (4.0 μmol monomer units)/mL. [**2**-Na]/[poly-**1**-HCl] = 0.5.

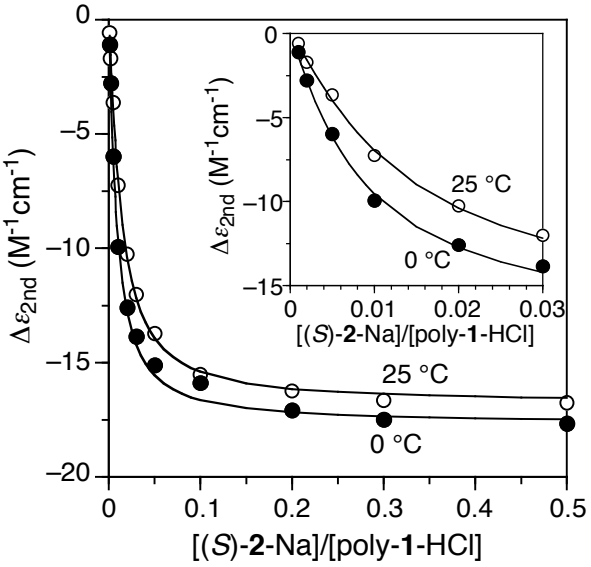

Figure 1-2. Titration curves of poly-**1**-HCl ($\Delta\varepsilon_{2nd}$) with (*S*)-**2**-Na in water (pH 4.9—5.4) at 25 and 0 °C. Inset shows expanded detail of the titration curves. Curves in the plots were the calculated ones using $K = 1.9 \times 10^4$ and 3.0×10^4 at 25 and 0 °C, respectively.

Table 1-1. Signs and Difference in Exciton Coefficient of the Second Cotton ($\Delta\varepsilon_{2nd}$) for the Complexes of Poly-**1**-HCl with Chiral Carboxylates in Water[a]

			second Cotton [λ (nm) and $\Delta\varepsilon_{2nd}$ ($M^{-1}cm^{-1}$)]		
			25 °C	10 °C	0 °C
guest	pH	sign	$\Delta\varepsilon$ (λ)	$\Delta\varepsilon$ (λ)	$\Delta\varepsilon$ (λ)
(*S*)-**2**-Na	5.1	–	15.04 (361)	15.63 (361)	15.88 (361)
(*R*)-**2**-Na	5.2	+	14.75 (361)	15.45 (361)	15.67 (361)
(*S*)-**3**-Na	5.3	–	14.38 (361)	15.19 (361)	15.42 (362)
(*S*)-**4**-Na	5.4	–	15.85 (361)	16.30 (361)	16.42 (361)
(*S*)-**5**-Na	5.3	–	13.49 (361)	14.29 (362)	14.50 (362)
(*S*)-**6**-Na	5.3	–	7.33 (361)	8.87 (361)	9.20 (361)
(*S*)-**7**-Na	5.3	–	4.23 (361)	5.14 (361)	5.38 (361)
(*S*)-**8**-Na	5.1	–	10.43 (362)	11.73 (362)	11.93 (362)
(*S*)-**9**-Na	5.0	–	3.99 (362)	8.60 (363)	10.91 (364)
(*S*)-**10**-Na	5.1	–	13.17 (362)	14.48 (363)	14.83 (363)
(*S*)-**11**-Na	5.4	–	3.04 (361)	3.88 (360)	3.92 (361)
(*S*)-**12**-Na	5.5	–	1.08 (362)	1.27 (362)	1.29 (362)
(*S*)-**13**-Na	5.3	–	11.83 (361)	12.88 (361)	13.23 (362)
l-**14**-Na	4.9	+	14.93 (362)	15.20 (362)	15.02 (362)

[a] The concentration of poly-**1**-HCl is 1.0 mg/mL, and [guest]/[poly-**1**-HCl] = 0.1.

The magnitude of the ICDs was influenced by the pH and salt (NaCl) concentration (Figure 1-3). The ICD magnitude dramatically decreased with a decrease in the pH in the region of pH < 4. Moreover, the addition of a small amount of aqueous 0.1 N NaOH resulted in precipitation of the polymer (pH > 6), which means that the generation of free diisopropylaminomethyl pendants remarkably reduces the solubility of the polymer in water due to the highly hydrophobic nature of the pendant. The addition of an achiral salt, such as NaCl, caused a decrease in the ICD magnitude. These results indicate that the nature of the interaction between poly-**1**-HCl and chiral acids may be mainly ionic rather than hydrophobic in water.

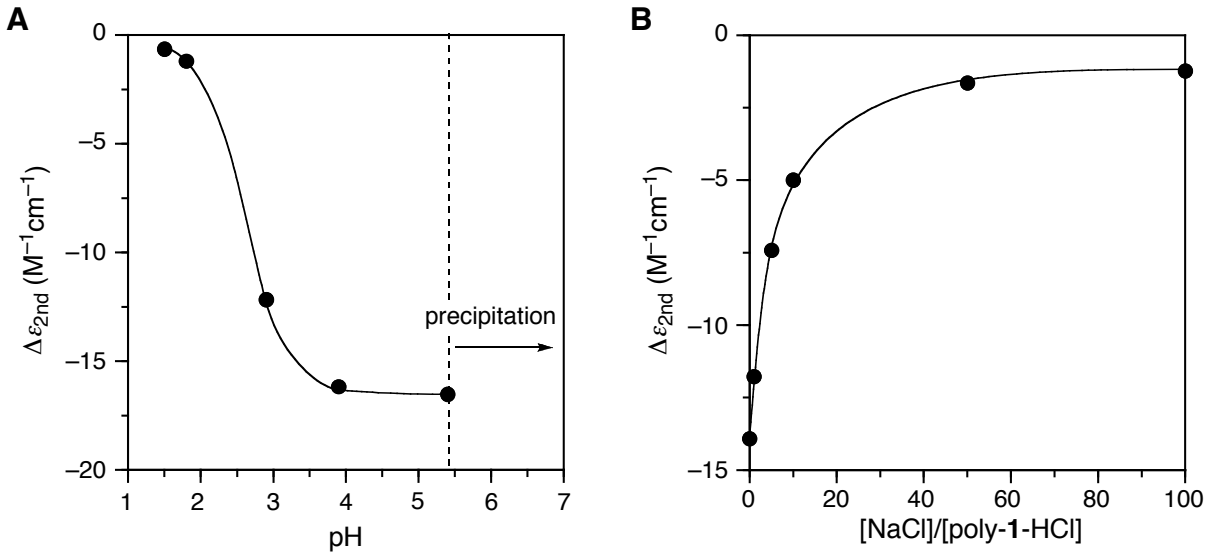

Figure 1-3. (A) pH dependence of ICD intensity ($\Delta\varepsilon_{2nd}$) in the complexation of poly-**1**-HCl (1.0 mg/mL) with (*S*)-**2**-Na ([(*S*)-**2**-Na]/[poly-**1**-HCl] = 0.5) in water at 25 °C. The pH was adjusted with 1 N HCl and 0.1 N HCl at room temperature. (B) Dependence of ICD intensity ($\Delta\varepsilon_{2nd}$) on NaCl concentration for the poly-**1**-HCl—(*S*)-**2**-Na in water at 25 °C. [(*S*)-**2**-Na]/[poly-**1**-HCl] = 0.1.

The results of the ICD studies for the complexes with other chiral aromatic and aliphatic carboxylates as well as α-hydroxy acid salts (Chart 1-1) are summarized in Table 1-1. The charged poly-**1**-HCl showed split-type ICDs in the presence of a very small amount of chiral α-hydroxy acid salts (**2**-Na—**7**-Na) ([α-hydroxy acid salt]/[poly-**1**-HCl] = 0.1) in water. The magnitude of the Cotton effects appears to reflect the bulkiness of the α-hydroxy acids and likely increased with an increase in the bulkiness of the chiral acids in the order of **2**-Na, **3**-Na, **4**-Na > **5**-Na > **6**-Na > **7**-Na. As previously reported, the neutral poly-**1** exhibited almost no or very weak ICDs in the presence of an excess of chiral carboxylic acids in organic solvents such as THF, whereas it showed moderate or weak ICDs in the presence of an excess of chiral α-hydroxy acids such as (*S*)-**3**.[9b] In organic solvents, the chelation-type complexation of the hydroxy group of the α-hydroxy acids to the amino group of poly-**1** together with the acid—base interaction was considered to be important for the appearance of the ICDs.[9] In water,

however, poly-**1**-HCl showed ICDs in the presence of a small amount of chiral carboxylates without an α-hydroxy group (**8**-Na—**14**-Na) ([carboxylate]/[poly-**1**-HCl] = 0.1). These results suggest that the additional intermolecular hydrogen bonding of the hydroxy group seems to be no longer essential for the helicity induction on the charged poly-**1**-HCl with chiral acids in water. The ICD magnitude of the poly-**1**-HCl—chiral carboxylate complexes also tends to increase with an increase in the bulkiness of the carboxylates at 25 °C, except for **9**-Na and **13**-Na. There was a good relation between the Cotton effect signs of the complexes and the absolute configurations of the chiral acids. The complexes showed the same Cotton effect signs if the absolute configurations of the chiral acids (**2**—**13**) are the same. Therefore, the induced Cotton effect signs corresponding to the helix sense of poly-**1**-HCl can be utilized for the chirality assignments of chiral carboxylic acids in water.

Poly-**1**-HCl also responded to other chiral acids, such as phosphoric (**15**-Na—**20**-Na, **21**-K, DNA) and sulfonic acids ((*R*)-**22**) and a bile acid (**23**-Na) (Chart 1-2), in water, and exhibited similar ICDs in their patterns in the UV-visible region (Table 1-2). As for chiral phosphoric acids, four ribonucleotides (**15**-Na—**18**-Na) with the same D-ribofuranoside residue were used in order to investigate whether poly-**1**-HCl could exhibit an ICD reflecting the difference in the nucleobases. Interestingly, poly-**1**-HCl complexed with guanosine 5'-monophosphate (**16**-Na) exhibited an opposite ICD pattern compared with those of the complexes with other nucleotides (**15**-Na, **17**-Na, and **18**-Na). A similar nucleobase-specific CD inversion has also been observed for the complexation of poly((4-dihydroxyborophenyl)acetylene) with **16**-Na among four ribonucleotides in water,[8b] although the mechanism for the nucleobase-selective inversion of the ICD is not clear. Among four ribonucleotides, **17**-Na showed a relatively weak ICD. These results indicate that the ribonucleotide bases play a critical role in the helix sense control of poly-**1**-HCl, and poly-**1**-HCl may be used as a probe for a sensory system of ribonucleotide base recognition by using CD spectroscopy.

Chart 1-2. Structures of Various Chiral Acids

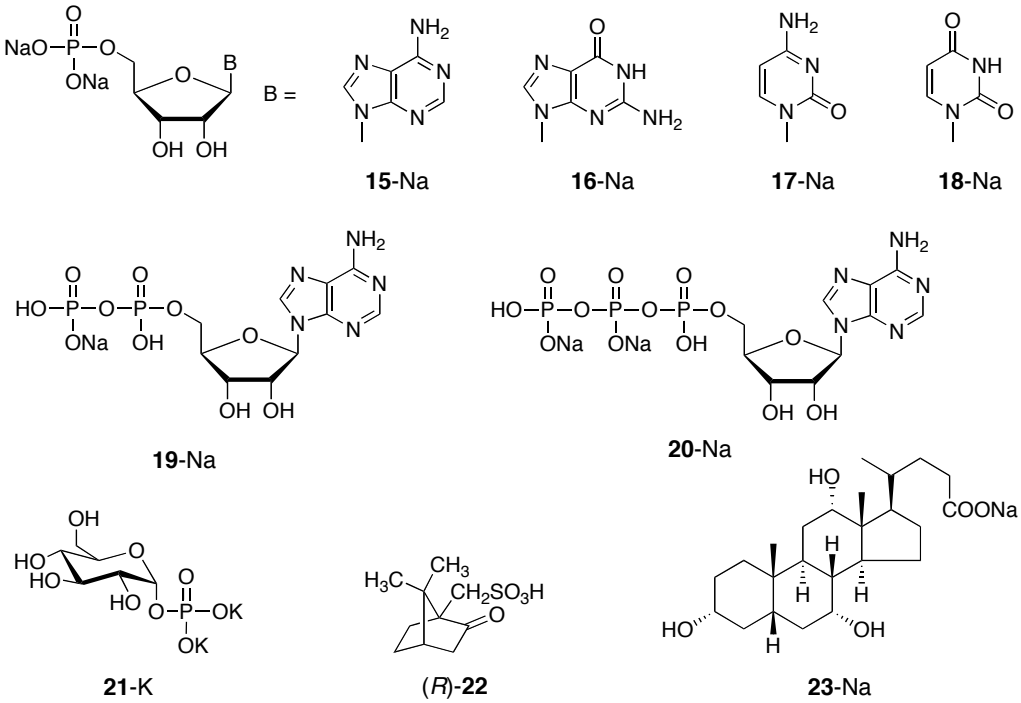

Nucleotides exist as di- and triphosphate types in nature. For example, adenosine can be isolated as 5'-diphosphate (ADP, **19**-Na) and 5'-triphosphate (ATP, **20**-Na) as well as 5'-monophosphate (AMP, **15**-Na), and ATP—ADP interconversion plays an important role in biological processes as a major energy source. The author then investigated the effect of the type of anionic phosphate residues on the helicity induction in the cationic poly-**1**-HCl using **15**-Na, **19**-Na, and **20**-Na as the helix inducer (Table 1-2). The magnitude of the observed ICDs increased in the following order: triphosphate (**20**-Na) > diphosphate (**19**-Na) > monophosphate (**15**-Na), indicating that the multiple interactions between the phosphoric acid residues and the positively charged pendants of poly-**1**-HCl appear to be favorable for the induction of helicity with an excess one-handedness in poly-**1**-HCl. The positively charged poly-**1**-HCl can also interact with the negatively charged DNA from salmon testes to give an apparent ICD without precipitation of the complex at a low DNA concentration ([DNA] < 0.01 mg/mL). A bile acid **23**-Na with remote stereogenic centers also produced a weak ICD (Table 1-2).

Table 1-2. Signs and Difference in Exciton Coefficient of the Second Cotton ($\Delta\varepsilon_{2nd}$) for the Complexes of Poly-**1**-HCl with Chiral Phosphoric and Sulfonic Acids in Water[a]

			second Cotton [λ (nm) and $\Delta\varepsilon_{2nd}$ (M^{-1} cm^{-1})]		
			25 °C	10 °C	0 °C
guest	pH	sign	$\Delta\varepsilon$ (λ)	$\Delta\varepsilon$ (λ)	$\Delta\varepsilon$ (λ)
phosphoric acid					
15-Na	5.3	+	8.09 (361)	9.67 (361)	10.17 (361)
16-Na	5.3	–	12.41 (361)	12.49 (362)	12.17 (362)
17-Na	5.6	+	5.36 (363)	7.39 (362)	8.13 (362)
18-Na	5.6	+	10.27 (362)	12.34 (362)	12.87 (362)
19-Na	4.9	+	13.66 (361)	14.81 (361)	15.14 (361)
20-Na	4.2	+	13.90 (361)	15.40 (361)	15.62 (361)
21-K	5.5	+	0.49 (361)	0.69 (364)	0.75 (361)
DNA[b]	5.7	–	0.12 (360)	0.13 (360)	0.14 (361)
sulfonic acid					
(*R*)-**22**	4.4	–	15.42 (359)	15.87 (360)	15.87 (360)
bile acid					
23-Na	5.8	–	0.19 (357)	0.14 (357)	0.12 (363)

[a] The concentration of poly-**1**-HCl is 1.0 mg/mL, and [guest]/[poly-**1**-HCl] = 0.1. [b] The concentration of salmon DNA is 0.01 mg/mL.

Amino acids are also important optically active biomolecules, and can complex with poly-**1**-HCl, thus showing characteristic ICDs. The ICD results for the complexes of poly-**1**-HCl with several amino acids and its derivatives and some chiral alcohols (Chart 1-3) are summarized in Table 1-3. The complexes with amino acids exhibited rather weak ICDs except for tryptophan (Trp) and phenylalanine (Phe) bearing bulky aromatic substituents compared with those with chiral carboxylic acids even at 0 °C. The electrostatic repulsions between the positively charged pendants of poly-**1**-HCl and the ammonium ion of the amino acids may disturb the attractive interaction because amino acids exist in the twitter ionic form in the pH region where the CD measurements were performed (3.7 < pH < 5.3). Therefore, *N*-protected amino acids with Boc groups resulted in a dramatic increase in the ICD intensities.

Chart 1-3. Structures of Amino Acids and Chiral Alcohols

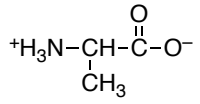

L-Ala

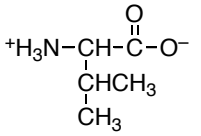

L-Val

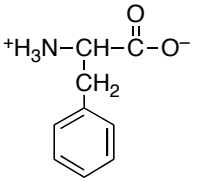

L-Phe

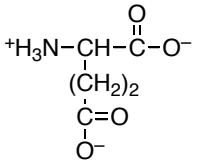

L-Glu

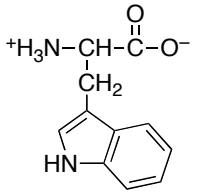

L-Trp

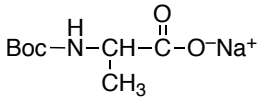

N-Boc-L-Ala-Na

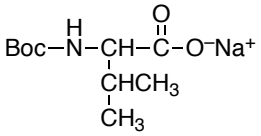

N-Boc-L-Val-Na

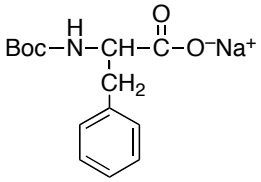

N-Boc-L-Phe-Na

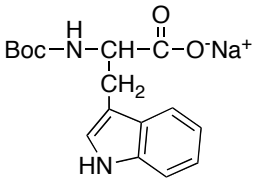

N-Boc-L-Trp-Na

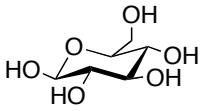

L-**24**

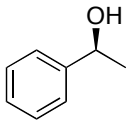

(*S*)-**25**

(*S*)-**26**

As for the relationship between the observed Cotton effect signs and the absolute configurations of the amino acids, there is a good relationship for the *N*-Boc amino acids, although such a relationship could not be observed for the free amino acids. For L-Phe, the Cotton effect sign became inverted from positive to negative at 0 °C, but the reason for this change is not clear at present.

Table 1-3. Signs and Difference in Exciton Coefficient of the Second Cotton ($\Delta\varepsilon_{2nd}$) for the Complexes of Poly-**1**-HCl with L-Amino Acids and Chiral Alcohols in Water[a]

			second Cotton [λ (nm) and $\Delta\varepsilon_{2nd}$ (M^{-1} cm^{-1})]			
				25 °C	10 °C	0 °C
guest	[guest]/ [poly-**1**-HCl]	pH	sign	$\Delta\varepsilon$ (λ)	$\Delta\varepsilon$ (λ)	$\Delta\varepsilon$ (λ)
amino acid						
L-Ala	100	5.3	–	0.37 (363)	0.46 (361)	0.48 (363)
	0.1	5.1	–	*b*	*b*	0.10 (358)
L-Phe	40	5.1	*c*	+5.08 (362)	+0.64 (361)	–4.55 (361)
	0.1	5.2	+	*b*	*b*	0.095 (360)
L-Glu	5	3.7	–	*b*	*b*	0.10 (365)
L-Val	0.1	5.1	–	*b*	*b*	0.076 (367)
L-Trp	7	5.2	+	9.13 (362)	11.1 (362)	12.1 (362)
	0.1	5.2	+	0.22 (360)	0.41 (360)	0.46 (359)
N-Boc-L-Ala	0.1	4.7	–	3.81 (362)	4.27 (362)	4.25 (362)
N-Boc-L-Val-Na	0.1	5.1	–	0.69 (361)	1.44 (361)	1.77 (361)
N-Boc-L-Phe-Na	0.1	5.0	–	9.84 (361)	11.72 (361)	12.38 (361)
N-Boc-L-Trp-Na	0.1	5.3	–	12.56 (361)	12.73 (361)	12.53 (361)
alcohol						
L-**24**	10	5.3	–	0.061 (363)	0.070 (367)	0.076 (364)
(*S*)-**25**	10	5.3	–	10.25 (362)	11.01 (362)	11.01 (362)
	1	4.0	–	1.71 (363)	2.36 (363)	2.48 (363)
(*S*)-**26**	10	5.6	–	0.93 (361)	1.11 (360)	1.11 (360)

[a] The concentration of poly-**1**-HCl is 1.0 mg/mL. [b] No distinctive CD. [c] The Cotton effect sign was inverted depending on temperatures

Aromatic amino acids, such as Trp and Phe, induced a particularly intense ICD among the tested amino acids without protection of the amino group. In this case, not only the electrostatic attractive interaction, but also the hydrophobic interaction might play an important role in the helicity induction on poly-**1**-HCl in water. Recently, Yashima et al. reported that poly(phenylacetylene)s bearing crown ether pendants also exhibited intense ICDs in the presence of aromatic amino acids, Trp and Phe, as well as an aromatic alcohol **25** in water, and the hydrophobic interaction between the polymers and these chiral guests functions as a chiral bias for inducing an excess one-handed helicity in water.[21] The author then investigated the importance of the hydrophobic interaction for helicity induction in poly-**1**-HCl using chiral neutral alcohols (L-**24**, (*S*)-**25**, and (*S*)-**26** in Chart 1-3) having no negatively charged groups capable of interacting with poly-**1**-HCl through electrostatic interactions as a helix inducer. Among these chiral alcohols, an aromatic alcohol (*S*)-**25** gave an intense ICD, which suggests that poly-**1**-HCl can also be used to detect the chirality of chiral neutral molecules through hydrophobic interactions in water.

Chiral Amplification and Nonlinear Effects in Water. Previously, Yashima et al. reported that the complex formation of poly(phenylacetylene)s bearing carboxy, phosphonate, or crown ether residues as the pendants with partially resolved chiral compounds, such as amines and amino acids, showed a unique positive nonlinear relationship (chiral amplification or "majority rule") between the enantiomeric excess (ee) of the chiral compounds and the observed ICD intensities in water as well as in organic solvents.[6b,7,10,22] The author then investigated if a similar chiral amplification could be possible for poly-**1**-HCl in water. The chiral carboxylate **2**-Na was selected as a helix inducer because it produced the most intense ICD in water among the chiral acids used in this study as **4**-Na did (Table 1-1). The changes in the ICD intensity of poly-**1**-HCl with respect to the ee's of **2**-Na in water are depicted in Figure 1-4. The CD intensities of poly-**1**-HCl, corresponding to the helical sense excesses, were out of proportion to the ee's of **2**-Na, showing a convex deviation from the linearity in

water. The extent of the departure from linearity slightly increased with the decreasing temperature. When poly-**1**-HCl was dissolved in water with an only 0.1-fold excess **2**-Na of 60 % ee ((*S*) rich), the complex showed the full ICD as induced by 100% ee of **2**-Na (Figure 1-4A). The excess enantiomer bound to the polymer induces an excess of a single-handed helix despite its proportion, which will result in a more intense ICD than that expected from the ee of **2**-Na. The positive nonlinear effect of poly-**1**-HCl versus the ee of **2**-Na increased with an increase in the amount of **2**-Na. As shown in Figure 1-4B, the extent of the departure from linearity increased, especially in the low ee region of **2**-Na (< 60% ee) when poly-**1**-HCl was dissolved in water with a 0.5-fold excess **2**-Na. Therefore, a stronger nonlinear effect would be expected for poly-**1**-HCl in the presence of greater amounts of the chiral acid. However, the further addition of (*S*)-**2**-Na (> 0.5 equiv) resulted in precipitation of the polymer because the solution pH became higher with the increasing amount of (*S*)-**2**-Na, and therefore, further experiments were difficult.

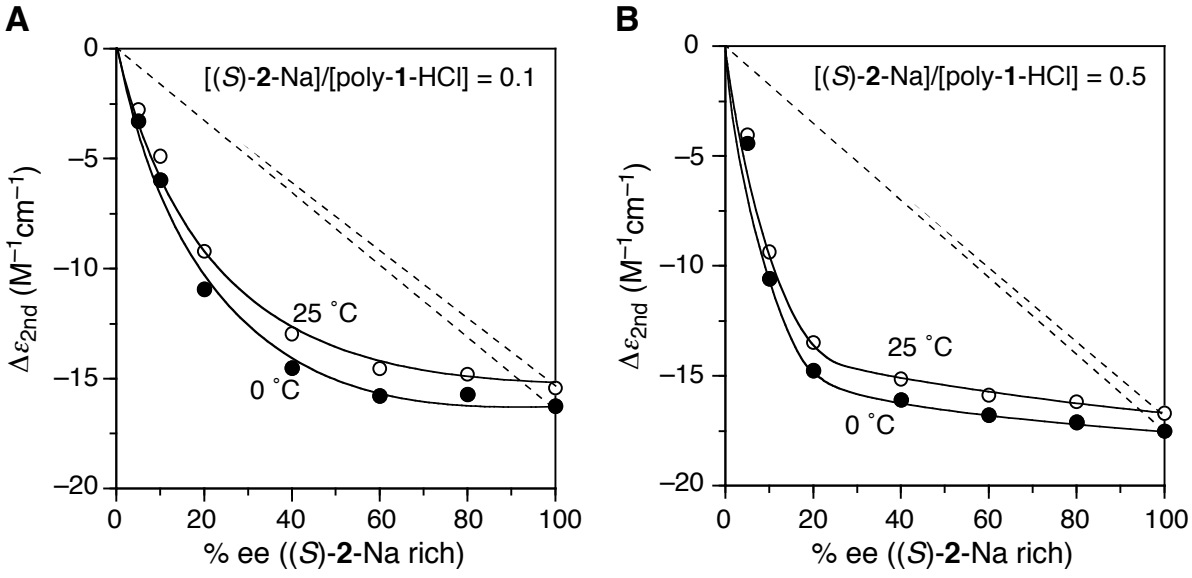

Figure 1-4. Changes in ICD intensity ($\Delta\varepsilon_{2nd}$) of poly-**1**-HCl (1.0 mg/mL) versus the % ee of **2**-Na ([**2**-Na]/[poly-**1**-HCl] = 0.1; pH 5.1–5.4) (A), ([**2**-Na]/[poly-**1**-HCl] = 0.5; pH 5.4–5.5) (B) in water at 25 and 0 °C during the complexation with poly-**1**-HCl.

Conclusions

In summary, the author has found that a positively charged poly(phenylacetylene) derivative bearing the hydrochloride of the diisopropylaminomethyl group as the pendants formed a predominantly one-handed helical conformation induced by a noncovalent interaction with various chiral acids in water and the complexes exhibited characteristic ICDs in the UV-visible region even in the presence of a small amount of chiral acids with a low optical activity. Poly-**1**-HCl was highly sensitive to the chirality of the carboxylic acids and showed the same Cotton effect signs if the configurations were the same. The present results demonstrate that the poly-**1**-HCl can be utilized as a chirality sensing probe for chiral acids in water. On the other hand, the neutral poly-**1** was not sensitive to the chirality of chiral acids in organic solvents and other noncharged neutral polyacetylenes also showed a weak chiral amplification in water. These results suggest that the polyelectrolyte function of the poly-**1**-HCl may play an important role in the high chiral amplification property in water. This finding will contribute to the design and construction of more sensitive helical polyacetylenes for the detection of chirality of target molecules in water.

Experimental Section

Materials. Deionized, distilled water was degassed with nitrogen before use for all experiments. Optically active acids and alcohols were obtained from Aldrich or Tokyo Kasei (TCI, Tokyo, Japan). The sodium salt of **2** was prepared by neutralization of **2** with aqueous 1 N NaOH, followed by precipitation into a large amount of acetone. The other sodium salts of optically active carboxylic acids (**3**–**14**) were prepared by mixing the solution of the corresponding acids in water or ethanol with aqueous 1 N NaOH ([acids]/[NaOH] = 1.0 (mol/mol)), followed by lyophilization. Nucleotides (**15**—**20**-Na) and DNA from salmon testes were purchased from Sigma and used as received.

Cis-transoidal poly-**1** was prepared by polymerization of 4-(*N*,*N*-diisopropylaminomethyl)phenylacetylene with $[Rh(nbd)Cl]_2$ (nbd = norbornadiene) in THF according to the previously reported method.[9a,b] Poly-**1** was quantitatively converted to its HCl salt (poly-**1**-HCl) by dissolving poly-**1** in aqueous 1 N HCl, followed by precipitation into acetone and filtration. The recovered polymer was dissolved in water and the solution was lyophilized. The stereoregularity of the poly-**1**-HCl was investigated by NMR spectroscopy.[23] However, the author could not estimate the stereoregularity of the poly-**1**-HCl by its ^{1}H NMR spectrum in D_2O because of the broadening of the main chain protons even at 80 °C, which may be due to the rigidity of the polymers' main chains. The Raman spectrum of poly-**1**-HCl gave useful information and showed intense peaks at 1580, 1353, and 974 cm^{-1}, which can be assigned to the C=C, C–C, and C–H bond vibrations in the *cis* polyacetylenes, while those in the *trans* polyacetylene were not observed, indicating that the poly-**1**-HCl possesses a highly *cis-transoidal* structure (Figure 1-5).[24] The number-average molecular weight (M_n) and molecular weight distribution (M_w/M_n) of poly-**1**-HCl were 3.4×10^5 and 2.2, respectively, as determined by SEC using poly(ethylene oxide) and poly(ethylene glycol) standards in water containing 9 mM tartaric acid and the 0.1 mM tartaric acid disodium salt as the eluent at a flow rate of 0.6 mL/min.

Spectroscopic data of poly-**1**-HCl: ^{1}H NMR (D_2O, 80 °C): δ 1.34 (br, CH_3, 12H), 3.76 (br, CH × 2 and CH_2, 4H), 5.75 (br, =CH, 1H), 6.0—9.6 (br, aromatic, 4H). Anal. Calcd for $(C_{15}H_{22}ClN)_n$: C, 71.55; H, 8.81; N, 5.56. Found: C, 71.55; H, 8.93; N, 5.75.

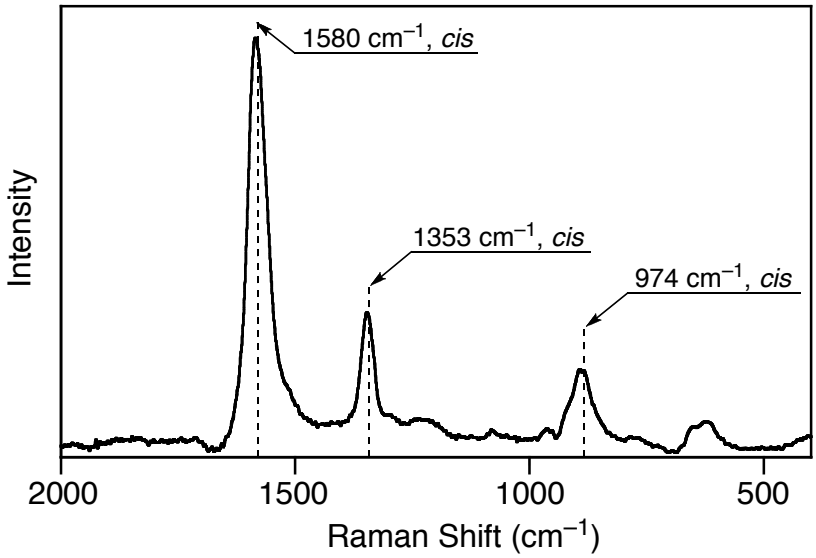

Figure 1-5. Laser Raman spectrum of poly-**1**-HCl.

Instruments. Melting point was measured on a Yanakao melting point apparatus and is uncorrected. The solution pH was measured with a B-211 pH meter (Horiba, Japan). NMR spectra were taken on a Varian Mercury 300 operating at 300 MHz for ^{1}H and a Varian VXR-500S operating at 500 MHz for ^{1}H and 125 MHz for ^{13}C in D_2O using acetonitrile as the internal standard. Elemental analyses were performed by the Nagoya University Analytical Laboratory in School of Engineering. SEC measurements were performed with a JASCO PU-980 liquid chromatograph (JASCO, Hachioji, Japan) equipped with a UV (254 nm; JASCO UV-970) detector. A Tosoh (Tokyo, Japan) TSK-GEL SuperAWM-H column (30 cm) was connected and a water solution containing 9 mM tartaric acid and the 0.1 mM tartaric acid sodium salt was used as the eluent at a flow rate of 0.6 mL/min. The molecular weight calibration curve was obtained with poly(ethylene oxide) and poly(ethylene glycol) standards (Tosoh). IR spectra were recorded with a JASCO Fourier Transform IR-620

spectrophotometer. Laser Raman spectra were taken on a JASCO RMP-200 spectrophotometer. The absorption and CD spectra were measured in a 0.1-, 0.5-, 1.0-, or 10-mm quartz cell on a JASCO V-570 spectrophotometer and a JASCO J-725 or J-820 spectropolarimeter, respectively. The temperature (0–25 °C) was controlled with a JASCO ETC 505T (for absorption spectral measurements) and a JASCO PTC-423L apparatus (for CD spectral measurements).

CD Measurements. The concentration of poly-**1**-HCl was calculated on the basis of the monomer units and was 1 mg/mL (4.0 mM monomer units) unless otherwise stated. In the complexation of poly-**1**-HCl with optically active acids, a stock solution of poly-**1**-HCl (2 mg/mL) in water was prepared in a 5-mL flask equipped with a stopcock. A 500 μL aliquot of the poly-**1**-HCl solution was transferred to a 1-mL flask equipped with a stopcock using a micropipette (Mettler-Toledo GmbH, Switzerland). An appropriate amount of sodium salts of optically active acids was added to the flask and the solution was diluted with water to keep the poly-**1**-HCl concentration at 1.0 mg/mL and absorption and CD spectra were taken.

CD titrations of Poly-1-HCl with (*S*)-2-Na and Hill plots. A stock solution of poly-**1**-HCl (2.0 mg/mL, 7.9 mM) in water was prepared in a 5-mL flask equipped with a stopcock. Stock solutions of (*S*)-**2**-Na (0.20, 0.40, 1.99, and 7.94 mM) in water were also prepared in 100-, 100-, 25-, and 5-mL flasks, respectively. The 0.50 mL aliquots of the poly-**1**-HCl solution were transferred to eleven 1-mL flasks equipped with stopcocks and increasing amounts of the stock solutions of the (*S*)-**2**-Na were added to the flasks; the molar ratios of (*S*)-**2**-Na to poly-**1**-HCl were 0.001, 0.002, 0.005 (0.20 mM (*S*)-**2**-Na), 0.01, 0.02, 0.03 (0.40 mM (*S*)-**2**-Na), 0.05, 0.1 (1.99 mM (*S*)-**2**-Na), and 0.2, 0.3, 0.5 (7.94 mM (*S*)-**2**-Na), and the resulting solutions were diluted with water to keep the poly-**1** concentrations at 1.0 mg/mL (4.0 mM). The absorption and CD spectra were then taken for each flask to determine the changes in the CD spectra (Figure 1-2). Plots of the CD intensities of the second Cotton ($\Delta\varepsilon_{2nd}$) of poly-**1**-HCl as a function of concentration of (*S*)-**2**-Na gave a saturation binding

isotherm at 25 and 0 °C. The Hill plot analysis of the data resulted in apparent binding constants (*K*s) according to the Hill equation, log(Y/(1-Y)) = *n*log[G] + *n*log*K*, where Y, *n*, and [G] represent the fractional saturation, the Hill coefficient, and the concentration of the guest, respectively.[20] The *n* values were 1.20 and 1.14 with a correlation coefficient $r > 0.999$ at 25 and 0 °C, respectively.

Nonlinear Effects. The nonlinear effect between intensities of ICD and percent ee of **2**-Na in the complexation with poly-**1**-HCl was investigated in water. The molar ratio of **2**-Na to the monomer units of poly-**1**-HCl ([**2**-Na]/[poly-**1**-HCl]) was held constant at 0.1 or 0.5 (mol/mol). A typical experimental procedure using **2**-Na ([**2**-Na]/[poly-**1**-HCl] = 0.5) is described below. Stock solutions of poly-**1**-HCl (2 mg/mL, 10 mL), (*S*)-**2**-Na (5 mM, 25 mL), and (*R*)-**2**-Na (5 mM, 25 mL) were prepared. Aliquots of the stock solutions of (*S*)- and (*R*)-**2**-Na were placed into seven 1 mL flasks so that the percent ee of the mixtures (*S* rich) became 5, 10, 20, 40, 60, 80, and 100, respectively. To the flasks was added a 0.50 mL aliquot of the stock solution of poly-**1**-HCl and the resulting solutions were diluted with water to keep the poly-**1**-HCl concentration at 1.0 mg/mL (4.0 mM). The absorption and CD spectra were then taken for each flask to determine the changes in the CD spectra (Figure 1-4B). The same procedure was performed in the experiment with poly-**1**-HCl and **2**-Na ([**2**-Na]/[poly-**1**-HCl] = 0.1).

References and Notes

(1) (a) Coppola, G. M.; Schuster, H. F. *α-Hydroxyl Acids in Enantioselective Syntheses*; VCH: Weinheim, 1997. (b) Aboul-Enein, H. Y.; Wainer, I. W., Eds. *The Impact of Stereochemistry on Drug Development and Use*; John Wiley & Sons: New York, 1997. (c) Ojima, I., Ed. *Catalytic Asymmetric Synthesis, 2nd ed*.; VCH: New York, 2000. (d) Challener, C. A., Ed. *Chiral Intermediates*; Ashgate: Hampshire, 2001.

(2) (a) Xu, M.; Lin, J.; Hu, Q.; Pu, L. *J. Am. Chem. Soc.* **2002**, *124*, 14239–14246. (b) Mei, X.; Wolf, C. *J. Am. Chem. Soc.* **2004**, *126*, 14736–14737. (c) Zhao, J.; Davidson, M. G.; Mahon, M. F.; Kociok-Köhn, G.; James, T. D. *J. Am. Chem. Soc.* **2004**, *126*, 16179–16186. (d) Lin, J.; Rajaram, A. R.; Pu, L. *Tetrahedron* **2004**, *60*, 11277–11281. (e) Pu, L. *Chem. Rev.* **2004**, *104*, 1687–1716.

(3) (a) Kabuto, K.; Sasaki, K.; Sasaki, Y. *Tetrahedron: Asymmetry* **1992**, *3*, 1357–1360. (b) Sessler, J. L.; Andrievsky, A.; Král, V.; Lynch, V. *J. Am. Chem. Soc.* **1997**, *119*, 9385–9392. (c) Voyer, N.; Côté, S.; Biron, S.; Beaumont, M.; Chaput, M.; Levac, S. *J. Supramol. Chem.* **2001**, *1*, 1–5. (d) Laurent, P.; Miyaji, H.; Collinson, S. R.; Prokes, I.; Moody, C. J.; Tucker, J. H. R.; Slawin, A. M. Z. *Org. Lett.* **2002**, *4*, 4037–4040. (e) Zheng, Y.; Zhang, C. *Org. Lett.* **2004**, *6*, 1189–1192. (f) Yang, X.; Wu, X.; Fang, M.; Yuan, Q.; Fu, E. *Tetrahedron: Asymmetry* **2004**, *15*, 2491–2497. (g) Seco, J. M.; Quiñoá, E.; Riguera, R. *Chem. Rev.* **2004**, *104*, 17–117. (h) Bell, T. W.; Hext, N. M. *Chem. Soc. Rev.* **2004**, *33*, 589–598.

(4) (a) Katzin, L. *Inorg. Chem.* **1968**, *7*, 1183–1191. (b) Takeuchi, M.; Imada, T.; Shinkai, S. *Angew. Chem., Int. Ed.* **1998**, *37*, 2096–2099. (c) Rickman, B. H.; Matile, S.; Nakanishi, K.; Berova, N. *Tetrahedron* **1998**, *54*, 5041–5064. (d) Proni, G.; Pescitelli, G.; Huang, X.; Quraishi, N. Q.; Nakanishi, K.; Berova, N. *Chem. Commun.* **2002**, 1590–1591. (e) Yang, Q.; Olmsted, C.; Borhan, B. *Org. Lett.* **2002**, *4*, 3423–3426. (f) Proni, G.; Pescitelli, G.; Huang, X.; Nakanishi, K.; Berova, N. *J. Am. Chem. Soc.* **2003**, *125*, 12914–12927.

(5) (a) Nakanishi, K.; Berova, N. In *Circular Dichroism— Principles and Applications, 2nd ed.;* Nakanishi, K.; Berova, N.; Woody, R. W., Eds.; VCH: New York, 2000; Chapter 12. (b) Canary, J. W.; Holmes, A. E.; Liu, J. *Enantiomer* **2001**, *6*, 181–188. (c) Tsukube, H.; Shinoda, S. *Chem. Rev.* **2002**, *102*, 2389–2403. (d) Allenmark, S. *Chirality* **2003**, *15*, 409–422.

(6) (a) Yashima, E.; Matsushima, T.; Okamoto, Y. *J. Am. Chem. Soc.* **1995**, *117*, 11596–11597. (b) Yashima, E.; Matsushima, T.; Okamoto, Y. *J. Am. Chem. Soc.* **1997**, *119*, 6345–6359. (c) Yashima, E.; Maeda, K.; Okamoto, Y. *Nature* **1999**, *399,* 449–451. (d) Ashida, Y.; Sato, T.; Morino, K.; Maeda, K.; Okamoto, Y.; Yashima, E. *Macromolecules* **2003**, *36*, 3345–3350. (e) Maeda, K.; Morino, K.; Okamoto, Y.; Sato, T.; Yashima, E. *J. Am. Chem. Soc.* **2004**, *126*, 4329–4342. (f) Maeda, K.; Hatanaka, K.; Yashima, E. *Mendeleeve Commun.* **2004**, *14*, 231–233. (g) Morino, K.; Watase, N.; Maeda, K.; Yashima, E. *Chem. –Eur. J.* **2004**, *10*, 4703–4707.

(7) (a) Onouchi, H.; Kashiwagi, D.; Hayashi, K.; Maeda, K.; Yashima, E. *Macromolecules* **2004**, *37*, 5495–5503. (b) Nishimura, T.; Tsuchiya, K.; Ohsawa, S.; Maeda, K.; Yashima, E.; Nakamura, Y.; Nishimura, J. *J. Am. Chem. Soc.* **2004**, *126*, 11711–11717. (c) Onouchi, H.; Miyagawa, T.; Furuko, A.; Maeda, K.; Yashima, E. *J. Am. Chem. Soc.* **2005**, *127*, 2960–2965. (d) Miyagawa, T.; Furuko, A.; Maeda, K.; Katagiri, H.; Furusho, Y.; Yashima, E. *J. Am. Chem. Soc.* **2005**, *127*, 5018–5019.

(8) (a) Yashima, E.; Nimura, T.; Matsushima, T.; Okamoto, Y. *J. Am. Chem. Soc.* **1996**, *118*, 9800–9801. (b) Kawamura, H.; Maeda, K.; Okamoto, Y.; Yashima, E. *Chem. Lett.* **2001**, 58–59.

(9) (a) Yashima, E.; Maeda, Y.; Okamoto, Y. *Chem. Lett.* **1996**, 955–956. (b) Yashima, E.; Maeda, Y.; Matsushima, T.; Okamoto, Y. *Chirality* **1997**, *9*, 593–600. (c) Maeda, K.; Okada, S.; Yashima, E.; Okamoto, Y. *J. Polym. Sci., Part A: Polym. Chem.* **2001**, *39*, 3180–3189.

(10) Nonokawa, R.; Yashima, E. *J. Am. Chem. Soc.* **2003**, *125*, 1278–1283.

(11) Yashima, E. *Anal. Sci.* **2002**, *18*, 3–6.

(12) (a) Yashima, E.; Okamoto, Y. In *Circular Dichroism: Principles and Applications,* 2nd ed.; Berova, N., Nakanishi, K., Woody, R. W., Eds.; Wiley-VCH: New York, 2000; chapter 18. (b) Yashima, E.; Maeda, K.; Nishimura, T. *Chem. –Eur. J.* **2004**, *10*, 42–51 and references therein.

(13) For reviews of dynamic helical polymers, see: (a) Green, M. M.; Park, J.-W.; Sato, T.; Teramoto, A.; Lifson, S.; Selinger, R. L. B.; Selinger, J. V. *Angew. Chem., Int. Ed.* **1999**, *38*, 3138-3154. (b) Nakano, T.; Okamoto, Y. *Chem. Rev.* **2001**, *101*, 4013–4038. (c) Cornelissen, J. J. L. M.; Rowan, A. E.; Nolte, R. J. M.; Sommerdijk, N. A. J. M. *Chem. Rev.* **2001**, *101*, 4039–4070. (d) Nomura, R.; Nakako, H.; Masuda, T. *J. Mol. Catl. A* **2002**, *190*, 197–205. (e) Fujiki, M.; Koe, J. R.; Terao, K.; Sato, T.; Teramoto, A.; Watanabe, J. *Polym. J.* **2003**, *35*, 297–344. For recent examples of helical polyacetylenes with optically active pendants, see: (f) Nomura, R.; Fukushima, Y.; Nakako, H.; Masuda, T. *J. Am. Chem. Soc.* **2000**, *122*, 8830–8836. (g) Li, B. S.; Cheuk, K. K. L.; Salhi, F.; Lam, J. W. Y.; Cha, J. A. K.; Xiao, X.; Bai, C.; Tang, B. Z. *Nano Lett.* **2001**, *1*, 323–328. (h) Yashima, E.; Maeda, K.; Sato, O. *J. Am. Chem. Soc.* **2001**, *123*, 8159–8160. (i) Morino, K.; Maeda, K.; Okamoto, Y.; Yashima, E.; Sato, T. *Chem. –Eur. J.* **2002**, *8*, 5112–5120. (j) Schenning, A. P. H. J.; Fransen, M.; Meijer, E. W. *Macromol. Rapid Commun.* **2002**, *23*, 265–270. (k) Percec, V.; Obata, M.; Rudick, J. G.; De, B. B.; Glodde, M.; Bera, T. K.; Magonov, S. N.; Balagurusamy, V. S. K.; Heiney, P. A. *J. Polym. Sci., Part A: Polym. Chem.* **2002**, *40*, 3509–3533. (l) Li, B. S.; Cheuk, K. K. L.; Ling, L.; Chen, J.; Xiao, X.; Bai, C.; Tang, B. Z. *Macromolecules* **2003**, *36*, 77–85.

(14) For reviews of molecular recognition in water; see: (a) Murakami, Y.; Kikuchi, J.; Hisaeda, Y.; Hayashida, O. *Chem. Rev.* **1996**, *96*, 721–758. (b) Lemieux, R. U. *Acc. Chem. Res.* **1996**, *29*, 373–380. (c) Schmidtchen, F. P.; Berger, M. *Chem. Rev.* **1997**, *97*, 1609–1646.

(15) For recent examples of chiral and/or molecular recognition of free amino acids or peptides based on electrostatic interactions in water, see: (a) Hossain, M. A.; Schneider, H.-J. *J. Am. Chem. Soc.* **1998**, *120,* 11208–11209. (b) Bell, T. W.; Khasanov, A. B.; Drew M. G. B.; Filikov, A.; James, T. L. *Angew. Chem. Int. Ed.* **1999**, *38*, 2543–2547. (c) Herm, M.; Molt, O.; Schrader, T. *Chem. –Eur. J.* **2002**, *8*, 1485–1499. (d) Wada, K.; Mizutani, T.; Matsuoka, H.; Kitagawa, S. *Chem. –Eur. J.* **2003**, *9*, 2368–2380. (e) Imai, H.; Munakata, H.; Uemori, Y.; Sakura, N. *Inorg. Chem.* **2004**, *43*, 1211–1213. (f) Schmuck, C.; Geiger, L. *J. Am. Chem. Soc.* **2004**, *126*, 8898–8899.

(16) (a) Oosawa, F. *Polyelectrolytes*; Dekker: New York, 1971. (b) Manning, G. S. *Acc. Chem. Res.* **1979**, *12*, 443–449. (c) *Molecular Conformation and Dynamics of Macromolecules in Condensed System*, Nagasawa, M., Ed.; Elsevier: New York, 1998. (d) Manning, G. S.; Ray, J. *J. Biomol. Struct. Dyn.* **1998**, *16*, 461–476.

(17) (a) Saito, M. A.; Maeda, K.; Onouchi, H.; Yashima, E. *Macromolecules* **2000**, *33,* 4616–4618. (b) Onouchi, H.; Maeda, K.; Yashima, E. *J. Am. Chem. Soc.* **2001**, *123*, 7441–7442.

(18) Maeda, K.; Takeyama, Y.; Sakajiri, K.; Yashima, E. *J. Am. Chem. Soc.* **2004**, *126*, 16284–16285.

(19) (a) Schlitzer, D. S.; Novak, B. M. *J. Am. Chem. Soc.* **1998**, *120*, 2196–2197. (b) Norris, I. D.; Kane-Maguire, L. A. P.; Wallace, G. G. *Macromolecules* **1998**, *31*, 6529–6533 (c) Maeda, K.; Yamamoto, N.; Okamoto, Y. *Macromolecules* **1998**, *31*, 5924–5926. (d) Nielsen, P. E. *Acc. Chem. Res.* **1999**, *32*, 624–630. (e) Yashima, E.; Maeda, K.; Yamanaka, T. *J. Am. Chem. Soc.* **2000**, *122*, 7813–7814. (f) Prince, R. B.; Barnes, S. A.; Moore, J. S. *J. Am. Chem. Soc.* **2000**, *122,* 2758–2762. (g) Inai, Y.; Ishida, Y.; Tagawa, K.; Takasu, A.; Hirabayashi, T. *J. Am. Chem. Soc.* **2002**, *124,* 2466–2473. (h) Ishikawa, M.; Maeda, K.; Yashima, E. *J. Am. Chem. Soc.* **2002**, *124,* 7448–7458. (i) Tabei, J.; Nomura, R.; Sanda, F.; Masuda, T. *Macromolecules* **2003**, *36*, 8603–8608. (j) Nilsson, K. P. R.; Rydberg, J.; Baltzer, L.; Inganäs, O. *Proc. Nat. Acad. Sci., USA* **2004**,

101, 11197–11202. (k) Sakai, R.; Satoh, T.; Kakuchi, R.; Kaga, H.; Kakuchi, T. *Macromolecules* **2004**, *37*, 3996–4003. For reviews of helical polymers and oligomers (foldamers), see: ref 13 and (l) Gellman, S. H. *Acc. Chem. Res.* **1998**, *31*, 173–180. (m) Srinivasarao, M. *Curr. Opin. Colloid Interface Sci.* **1999**, *4,* 370–376. (n) Fujiki, M. *Macromol. Rapid Commun.* **2001**, *22*, 539–563. (o) Hill, D. J.; Mio, M. J.; Prince, R. B.; Hughes, T. S.; Moore, J. S. *Chem. Rev.* **2001**, *101*, 3893–4011. (p) Brunsveld, L.; Folmer, B. J. B.; Meijer, E. W.; Sijbesma, R. P. *Chem. Rev.* **2001**, *101*, 4071–4097. (q) Huc, I. *Eur. J. Org. Chem.* **2004**, 17–29.

(20) Connors, K. A. *Binding Constants*; John Wiley: New York, 1987.

(21) (a) Nonokawa, R.; Oobo, M.; Yashima, E. *Macromolecules* **2003**, *36,* 6599–6606. (b) Nonokawa, R.; Yashima, E. *J. Polym. Sci., Part A: Polym. Chem.* **2003**, *41*, 1004–1013.

(22) (a) Selinger, J. V.; Selinger, R. L. B. *Phys. Rev. Lett.* **1996**, *76*, 58–61. For other references of majority rule in helical polymers, see: (b) Green, M. M.; Garetz, B. A.; Munoz, B.; Chang, H.; Hoke, S.; Cooks, R. G. *J. Am. Chem. Soc.* **1995**, *117*, 4181–4182. (c) Okamoto, Y.; Nishikawa, M.; Nakano, T.; Yashima, E.; Hatada, K. *Macromolecules*. **1995**, *28*, 5135–5138. (d) Takei, F.; Onitsuka, K.; Takahashi, S. *Polym. J.* **1999**, *31*, 1029–1032. (e) Li, J.; Schuster, G. B.; Cheon, K.-S.; Green, M. M.; Selinger, J. V. *J. Am. Chem. Soc.* **2000**, *122*, 2603–2612. (f) Tabei, J.; Nomura, R.; Masuda, T. *Macromolecules* **2002**, *35*, 5405–5409. For reviews, see: (g) Green, M. M.; Peterson, N. C.; Sato, T.; Teramoto, A.; Cook, R.; Lifson, S. *Science* **1995**, *268,* 1860–1866.

(23) (a) Simionescu, C. I.; Percec, V.; Dumitrescu, S. *J. Polym. Sci: Polym. Chem. Ed.* **1977**, *15*, 2497–2509. (b) Simionescu, C. I.; Percec, V. *Prog. Polym. Sci.* **1982**, *8*, 133–214. (c) Furlani, A.; Napoletano, C.; Russo, M. V.; Feast, W. *J. Polym. Bull.* **1986**, *16*, 311–317. (d) Matsunami, S.; Kakuchi, T.; Ishii, F. *Macromolecules* **1997**, *30*, 1074–1078. (e) Kishimoto, Y.; Eckerle, P.; Miyatake, T.; Kainosho, M.; Ono, A.; Ikariya, T.; Noyori, R. *J. Am. Chem. Soc.* **1999**, *121*, 12035–12044.

(24) (a) Shirakawa, H.; Ito, T.; Ikeda, S. *Polym. J.* **1973**, *4*, 469–462. (b) Tabata, M.; Tanaka, Y.; Sadahiro, Y.; Sone, T.; Yokota, K.; Miura, I. *Macromolecules* **1997**, *30*, 5200–5204.

Chapter 2

Hierarchical Amplification of Macromolecular Helicity in a Lyotropic Liquid Crystalline Charged Poly(phenylacetylene) by Nonracemic Dopants in Water and Its Helical Structure

Abstract: A unique hierarchical amplification of chiral information from a nonracemic guest to macromolecular helicity, followed by a mesoscopic, supramolecular cholesteric twist in water is reported. This remarkable chiral amplification involves two-step chirality transfer processes, which enable the detection and sensing of an extremely small imbalance in chiral guest molecules. The macromolecular helicity with an excess single-handed helix was first induced in the positively charged, chromophoric poly(phenylacetylene), the hydrochloride of poly(4-(*N*,*N*-diisopropylaminomethyl)phenylacetylene) (poly-**1**-HCl) upon complexation with an oppositely charged nonracemic acid as a dopant through electrostatic interaction in dilute water. Subsequently, the macromolecular helicity was further amplified in the polymer backbone as a greater excess of a single-handed helix through self-assembly into a lyotropic cholesteric liquid crystal (LC). Direct evidence for the hierarchical amplification process of the helical sense excess of the polymer during the cholesteric LC formation was demonstrated by direct comparison of the excess of the one helical sense of the polymer in dilute solution with that in the cholesteric LC state. Poly-**1**-HCl formed a lyotropic nematic LC in water in the absence of chiral acids, indicating its rigid-rod characteristic regardless of the lack of a single-handed helix, as evidenced by the long persistence lengths before (26 nm) and after (28 nm) the one-handed helicity induction in the polymer. X-ray diffraction of the oriented films of the nematic and cholesteric liquid crystalline poly-**1**-HCls exhibited almost the same diffraction pattern, suggesting that both polymers may have the same helical structure in spite of the substantial difference in their helical characteristics; dynamically racemic and one-

handed helices in dilute solution, respectively. On the basis of the X-ray analyses, the most plausible helical structure of poly-**1**-HCl is proposed to be a 23 unit / 10 turn (23/10) helix.

Introduction

Biological macromolecules, such as DNA and proteins, adopt an elaborate one-handed helical structure, which further self-assembles into lyotropic cholesteric liquid crystals (LCs) in water because of their stiff helical backbones.[1] Since the discovery of their biological helices and liquid crystallinities, significant attention has been paid to developing artificial helical polymers with a controlled helix-sense[2] and liquid crystallinity because of the great interest from fundamental and biological viewpoints as well as for attractive applications in chiral materials science.[3] Several synthetic polymers bearing optically active pendants through covalent bonding also exhibit cholesteric LCs due to their rigid helical backbones in organic solvents or in the melt.[2a,4] However, aqueous cholesteric LCs derived from synthetic helical polymers are rare,[1b] in spite of their potential for a wide range of applications including biomimetic composite materials and electric-field responsive materials.[5]

In a series of studies, Yashima and co-workers reported the unique feature of dynamic helical, chromophoric poly(phenylacetylene)s with various functional groups as the pendants for the chirality detection and sensing of chiral small molecules in dilute solution. The poly(phenylacetylene)s formed an excess of one helical sense induced by noncovalent specific interactions with chiral guests, and the complexes exhibited a characteristic induced circular dichroism (ICD) in the polymer backbone regions in dilute solution.[2j,6] The interactions that occurred in the remote pendants are highly cooperative, so that the molecular chirality of the guests transforms into dynamic helical poly(phenylacetylene)s, resulting in the generation of an easily measurable excess of the one helical sense as detected by circular dichroism (CD), since the complexation with chiral guests remarkably alters the population of the right- and left-handed helices of the dynamically racemic helical polymers separated by helical reversals.[7,8] However, the induced helical poly(phenylacetylene)s prepared so far showed no LC phase in organic solvents probably because of their rather flexible backbones.

Recently, Yashima et al. have found that a positively charged poly(phenylacetylene), the hydrochloride of poly(4-(*N*,*N*-diisopropylaminomethyl)phenylacetylene) (poly-**1**-HCl; Chart

2-1) also forms a predominantly one-handed helix upon complexation with various chiral acids including carboxylic acids, phosphonic and sulfonic acids, and amino acids and exhibits similar ICDs through the significant amplification of chirality in water.[9] The polymer is very sensitive to the chirality of chiral acids as evidenced by the appearance of an ICD in the presence of a tiny amount of chiral carboxylic acids such as the sodium salt of phenyl lactic acid ((*S*)-**2** in Chart 2-1) as the dopant and even with **2** of a low enantiomeric excess (ee) in dilute water solution.[9] Moreover, the poly-**1**-HCl formed a lyotropic LC phase in concentrated water solutions, resulting in the first polyacetylene-based aqueous LC.[9a,10] The polyelectrolyte function of poly-**1**-HCl accompanied by the hydrophobic pendants of this polymer seems to be important for the appearance of the LC phase in water because the neutral poly-**1** showed no LC phase in any organic solvents.[9a]

Interestingly, the helix-sense excess of poly-**1**-HCl was further amplified in the cholesteric LC phase in the presence of the nonracemic **2** than that in dilute solution.[9a,11,12] This concept of the amplification of the helical chirality in the LC state was first demonstrated by Green et al. using the optically inactive poly(*n*-hexyl isocyanate), a typical stiff dynamic helical polymer.[2a,b] They found that the lyotropic nematic liquid crystalline polyisocyanate converted to the cholesteric counterpart by doping with optically active polyisocyanates in organic solvents, and discovered the amplification of the helical sense excess of the polyisocyanate by the LC state over that in dilute solutions.[4e] This is called the "bad neighbors" rule. These precedent observations together with our preliminary results prompted us to explore if the poly-**1**-HCl could work as a general-purpose chirality sensing probe for other various chiral acids including important biomolecules, such as amino acids and nucleotides, in an aqueous LC state, and the results were compared with those in a dilute water system reported previously.[9]

Chart 2-1. Structures of Poly-**1**-HCl and Optically Active Dopants

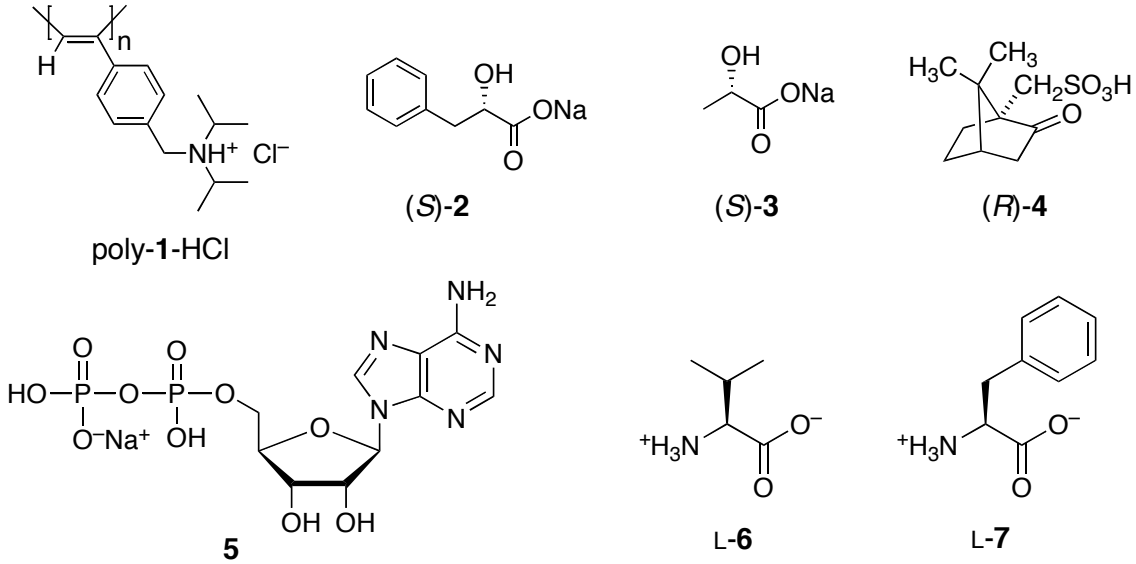

In addition, the fact that dynamically racemic and preferred-sense helical poly-**1**-HCls form nematic and cholesteric LCs makes possible the analysis of their helical structures by X-ray diffraction, because we can make shear-oriented films from the LC samples. Although a large number of stereoregular *cis-transoidal* polyacetylenes with aliphatic and aromatic pendants have been synthesized with much interest,[6,10,13] their exact structures have not yet been determined. Previous X-ray studies of *cis-transoidal* aliphatic and aromatic polyacetylenes revealed their lateral packing of the polymer molecules, and a pseudohexagonal columnar packing structure composed of helical polyacetylenes in the solid state was proposed based on the X-ray diffraction results.[10c-e,g,14] Computational studies suggested that the most energetically preferred conformation of the *cis-transoidal* helical polyacetylenes was a nearly 7/3 helix.[6e,15]

In sharp contrast to the other stiff rodlike helical polymers, such as polyisocyanates and polysilanes, with a long persistence length (q) which stands for the backbone stiffness (20–45[16] and ca. 70 nm,[17] respectively) and a very large helical domain,[2a,b,f] the previously prepared substituted polyacetylenes appear to be rather flexible with a low population of such

a helical domain[7,18] As a result, there has been no structural information available to define the main chain helical structures of the polyacetylenes.

In this study, the author reports convincing evidence for the hierarchical amplification of the helicity of poly-**1**-HCl in the LC state, that is, the strong enhancement of preferred handedness through the cholesteric twist. The author also demonstrates that the lyotropic solution can be used as a simple indicator of enantiomeric excess of various small chiral molecules. To more quantitatively analyze the helicity induction in poly-**1**-HCl with chiral amplification in the LC state, the persistence length of poly-**1**-HCl before and after the single-handed helicity induction with chiral acids was determined. Finally, the author shows the X-ray data of the oriented poly-**1**-HCl films prepared from nematic and cholesteric LC samples and propose the possible helical structures of the poly-**1**-HCls. On the basis of these results, the mechanism of the preferred-sense helicity induction in poly-**1**-HCl with chiral acids in dilute solution followed by amplification of the macromolecular helicity process in the LC state is discussed.

Results and Discussion

Helicity Induction in Dilute Solution and Cholesteric Liquid Crystal Formation in Concentrated Solution. The *cis-transoidal* poly-**1**-HCl was prepared according to a previously reported method.[9] The stereoregularity of poly-**1**-HCl was confirmed to be highly *cis-transoidal* (*cis* content = 96%) based on ^{1}H NMR spectroscopy of original poly-**1** (see Figure 2-6 and the Experimental Section). The number average molecular weight (M_n) and its distribution (M_w/M_n) were 2.36×10^5 and 1.43, respectively, as estimated by atomic force microscopy (AFM) (see Figure 2-8 and the Experimental Section).[19] As previously reported, poly-**1**-HCl was highly sensitive to the chirality of various acids, as already demonstrated by the appearance of ICDs in the presence of an extremely small amount of chiral acids, such as (*S*)-**2** and **2** of low ee, in dilute aqueous solution.[9] Figure 2-1A shows the typical CD and absorption spectra of poly-**1**-HCl with (*S*)- and (*R*)-**2** in water. In a concentrated water

solution (above 8 wt %), poly-**1**-HCl formed a birefringent nematic phase (Figure 2-1D). The addition of nonracemic acids to a concentrated poly-**1**-HCl solution brought about the LC state with a fingerprint texture typical of the cholesteric LC, where the spacing of the fringes defines half of the cholesteric pitch and a smaller pitch represents an increased preference of the one helical sense in the cholesteric phase[3a,9a] (for the typical textures, see E–I in Figure 2-1).

Yashima et al. previously performed titration experiments with (*S*)-**2** and **2** of different ee's by following either the changes in the CD intensity of the second Cotton effect ($\Delta\varepsilon_{2nd}$) in dilute solution and the cholesteric pitch (p) in the LC state in order to explore if the macromolecular helicity induced in poly-**1**-HCl by chiral **2** in dilute solution would be further amplified in the LC state by comparing their nonlinear responses to the chirality of **2** in each pair of titrations.[9a] In Figures 2-1B and 2-1C, the previously reported titration experiment results using (*S*)-**2** and **2** of different ee's in the LC state[9a] are shown, along with additional experiments, in the plot of the cholesteric wavenumber q_c (defined by $2\pi/p$) versus the concentration of (*S*)-**2** and the % ee of **2**, respectively; the CD titration results in a dilute water solution[9a] are also shown for comparison. A remarkable chiral amplification in the LC state over that in the dilute solution was observed during the titrations with (*S*)-**2** and nonracemic **2**; for instance, the q_c value increased with the increasing ee and reached a constant value at about 40–50% ee, while in dilute solution, the $\Delta\varepsilon_{2nd}$ value became constant at over 75% ee (Figure 2-1C). The sudden onset and more rapid increase in the q_c value over that in the $\Delta\varepsilon_{2nd}$ value in dilute solution suggest a subsequent amplification of the helical sense excess in the LC state. In the titrations with (*S*)-**2** in dilute and concentrated solutions, the difference in their increments is also significant (Figure 2-1B).

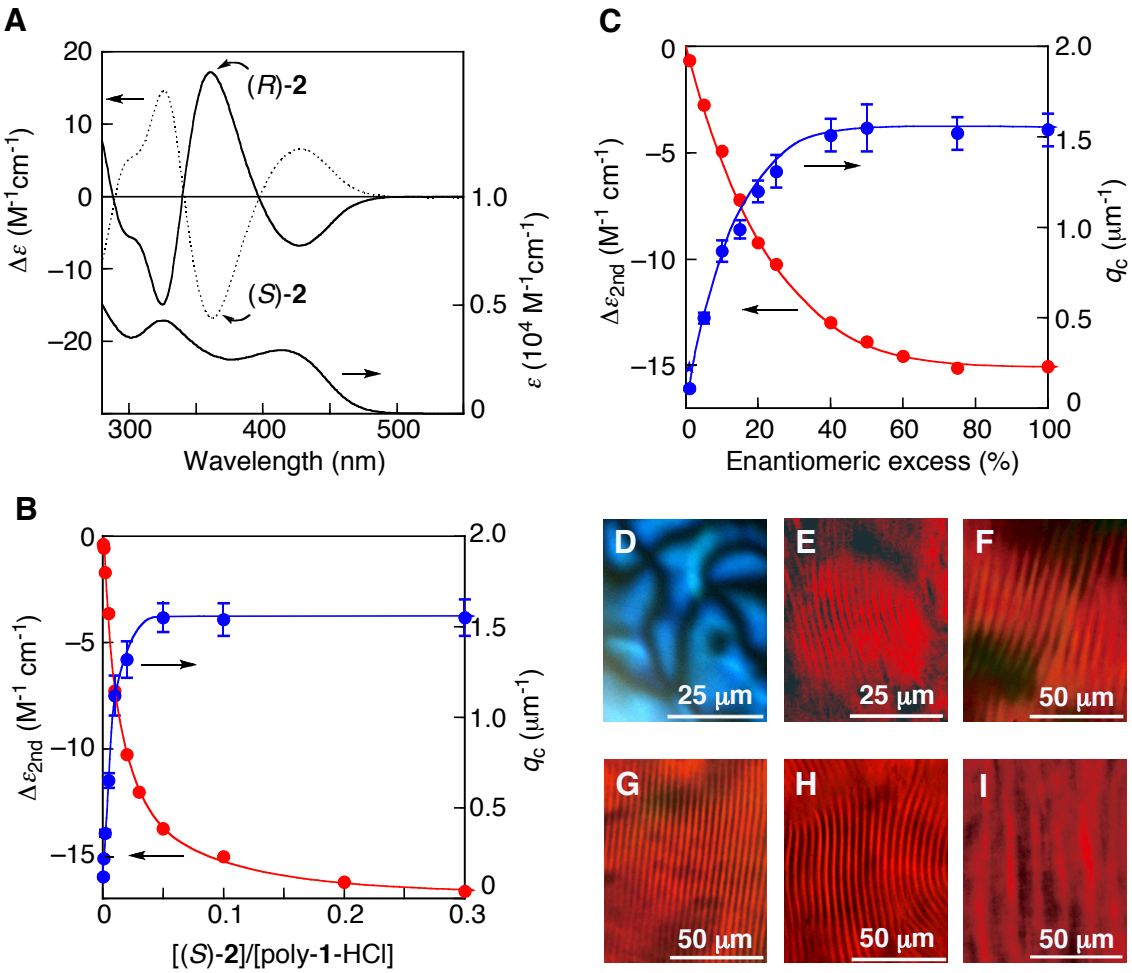

Figure 2-1. (A) CD spectra of poly-**1**-HCl with (*S*)- and (*R*)-**2** in water at 25 °C. Absorption spectrum of poly-**1**-HCl with (*R*)-**2** at 25 °C is also shown. The concentration of poly-**1**-HCl is 1.0 mg (4.0 μmol monomer units)/mL. [**2**]/[poly-**1**-HCl] = 0.5. (B) Changes in the ICD intensity ($\Delta\varepsilon_{2nd}$) (●) and the cholesteric wavenumber (q_c) (●) of poly-**1**-HCl versus the concentration of (*S*)-**2** in dilute (1 mg/mL) and concentrated (20 wt %) water solutions, respectively. (C) Changes in the ICD intensity (●) and q_c (●) of poly-**1**-HCl versus the % ee of **2** (*S*-rich) in dilute (1 mg/mL) and concentrated (20 wt %) water solutions, respectively. The molar ratio of **2** to the monomeric units of poly-**1**-HCl is 0.1 equiv (D—I) Polarized optical micrographs of a nematic LC phase of poly-**1**-HCl (20 wt %) (D) and cholesteric LC phases of poly-**1**-HCl (20 wt %) in the presence of 50 (E) and 5% ee (F) (*S* rich) of **2** (0.1 equiv), (*S*)-**3** (0.1 equiv) (G), (*R*)-**4** (0.01 equiv) (H), and L-**6** (0.1 equiv) (I) in water. The error bars in B and C represent the standard deviation estimated by an evaluation of ca. 30 fingerprint spacings (see Table 2-1).

The cholesteric wavenumber q_c of helical polymer solutions strongly depends on the polymer concentration, temperature, and the solvent.[4d,e] If the solution contains enantiomers, i.e., the right- and left-handed helices, q_c also depends on the excess of one helical sense. It can be theoretically shown that q_c of such a solution is given by[20]

$$q_c = q_{c,max}(f_M - f_P) \tag{2-1}$$

where f_M (f_P) is the fraction of the left-handed (right-handed) helix component, and $q_{c,max}$ is q_c at $f_M = 1$ and $f_P = 0$. For the cholesteric LC solution of a helical poly-**1**-HCl induced by a chiral acid, $q_{c,max}$ is experimentally available from the titration experiments under the fixed polymer concentration and temperature, if the chiral acid used as a dopant only acts to change the population of the right- and left-handed helices of the dynamically racemic helical poly-**1**-HCl chain through complexation in water, and dissociated acid ions do not directly contribute to the twisting of the helical polymer chains at all. Thus, we can estimate the excess of one helical sense ee_h ($= f_M - f_P$) of the poly-**1**-HCl in a particular cholesteric LC solution showing a different cholesteric pitch under the conditions from eq 2-1 or by

$$ee_h \text{ (in the LC state)} = q_c / q_{c,max} \tag{2-2}$$

while the ee_h in the dilute solution is estimated from $\Delta\varepsilon_{2nd}$ by

$$ee_h \text{ (in the dilute solution)} = \Delta\varepsilon_{2nd} / \Delta\varepsilon_{2nd,max} \tag{2-3}$$

along with the maximum value of $\Delta\varepsilon_{2nd}$ ($\Delta\varepsilon_{2nd,max}$).

The titration experiments with (*S*)-**2** in the aqueous LC state under the constant polymer concentration of 20 wt % at ca. 25 °C gave the minimum cholesteric pitch of 4.06 μm in the presence of 0.3 equiv of (*S*)-**2**, at which the polymer has a single-handed helix in the LC state. The maximum q_c value ($q_{c,max}$) was determined from the titration result. The q_c values were plotted versus the inverse [(*S*)-**2**]/[poly-**1**-HCl], and the maximum q_c value ($q_{c,max}$) was estimated from its intercept ($q_{c,max}$ = 1.55 μm^{-1}) (Figure 2-2A). In the same way, the

maximum $\Delta\varepsilon_{2nd}$ value could be determined to be –17.2 from the CD titration results using (*S*)-**2** in a dilute water solution, at which the polymer is anticipated to have a complete single-handed helix (Figure 2-2B). Based on these values as the base ones, the ee_h values of poly-**1**-HCl induced by chiral acids in a dilute solution and in the LC state can be separately estimated from eqs 2-3 and 2-2, respectively, leading to the direct evaluation for the amplification of the intrinsic helical sense excess of the poly(phenylacetylene) by the LC state that can be demonstrated by comparing the ee_h values.[21]

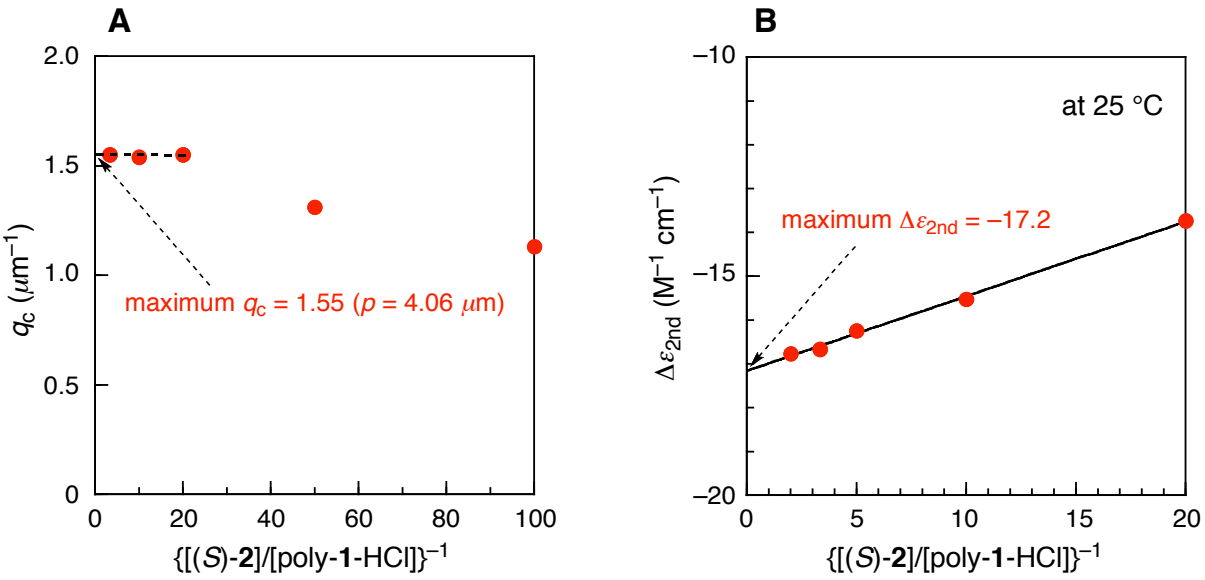

Figure 2-2. (A) Plots of the q_c of poly-**1**-HCl ([poly-**1**-HCl] = 20 wt %) versus {[(*S*)-**2**]/[poly-**1**-HCl]}$^{-1}$ in concentrated water solution at ca. 25 °C. (B) Plots of the ICD intensity ($\Delta\varepsilon_{2nd}$) of poly-**1**-HCl ([poly-**1**-HCl] = 1 mg/mL) versus {[(*S*)-**2**]/[poly-**1**-HCl]}$^{-1}$ in water at 25 °C.

As chiral acids, the author selected different functional acids (**2**–**7**; Chart 2-1) as excellent (**2**, **4**, and **5**), moderate (**3**), and poor (**6** and **7**) helicity inducers in dilute water according to the recently reported results,[9b] and the ee_h values of poly-**1**-HCl in dilute and concentrated liquid crystalline water solutions were calculated using the maximum $\Delta\varepsilon_{2nd}$ and q_c values of –17.2 M^{-1} cm^{-1} and 1.55 μm^{-1} as the base values, respectively, as described above.

These results are summarized in Table 2-1 and the calculated ee_h values of poly-**1**-HCl in the cholesteric LC state are plotted versus those in dilute water (Figure 2-3). If the helical sense ratio of the poly-**1**-HCl induced by the chiral acids in dilute water remained in the LC state, we should observe a linear relation between the ee_h values in dilute solution and cholesteric LC. However, a positive nonlinear relationship between the helix-sense excesses of poly-**1**-HCl in dilute solution and those in the cholesteric LC state was observed, which clearly demonstrates the amplification of the helical sense excess in the LC state (Figure 2-3). As well as **2**, a chiral aliphatic carboxylic acid (**3**), sulfonic and phosphoric acids (**4** and the sodium salt of adenosine diphosphate (ADP, **5**), respectively), and amino acids (**6** and **7**) were found to assist in the cholesteric LC formation in the concentrated aqueous poly-**1**-HCl solutions.

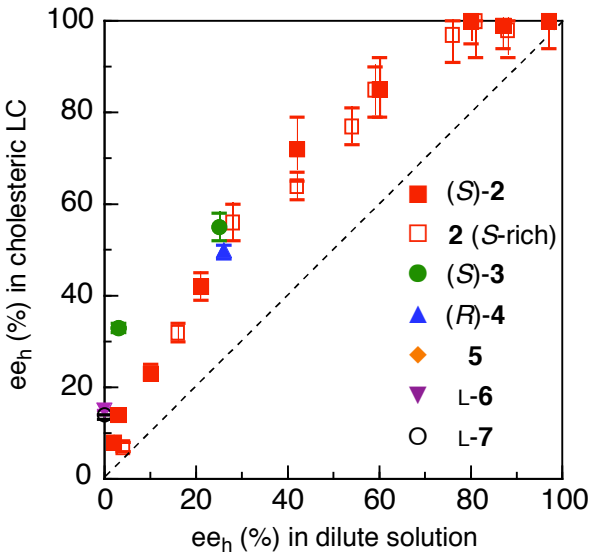

Figure 2-3. Plots of the calculated ee_h values of poly-**1**-HCl in the presence of chiral dopants ((*S*)-**2** (■), **2** (*S* rich) (□), (*S*)-**3** (●), (*R*)-**4** (▲), **5** (◆), L-**6** (▼), and L-**7** (○)) in the cholesteric LC state versus those in dilute water (see Table 2-1). The ee_h values of poly-**1**-HCl in dilute and concentrated liquid crystalline water solutions were calculated using the maximum $\Delta\varepsilon_{2nd}$ and q_c values of –17.2 and 1.55 as the base values, respectively.

Poly-**1**-HCl formed an excess one helical sense over of 80% ee_h in the presence of (*S*)-**2** equal or greater than 0.05 equiv and **2** of more than 50% ee in a dilute solution (runs 1–3, 10, and 11 in Table 2-1). In the LC state, however, the ee_h value became slightly higher, resulting in the almost perfect single-handed helix in the LC state. A noticeable chiral amplification of poly-**1**-HCl in the LC state was observed when smaller amounts of (*S*)-**2** and **2** of low ee were used (runs 4–9 and 12–18 in Table 2-1). The excess of a one helical sense induction in poly-**1**-HCl through a noncovalent bonding interaction with chiral acids such as (*S*)-**2** involves an equilibrium, so that one may think that the ICD intensity may depend on the concentration of the polymer. However, the ICD intensity scarcely changed in the polymer concentrations ranging from 0.1 to 5.0 wt % in the presence of 0.1 equiv of a 20% ee of (*S*)-**2** (run 14 in Table 2-1). The author further estimated the degree of complexation (f_c) of poly-**1**-HCl with **2** of 20% ee (*S* rich) by potentiometric pH titration according to the reported procedure,[22] since the amino group of poly-**1**-HCl must take one of the two following forms: the complex form with **2** (20% ee) and the free ammonium ion in an aqueous solution. The determined f_c value thus obtained for the solutions with the polymer concentrations ranging from 0.1 to 1.0 wt % in the presence of 0.1 equiv **2** (20% ee) was almost 0.1 irrespective of the polymer concentration. This indicates that all the **2** (20% ee) in the polymer solution are complexed with the amino groups of the polymer. Since we can expect that the degree of complexation maintains this value with the further increasing polymer concentration under the condition of [**2** (20% ee)]/[poly-**1**-HCl] = 0.1, the author concluded that the content of the complexed monomer units in the poly-**1**-HCl does not depend on the polymer concentration. This is consistent with the polymer concentration independence of the ICD intensity, and furthermore, verifies that the chiral amplification in the LC phase takes place at the constant content of the complexed monomer units in the poly-**1**-HCl. The chiral sulfonic and phosphoric acids ((*R*)-**4** and **5**) could also induce an excess of a one helical sense in poly-**1**-HCl with 0.1 equiv of the acids in dilute solution (runs 21 and 23 in Table 2-1). However, 0.01 equiv (*R*)-**4** and 0.001 equiv **5** induced a only slightly excess of the one-helical sense and an almost racemic helix in

the poly-**1**-HCl, respectively, in dilute solution (runs 22 and 24 in Table 2-1). In the LC state, however, the helicity was amplified, resulting in the larger helical sense excess in the polymer. The author notes that the L-amino acids **6** and **7** (0.1 equiv) are poor helicity inducers, and could not induce an ICD in poly-**1**-HCl at all in the dilute (0.1 wt %) and more concentrated polymer solutions (5 wt %) (runs 25 and 26 in Table 2-1). However, in the LC state (20 wt %), the chirality is in fact amplified, leading to a cholesteric LC, where the polymer has an excess helical sense of 14–15% ee_h. These convincing results provide a direct evidence for the amplification of chirality in the LC state, and demonstrate a highly sensitive chirality sensing system.

Table 2-1. Signs and $\Delta\varepsilon_{2nd}$ Values in Dilute Solution, Cholesteric Helical Pitch (p) and Cholesteric Wavenumber (q_c) in Concentrated Solution, and Excess of One Helical Sense (ee_h) of Poly-**1**-HCl Induced by Chiral Dopants in Dilute and Concentrated LC Solutions

run	chiral dopant	[dopant]/ [poly-**1**-HCl]	dilute solution (1 mg/mL)		lyotropic LC (20 wt %)		
			$\Delta\varepsilon_{2nd}$(M^{-1} cm^{-1}) [λ (nm)]	ee_h (%)[a]	p (μm)[b]	q_c (μm^{-1})[b]	ee_h (%)[c]
1	(*S*)-**2**	0.3	–16.7 (361)	97	4.06 ± 0.25	1.55 ± 0.10	100 ± 6
2	(*S*)-**2**	0.1	–15.0 (361)[d]	87	4.10 ± 0.25	1.54 ± 0.09	99 ± 6
3	(*S*)-**2**	0.05	–13.7 (361)	80	4.06 ± 0.22	1.55 ± 0.08	100 ± 5
4	(*S*)-**2**	0.02	–10.3 (361)	60	4.79 ± 0.38	1.32 ± 0.10	85 ± 6
5	(*S*)-**2**	0.01	–7.26 (361)	42	5.66 ± 0.54	1.12 ± 0.11	72 ± 7
6	(*S*)-**2**	0.005	–3.63 (361)	21	9.64 ± 0.62	0.65 ± 0.04	42 ± 3
7	(*S*)-**2**	0.002	–1.70 (361)	10	17.5 ± 1.0	0.36 ± 0.02	23 ± 1
8	(*S*)-**2**	0.001	–0.58 (361)	3	28.9 ± 1.9	0.22 ± 0.01	14 ± 1
9	(*S*)-**2**	0.0005	–0.39 (358)	2	53.6 ± 3.3	0.12 ± 0.01	8 ± 1
10	**2** (75% ee)[e]	0.1	–15.1 (361)	88	4.15 ± 0.25	1.52 ± 0.09	98 ± 6
11	**2** (50% ee)[e]	0.1	–13.9 (360)	81	4.06 ± 0.36	1.55 ± 0.13	100 ± 8
12	**2** (40% ee)[e]	0.1	–13.0 (361)	76	4.19 ± 0.24	1.51 ± 0.09	97 ± 6
13	**2** (25% ee)[e]	0.1	–10.2 (361)	59	4.82 ± 0.32	1.31 ± 0.09	85 ± 6
14	**2** (20% ee)[e]	0.1	–9.22 (361)[f]	54	5.25 ± 0.25	1.20 ± 0.06	77 ± 4
15	**2** (15% ee)[e]	0.1	–7.20 (361)	42	6.35 ± 0.34	0.99 ± 0.05	64 ± 3
16	**2** (10% ee)[e]	0.1	–4.90 (361)	28	7.27 ± 0.50	0.87 ± 0.06	56 ± 4
17	**2** (5% ee)[e]	0.1	–2.76 (361)	16	12.5 ± 0.6	0.50 ± 0.03	32 ± 2
18	**2** (1% ee)[e]	0.1	–0.65 (359)	4	58.0 ± 2.8	0.11 ± 0.01	7 ± 1
19	(*S*)-**3**	0.1	–4.23 (361)[d]	25	7.42 ± 0.37	0.85 ± 0.04	55 ± 3
20	(*S*)-**3**	0.01	–0.56 (361)	3	12.5 ± 0.6	0.51 ± 0.02	33 ± 1
21	(*R*)-**4**	0.1	–15.4 (359)[d]	90	—	—	—
22	(*R*)-**4**	0.01	–4.39 (360)	26	8.21 ± 0.16	0.77 ± 0.02	50 ± 1
23	**5**	0.1	+13.7(361)[d]	80	—	—	—
24	**5**	0.001	+0.32 (361)	2	52.2 ± 3.4	0.12 ± 0.01	8 ± 1
25	L-**6**	0.1	[d,g]	~0	27.3 ± 0.9	0.23 ± 0.01	15 ± 1
26	L-**7**	0.1	[d,g]	~0	29.4 ± 1.2	0.21 ± 0.01	14 ± 1

[a] Estimated using $\Delta\varepsilon_{2nd}$ = –17.2 as the base value. [b] Estimated on the basis of an evaluation of ca. 30 fingerprint spacings. [c] Estimated using the maximum q_c = 1.55 as the base value. [d] Cited from ref 9b. [e] (*S*)-Isomer rich. [f] Almost no change in the $\Delta\varepsilon_{2nd}$ value was observed when the concentration of poly-**1**-HCl was 1, 5, 10, and 50 mg/mL (0.1, 0.5, 1.0, and 5 wt %). [g] No distinctive CD was observed even when the concentration of poly-**1**-HCl was 1 and 50 mg/mL (0.1 and 5 wt %).

Persistence Length Measurements. The author next estimated the backbone stiffness (persistence length (q)) of poly-**1**-HCl before and after the single-handed helicity induction thus showing nematic and cholesteric LC phases in concentrated water solutions, respectively, by measuring their isotropic–LC phase boundary concentrations.[23] The cholesteric and nematic LC poly-**1**-HCl solutions were prepared in water (10 wt %) in the presence of 0.1 equiv of (*S*)-**2** and NaCl, respectively. NaCl was used to reduce the effect of the salt concentration on the phase boundary concentration measurements for the nematic LC poly-**1**-HCl. These solutions were gradually diluted with water until the birefringence disappeared during polarizing optical microscopy. The concentration at which the birefringence disappeared was taken as the isotropic–LC phase boundary concentration C_i. The q values can be calculated by the theory of Khokhlov and Semenov[23] combined with the theory of Stroobants et al.[23c] when the molar mass per unit contour length (M_L), the C_i, and the isotropically averaged effective molecular diameter d_{eff}[24] are given (see the Experimental Section). The author notes the determined q values thus obtained for an optically inactive poly-**1**-HCl and a single-handed helical poly-**1**-HCl in the nematic and cholesteric LC states were 26.2 and 28.0 nm, respectively. These large q values indicate that both the poly-**1**-HCls are rigid and their LC formations are definitely based on their main chain stiffness.[25] The author notes that the q values are almost the same for both the optically active and inactive poly-**1**-HCls or the latter is only a little smaller than the former.

The author first considered that the optically inactive poly-**1**-HCl might have a shorter persistence length than the single-handed helical poly-**1**-HCl, since the former poly-**1**-HCl chain is expected to have more helical reversals. However, the optically active and inactive poly-**1**-HCls actually have similar q values, indicating that kinks due to the helical reversal in the polymer chain are too few to contribute to the chain flexibility and the alternative contribution of the torsional fluctuation in the polyacetylene chain may be predominant.[7] Consequently, the dynamically racemic poly-**1**-HCl helices may have a long helical sequence with few helical reversals. Such a stiff helical polyacetylene is expected to form a regular

helical structure over long distance so that the helical conformation may be determined from the X-ray analysis. In fact, the helical structures of the liquid crystalline polyisocyanates and polysilanes having a large persistence length have been determined by the X-ray analyses of the corresponding oriented films to be 8 unit / 3 turn helix (8/3)[26] and 7 unit / 3 turn helix (7/3), respectively.[4g,27]

Helical Structure. *Cis-transoidal* poly(phenylacetylene)s have been considered to have a helical conformation because of the steric effect between the main chain protons and the phenyl substituents at the vicinal units that may cause a deviation from planarity,[6,7,10c-e,g,13-15] although their exact helical structures have not yet been determined.[28] The three-dimensional solid-state structures of the optically inactive and active poly-**1**-HCls were then investigated by X-ray analysis. Figures 2-4A and 2-4B show the wide angle X-ray diffraction (WAXD) patterns of the uniaxially oriented poly-**1**-HCl and poly-**1**-HCl—(*S*)-**2** films prepared from concentrated nematic and cholesteric LC water solutions, respectively. X-ray photographs were taken from the edge-view position with a beam parallel to the film surface at ambient temperature (20—25 °C). Any heat treatment of the samples was not performed, because the poly-**1**-HCl is thermally unstable and *cis*-to-*trans* isomerization took place at high temperature (>100 °C), although the poly-**1**-HCl is quite stable in solution and in the solid state at ambient temperature (20—25 °C) for a long time and the diffraction patterns did not change after ca. one month at ambient temperature (20—25 °C).

Surprisingly, the X-ray diffractions of an oriented optically inactive poly-**1**-HCl film (Figure 2-4A) and an optically active, single-handed helical poly-**1**-HCl—(*S*)-**2** film ([(*S*)-**2**]/[poly-**1**-HCl] = 0.1) (Figure 2-4B) showed essentially the same pattern, exhibiting diffuse, but apparent equatorial and near- and off-meridional reflections (for the WAXD patterns with different ranges of sensitivities, see Figure 2-9 in the Experimental Section). In Figures 2-4A and 2-4B, the WAXD intensities were not perfectly symmetrical and the meridian directions in both the WAXD patterns are not perfectly vertical-aligned. Because the samples were made

by piling up several uniaxially oriented, thin and rectangle-shaped films of ca. 10 mm length, 1.5 mm width, and 0.02 mm thickness (Experimental Section), it was difficult to align perfectly the samples with the orientation axes in each film. In addition, the samples were so soft and flexible and had a slightly arc-like shape, which made it difficult to set the oriented samples perfectly normal to the beam, that is, the helical axes of the films were not perfectly parallel to the meridian direction, which may also cause the different pass lengths in the top and bottom half, resulting in slightly dissymmetrical WAXD intensities.[29] The four equatorial reflections, 17.23, 9.92, 8.59, and 6.50 Å for poly-**1**-HCl and 16.64, 9.61, 8.32, and 6.31 Å for poly-**1**-HCl—(*S*)-**2**, can be visually indexed with a two-dimensional hexagonal lattice of a = 19.84 and 19.21 Å, respectively, and the observed d-spacings are listed in Table 2-2. The author then determined the fiber periods to be 49.74 Å (= c) from the layer lines, and attempted to index the reflections based on the hexagonal unit cell, but the 3rd and 5th layer line reflections could not be indexed.

Next, the author used a larger orthogonal lattice with the hexagonal symmetry, and found that all the reflections including a series of equally spaced layer line reflections (1/49.74 $Å^{-1}$ apart) attributed to the helical poly-**1**-HCl and poly-**1**-HCl—(*S*)-**2** structures can be reasonably indexed to an orthorhombic unit cell with a = 34.36, b = 19.84, and c = 49.74 Å for poly-**1**-HCl and a = 33.29, b = 19.21, and c = 49.74 Å for poly-**1**-HCl—(*S*)-**2**, where the reflections on the 3rd and 5th layer lines can also be reasonably indexed to (213) and (123), and (415), respectively (Table 2-2).[30] Although the author could not observe a meridional reflection on the 23rd layer line (2.16 Å) (see Table 2-2) corresponding to the unit height (h) of the helical structures even when the X-ray measurements were performed using a cylindrical camera with the samples tilted ca. 21° normal to the beam, the most plausible structure of the helical poly-**1**-HCl and poly-**1**-HCl—(*S*)-**2** can be proposed to be a 23 unit / 10 turn helix (23/10) by considering the density measurement results[31] combined with the layer lines observed in the X-ray diffraction patterns. The orthorhombic unit cell of the poly-**1**-HCl is assumed to contain four helices or two double helices of the polymer chain, which

requires the density of 1.135 g/cm^3, that is in good agreement with the observed value (1.142 g/cm^3).[31] In addition, when the number of repeating units per the fiber period is assumed to be other than 23, the observed density was considerably different from the calculated density (see the Experimental Section). On the other hand, the observed density of the poly-**1**-HCl—(*S*)-**2** ([(*S*)-**2**]/[poly-**1**-HCl] = 0.1) film (1.178 g/cm^3)[31] was different from the calculated value (1.272 g/cm^3) for this unit cell containing four helices of the poly-**1**-HCl chain complexed with 0.1 equiv (*S*)-**2**. The reason is not clear at the present, but highly disordered location of the 0.1 equiv (*S*)-**2** molecules in the film and NaCl precipitation during the sample preparation, resulting in the formation of defects and giving rise to voids between polymer films and NaCl particles, respectively, should be taken into consideration for the lower observed density of the poly-**1**-HCl—(*S*)-**2** film. Although the relatively strong reflections on the 10th and 13th layer lines corresponding to the first-order Bessel functions are consistent with the helical diffraction theory,[32] the rather strong reflection observed in the 8th layer line reflection is not clearly understood. The validity of the 23/10 helical structure has been confirmed by Miyazawa's equation. (see Figure 2-11 and the Experimental Section).

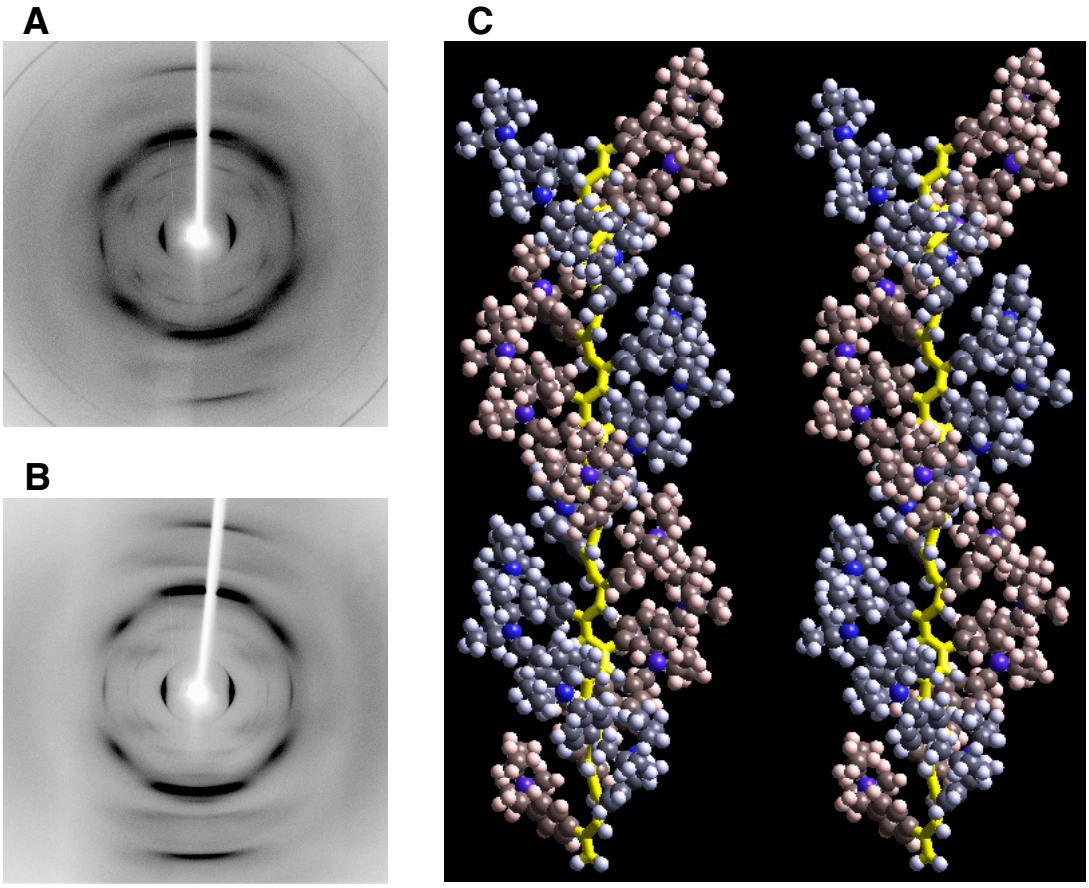

Figure 2-4. X-ray diffraction patterns of oriented optically inactive poly-**1**-HCl film (A) and optically active poly-**1**-HCl—(*S*)-**2** film (B) taken from the edge-view position with a beam parallel to the film surface; the vertical direction is nearly corresponding to the helical axis. The two Debye-Scherrer rings that appeared on the higher angle side in B are assigned to the 111 (3.26 Å) and 200 (2.82 Å) reflections from the precipitated NaCl during the sample preparation. Stereoview of a possible 23/10 helical structure of poly-**1** (23-mer) is shown in C using the space-filling model. The main chain carbon atoms are shown in yellow using the cylinder model for clarity. The 4-(*N*,*N*-diisopropylaminomethyl)phenyl substituents, represented by light blue and red for clarity, arrange in a helical array with a predominant screw-sense along the polymer backbone.

Table 2-2. X-ray Diffraction Data of Optically Inactive (Poly-**1**-HCl) and Optically Active (Poly-**1**-HCl—(*S*)-**2**) Oriented Films

layer line *l*	optically inactive poly-**1**-HCl				optically active poly-**1**-HCl—(*S*)-**2**			
	d_{obs} / Å[a]	d_{cal} / Å[b]	*h k*[b]	I_{obs}[c]	d_{obs} / Å[a]	d_{cal} / Å[d]	*h k*[d]	I_{obs}[c]
0	17.23	17.18	1 1, 2 0	vs	16.64	16.64	1 1, 2 0	vs
	9.92	9.92	0 2, 3 1	vw	9.61	9.61	0 2, 31	vw
	8.59	8.59	2 2 , 4 0	m	8.32	8.32	2 2, 4 0	m
	6.50	6.49	13,42,51	s	6.31	6.29	13,42,51	s
2	9.29	9.21	0 2, 3 1	w	8.93	8.96	0 2, 3 1	w
3					11.79	11.74	1 1, 2 0	vw
	10.19	10.22	2 1	m				
					8.31	8.31	0 2, 3 1	m
	8.12	8.26	1 2	m				
					7.50	7.44	2 2, 4 0	w
5	8.67	8.61	1 1, 2 0	w	8.59	8.54	1 1, 2 0	m
	6.10	6.18	4 1	vs	6.07	6.06	4 1	s
6	8.19	8.29	nm[e]	vw				
7	7.12	7.10	nm[e]	m				
					6.56	6.53	1 1, 2 0	m
8	6.12	6.22	streak	vs	6.11	6.22	streak	vs
9	5.55	5.53	nm[e]	m	5.57	5.53	nm[e]	m
10	4.83	4.82	0 1	m				
	4.63	4.64	2 1	w	4.58	4.62	2 1	w
					4.27	4.27	2 2, 4 0	vw
13	3.83	3.83	nm[e]	s	3.83	3.83	nm[e]	s
23	*f*	2.16	0 0		*f*	2.16	0 0	

[a] Spacings observed in X-ray diffraction patterns of poly-**1**-HCl oriented films. [b] Spacings calculated and indexed on the basis of an orthorhombic unit cell with parameters, a = 34.36, b = 19.84, and c = 49.74 Å. [c] Observed intensities; vs = very strong, s = strong, m = medium, w = weak, and vw = very weak. [d] Spacings calculated and indexed on the basis of an orthorhombic unit cell with parameters a = 33.29, b = 19.21, and c = 49.74 Å. [e] Near meridional reflections. These reflections may be indexed as 10*l*, which should be split across the meridian. However, the imperfect orientation of the films may result in such arc-like reflections linked at the meridian, and their calculated *d* values were estimated as the 00*l* reflections because these reflections were read along the meridian. [f] Not observed.

Figure 2-4C illustrates the molecular structure of the 23/10 helix of the right-handed helical poly-**1** model (23-mer), where the bond lengths (C=C: 1.374 Å and C–C: 1.466 Å), the bond angles (C–C=C: 128.8° and C=C–C: 124.8°), and the dihedral angles (C–C=C–C: 0° (*cis*), C=C–C=C: *transoid* (140.3°)) were used as the internal coordinates (see the Experimental Section). The author noted that when the poly-**1** main chain has a right-handed helical structure, poly-**1** has the opposite left-handed helical array of the pendants (23 unit / 1.5 turn helix with a helical pitch of 33.16 Å). All the diffractions could be indexed in a reasonable way based on this model, but due to the limited resolution and number of reflections and the unobservable repeat length reflection (unit height, h = 2.16 Å), the proposed 23/10 helix may need a further minor revision, because the author could not perfectly explain the observed X-ray diffraction intensities and could not determine the space group at the present time, which may result from the irregular twist of the phenyl rings, the random arrangement of the chloride ions, and a specific interdigitated or intertwined double-helical packing of the polymer chains. In particular, the determination of the packing-mode is difficult because there are a lot of things that should be decided, for instances, the helical-senses (right-handed and left-handed), the direction of the helical chain (upward and downward), and single or double-helical conformations, etc. Preliminary molecular modeling studies indicate that the orthorhombic unit cell can be totally filled with interdigitated four single-handed 23/10 helices of poly-**1** without any unfavorable overlapping of the chains. The interdigitated dense packing of the chains requires favorable nonbonded interactions between the surface of the helices in a "ridges-and-grooves" fashion as reported for helical polypeptides.[33] In a similar way, a double-helical structure model[33a,f] may be assumed, when the unit cell is filled with two double-helices, located in the center and at the corner of the lattice.[30a–e] In this packing-mode, the hexagonal symmetry is also maintained. In addition, the systematic absence of the reflections, (h + k) odd for hk0 may be reasonable. Such single- and double-helices packing structures must influence the observed X-ray intensities. Further three-dimensional structural refinements including a double helix are in progress.

Although the packing-mode has not been elucidated yet, these X-ray results suggest that the poly-**1**-HCls before and after the preferred-sense helicity induction may possess the same helical conformation (23/10 helix) independent of their helical sense ratio, specifically in the solid state prepared from the liquid crystalline water solutions, as evidenced by their essentially same layer reflections. The author first thought that the poly-**1**-HCl might show rather broad and different X-ray diffractions from those of the single-handed helical poly-**1**-HCl—(*S*)-**2** because the poly-**1**-HCl consists of equal amounts of interconvertible right- and left-handed helical conformations separated by helix reversals in dilute solution, and the kink due to the helix reversal may cause more or less disordered packing of the polymer chains. However, the present X-ray results together with the fact that both polymers have almost the same persistence length support our speculation that poly-**1**-HCl may have a stiff helical polymer with long alternating left- and right-handed helical segments (long helical persistence length) separated by rarely occurring helix reversals even in dilute solution, the population of which may be further reduced even in the nematic LC state to form the racemic single-handed helices (see Figure 2-5). As a result, the poly-**1**-HCl exhibited the same X-ray diffraction pattern as that of the single-handed helical poly-**1**-HCl. The possibility that the original poly-**1**-HCl has very few helical reversals in dilute solution cannot be excluded. However, the fact that the helical sense excess is further amplified in the LC state suggests that the original poly-**1**-HCl may have more or less helical reversals, the population of which may be reduced during the LC formation.[4e] Apparently, the author needs further experiments to estimate the helical persistence length of the polymer[34] before and after the preferred-sense helicity induction in a dilute water solution. This, however, may be the first unambiguous evidence that poly(phenylacetylene)s are in fact a dynamically racemic helical polymer composed of interconvertible right- and left-handed helical segments, and this unique helical characteristic is responsible for their remarkable amplification of the chirality in dilute solution and further in the LC state.

On the basis of these results, the author proposes a possible mechanism for the hierarchical amplification process of the macromolecular helicity of poly-**1**-HCl mediated by a nonracemic dopant in dilute and concentrated water solutions (Figure 2-5). The original poly-**1**-HCl is a rigid rod dynamic helical polymer with interconvertible long right- and left-handed helical segments separated by rarely occurring helix reversals in dilute solution. Therefore, upon complexation with a small amount nonracemic acid or even with that of a low ee, a greater excess one helical sense than that expected from the amount or ee of the acid is induced in the polymer ("sergeants and soldiers"[35] and "majority" effects[36]),[2a,b,j] thus showing an ICD, whereby the chiral information of the nonracemic acid transfers to the polymer backbone as an excess of a single-handed helix with high cooperativity in dilute solution. The macromolecular helicity induced in the polymer is further amplified in the LC matrix, resulting in the increase in the helical sense excess of the polymer, probably by the reduction in population of the helical reversals as observed in the polyisocyanates by Green et al.[4e]

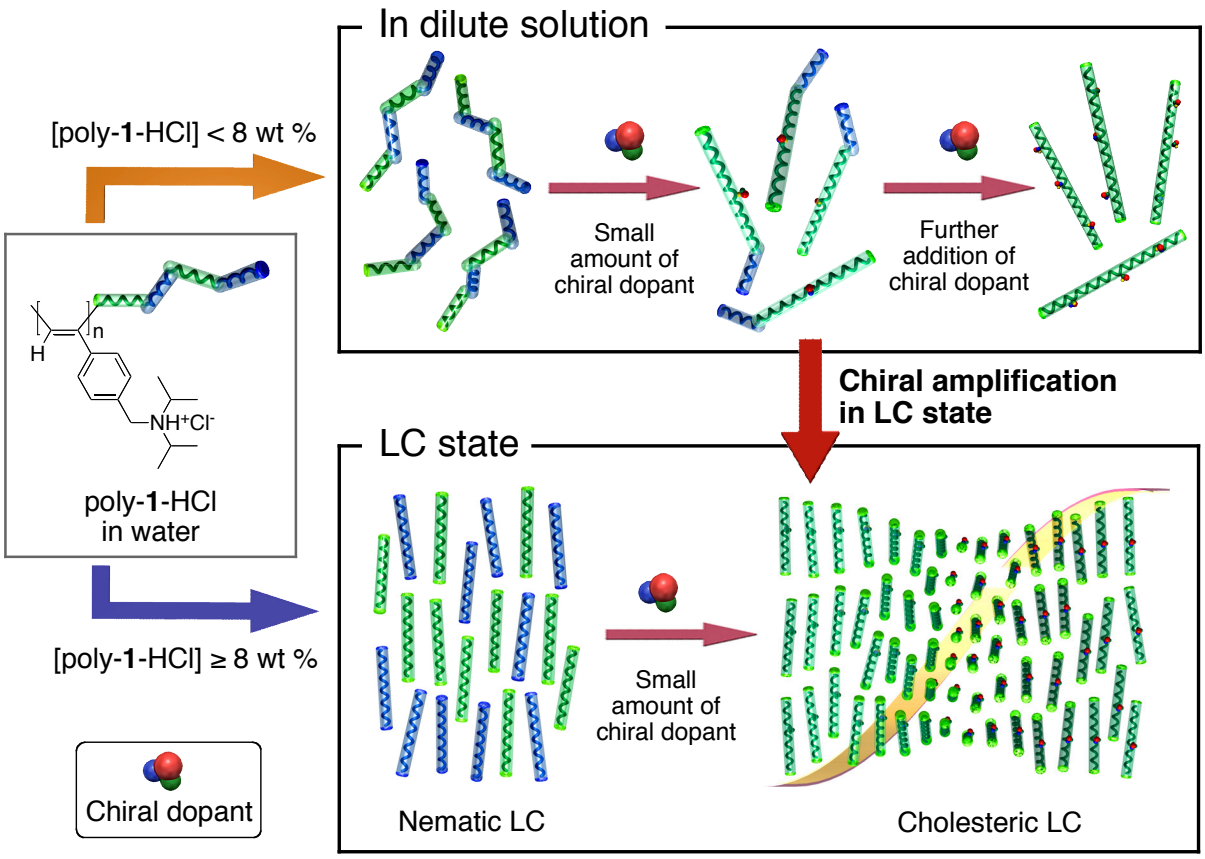

Figure 2-5. A possible mechanism of the hierarchical amplification process of the macromolecular helicity of poly-**1**-HCl mediated by a nonracemic dopant in dilute and concentrated water solutions. Poly-**1**-HCl has interconvertible, right- (green) and left-handed (blue) dynamic helical conformations separated by rarely occurring helix reversals in dilute solution. Excess of preferred-sense helical sense (right- or left-handed helix) of poly-**1**-HCl is induced with a small amount of chiral dopant and further addition of the chiral dopant is required for a complete single-handed helix formation in poly-**1**-HCl in dilute solution (upper). In LC state, the population of helix reversals may be reduced even in the nematic LC state to form the racemic single-handed helices. In the presence of a small amount of chiral dopant, chirality is significantly amplified, resulting in a single-handed helical supramolecular assembly, thus showing a cholesteric LC phase (bottom).

Conclusions

In summary, the author has demonstrated a novel hierarchical amplification of chirality during the transfer of chiral information from nonracemic guests to the helical systems either at macromolecular and subsequent supramolecular mesoscopic levels, leading to an easily measurable excess of one helical sense in a dynamic helical polyacetylene, which can be detected by measuring the CD of the polymer or the mesoscopic cholesteric twist in the LC state if the CD is not available. The main chain stiffness with a dynamic helical characteristic that allows a formation of the LC phase is essential for realizing this hierarchical amplification of the chirality system for detecting and sensing a small chiral bias of the guest molecules. The present results including the helical structure (23/10 helix) proposed by the X-ray diffraction studies will contribute to developing a more efficient chirality-sensing system based on liquid crystalline helical polyacetylenes through the hierarchical amplification of chirality in the LC state.

Experimental Section

Materials. Deionized distilled water was used in all the experiments unless otherwise noted. Optically active compounds were obtained from Aldrich or Tokyo Kasei (TCI, Tokyo, Japan). (*S*)- and (*R*)-**2** and (*S*)-**3** were prepared by the reaction of the corresponding carboxylic acids with aqueous NaOH. The stereoregular *cis-transoidal* poly-**1** was prepared by the polymerization of the corresponding monomer with a rhodium catalyst according to the previously reported method.[6c,d,9] The resulting polymer was quantitatively converted to its HCl salt (poly-**1**-HCl) with aqueous HCl, followed by precipitation into acetone; its number-average molecular weight (M_n) and molecular weight distribution (M_w/M_n) were 3.4×10^5 and 2.21, respectively, as determined by size exclusion chromatography (SEC).[9] The M_n and M_w/M_n were also estimated by atomic force microscopy (AFM)[19] and were 2.36×10^5 and 1.43, respectively. The stereoregularity of the original poly-**1** and poly-**1**-HCl were investigated by ^{1}H NMR and laser Raman spectroscopies.[13a,14a,37] Previously, the author reported that the stereoregularity of poly-**1**-HCl could not be determined by its ^{1}H NMR spectrum in D_2O because of the broadening of the main chain protons even at 80 °C, probably due to the rigidity of the polymers' main chains.[9] However, the ^{1}H NMR spectrum of the original poly-**1** in CD_3CN in the presence of CF_3CO_2D showed a sharp singlet centered at 5.76 ppm, due to the main chain proton, indicating that poly-**1** possesses a highly *cis-transoidal*, stereoregular structure (Figure 2-6). The exact *cis* content was estimated to be 96% by using the following equation based on the literature method for poly(phenylacetylene)[14a,37d]

$$\% \; cis = [A_{5.76}/(A_{total}/21)] \times 100 \qquad (2\text{-}4)$$

where $A_{5.76}$ and A_{total} represent the area of the main chain proton resonance at 5.76 ppm and the total area of all proton resonances of poly-**1** in its ^{1}H NMR spectrum (Figure 2-6). Poly-**1**-HCl was then converted to poly-**1** by treatment with aqueous NaOH and its ^{1}H NMR spectrum of the recovered poly-**1** was measured under the same conditions. The recovered poly-**1** exhibited the identical spectrum as that of the original poly-**1**, indicating that poly-**1**-

HCl also has a highly *cis-transoidal* structure. The Raman spectra of poly-**1** and poly-**1**-HCl (Figure 2-7) also support this conclusion; poly-**1** and poly-**1**-HCl showed characteristic vibrations in the *cis* polyacetylenes, while those in the *trans* polyacetylene were scarcely observed.[38] Consequently, the poly-**1**-HCl is a highly stereoregular *cis-transoidal* (*cis* content > 96%) polymer.

The author also carefully examined the thermal stability of poly-**1**-HCl with (*R*)-**2** and confirmed that the polymer was quite stable in water. The thermal stability of poly-**1**-HCl with (*R*)-**2** ([poly-**1**-HCl] = 1.0 mg/mL, [(*R*)-**2**]/[poly-**1**-HCl] = 0.5) in water was investigated by CD and absorption spectroscopies and SEC measurements. After heating the complex solution at 60 °C for 8 h under an anaerobic atmosphere, the complex showed a slight decrease in the CD intensity of ca. 8% without any change in the absorption spectrum. The M_n of the annealed sample slightly decreased (ca. 7%) with a negligible change in its distribution (M_w/M_n). Moreover, the CD intensity did not change after leaving the sample for 15 days at room temperature. These results suggest that the polymer is quite stable in water.[39]

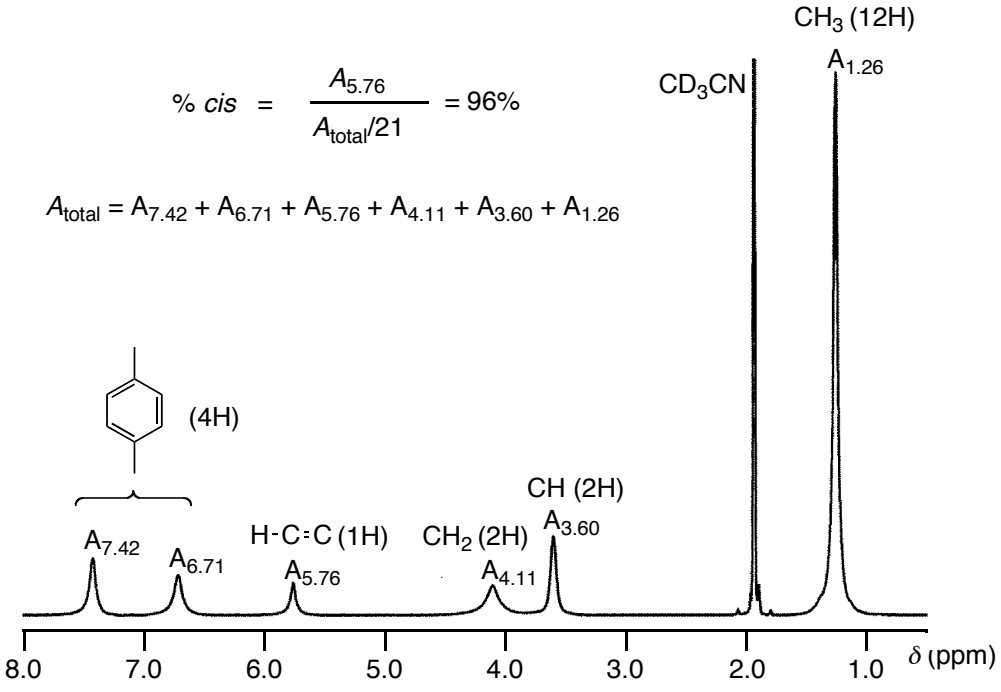

Figure 2-6. ^{1}H NMR spectrum of poly-**1** in CD_3CN with CF_3CO_2D ([CF_3CO_2D]/[poly-**1**] = 2) at 60 °C.

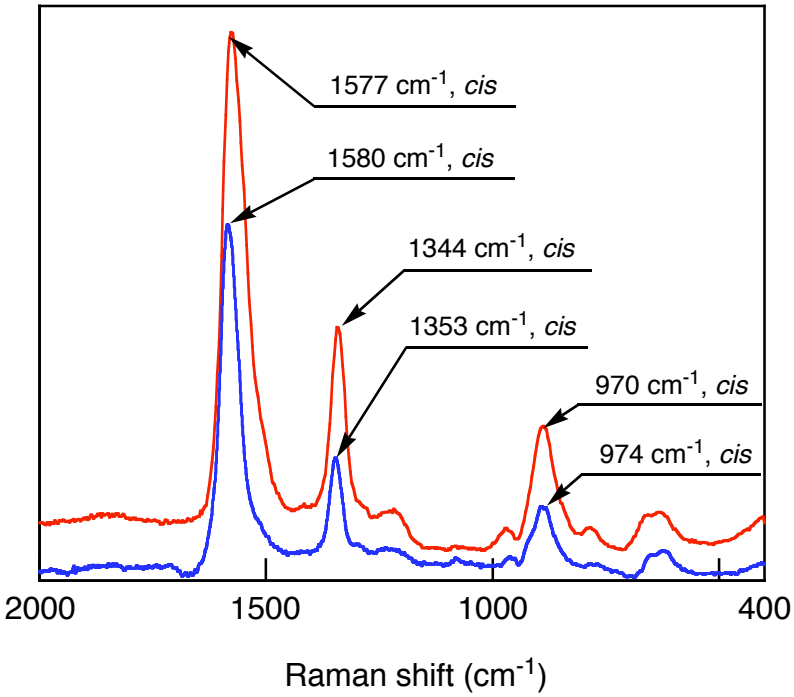

Figure 2-7. Laser Raman spectra of poly-**1** (red line) and poly-**1**-HCl (blue line).

Instruments. ^{1}H NMR spectra were taken using a Varian VXR-500S spectrometer operating at 500 MHz for ^{1}H. Laser Raman spectra were measured on a JASCO NRS-1000 spectrophotometer. Absorption (JASCO V-570, Hachioji, Japan) and CD (JASCO J-725) spectra were measured in water in a 1.0-mm quartz cell at 25 °C. AFM measurements were performed on a Nanoscope IIIa microscope (Veeco, Santa Barbara, CA) in air at ambient temperature (20–25 °C) with standard silicon tips (NCH-10V) in the tapping mode. AFM images were measured at the resonance frequency of the tips with 125-μm-long cantilevers (200–300 Hz) and a spring constant of approximately 40 N/m. All the images were collected with the maximum available number of pixels (512) in each direction. The scanning speed was at a line frequency of 1.0 Hz. The effective silicon tip radii were estimated with Au colloids (5 nm; ICN Biomedicals, Inc., Aurora, OH) as imaging standards[40] and were 5–10 nm. X-ray measurements were performed with a Rigaku R-AXIS VII detector system equipped with a Rigaku FR-E rotating-anode generator with confocal mirror monochromated Cu Kα radiation (0.15418 nm) focused through a 0.5 mm pinhole collimator, which was

supplied at 45 kV voltage and 45 mA current, equipped with a flat imaging plate of specimen-to-plate distance 300 mm. Elemental analysis was performed by the Nagoya University Analytical Laboratory in School of Engineering. The solution pH was measured with a B-211 pH meter (Horiba, Japan). The molecular modeling and molecular mechanics (MM) calculation were performed on the program system MS Modeling software (version 3.1, Accelrys Inc., San Diego, CA).

Absorption and CD Measurements in Dilute Solution. The concentration of poly-**1**-HCl was calculated on the basis of the monomer units and was 1.0 mg/mL in dilute solution unless otherwise stated. On the complexation of poly-**1**-HCl with optically active acids, a stock solution of poly-**1**-HCl (2.0 mg/mL) in water was prepared in a 5-mL flask equipped with a stopcock. A 500 μL aliquot of the poly-**1**-HCl solution was transferred to a vessel equipped with a screwcap using a micropipette (Nichiryo Nichipet EX, Japan). An appropriate amount of (*R*)- or (*S*)-acid was added to the vessel and the solution was diluted with water to keep the poly-**1**-HCl concentration at 1.0 mg/mL and absorption and CD spectra were measured. The changes in the ICD intensity of poly-**1**-HCl with respect to the ee of **2** (1% < ee < 100%, nonlinear effects) were investigated as follows.[9] The molar ratio of **2** to the monomer units of poly-**1**-HCl was held constant at 0.1. Stock solutions of the (*S*)- and (*R*)-**2** (0.93 mg/mL) in water were prepared in separate 25-mL flasks. The 0.50 mL aliquots of the poly-**1**-HCl solution (2.0 mg/mL) were transferred to eleven 1-mL flasks equipped with stopcocks. Aliquots of the stock solutions of (*S*)- and (*R*)-**2** were then placed in the flasks so that the percent ee of the mixtures (*S*-rich) was 1, 5, 10, 15, 20, 25, 40, 50, 60, 75 and 100, and the solutions were finally diluted with water to maintain the poly-**1**-HCl concentration at 1.0 mg/mL. After mixing the solutions, the CD and absorption spectra were measured for each flask (A–C in Figure 2-1 and Table 2-1). The maximum $\Delta\varepsilon_{2nd}$ value was estimated to be –17.2 from the titration results with (*S*)-**2** in dilute water. The $\Delta\varepsilon_{2nd}$ values were plotted versus the inverse [(*S*)-**2**]/[poly-**1**-HCl] and the data points almost obey a straight line with a positive slope. From the intercept, the maximum $\Delta\varepsilon_{2nd}$ at 25 °C in water was determined (Figure 2-2B).

Preparation of Liquid Crystal Samples for Polarized Microscopy Studies. The concentrated poly-**1**-HCl (5 mg) solution in water (20 wt %; (weight of total polymer) / [(weight of total polymer) + (weight of water)]) was prepared in a 2-mL test tube, for the nematic liquid crystalline poly-**1**-HCl. After the polymer was completely dissolved to give a clear and homogeneous solution, the solution was transferred to a 1.0-mm (i.d.) glass capillary by pipette and the ends then sealed. The cholesteric solutions were prepared in the same way using a 20 wt % poly-**1**-HCl solution in water in the presence of appropriate amounts of optically active acids. The samples were left at ambient temperature (20—25 °C) for one hour or days until stable fingerprint textures were obtained. The fingerprint textures showing the retardation lines for the cholesteric LCs were observed using a NIKON E600POL polarized microscope. The fingerprint spacings, which are equal to the half pitch of the cholesteric helical structure, were measured by comparing it to a photograph of a standard microscopic ruler. The average cholesteric pitches (p) were estimated on the basis of an evaluation of about 30 fingerprint spacings. The maximum q_c ($2\pi/p$) value was determined to be 1.55 μm^{-1} from the titration results with (*S*)-**2** in a concentrated water solution (20 wt %) at ca. 25 °C. The q_c values were plotted versus the inverse [(*S*)-**2**]/[poly-**1**-HCl]. The q_c value reached an almost constant value at 0.05 to 0.3 equiv of (*S*)-**2**. From the intercept, the maximum q_c was determined (Figure 2-2A).

Molecular Length (Weight) and Its Distribution Measurements. AFM was used to estimate the molecular length (weight) of poly-**1**-HCl and its distribution. A stock solution of poly-**1**-HCl (0.0025 mg/mL) in 0.015 M aqueous HCl was prepared. An eight μL sample of the stock solution was dropped on a freshly cleaved mica, the solution was blown off simultaneously with a stream of nitrogen, then the mica substrate was dried *in vacuo* overnight to measure the AFM images in the tapping-mode (Figure 2-8A). Under a dilute condition, single molecules of poly-**1**-HCl could be observed, and such a molecular resolution allowed direct measurements of the average molecular length of poly-**1**-HCl.[19] On the basis of an evaluation of 256 molecules in the AFM images including the image in Figure 2-8A, the

number-average molecular length (L_n = 203 nm), the weight-average molecular length (L_w = 290 nm), and the length distribution (L_w/L_n = 1.43) of poly-**1**-HCl were estimated (Figure 2-8B). These values were measured without compensation for the tip radius of curvature (ca. 10 nm), and so the measured values were overestimated because of the broadening effect of the tip. However, the tip broadening played a minor role in the determination of the contour length of the rodlike species.[41] Polymer lengths were measured using the NIH Image program, developed at the National Institutes of Health (available on the Internet at http://rsb.info.nih.gov/nih-image/). The number-average molecular weight was then calculated to be 2.36×10^5 from the equation, $M_n = (L_n/h) \times M_0$, where h and M_0 represent the unit height (0.2162 nm) estimated from the X-ray analysis of poly-**1**-HCl and the molecular weight (251.79) of the repeating unit of poly-**1**-HCl, respectively.

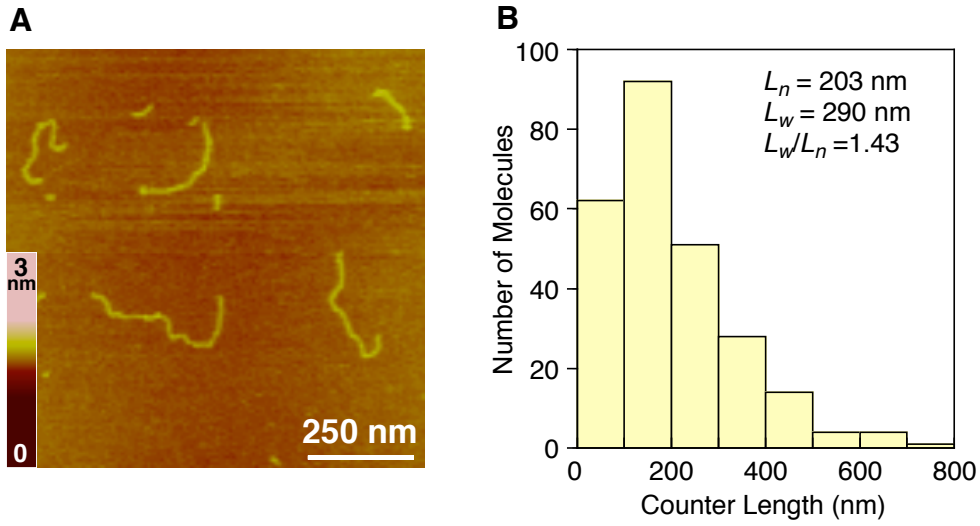

Figure 2-8. (A) The typical tapping-mode AFM height image of poly-**1**-HCl on mica. (B) Histogram of the molecular length distribution of poly-**1**-HCl obtained from the AFM images. Based on of an evaluation of 256 molecules, L_n, L_w, and L_w/L_n were estimated.

Phase Boundary Concentration Measurements. The cholesteric and nematic liquid crystalline poly-**1**-HCl (20.9 mg) solutions were prepared in Mili-Q water (10 wt %) in the presence of 0.1 equiv of (*S*)-**2** and 0.1 equiv of NaCl, respectively, in 3-mL test tubes. NaCl was used to reduce the effect of the salt concentration on the phase boundary concentration measurement for the nematic LC poly-**1**-HCl. The poly-**1**-HCl formed a one-handed helical structure in the presence of 0.1 equiv of (*S*)-**2** in dilute solution, thus showing an almost full ICD. These concentrated solutions were then gradually diluted with Mili-Q water until the optical anisotropy disappeared during polarizing optical microscopy. The concentration where the optical anisotropy disappeared, namely the isotropic-anisotropic LC phase boundary concentration was taken as C_i. The isotropic-nematic LC phase boundary concentration ($C_{i\text{-}n}$) in the presence of 0.1 equiv of NaCl and the isotropic-cholesteric LC phase boundary concentration ($C_{i\text{-}c}$) in the presence of 0.1 equiv of (*S*)-**2** were 0.0784 and 0.0700 g/cm^3, respectively.

Persistence Length Measurements. If the persistence length q, the molar mass per unit contour length M_L (= M_0/h = 1165 nm^{-1}), and the isotropically averaged effective molecular diameter[24] d_{eff} are given, the theory of Khokhlov and Semenov[23a,b,d] allows calculating C_i using

$$C_i = [(3.34 + 11.94N + 6.34N^2)/\{(1 + 0.5868N)N\}](d_{eff}/2q)/\{\pi(d_{eff}/2)^2 N_A/M_L\} \quad (2\text{-}5)$$

where N and N_A are the Kuhn statistical segment number defined by $N = M_w/2qM_L$ and Avogadro's constant, respectively. Although eq 2-5 uses the second virial approximation,[23a,b,d] the higher virial terms are not very important in C_i if C_i is low enough.[1h,42]

According to Stroobants et al.,[23c] d_{eff} can be calculated using the equation

$$d_{eff} = \kappa^{-1}\{\ln(2\pi\nu_{eff}^2 Q/\kappa) + \gamma + \ln 2 - 1/2\} \quad (2\text{-}6)$$

where, κ is the Debye screening length, ν_{eff} is the effective linear charge density, Q is the Bjerrum length (= 0.714 nm in 25 °C water), and γ is Euler's constant (= 0.5772). The value of κ may be calculated by[1h,42b]

$$\kappa^2 = 8\pi Q N_A (C_s + \Gamma z_p C_i / M_w) \quad (2\text{-}7)$$

with the molar concentration C_s of the added salt, the Donnan salt exclusion coefficient Γ, and the valence z_p of the polyion. According to the Manning theory[43] of polyelectrolytes, we write Γ as $1/(4\xi)$, where ξ is the Manning charge density parameter. Since we have checked the full ionization of poly-**1**-HCl in the solution by pH measurements, we can calculate z_p and ξ by $z_p = M_w/M_0$ and $\xi = Q/h$.

Using the Philip-Wooding solution[44] of the Poisson-Boltzmann equation for the charged cylinder, Stroobants et al.[23c] proposed calculating ν_{eff} using

$$\nu_{eff} = 1/\{2QK_0(R^*)\} \quad (2\text{-}8)$$

Here, K_0 is the zero-order modified Bessel function of the second kind, and R^* is given as the solution of

$$1 + (\beta/2)\cot[(\beta/2)\ln(\kappa d/2R^*) + \sin^{-1}\{\beta/(e^{1/2}R^*)\}] = \xi \quad (2\text{-}9)$$

in case of eq 2-9 of the Philip-Wooding solution,[44] where $\beta = 2.65$ and 2.59 for the nematic and cholesteric systems, respectively, and the molecular diameter d is estimated to be 1.918 nm from a model of poly-**1**. The author notes that eq 2-9 has two solutions of R^* for our system. From the criterion that the solution of R^* in case of eq 2-9 must be connected to the solution in case of eq 2-7 with a decreasing ξ, the small R^* is a suitable solution.

The author has searched for values of q leading to the best fit of the experimental $C_{i\text{-}n}$ and $C_{i\text{-}c}$ for the nematic and cholesteric systems, respectively, to the theoretically calculated values from the above equations. It is noted that eq 2-7 contains C_i so that the calculation of C_i must

be iteratively made to produce a consistent C_i in eqs 2-5 and 2-7. The values of q determined by this method were 26.2 and 28.0 nm for the nematic and cholesteric systems, respectively.

X-ray Measurements. Oriented poly-**1**-HCl films were prepared for the X-ray analyses by shearing a uniaxially LC nematic and cholesteric water solutions of poly-**1**-HCl cast on a glass plate. After drying in air, the oriented poly-**1**-HCl films were floated off from the glass substrates onto an acetone surface, carefully collected, and then dried. Any trace amounts of residual water were not detected by elemental analysis. Several uniaxially oriented thin and rectangle-shaped poly-**1**-HCl films of ca. 10 mm length, 1.5 mm width, and 0.02 mm thickness were prepared and piled up parallel to each other for the X-ray measurements. In the same way, the oriented poly-**1**-HCl—(*S*)-**2** films were prepared from a cholesteric LC solution of poly-**1**-HCl with 0.1 equiv of (*S*)-**2** in water. X-ray photographs were taken at ambient temperature (20—25 °C) from the edge-view position with a beam parallel to the film surface, without any heat treatment of the samples because poly-**1**-HCl is thermally unstable and *cis-to-trans* isomerization took place at high temperature (>100 °C), although the poly-**1**-HCl is quite stable in solution and in the solid state at ambient temperature for a long time and the diffraction patterns did not change after ca. one month at ambient temperature (20—25 °C).

Figure 2-9 shows the X-ray diffraction patterns of an oriented optically inactive poly-**1**-HCl film (Figure 2-9A) and an optically active, single-handed helical poly-**1**-HCl—(*S*)-**2** film ([(*S*)-**2**]/[poly-**1**-HCl] = 0.1) (Figure 2-9B) with different ranges of sensitivities to show both the strong and weak reflections (see also Figures 2-4A and 2-4B for comparison), where the main layer lines have been indicated and the indices of the main reflections have been labeled.

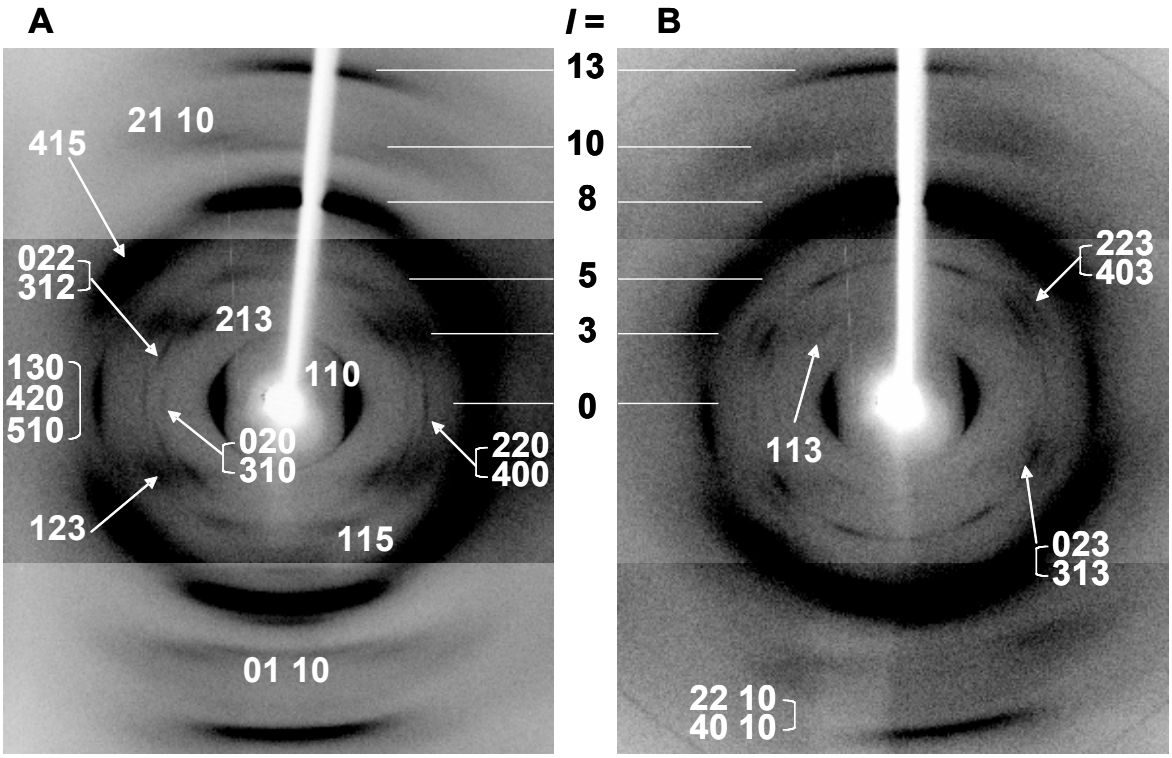

Figure 2-9. The X-ray diffraction patterns of an oriented optically inactive poly-**1**-HCl film (A) and an optically active, single-handed helical poly-**1**-HCl—(*S*)-**2** film ([(*S*)-**2**]/[poly-**1**-HCl] = 0.1) (B) with different ranges of sensitivities; the representative layer lines and the main reflections are labeled.

Figure 2-10 shows the flow charts for the determination processes of the unit cell (A) and the helical structure of poly-**1**-HCl (B) on the basis of the X-ray diffraction patterns (Figure 2-9) together with the density measurement results and the geometrical analyses using Miyazawa's equation (see below).

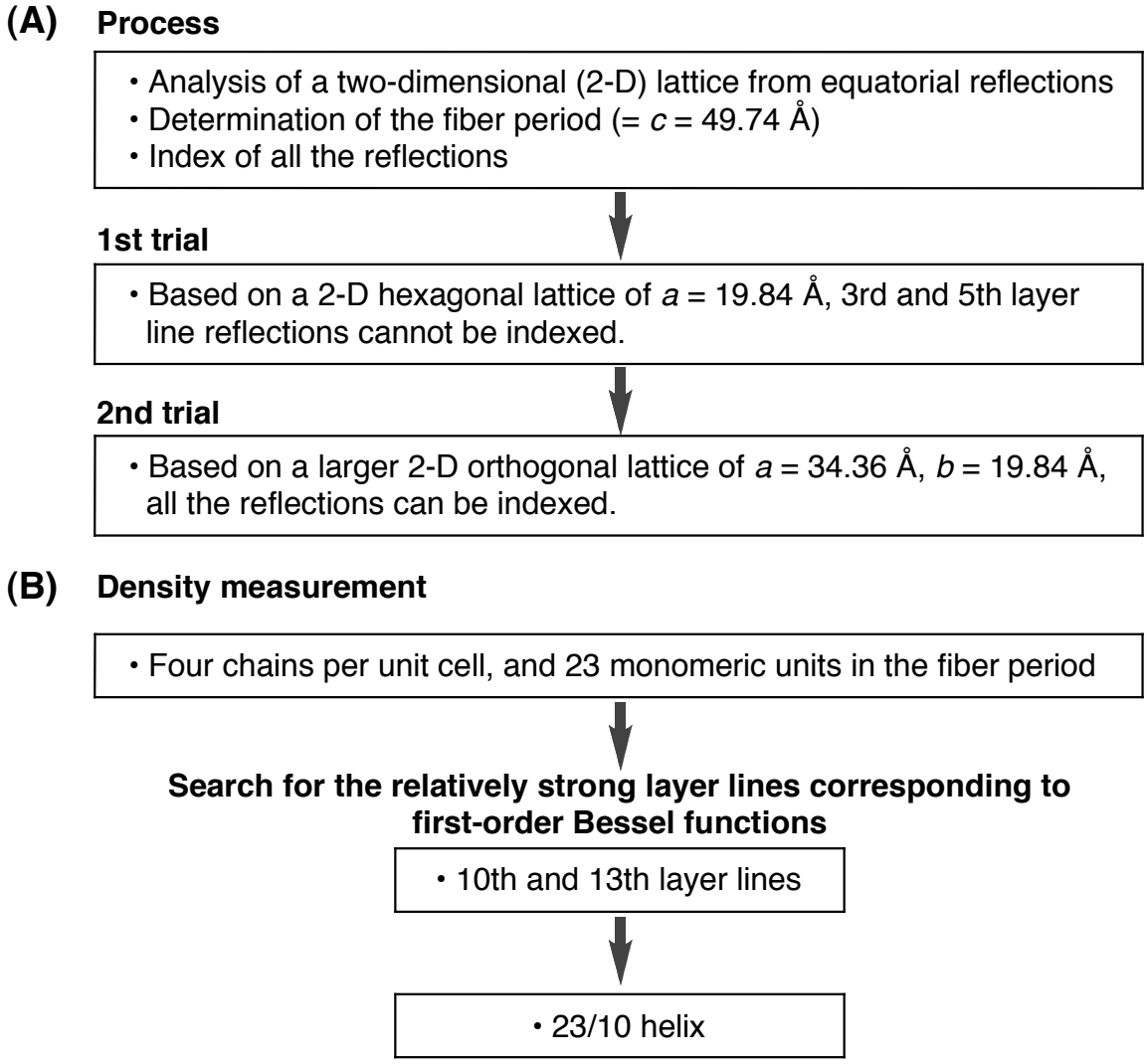

Figure 2-10. The determination processes of the unit cell for poly-**1**-HCl (A) and the helical structure of poly-**1**-HCl (B)

Although the most probable helical conformation of poly-**1** is considered to be the 23/10 helix on the basis of the X-ray diffraction analyses and the density measurement results, the meridional reflection on the 23rd layer line (2.16 Å) corresponding to the unit height (*h*) could not be detected. In order to justify the validity of this 23/10 helix model, the author explored the geometrically allowed helical conformations of poly-**1** using Miyazawa's

equation.[45] According to Miyazawa, helical conformations of infinite (periodic) polymer chains can be described by the helical parameters including the unit height (h), the number of repeating units (n) per one helical turn, and the backbone dihedral angle if the internal coordinates, such as the bond lengths, the bond angles, and the internal torsion angles are given. The internal coordinates were determined by *ab initio* quantum chemical calculations as follows: the bond lengths (C=C: 1.374 Å and C–C: 1.466 Å) and the bond angles (C–C=C: 128.8° and C=C–C: 121.3°), and the double bond geometry and the main chain dihedral angle defined by C–C=C–C were fixed to *cis* and 0°, respectively. The dihedral angle (ϕ) of a single bond from planarity (C=C–C=C) can be varied from 0 to 180° (n = 2). The helical parameters h and n were then calculated for each poly-**1** conformation defined as a function of ϕ according to Miyazawa's equation, which allows geometrically possible helical conformations of poly-**1** as a function of h and n (green solid line in Figure 2-11); in other words, helical conformations away from the green line can be excluded due to a geometrical reason. This profile was hardly changed when the reported bond lengths (C=C: 1.35 Å and C–C: 1.46 Å) and bond angles (C–C=C: 125.1° and C=C–C: 125.1°) for a nonsubstituted polyacetylene were employed as the internal coordinates.[46]

The author then calculated the possible helical forms of poly-**1** defined by the helical parameters h and n (= m residues per l turns) including the 23 unit /10 turn (23/10) helix, where the number of turns (l) was taken from the layer line reflections (l = 7, 8, 9, 10, and 13) in Table 2-2 and the number of residues (m) was selected so as to satisfy the X-ray diffraction data in Table 2-2. The results are plotted as circles with different colors in Figure 2-11, where the number represents the residues (m). Among all the possible helical forms plotted in Figure 2-11, the geometrically allowed helical conformations that fit the green line were 23/10, 27/10, and 38/13 helices. However, the calculated densities for the 27/10 and 38/13 helical forms of poly-**1**-HCl are 1.332 and 1.875 g/cm^3, respectively, which are much higher than that of the observed density (1.142 g/cm^3), while the calculated density (1.135 g/cm^3) for the 23/10 helix

agrees well with the observed density. Consequently, the 23/10 helix appears to be the most plausible helical conformation for the poly-**1** (Figure 2-4C).

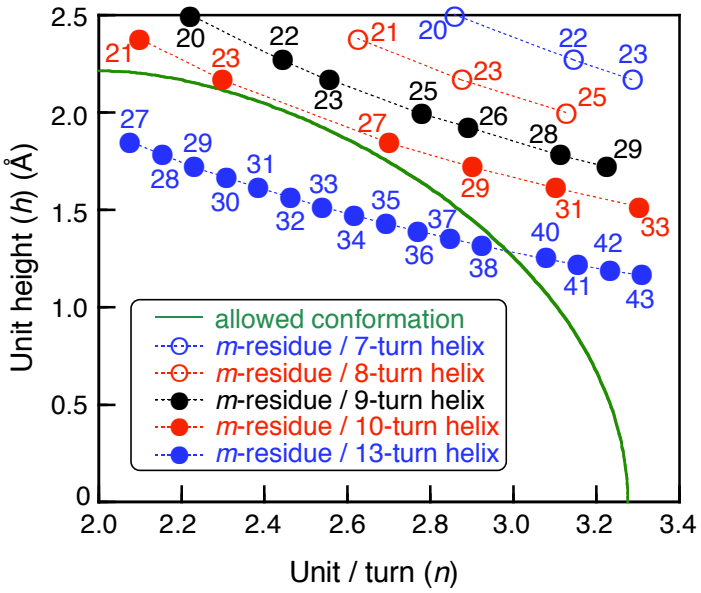

Figure 2-11. The geometrically allowed helical conformation (green solid line), namely the relationship between the number of repeating units (*n*) per one turn and the unit height (*h*) calculated from Miyazawa's equation. The circles show the candidates for the helical forms derived from the X-ray results (Table 2-2), where the number (*m*) represents the number of the residues per *l* turns and the number of turns (*l*) was taken from the layer line reflections (*l* = 7, 8, 9, 10, and 13) in Table 2-2.

Molecular Modeling of Poly-1. Molecular modeling and molecular mechanics calculations were conducted using the Compass force field[47] as implemented in the MS Modeling software (version 3.1, Accelrys Inc., San Diego, CA) operated using a PC running under Windows® XP. The polymer model of poly-**1** (23 repeating monomer units) was constructed using a Polymer Builder module in MS Modeling software based on the X-ray analysis results. The starting main chain conformation (23 unit / 10 turn helix) of a poly-**1** model was defined by the bond lengths (C=C: 1.374 Å and C–C: 1.466 Å), the bond angles (C=C–C: 124.8° and C–C=C: 128.8°), and the dihedral angles (C–C=C–C: 0° (*cis*) and C=C–

C=C: 140.3° (*transoid*)). These initial parameters were set on the basis of the calculated structure of a *cis-transoidal* phenylacetylene heptamer using the density functional theory (DFT) at the B3LYP level[48] and the 6-31G basis set in Gaussian 03 program (Gaussian, Inc., Pittsburgh, PA).[49] The bond lengths and bond angle (C–C=C) of the central monomer unit of the optimized heptamer were employed in order to avoid any influence by the end groups. Although the calculated bond angle (C=C–C) obtained by DFT was 121.3°, this value was changed to 124.8° so as to satisfy the X-ray result (2.3 unit/turn and 2.162(5) Å as the unit height). This bond angle is similar to that (125.1°) of the reported value for a nonsubstituted polyacetylene. The dihedral angles were then estimated using Miyazawa's equation.[45] These geometrical parameters for the helical poly-**1** backbone structure were fixed during the following force field optimization. The dielectric constant was set to 1.0. The calculation was used with setup parameters that include a 10.0 kcal mol^{-1} $Å^{-1}$ final convergence for minimization. Geometry optimizations were carried out without any cutoff in two steps. First, the starting conformation was subject to the steepest decent optimization in order to eliminate the worse steric conflicts. Second, subsequent optimization until the convergence using a conjugate gradient algorithm was performed. The final poly-**1** model as shown in Figure 2-4C was reconstructed by adopting the geometry of the central monomer unit of the optimized poly-**1** structure to avoid the end-group effect.

References and Notes

(1) Robinson, C.; Ward, J. C. *Nature* **1957**, *180*, 1183–1184. (b) Tsujita, Y.; Yamanaka, I.; Takizawa, A. *Polym. J.* **1979**, *11*, 749–754. (c) Livolant, F.; Bouligand, Y. *J. Physique* **1986**, *47*, 1813–1827. (d) Strzelecka, T. E.; Davidson, M. W.; Rill, R. L. *Nature* **1988**, *331*, 457–460. (e) Livolant, F.; Levelut, A. M.; Doucet, J.; Benoit, J. P. *Nature* **1989**, *339*, 724–726. (f) Fortin, S.; Charlet, G. *Macromolecules* **1989**, *22*, 2286–2292. (g) Wen, X.; Meyer, R. B.; Casper, D. L. D. *Phys. Rev. Lett.* **1989**, *63*, 2760–2763. (h) Inatomi, S.; Jinbo, Y.; Sato, T.; Teramoto, A. *Macromolecules* **1992**, *25*, 5013–5019. (i) Yu, S. M.; Conticello, V. P.; Zhang, G.; Kayser, C.; Fournier, M. J.; Mason, T. L.; Tirrel, D. A. *Nature* **1997**, *389*, 167–170. (j) Dogic, Z.; Fraden. S. *Phys. Rev. Lett.* **1997**, *78*, 2417–2420.

(2) Reviews: (a) Green, M. M.; Peterson, N. C.; Sato, T.; Teramoto, A.; Cook, R.; Lifson, S. *Science* **1995**, *268,* 1860–1866. (b) Green, M. M.; Park, J.-W.; Sato, T.; Teramoto, A.; Lifson, S.; Selinger, R. L. B.; Selinger, J. V. *Angew. Chem., Int. Ed.* **1999**, *38*, 3138–3154. (c) Nielsen, P. E. *Acc. Chem. Res.* **1999**, *32*, 624–630. (d) Nakano, T.; Okamoto, Y. *Chem. Rev.* **2001**, *101*, 4013–4038. (e) Cornelissen, J. J. L. M.; Rowan, A. E.; Nolte, R. J. M.; Sommerdijk, N. A. J. M. *Chem. Rev.* **2001**, *101*, 4039–4070. (f) Fujiki, M. *Macromol. Rapid Commun.* **2001**, *22*, 539–563. (g) Nomura, R.; Nakako, H.; Masuda, T. *J. Mol. Catl. A* **2002**, *190*, 197–205. (h) Fujiki, M.; Koe, J. R.; Terao, K.; Sato, T.; Teramoto, A.; Watanabe, J. *Polym. J.* **2003**, *35*, 297–344. (i) Elemans, J. A. A. W.; Rowan, A. E.; Nolte, R. J. M. *J. Mater. Chem.* **2003**, *13*, 2661–2670. (j) Yashima, E.; Maeda, K.; Nishimura, T. *Chem. –Eur. J.* **2004**, *10*, 42–51. For reviews of helical oligomers (foldamers) and helical assemblies, see: (k) Lehn, J. M. *Supramolecular Chemistry*; VCH: Weinheim, Germany, 1995. (l) Gellman, S. H. *Acc. Chem. Res.* **1998**, *31*, 173–180. (m) Srinivasarao, M. *Curr. Opin. Colloid Interface Sci.* **1999**, *4,* 370–376. (n) Hill, D. J.; Mio, M. J.; Prince, R. B.; Hughes, T. S.; Moore, J. S. *Chem. Rev.* **2001**, *101*, 3893–4011. (o) Brunsveld, L.; Folmer, B. J. B.; Meijer, E. W.; Sijbesma, R. P.

Chem. Rev. **2001**, *101*, 4071–4097. (p) Huc, I. *Eur. J. Org. Chem.* **2004**, 17–29. (q) Seebach, D.; Beck, A. K.; Bierbaum, D. J. *Chem. Biodiv.* **2004**, *1*, 1111–1239. (r) Hoeben, F. J. M.; Jonkheijm, P.; Meijer, E. W.; Schenning, A. P. H. J. *Chem. Rev.* **2005**, *105*, 1491–1546. (s) Tanatani, A.; Yokoyama, A.; Azumaya, I.; Takakura, Y.; Mitsui, C.; Shiro, M.; Uchiyama, M.; Muranaka, A.; Kobayashi, N.; Yokozawa, T. *J. Am. Chem. Soc.* **2005**, *127*, 8553–8561.

(3) (a) Chandrasekaran, S. *Liquid Crystals*, 2nd ed.; Cambridge University Press: Cambridge, 1992; Chapter 4. (b) Okamoto, Y.; Yashima, E. *Angew. Chem., Int. Ed.* **1998**, *37*, 1021–1043. (c) Amabilino, D. B.; Pérez-García, L. *Chem. Soc. Rev.* **2002**, *31*, 342–356. (d) Kato, T. *Science* **2002**, *295*, 2414–2418. (e) Yamamoto, C.; Okamoto, Y. *Bull. Chem. Soc. Jpn.* **2004**, *77*, 227–257. (f) Reggelin, M.; Doerr, S.; Klussmann, M.; Schultz, M.; Holbach, M. *Proc. Natl. Acad. Sci. U. S. A.* **2004**, *101*, 5461–5466.

(4) For leading references for liquid crystalline polyisocyanates: (a) Aharoni, S. M. *Macromolecules* **1979**, *12*, 94–103. (b) Itou, T.; Teramoto, A. *Macromolecules* **1988**, *21*, 2225–2230. (c) Green, M. M.; Weng, D.; Shang, W.; Labes, M. M. *Angew. Chem., Int. Ed. Engl.* **1992**, *31*, 88–90. (d) Sato, T.; Sato, Y.; Umemura, Y.; Teramoto, A.; Nagamura, Y.; Wagner, J.; Weng, D.; Okamoto, Y.; Hatada, K.; Green, M. M. *Macromolecules* **1993**, *26*, 4551–4559. (e) Green, M. M.; Zanella, S.; Gu, H.; Sato, T.; Gottarelli, G.; Jha, S. K.; Spada, G. P.; Schoevaars, A. M.; Feringa, B.; Teramoto, A. *J. Am. Chem. Soc.* **1998**, *120*, 9810–9817. (f) Tang, K.; Green, M. M.; Cheon, K. S.; Selinger, J. V.; Garetz, B. A. *J. Am. Chem. Soc.* **2003**, *125*, 7313–7323. Liquid crystalline polysilanes: (g) Watanabe, J.; Kamee, H.; Fujiki, M. *Polym. J.* **2001**, *33*, 495–497. (h) Okoshi, K.; Kamee. H.; Suzaki, G.; Tokita, M.; Fujiki, M.; Watanabe, J. *Macromolecules* **2002**, *35*, 4556–4559. (i) Okoshi, K.; Saxena, A.; Naito, M.; Suzaki, G.; Tokita, M.; Watanabe, J.; Fujiki, M. *Liq. Cryst.* **2004**, *31*, 279–283. Liquid crystalline polyisocyanides: (j) Cornelissen, J. J. L. M.; Donners, J. J. J. M.; de Gelder, R.; Graswinckel, W. S.; Metselaar, G. A.; Rowan, A. E.; Sommerdijk, N. A. J. M.;

Nolte, R. J. M. *Science* **2001**, *293*, 676–680. (k) Samorí, P.; Ecker, C.; Gösell, I.; de Witte, P. A. J.; Cornelissen, J. J. L. M.; Metselaar, G. A.; Otten, M. B. J.; Rowan, A. E.; Nolte, R. J. M.; Rabe, J. P. *Macromolecules* **2002**, *35*, 5290–5294. (l) Cornelissen, J. J. L. M.; Graswinckel, W. S.; Rowan, A. E.; Sommerdijk, N. A. J. M.; Nolte, R. J. M. *J. Polym. Sci., Part A: Polym. Chem.* **2003**, *41*, 1725–1736. Liquid crystalline polyguanidiens: (m) Kim, J.; Novak, B. M.; Waddon, A. J. *Macromolecules* **2004**, *37*, 1660–1662. (n) Kim, J.; Novak, B. M.; Waddon, A. J. *Macromolecules* **2004**, *37*, 8286–8292.

(5) Bellomo, E. G.; Davidson, P.; Impéror-Clerc, M.; Deming, T. J. *J. Am. Chem. Soc.* **2004**, *126*, 9101–9105.

(6) (a) Yashima, E.; Matsushima, T.; Okamoto, Y. *J. Am. Chem. Soc.* **1995**, *117*, 11596–11597. (b) Yashima, E.; Nimura, T.; Matsushima, T.; Okamoto, Y. *J. Am. Chem. Soc.* **1996**, *118*, 9800–9801. (c) Yashima, E.; Maeda, Y.; Okamoto, Y. *Chem. Lett.* **1996**, 955–956. (d) Yashima, E.; Maeda, Y.; Matsushima, T.; Okamoto, Y. *Chirality* **1997**, *9*, 593–600. (e) Yashima, E.; Matsushima, T.; Okamoto, Y. *J. Am. Chem. Soc.* **1997**, *119*, 6345–6359. (f) Yashima, E.; Maeda, K.; Okamoto, Y. *Nature* **1999**, *399*, 449–451. (g) Nonokawa, R.; Yashima, E. *J. Am. Chem. Soc.* **2003**, *125*, 1278–1283. (h) Maeda, K.; Morino, K.; Okamoto, Y.; Sato, T.; Yashima, E. *J. Am. Chem. Soc.* **2004**, *126*, 4329–4342. (i) Kamikawa, Y.; Kato, T.; Onouchi, H.; Kashiwagi, D.; Maeda, K.; Yashima, E. *J. Polym. Sci., Part A: Polym. Chem.* **2004**, *42*, 4580–4586. (j) Morino, K.; Watase, N.; Maeda, K.; Yashima, E. *Chem. –Eur. J.* **2004**, *10*, 4703–4707. (k) Onouchi, H.; Kashiwagi, D.; Hayashi, K.; Maeda, K.; Yashima, E. *Macromolecules* **2004**, *37*, 5495–5503. (l) Nishimura, T.; Tsuchiya, K.; Ohsawa, S.; Maeda, K.; Yashima, E.; Nakamura, Y.; Nishimura, J. *J. Am. Chem. Soc.* **2004**, *126*, 11711–11717. (m) Miyagawa, T.; Furuko, A.; Maeda, K.; Katagiri, H.; Furusho, Y.; Yashima, E. *J. Am. Chem. Soc.* **2005**, *127*, 5018–5019. (n) Onouchi, H.; Hasegawa, T.; Kashiwagi, D.; Ishiguro, H.; Maeda, K.; Yashima, E. *Macromolecules* **2005**, *38*, 8625–8633.

(7) Ashida, Y.; Sato, T.; Morino, K.; Maeda, K.; Okamoto, Y.; Yashima, E. *Macromolecules* **2003**, *36*, 3345–3350.

(8) For helicity induction through noncovalent chiral interactions in related aliphatic polyacetylenes and other polymers bearing functional groups as the pendants. See: (a) Schlitzer, D. S.; Novak, B. M. *J. Am. Chem. Soc.* **1998**, *120*, 2196–2197. (b) Norris, I. D.; Kane-Maguire, L. A. P.; Wallace, G. G. *Macromolecules* **1998**, *31*, 6529–6533 (c) Maeda, K.; Yamamoto, N.; Okamoto, Y. *Macromolecules* **1998**, *31*, 5924–5926. (d) Yashima, E.; Maeda, K.; Yamanaka, T. *J. Am. Chem. Soc.* **2000**, *122*, 7813–7814. (e) Inai, Y.; Ishida, Y.; Tagawa, K.; Takasu, A.; Hirabayashi, T. *J. Am. Chem. Soc.* **2002**, *124,* 2466–2473. (f) Ishikawa, M.; Maeda, K.; Yashima, E. *J. Am. Chem. Soc.* **2002**, *124,* 7448–7458. (g) Sakai, R.; Satoh, T.; Kakuchi, R.; Kaga, H.; Kakuchi, T. *Macromolecules* **2003**, *36*, 3709–3713. (h) Tabei, J.; Nomura, R.; Sanda, F.; Masuda, T. *Macromolecules* **2003**, *36*, 8603–8608. (i) Guo, Y.-M.; Oike, H.; Aida, T. *J. Am. Chem. Soc.* **2004**, *126,* 716–717. (j) Ishikawa, M.; Maeda, K.; Mitsutsuji, Y.; Yashima, E. *J. Am. Chem. Soc.* **2004**, *126,* 732–733. (k) Arnt, L.; Tew, G. N. *Macromolecules* **2004**, *37*, 1283–1288. (l) Sakai, R.; Satoh, T.; Kakuchi, R.; Kaga, H.; Kakuchi, T. *Macromolecules* **2004**, *37*, 3996–4003. (m) Nilsson, K. P. R.; Rydberg, J.; Baltzer, L.; Inganäs, O. *Proc. Nat. Acad. Sci., USA* **2004**, *101*, 11197–11202. (n) Kakuchi, R.; Sakai, R.; Otsuka, I.; Satoh, T.; Kaga, H.; Kakuchi, T. *Macromolecules* **2005**, *38*, 9441–9447.

(9) (a) Maeda, K.; Takeyama, Y.; Sakajiri, K.; Yashima, E. *J. Am. Chem. Soc.* **2004**, *126*, 16284–16285. (b) Nagai, K.; Maeda, K.; Takeyama, Y.; Sakajiri, K.; Yashima, E. *Macromolecules* **2005**, *38*, 5444–5451.

(10) For reviews of liquid crystalline polyacetylenes with mesogenic pendants, see: (a) Akagi, K.; Shirakawa, H. In *Electrical and Optical Polymer Systems*; Donald, L. W., Eds.; Marcel Dekker: New York, 1998; Chapter 28. (b) Lam, J. W. Y.; Tang, B. Z. *J. Polym. Sci., Part A: Polym. Chem.* **2003**, *41*, 2607–2629. (c) Lam, J. W. Y.; Tang, B. Z. *Acc. Chem. Res.* **2005**, *38*, 745–754. For thermotropic liquid crystalline polyacetylenes,

see: (d) Schenning, A. P. H. J.; Fransen, M.; Meijer, E. W. *Macromol. Rapid Commun.* **2002**, *23*, 265–270. (e) Percec, V.; Obata, M.; Rudick, J. G.; De, B. B.; Glodde, M.; Bera, T. K.; Magonov, S. N.; Balagurusamy, V. S. K.; Heiney, P. A. *J. Polym. Sci., Part A: Polym. Chem.* **2002**, *40*, 3509–3533. (f) Lam, J. W. Y.; Dong, Y.; Law, C. C. W.; Dong, Y.; Cheuk, K. K. L.; Lai, L. M.; Li, Z.; Sun, J.; Chen, H.; Zheng, Q.; Kwok, H. S.; Wang, M.; Feng, X.; Shen, J.; Tang, B. Z. *Macromolecules* **2005**, *38*, 3290–3300. (g) Percec, V.; Rudick, J. G.; Peterca, M.; Wagner, M.; Obata, M.; Mitchell, C. M.; Cho, W.-D.; Balagurusamy, V. S. K.; Heiney, P. A. *J. Am. Chem. Soc.* **2005**, *127*, 15257–15264.

(11) Cholesteric induction by doping nematic LCs with nonracemic chiral compounds is a typical and versatile example of chiral amplification on a macroscopic level and allows the detection of even trace amounts of chiral dopants. (a) Penot, J. P.; Billard, J. J. et J. *Tetrahedron Lett.* **1968**, 4013–4016. (b) Bertocchi, G.; Gottarelli, G.; Prati, R. *Talanta* **1984**, *31*, 138–140. (c) Huck, N. P. M.; Jager, W. F.; Lange, B.; Feringa, B. L. *Science* **1996**, *273*, 1686–1688. (d) Gottarelli, G.; Samori, B.; Fuganti, C.; Grasselli, P. *J. Am. Chem. Soc.* **1997**, *119*, 471–472. (e) Proni, G.; Spada, G. *Enantiomer* **2001**, *6*, 171–179. (f) Delden, R. A.; Feringa, B. L. *Angew. Chem., Int. Ed.* **2001**, *40*, 3198–3200. For reviews of chirality sensing by CD, see: ref 2j and (g) Ogoshi, H.; Mizutani, T. *Acc. Chem. Res.* **1998**, *31*, 81–89. (h) Nakanishi, K.; Berova, N. In *Circular Dichroism—Principles and Applications, 2nd ed.;* Nakanishi, K.; Berova, N.; Woody, R. W., Eds.; VCH: New York, 2000; Chapter 12. (i) Canary, J. W.; Holmes, A. E.; Liu, J. *Enantiomer* **2001**, *6*, 181–188. (j) Shinkai, S.; Ikeda, M.; Sugasaki, A.; Takeuchi, M. *Acc. Chem. Res.* **2001**, *34*, 494–503. (k) Tsukube, H.; Shinoda, S. *Chem. Rev.* **2002**, *102*, 2389–2403. (l) Allenmark, S. *Chirality* **2003**, *15*, 409–422. (m) Borovkov, V. V.; Hembury, G. A.; Inoue, Y. *Acc. Chem. Res.* **2004**, *37*, 449–459.

(12) Recently, a similar hierarchical amplification of chirality in LC media has been reported for small molecular systems. Eelkema, R.; Feringa, B. L. *J. Am. Chem. Soc.* **2005**, *127*, 13480–13481.

(13) For reviews: (a) Simionescu, C. I.; Percec, V. *Prog. Polym. Sci.* **1982**, *8*, 133–214. (b) Masuda, T.; Higashimura, T. *Adv. Polym. Sci.* **1987**, *81*, 121–165. (c) Shirakawa, H.; Masuda, T.; Takeda, K. In *The Chemistry of Triple-Bond Functional Groups*; Patai, S., Ed.; John Wiley & Sons: New York, 1994; Chapter 17. (d) Mayershofer, M. G.; Nuyken, O. *J. Polym. Sci., Part A: Polym. Chem.* **2005**, *43*, 5723–5747. (e) Aoki, T.; Kaneko, T. *Polym. J.* **2005**, *37*, 717–735. For recent examples of helical polyacetylenes with optically active substituents, see ref 10c—10e,g and: (f) Nomura, R.; Fukushima, Y.; Nakako, H.; Masuda, T. *J. Am. Chem. Soc.* **2000**, *122*, 8830–8836. (g) Li, B. S.; Cheuk, K. K. L.; Salhi, F.; Lam, J. W. Y.; Cha, J. A. K.; Xiao, X.; Bai, C.; Tang, B. Z. *Nano Lett.* **2001**, *1*, 323–328. (h) Yashima, E.; Maeda, K.; Sato, O. *J. Am. Chem. Soc.* **2001**, *123*, 8159–8160. (i) Morino, K.; Maeda, K.; Okamoto, Y.; Yashima, E.; Sato, T. *Chem. –Eur. J.* **2002**, *8*, 5112–5120. (j) Li, B. S.; Cheuk, K. K. L.; Ling, L.; Chen, J.; Xiao, X.; Bai, C.; Tang, B. Z. *Macromolecules* **2003**, *36*, 77–85. (k) Aoki, T.; Fukuda, T.; Shinohara, K.; Kaneko, T.; Teraguchi, M.; Yagi, M. *J. Polym. Sci., Part A: Polym. Chem.* **2004**, *42*, 4502–4517. (l) Lam, J. W. Y.; Dong, Y.; Cheuk, K. K. L.; Law, C. C. W.; Lai, L. M.; Tang, B. Z. *Macromolecules* **2004**, *37*, 6695–6704. (m) Tabei, J.; Shiotsuki, M.; Sanda, F.; Masuda, T. *Macromolecules* **2005**, *38*, 5860–5867. (n) Percec, V; Rudick, J. G.; Aqad, E. *Macromolecules* **2005**, *38*, 7205–7206. (o) Kaneko, T.; Umeda, Y.; Yamamoto, T.; Teraguchi, M.; Aoki, T. *Macromolecules* **2005**, *38*, 9420–9426. (p) Tabei, J.; Shiotsuki, M.; Sanda, F.; Masuda, T. *Macromolecules* **2005**, *38*, 9448–9454.

(14) (a) Simionescu, C. I.; Percec, V.; Dumitrescu, S. *J. Polym. Sci. Polym. Chem. Ed.* **1977**, *15*, 2497–2509. (b) Lee, D.-H.; Lee, D.-H.; Soga, K. *Makromol. Chem., Rapid Commun.* **1990**, *11*, 559–563. (c) Tabata, M.; Sadahiro, Y.; Nozaki, Y.; Inaba, Y.; Yokota, K.

Macromolecules **1996**, *29*, 6673–6675. (d) Lam, J. W. Y.; Kong, X.; Dong, Y.; Cheuk, K. K. L.; Xu, K.; Tang, B. Z. *Macromolecules* **2000**, *33*, 5027–5040. (e) Kozuka, M.; Sone, T.; Sadahiro, Y.; Tabata, M.; Endo, T. *Macromol. Chem. Phys.* **2002**, *203*, 66–70. (f) Ye, C.; Xu, G.; Yu, Z.-Q.; Lam, J. W. Y.; Jang, J. H.; Peng, H.-L.; Tu, Y.-F.; Liu, Z.-F.; Jeong, K.-U.; Cheng, S. Z. D.; Chen, E.-Q.; Tang, B. Z. *J. Am. Chem. Soc.* **2005**, *127*, 7668–7669.

(15) (a) Yashima, E.; Huang, S.; Matsushima, T.; Okamoto, Y. *Macromolecules* **1995**, *28*, 4184–4193. (b) Nakako, H.; Nomura, R.; Masuda, T. *Macromolecules* **2001**, *34*, 1496–1502.

(16) (a) Murakami, H.; Norisuye, T.; Fujita, H. *Macromolecules* **1980**, *13*, 345–352. (b) Itou, S.; Chikiri, H.; Teramoto, A.; Aharoni, S. M. *Polym. J.* **1988**, *20*, 143–151. (c) Takada, S.; Itou, T.; Chikiri, H. Einaga, Y.; Teramoto, A. *Macromolecules* **1989**, *22*, 973–979. (d) Sato, T.; Teramoto, A. *Adv. Polym. Sci.* **1996**, *126*, 85–161.

(17) Natsume, T.; Wu, L.; Sato, T.; Terao, K.; Teramoto, A.; Fujiki, M. *Macromolecules* **2001**, *34*, 7899–7904.

(18) The reported *q* values are 8.6 and 13.5 nm for a helical poly(4-carboxyphenylacetylene) induced by chiral amines[7] and a polypropargylamide, respectively. For the *q* value of a polypropargylamide, see: Nomura, R.; Tabei, J.; Nishiura, S.; Masuda, T. *Macromolecules* **2003**, *36*, 561–564.

(19) For the molecular weight determination by AFM, see: (a) Prokhorova, S. A.; Sheiko, S. S.; Möller, M.; Ahn, C.-H.; Percec, V. *Macromol. Rapid Commun.* **1998**, *19*, 359–366. (b) Thomas, B. N.; Corcoran, R. C.; Cotant, C. L.; Lindemann, C. M.; Kirsch, J. E.; Persichini, P. J. *J. Am. Chem. Soc.* **1998**, *120*, 12178–12186. (c) Börner, H. G.; Beers, K.; Matyjaszewski, K.; Sheiko, S. S.; Möller, M. *Macromolecules* **2001**, *34*, 4375–4383. (d) Cornellissen, J. J. L. M.; Graswinckel, W. S.; Adams, P. J. H. M.; Nachtegaal, G. H.; Kentgens, A. P. M.; Sommerdijk, N. A. J. M.; Nolte, R. J. M. *J. Polym. Sci. Part A:*

Polym. Chem. **2001**, *39*, 4255–4264. (e) Sakurai, S.-i.; Kuroyanagi, K.; Nonokawa, R.; Yashima, E. *J. Polym. Sci., Part A: Polym. Chem.* **2004**, *42*, 5838–5844.

(20) (a) Sato, T.; Nakamura, J.; Teramoto, A.; Green, M. M. *Macromolecules,* **1998**, *31,*1398–1405. (b) Gu, H. Doctoral Thesis, Osaka University, 1997.

(21) Green et al. demonstrated the amplification of the helical sense excess of a dynamically racemic helical polyisocyanate in the LC state doped with two different optically active polyisocyanates in their helical characteristics, one of which has a single-handed helix and the other, unequal interconverting right- and left-handed helical senses. They observed a nonlinear relationship between their dilute solution optical activities and cholesteric properties in the latter system, giving rise to higher q_c values than the former system. Green et al. proposed the amplification mechanism that is driven by the reduction in population of the mobile kinked helical reversals.[4e]

(22) Kimura, Y.; Sato, T. *Polym. J.* **2006**, *38*, 190–196.

(23) (a) Khokhlov, A. R.; Semenov, A. N. *Physica A* **1981**, *108*, 546–556. (b) Khokhlov, A. R.; Semenov, A. N. *Physica A* **1982**, *112*, 605–614. (c) Stroobants, A.; Lekkerkerker, H. N. W.; Odijk, Th. *Macromolecules* **1986**, *19*, 2232–2238. (d) Itou, T.; Teramoto, A. *Macromolecules* **1988**, *21*, 2225–2230.

(24) Onsager, L. *Ann. N. Y. Acad. Sci.* **1949**, *51*, 627–659.

(25) Recently, Yashima et al. found that helical poly(phenylacetylene)s bearing L- or D- and DL-alanine residues with a long alkyl chain as the pendants form lyotropic cholesteric and nematic LC phases, respectively, in organic solvents due to a rigid-rod helical conformation, and their *q* values were determined to be ca. 40 and 16 nm, respectively. Okoshi, K.; Sakajiri, K.; Kumaki, J.; Yashima, E. *Macromolecules* **2005**, *38*, 4061–4064.

(26) Shmueli, U.; Traub, W.; Rosenheck, K. *J. Polym. Sci., Part A-2* **1969**, *7*, 515–524.

(27) Klemann, B.; West, R.; Koutsky, J. A. *Macromolecules* **1993**, *26*, 1042–1046.

(28) Very recently, Yashima et al. have proposed a helical structure of poly(phenylacetylene)s bearing L- or D-alanine residues with a long alkyl chain as the pendants by AFM observations together with their X-ray structural analyses. Sakurai, S.-i.; Okoshi, K.; Kumaki, J.; Yashima, E. *Angew. Chem., Int. Ed.* **2006**, *45*, 1245–1248.

(29) Similar dissymmetrical WAXD patterns were reported. For example, see: Miller, R. D.; Farmer, B. L.; Fleming, W.; Sooriyakumaran, R.; Rabolt, J. *J. Am. Chem. Soc.* **1987**, *109*, 2509–2510.

(30) As for other helical polymers reported so far, helical chains are often packed with a hexagonal symmetry, but orthorhombic unit cells with hexagonal symmetry like poly-**1**-HCl have been reported for some helical polymers: for examples, see: (a) Sasaki, S.; Yasumoto, Y.; Uematsu, I. *Macromolecules* **1981**, *14*, 1797–1801. (b) Kusanagi, H.; Chatani, Y.; Tadokoro, H. *Polymer* **1994**, *35*, 2028–2039. (c) Chatani, Y.; Kobatake, T.; Tadokoro, H.; Tanaka, R. *Macromolecules* **1982**, *15*, 170–176. (d) Sasaki, S.; Asakura, T. *Macromolecules* **2003**, *36*, 8385–8390. (e) Klemann, B.; West, R.; Koutsky, J. A. *Macromolecules* **1993**, *26*, 1042–1046.

(31) The densities of the poly-**1**-HCl and poly-**1**-HCl—(*S*)-**2** ([(*S*)-**2**]/[poly-**1**-HCl] = 0.1) films were measured by the standard flotation method in a carbon tetrachloride / *n*-heptane mixture at ambient temperature (20–25 °C).

(32) Cochran, W.; Crick, F. H. C.; Vand, V. *Acta Crystallogr.* **1956**, *5*, 581–586.

(33) (a) Crick, F. H. C. *Acta Crystallogr.* **1953**, *6*, 689–697. (b) Parsons, D. F.; Martius, U. *J. Mol. Biol.* **1964**, *10*, 530. (c) Chothia, C.; Levitt, M.; Richardson, D. *Proc. Natl. Acad. Sci. U. S. A.* **1977**, *74*, 4130–4134. (d) Cho, K. C.; Nemethy, G.; Sheraga, H. A. *J. Phys. Chem.* **1983**, *87*, 2869–2881. (e) Sasaki, S. *Polymer* **1986**, *27*, 849–855. (f) Watanabe, J.; Ono, H. *Macromolecules* **1986**, *19*, 1079–1083.

(34) (a) Lifson, S.; Andreola, C.; Peterson, N.; Green, M. M. *J. Am. Chem. Soc.* **1989**, *111*, 8850–8858. (b) Gu, H.; Sato, T.; Teramoto, A.; Varichon, L.; Green, M. M. *Polym. J.* **1997**, *29*, 77–84. (c) Selinger, J. V.; Selinger, R. L. B. *Phys. Rev. E* **1997**, *55*, 1728–

1731. (d) Gu, H.; Sato, T.; Teramoto, A.; Green, M. M.; Jha, S. K.; Andreola, C.; Reidy, M. P. *Macromolecules* **1998**, *31*, 6362–6368. (e) Teramoto, A. *Prog. Polym. Sci.* **2001**, *26*, 667–720. (f) Morino, K.; Maeda, K.; Okamoto, Y.; Yashima, E.; Sato, T. *Chem. – Eur. J.* **2002**, *8*, 5112–5120.

(35) Green, M. M.; Reidy, M. P.; Johnson, R. J.; Darling, G.; O'Leary, D. J.; Willson, G. *J. Am. Chem. Soc.* **1989**, *111*, 6452–6454.

(36) Green, M. M.; Garetz, B. A.; Muñoz, B.; Chang, H.; Hoke, S.; Cooks, R. G. *J. Am. Chem. Soc.* **1995**, *117*, 4181–4182.

(37) (a) Furlani, A.; Napoletano, C.; Russo, M. V.; Feast, W. *J. Polym. Bull.* **1986**, *16*, 311–317. (b) Matsunami, S.; Kakuchi, T.; Ishii, F. *Macromolecules* **1997**, *30*, 1074–1078. (c) Kishimoto, Y.; Eckerle, P.; Miyatake, T.; Kainosho, M.; Ono, A.; Ikariya, T.; Noyori, R. *J. Am. Chem. Soc.* **1999**, *121*, 12035–12044. (d) Percec, V.; Rudick, J. G. *Macromolecules* **2005**, *38*, 7241–7250.

(38) (a) Shirakawa, H.; Ito, T.; Ikeda, S. *Polym. J.* **1973**, *4*, 469–462. (b) Tabata, M.; Tanaka, Y.; Sadahiro, Y.; Sone, T.; Yokota, K.; Miura, I. *Macromolecules* **1997**, *30*, 5200–5204.

(39) For the thermal stability of poly(phenylacetylene) derivatives, see: refs 13a, 13n, 14a, and 37d and Morino, K.; Asari, T.; Maeda, K.; Yashima, E. *J. Polym. Sci., Part A: Polym. Chem.* **2004**, *42*, 4711–4722.

(40) Vesenka, J.; Manne, S.; Giberson, R.; Marsh, T.; Henderson, E. *Biophys. J.* **1993**, *126*, 992–997.

(41) Samorí, P.; Francke, V.; Müllen, K.; Rabe, J. P. *Chem. –Eur. J.* **1999**, *5*, 2312–2317.

(42) (a) Sato, T.; Kakihara, T.; Teramoto, A. *Polymer* **1990**, *31*, 824–828. (b) Sato, T.; Teramoto, A. *Physica A* **1991**, *176*, 72–86.

(43) Mannig, G. S. *J. Chem. Phys.* **1969**, *51*, 924–933.

(44) Philip, J. R.; Wooding, R. A. *J. Chem. Phys.* **1970**, *52*, 953–959.

(45) Miyazawa, T. *J. Polym. Sci.* **1961**, *55*, 215–231.

(46) Chien, J. C. W.; Karasz, F. E.; Shimamura, K. *Macromolecules* **1982**, *15*, 1012–1017.

(47) Sun, H. *J. Phys. Chem. B* **1998**, *102*, 7338–7364.

(48) (a) Becke, A. D. *J. Chem. Phys.* **1993**, *98*, 5048–5652. (b) Lee, C.; Yang, W.; Parr, R. G. *Phys. Rev. B* **1988**, *37*, 785–789.

(49) Frisch, M. J.; Trucks, G. W.; Schlegel, H. B.; Scuseria, G. E.; Robb, M. A.; Cheeseman, J. R.; Montgomery, J. A., Jr.; Vreven, T.; Kudin, K. N.; Burant, J. C.; Millam, J. M.; Iyengar, S. S.; Tomasi, J.; Barone, V.; Mennucci, B.; Cossi, M.; Scalmani, G.; Rega, N.; Petersson, G. A.; Nakatsuji, H.; Hada, M.; Ehara, M.; Toyata, K.; Fukuda, R.; Hasegawa, J.; Ishida, M.; Nakajima, T.; Honda, Y.; Kitao, O.; Nakai, H.; Klene, M.; Li, X.; Knox, J. E.; Hratchian, H. P.; Cross, J. B.; Adamo, C.; Jaramillo, J.; Gomperts, R.; Stratmann, R. E.; Yazyev, O.; Austin, A. J.; Cammi, R.; Pomelli, C.; Ochterski, J. W.; Ayala, P. Y.; Morokuma, K.; Voth, G. A.; Salvador, P.; Dannenberg, J. J.; Zakrzewski, V. G.; Dapprich, S.; Daniels, A. D.; Strain, M. C.; Farkas, O.; Malick, D. K.; Rabuck, A. D.; Raghavachari, K.; Foresman, J. B.; Ortiz, J. V.; Cui, Q.; Baboul, A. G.; Clifford, S.; Cioslowski, J.; Stefanov, B. B.; Liu, G.; Liashenko, A.; Piskorz, P.; Komaromi, I.; Martin, R. L.; Fox, D. J.; Keith, T.; Al-Laham, M. A.; Peng, C. Y.; Nanayakkara, A.; Challacombe, M.; Gill, P. M. W.; Johnson, B.; Chen, W.; Wong, M. W.; Gonzalez, C.; Pople, J. A. *Gaussian 03*; Gaussian, Inc.: Pittsburgh, PA, 2003.

Chapter 3

Temperature-Induced Chiroptical Changes in a Helical Poly(phenylacetylene) Bearing *N*,*N*-Diisopropylaminomethyl Groups with Chiral Acids in Water

Abstract: A stereoregular poly(phenylacetylene) bearing an *N*,*N*-diisopropylaminomethyl group as the pendant (poly-**1**) changed its structure into the prevailing one-handed helical conformation upon complexation with optically active acids in water, and the complexes exhibited an induced circular dichroism (ICD) in the UV-visible region of the polymer backbone. Poly-**1** is highly sensitive to the chirality of chiral acids and can detect a small enantiomeric imbalance in the chiral acids, in particular, phenyl lactic acid in water; for example, a 0.005% enantiomeric excess of phenyl lactic acid can be detected by CD spectroscopy. The observed ICD intensity and pattern of poly-**1** were dependent on the temperature and concentration of poly-**1**, probably due to aggregations of the polymer at high temperature as revealed by dynamic light scattering and AFM measurements. On the basis of the temperature-dependent ICD changes, the preferred-handed helical sense of poly-**1** was found to be controlled by noncovalent bonding interactions using structurally different enantiomeric acids.

Introduction

The helix is an important structural motif among a variety of conformational states observed in molecular and supramolecular organizations as exemplified in DNA and proteins. Therefore, constructing artificial helical polymers[1] and oligomers (foldamers)[2] or supramolecular helical assemblies[3] with a controlled helicity has attracted significant interest in recent years in the fields of polymer and supramolecular chemistries and materials sciences because of their possible applications in chiroptical devices and chiral materials including enantioselective adsorbents and catalysts.[1a,g,4]

In a series of studies, Yashima and co-workers reported the unique helicity induction in optically inactive, stereoregular *cis-transoidal* poly(phenylacetylene)s bearing various functional groups such as carboxy,[5] phosphonate,[6] boronate,[7] sulfonate,[8] and amino groups,[9,10] or bulky crown ethers[11] as the pendants, which changed their dynamically racemic helical conformations into the preferred-handed helical conformations upon complexation with specific chiral guests in organic solvents[5,6,8,9,11] and water.[7,10,12] Their complexes exhibited a characteristic induced circular dichroism (ICD) in the UV-visible region of the polymer backbones. The Cotton effect signs can be used to predict the absolute configurations of the guest molecules.[11l,p,13]

Among the poly(phenylacetylene)s prepared to date, poly(4-(*N*,*N*-diisopropyl-aminomethyl)phenylacetylene) (poly-**1**) (Chart 3-1) is particularly interesting and unique because the hydrochloride of poly-**1** (poly-**1**-HCl) is soluble in water and formed an excess helical sense in the presence of a small amount of various chiral acids such as the sodium salt of phenyl lactic acid (**2**) of low enantiomeric excess (ee) through a significant amplification of the chirality in water, thus showing an ICD.[10] Moreover, the poly-**1**-HCl was, for the first time, found to form a lyotropic nematic liquid crystal (LC) in concentrated water solutions because of its stiff helical backbone with the long persistence length of 26 nm. In addition, the nematic LC phase converted to the cholesteric counterpart by doping with a tiny amount of chiral acids with a low ee and the helix-sense excess of the polymer backbone was further amplified

through interchain interactions in the cholesteric LC state compared to that in a dilute solution.[10a,c] This liquid crystalline feature of the induced helical poly-**1**-HCl enabled us to determine its helical structure by X-ray diffraction of the oriented films of the liquid crystalline poly-**1**-HCl.[10c] The polyelectrolyte function of the poly-**1**-HCl accompanied with the hydrophobic pendants[14] appears to be crucial for such a hierarchical amplification of the macromolecular helicity in dilute and concentrated water solutions because the neutral poly-**1** showed a poor sensitivity to the chirality of the chiral acids[9a,b] and produced no LC phase in organic solvents.[10a]

During the course of studies, the author has found that the neutral poly-**1**, which is not soluble in water, became soluble in water in the presence of excess amounts of free aromatic and aliphatic carboxylic acids in water ([acid]/[poly-**1**] > 2), which prompted us to investigate the helicity induction and chiral amplification of free poly-**1** with chiral acids in water.

Chart 3-1. Structures of Poly-**1** and Carboxylic and Sulfonic Acids

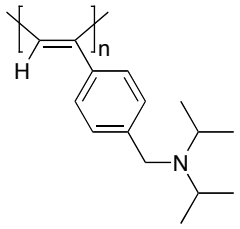

poly-**1**

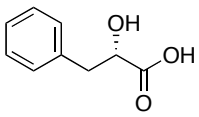

(*S*)-**2**

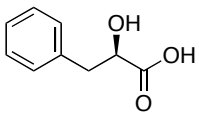

(*R*)-**2**

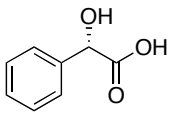

(*S*)-**3**

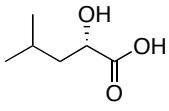

(*S*)-**4**

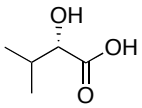

(*S*)-**5**

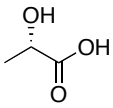

(*S*)-**6**

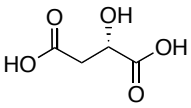

(*S*)-**7**

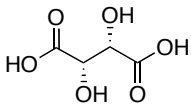

L-**8**

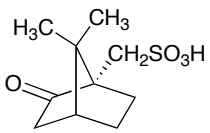

(*S*)-**9**

Results and Discussion

CD Studies of Helix Induction of Poly-1 with Chiral Acids in Water. Poly-**1** was prepared by the polymerization of the corresponding monomer (**1**) with $[Rh(nbd)Cl]_2$ (nbd = norbornadiene) according to a previously reported method.[9a,b,10] The stereoregularity of poly-**1** was confirmed to be highly *cis-transoidal* (*cis* content = 96%) based on the ^{1}H NMR spectroscopy (Figure 3-12 in the Experimental Section).[10c,15] The number average molecular weight (M_n) and its molecular weight distribution (M_w/M_n) were 3.4×10^5 and 2.21, respectively, as determined by size exclusion chromatography (SEC) as its hydrochloride salt (poly-**1**-HCl).[10]

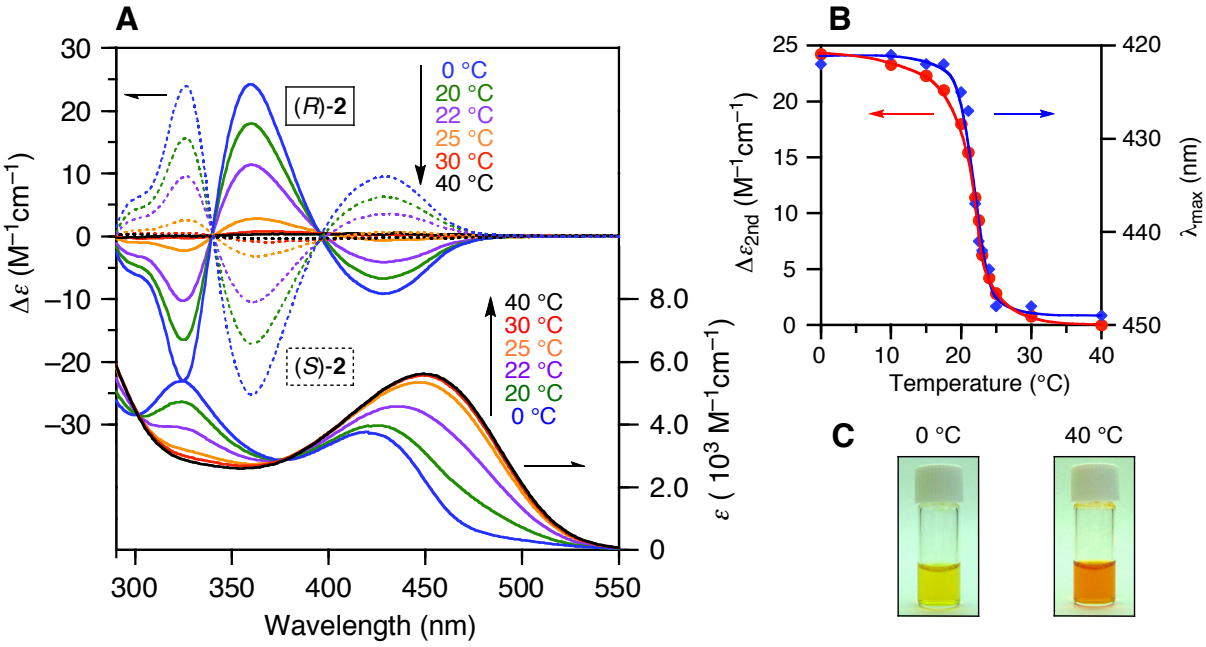

Figure 3-1. (A) CD spectral changes of poly-**1** with (*R*)- and (*S*)-**2** in water (pH 3.1) at various temperatures. Absorption spectral changes of poly-**1** with (*R*)-**2** in water are also shown. (B) Temperature-dependent $\Delta\varepsilon_{2nd}$ (●) and λ_{max} (◆) changes of poly-**1** with (*R*)-**2** in water. (C) Visible difference of poly-**1** with (*R*)-**2** in water at 0 and 40 °C. The concentration of poly-**1** is 1.0 mg (4.6 mmol monomer units)/mL. [**2**]/[poly-**1**] = 4.

Figure 3-1A shows the typical CD and absorption spectra of poly-**1** in the presence of (*R*)- and (*S*)-**2** (4 equiv to monomer units of poly-**1**) in water at 20 °C (green solid and dotted lines, respectively) together with their changes at various temperatures. The complexes exhibited mirror images of the split-type intense ICDs in the polymer backbone region at 20 °C; the CD and absorption spectral patterns and its ICD intensity were similar to those of the complex of poly-**1**-HCl with the sodium salt of (*S*)- or (*R*)-**2** ((*S*)- or (*R*)-**2**-Na) in water at 25 °C.[10a] However, in sharp contrast to the poly-**1**-HCl—(*S*)-**2**-Na complex in water, the ICD magnitude was sensitive to temperature, and increased with the decreasing temperature, but sharply decreased at around 22–25 °C and the ICD almost completely disappeared at 30 °C. The author notes poly-**1** became soluble in water in the presence of 3 equiv of (*S*)-**2**. CD titration experiments of poly-**1** with (*S*)-**2** at 0 °C revealed that the ICD intensities of the second Cotton effect ($\Delta\varepsilon_{2nd}$) reached an almost constant value in the presence of 3 equiv (*S*)-**2** (Figure 3-2).

This remarkable change in the ICD intensity was accompanied by a significant change in the absorption spectra; the absorbance maxima (λ_{max}) at 422 nm and 0 °C red-shifted to 449 nm at 30–40 °C, a peak at around 320 nm decreased with an increase in temperature with a clear isosbestic point at 302 and 375 nm, and the solution color changed from yellow to orange (A–C in Figure 3-1). These CD and absorption spectral changes are completely reversible and could be repeated at least ten times, which indicated that the helix-sense preference of the poly-**1** induced by (*S*)- or (*R*)-**2** increased with the decreasing temperature, and the conformation of the polymer backbone may change from a tightly twisted helix at lower temperatures to a rather relaxed, extended one at high temperatures. This speculation is supported by the fact that the CD intensity monotonically decreased while maintaining its spectral pattern along with the changes in the absorption maxima (Figure 3-1B). A similar thermo-reversible change in the absorption spectrum of poly-**1** also took place in the presence of achiral benzoic acid (Figure 3-3). The author noted that poly-**1**-HCl complexed with (*S*)- or (*R*)-**2**-Na ([**2**-Na]/[poly-**1**-HCl] = 0.5) did not show such a change in its absorption and CD

spectra in the same temperature range (0–40 °C). A similar temperature-dependent CD and absorption spectral change was reported for the poly(*N*-propagylamide)s, and this was considered to be due to a helix-to-random coil transition of the polymer backbones.[16]

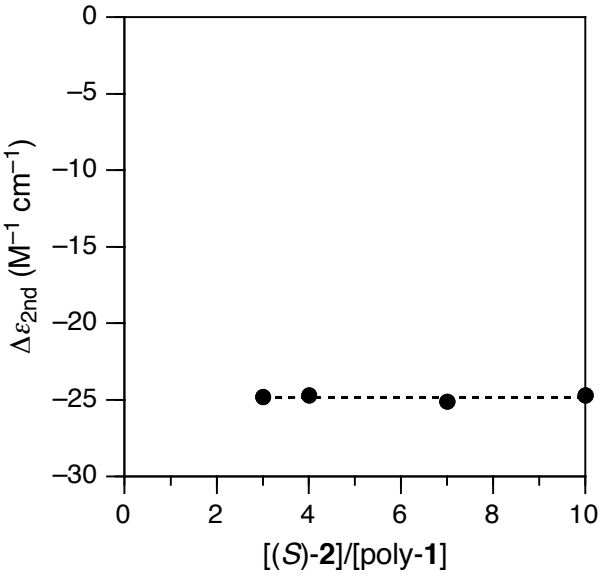

Figure 3-2. Plots of the ICD intensity ($\Delta\varepsilon_{2nd}$) of poly-**1** (1 mg/mL) in the complexation with (*S*)-**2** in water (pH 2.6–3.3) at 0 °C.

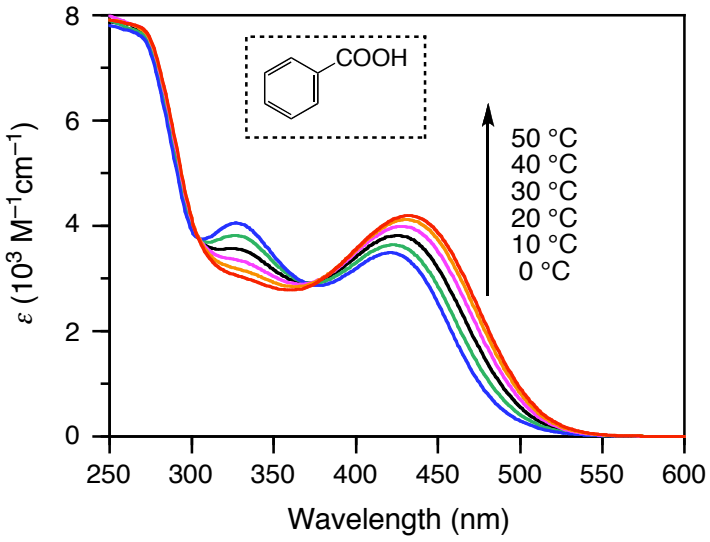

Figure 3-3. Absorption spectral changes of poly-**1** with benzoic acid in water (pH 3.5) at various temperatures. The concentration of poly-**1** is 1.0 mg (4.6 mmol monomer units)/mL. [benzoic acid]/[poly-**1**] = 4.

Another possible explanation for the changes in the absorption spectra to longer wavelengths may be due to aggregations of the polymer main chains at high temperature.[17] The author then measured the CD and absorption spectra of poly-**1** at different concentrations ([poly-**1**] = 1–0.01 mg/mL) in the presence of a constant (*S*)-**2** concentration at 25 °C (Figure 3-4). The ICD magnitude significantly increased with the decreasing concentration of poly-**1** accompanied by a blue-shift in the absorption spectra. The concentration-dependent changes in the CD and absorption spectra of the poly-**1**—**2** complex suggest the formation of poly-**1** aggregates at high temperature.

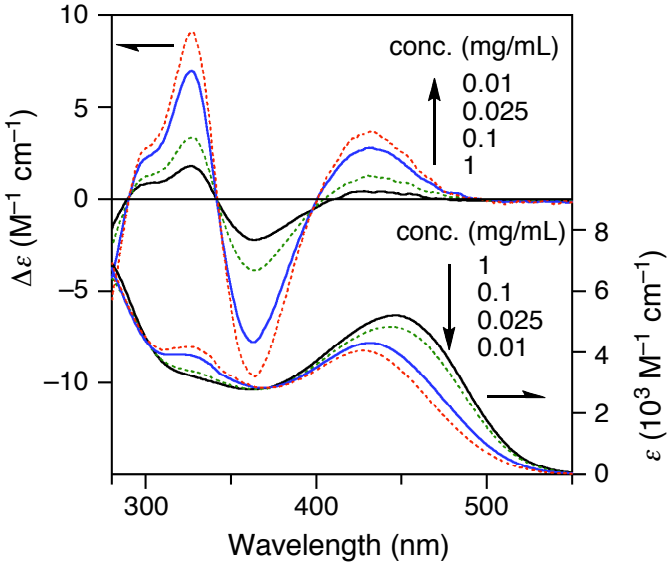

Figure 3-4. CD and absorption spectral changes of poly-**1** with (*S*)-**2** in water (pH 3.0–2.7) at various concentrations of poly-**1** (0.01–1 mg/mL) at 25 °C. The concentration of (*S*)-**2** is 3.1 mg (19 mmol)/mL.

Dynamic light scattering (DLS) measurements of the poly-**1**—(*S*)-**2** complex in water at high (38 °C) and low (3 °C) temperatures were then performed. The hydrodynamic radius (R_h) values of the polymer estimated in water at 3 and 38 °C were 43 nm and 2.35 μm, respectively. In addition, from a light intensity autocorrelation function ($g^{(2)}(\tau)$), it was found

that the time correlation delay was much faster at 3 °C than at 38 °C, indicating large particles were formed at 38 °C (Figure 3-5).

AFM measurements were also performed to obtain additional information with respect to the morphology of the poly-**1**—(*S*)-**2** aggregates at high and low temperatures (Figure 3-6). Individual poly-**1** chains complexed with (*S*)-**2** could be directly observed on mica prepared from a dilute solution at 0 °C, while a number of entwined polymer chains were observed when deposited at 40 °C. These results agreed with the assumption that the poly-**1**—(*S*)-**2** complex exists as aggregates at high temperature. The author assumes that the polymer forms an extended conformation at high temperatures probably because of the electrostatic repulsion between the charged pendants, resulting in the aggregations in the presence of **2**. This assumption is supported by the fact that the aggregation of poly-**1** complexed with (*S*)-**2** ([(*S*)-**2**]/[poly-**1**] = 4) considerably diminished at high temperature in the presence of an increasing amount of NaCl (Figure 3-7). The presence of a salt like NaCl is expected to attenuate the electrostatic interactions because of the charge-shielding effect of the salt, so that the polymer backbone may maintain its tightly twisted helix at high temperatures.

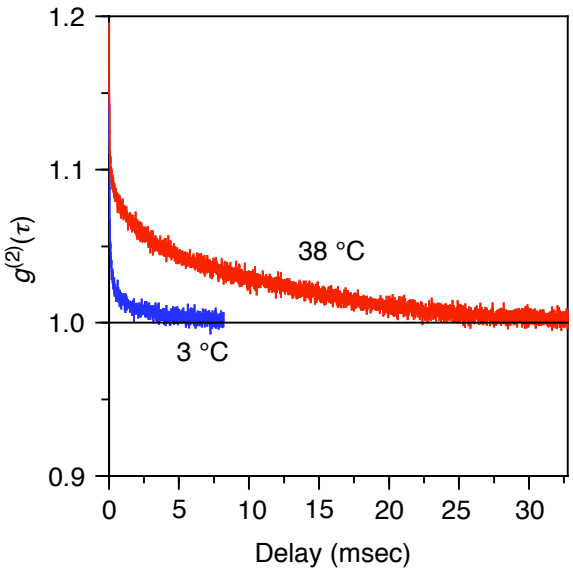

Figure 3-5. Autocorrelation function observed for poly-**1** with 4 equiv of (*S*)-**2** in water at 3 and 38 °C.

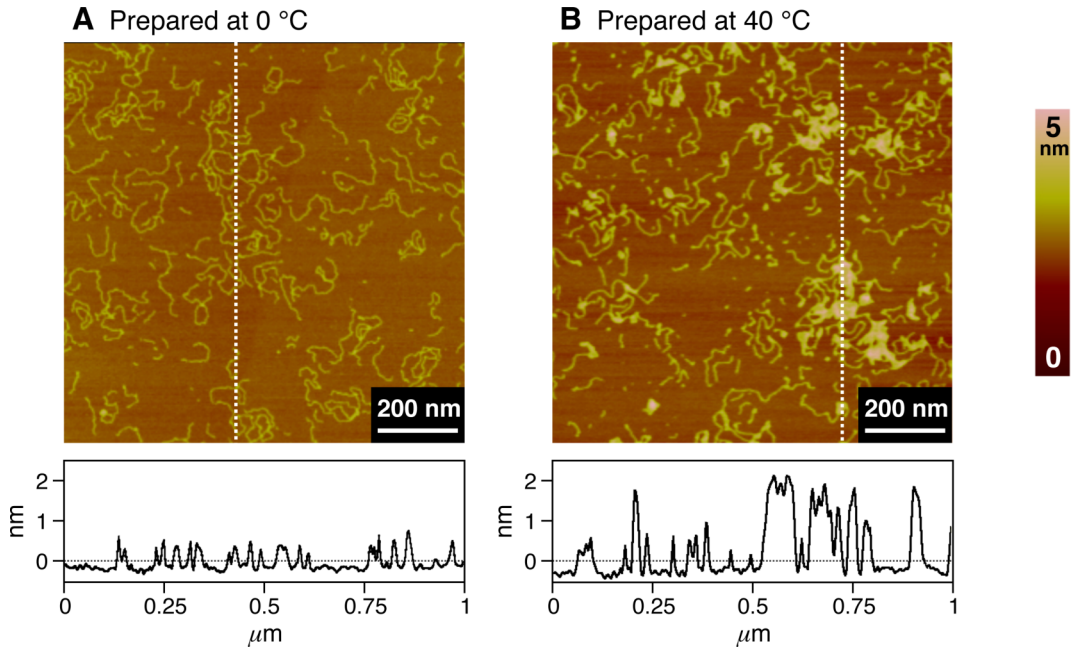

Figure 3-6. Tapping-mode AFM height images of the poly-**1**—(*S*)-**2** complex on mica prepared at 0 (A) and 40 °C (B). The concentrations of poly-**1** and (*S*)-**2** are 0.01 and 3.1 mg/mL ([**2**]/[poly-**1**] = 400), respectively. The height profiles measured along the dashed lines in the images are also shown.

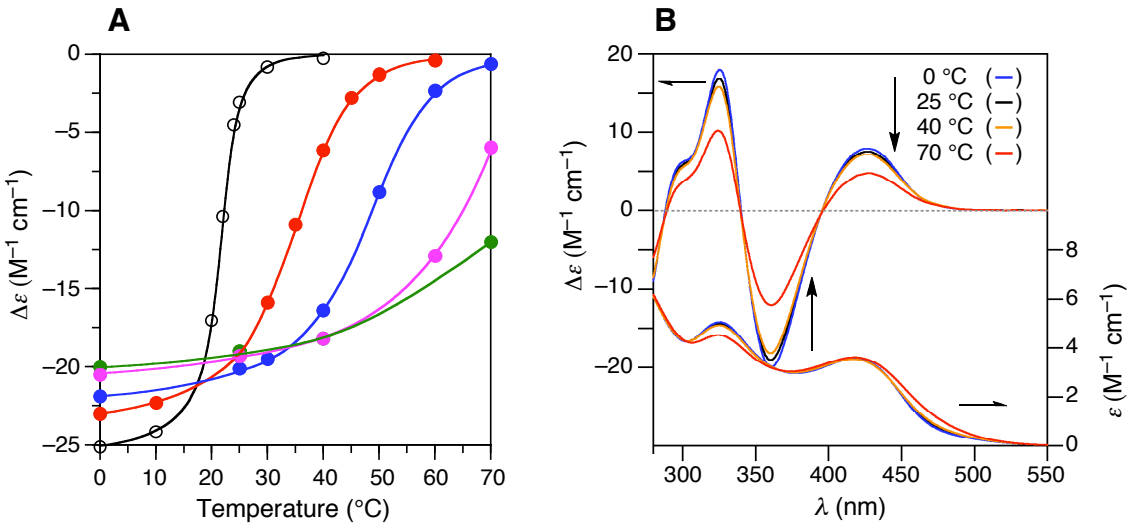

Figure 3-7. (A) Temperature-dependent $\Delta\varepsilon_{2nd}$ change of poly-**1**—(*S*)-**2** complex ([(*S*)-**2**]/[poly-**1**] = 4) in the presence of an increasing amount of NaCl (0 (○), 0.1 (●), 0.2 (●), 0.5 (●), and 1.0 equiv of NaCl (●)) in water. The concentration of poly-**1** is 1.0 mg (4.6 mmol monomer units)/mL. (B) CD and absorption spectral changes of the poly-**1**—(*S*)-**2** in the presence of 1.0 equiv of NaCl in water at various temperatures.

Poly-**1** also responded to other optically active free carboxylic and sulfonic acids (**3**–**9** in Chart 3-1) in water, and the complexes exhibited similar temperature-dependent ICDs in their patterns and the Cotton effect signs when the absolute configurations of the chiral carboxylic acids are the same (Figure 3-8 and Table 3-1); the ICD intensities significantly increased with the decreasing temperature.

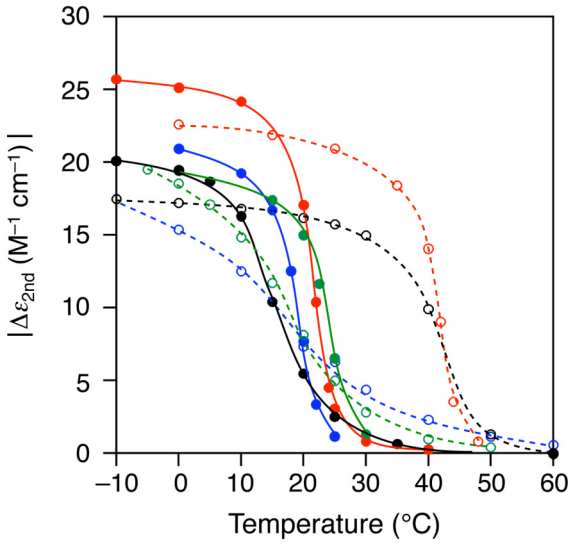

Figure 3-8. Temperature-dependent $|\Delta\varepsilon_{2nd}|$ value of poly-**1** with (*S*)-**2**(●), (*S*)-**3**(●), (*S*)-**4**(○), (*S*)-**5**(●), (*S*)-**6**(●), (*S*)-**7**(○), L-**8**(○), and (*S*)-**9**(○) in water. The concentration of poly-**1** is 1.0 mg (4.6 mmol monomer units)/mL. [(*S*)-**2** or (*S*)-**3**]/[poly-**1**] = 4, [(*S*)-**4**, (*S*)-**5**, or (*S*)-**6**]/[poly-**1**] = 10, and [(*S*)-**7** or L-**8**]/[poly-**1**] = 1.

Table 3-1. Signs and Difference in Exciton Coefficient of the Second Cotton Effect ($\Delta\varepsilon_{2nd}$) for the Complexes of Poly-**1** with Chiral Carboxylic and Sulfonic Acids in Water[a]

				second Cotton [λ (nm) and $\Delta\varepsilon_{2nd}$ ($M^{-1}cm^{-1}$)]		
	[acid]			25 °C	10 °C	0 °C
chiral acid	[poly-**1**]	pH	sign	$\Delta\varepsilon$ (λ)	$\Delta\varepsilon$ (λ)	$\Delta\varepsilon$ (λ)
(*S*)-**2**	4	3.1	–	3.07 (363)	24.2 (360)	25.1 (360)
(*R*)-**2**	4	3.1	+	2.81 (362)	23.3 (359)	24.2 (360)
(*S*)-**3**	4	3.2	–	2.51 (371)	16.3 (367)	19.4 (368)
(*S*)-**4**	10	2.6	–	20.9 (361)	—	22.6 (361)
(*S*)-**5**	10	2.6	–	1.16 (364)	19.2 (362)	20.9 (362)
(*S*)-**6**	10	2.6	–	6.52 (361)	—	19.4 (362)
(*S*)-**7**	1	3.2	–	15.7 (362)	16.8 (361)	17.2 (361)
L-**8**	1	3.3	–	6.28 (362)	12.5 (361)	15.4 (360)
(*S*)-**9**	4	2.5	+	4.99 (366)	14.8 (364)	18.5 (364)

[a] The concentration of poly-**1** is 1.0 mg/mL.

Chiral Amplification and Nonlinear Effects in Water. Chiral amplification[18] is one of the most unique and interesting features of dynamic helical polymers as reported for polyisocyanates,[1c,f,19] polysilanes,[1i,k,20] and poly(phenylacetylene)s with functional pendants.[1l,p,5b,h,6a,d,e,11] Previously, the author reported that the complex formation of poly-**1**-HCl with partially resolved chiral acids showed a strong positive nonlinear relationship (majority rule)[19a] between the ee of the chiral acids, such as **2**-Na, and the observed ICD intensities in water.[10] The positive nonlinear effect of poly-**1**-HCl increased with an increase in the amount of **2**-Na. However, the addition of **2**-Na (> 0.5 equiv.) resulted in precipitation of the polymer, and further experiments were difficult.[10c]

The author then investigated whether a similar nonlinear effect could be observed for poly-**1** with nonracemic, free carboxylic acids in water. The chiral carboxylic acid **2** was selected as a helix inducer because it produced the most intense ICD in water at 0 °C among

the chiral acids used in this study (Table 3-1). Poly-**1** complexed with four equiv of **2** ((*S*) rich) exhibited almost no nonlinear effect at 25 °C. However, the extent of a convex deviation from the linearity became remarkably greater with the decreasing temperature and even a 5% ee of **2** gave rise to the full ICD below 0 °C as induced by the 100% ee of **2** (Figure 3-9). This noticeable positive nonlinear effect of poly-**1** was superior to that observed for the poly-**1**-HCl—**2**-Na system and enabled the detection of the chirality of **2** with a very small ee of less than 0.005% in accuracy; almost linear relationship between the ee (from 0.1 to 0.005%) and the ICD values of poly-**1** was observed below 0 °C (Figure 3-10). These results indicate that poly-**1** is highly sensitive to the small enantiomeric imbalance of optically active acids in water.

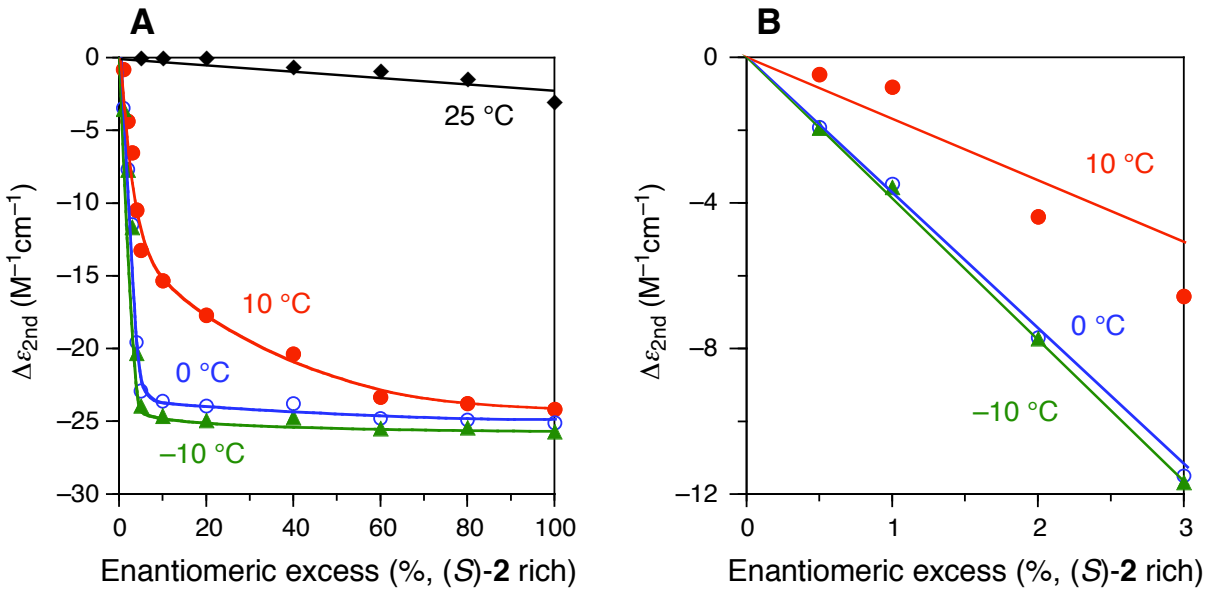

Figure 3-9. (A) Changes in ICD intensity ($\Delta\varepsilon_{2nd}$) of poly-**1** (1.0 mg/mL) versus the % ee of **2** ([**2**]/[poly-**1**] = 4; pH 3.0–3.2) during the complexation with poly-**1** in water at 25, 10, 0, and –10 °C. (B) Expanded detail of the ICD intensity at 10, 0, and –10 °C.

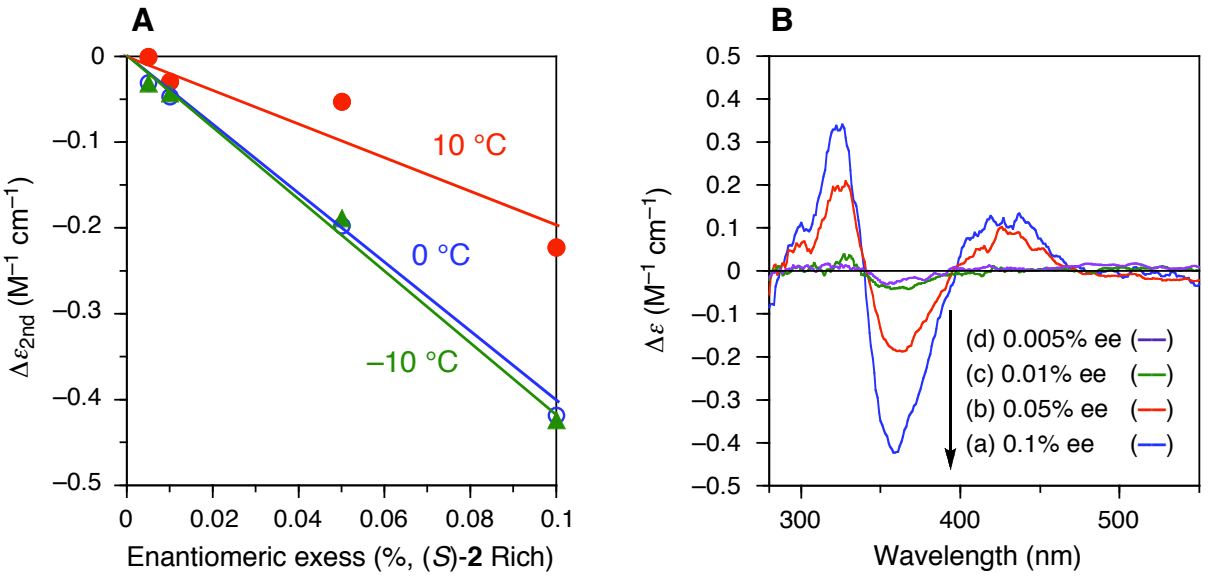

Figure 3-10. (A) Plots between the ICD intensity of poly-**1** in the presence of 0.1–0.005% ee of **2** (*S*-rich) at 10, 0, and –10 °C. (B) CD spectra of poly-**1** in the presence of 0.1 (blue line), 0.05 (red line), 0.01 (green line), and 0.005% ee of **2** (purple line) ([**2**]/[poly-**1**] = 4) in water at –10 °C. The concentration of poly-**1** is 1.0 mg (4.6 mmol monomer units)/mL.

Chiral Competition: Helix Inversion Controlled by Noncovalent Competition between Structurally Different Enantiomeric Acids. Another interesting and unique feature of dynamic helical polymers is the reversible helix inversion between right- and left-handed helices. Biological polymers, such as DNA[21] and polypeptides,[22] with specific sequences and several synthetic, dynamic helical polymers bearing optically active substituents through covalent bonding, are known to undergo an inversion of helicity regulated by external stimuli, such as a change in temperature[1g–l,n,p,17,19,23,24] and solvent.[1g–l,n,p,17,24,25] However, inversion of a macromolecular helicity induced by chiral stimuli through noncovalent bonding interactions is quite rare,[5i,6e,17,24b,25e,26] but can be used to sense the chirality of chiral guests as well as to produce enantiomeric helices[6e] based on the noncovalent "helicity induction and chiral memory" concept.[11,p,5c,f,27] In addition, Green et al. recently reported designer polyisocyanates showing an inversion of the helicity with a desired helix inversion temperature in dilute solution by the copolymerization of a pair of structurally different enantiomers, which are in

competition with each other in helical sense preferences.[28]

The author then investigated if such a macromolecular helicity inversion of poly-**1** could be possible using two different enantiomeric acids in water via noncovalent bonding interactions. The author examined a series of combinations of different enantiomeric acids in Chart 3-1 and found that (*S*)-**2** and D-**8** showing steep and gentle changes in the ICD intensities of poly-**1** versus temperature, respectively, could be used for the purpose.

Figure 3-11 shows the temperature-dependent ICD intensity changes of a mixture of poly-**1**, (*S*)-**2**, and D-**8** ([(*S*)-**2**]/[D-**8**]/[poly-**1**] = 0.4/1/1) in water. The Cotton effect sign inverted from a negative to positive value at around 25 °C, resulting from the differences in the binding affinity of each enantiomer to poly-**1** and the chiral twisting power between (*S*)-**2** and D-**8**, which may force the poly-**1** into either a right- or left-handed helix depending on the temperature. Consequently, inversion of the helicity of poly-**1** could be controlled by the noncovalent chiral competition.[28]

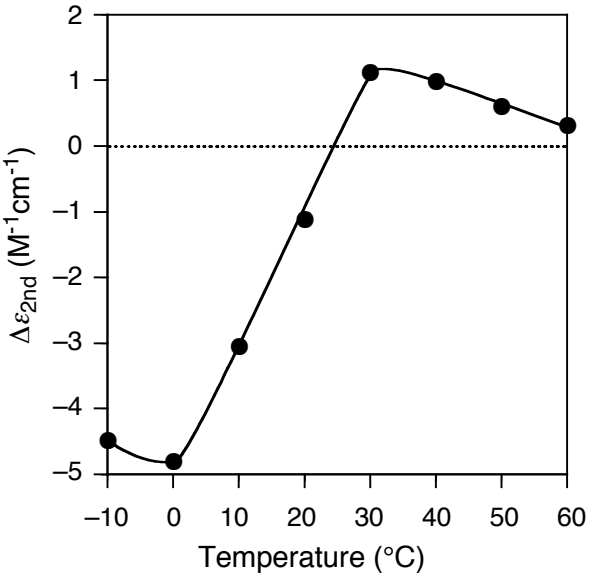

Figure 3-11. Temperature-dependent $\Delta\varepsilon_{2nd}$ value of poly-**1** with (*S*)-**2** and D-**8** ([(*S*)-**2**]/[D-**8**]/[poly-**1**] = 0.4/1/1) in water.

Conclusions

In summary, the author has found that a poly(phenylacetylene) bearing an *N*,*N*-diisopropylaminomethyl group as the pendant (poly-**1**) is highly sensitive to the chirality of chiral acids via formation of a predominantly one-handed helix in water, particularly at low temperature, and can detect an extremely small enantiomeric imbalance in carboxylic acids. The polyelectrolyte function of poly-**1** in the presence of chiral acids appears to be important for such a high sensitivity to the chirality because the poly-**1** showed a weak ICD even in the presence of excess chiral acids in organic solvents. Moreover, the preferred-handed helical sense of poly-**1** can be controlled by the temperature-dependent, noncovalent chiral competition between structurally different enantiomeric acids.

Experimental Section

Materials. Deionized, distilled water was degassed with nitrogen before use in all the experiments. Optically active acids were purchased from Aldrich (Milwaukee, WI) or Tokyo Kasei (TCI, Tokyo, Japan) and used as received. *Cis-transoidal* poly-**1** was prepared by the polymerization of 4-(*N*,*N*-diisopropylaminomethyl)phenylacetylene (**1**) with $[Rh(nbd)Cl]_2$ (nbd = norbornadiene) according to a previously reported method.[9a,b,10] The stereoregularity of the obtained poly-**1** was confirmed to be highly *cis-transoidal* (*cis* content = 96%) based on the ^{1}H NMR spectrum (Figure 3-12).[10c,15] The M_n and M_w/M_n of poly-**1** were estimated to be 3.4×10^5 and 2.21, respectively, as determined by SEC as its hydrochloride salt (poly-**1**-HCl).[10]

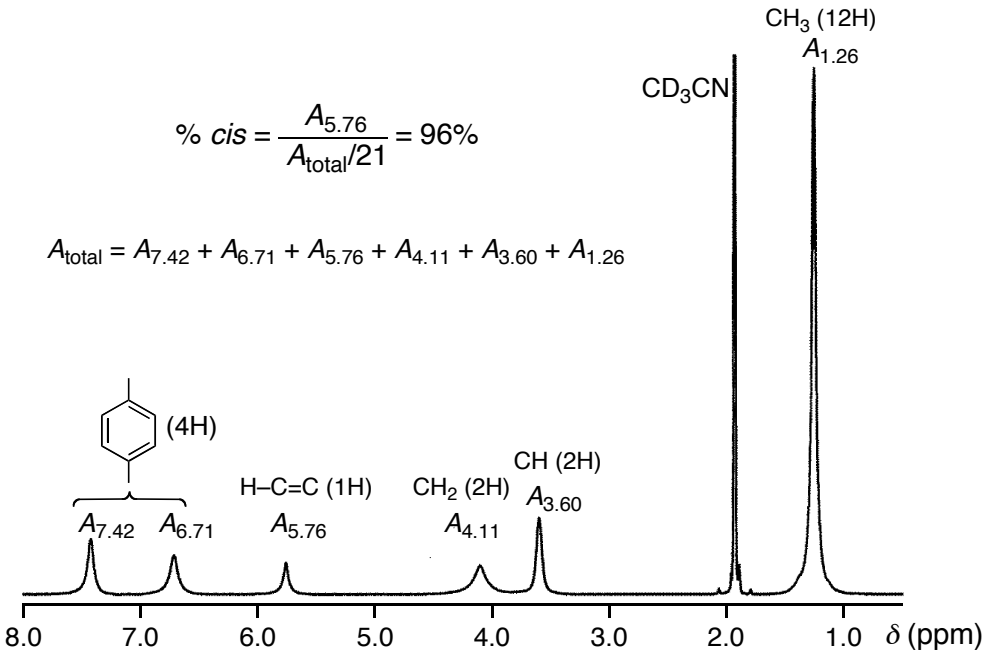

Figure 3-12. ^{1}H NMR spectrum of poly-**1** in CD_3CN with CF_3CO_2D ($[CF_3CO_2D]/[\text{poly-}\mathbf{1}] = 2$) at 60 °C.

Instruments. The solution pH was measured by a B-211 pH meter (Horiba, Japan). The NMR spectra were taken by a Varian INOVA-500 operating at 500 MHz for ^1H in CD_3CN. SEC measurements were performed with a JASCO PU-980 liquid chromatograph (JASCO, Hachioji, Japan) equipped with a UV (254 nm; JASCO UV-970) detector. A Tosoh (Tokyo, Japan) TSK-GEL SuperAWM-H column (30 cm) was connected and a water solution containing 9 mM tartaric acid and the 0.1 mM tartaric acid sodium salt was used as the eluent at the flow rate of 0.6 mL/min. The molecular weight calibration curve was obtained using poly(ethylene oxide) and poly(ethylene glycol) standards (Tosoh). The FT-IR spectra were measured in a 0.15-mm CaF_2 cell by a JASCO JV-2001YS spectrophotometer equipped with a temperature controller (EYELA NCB-1200). The concentration of poly-**1** was 5 mg/mL in D_2O. The laser Raman spectra were obtained using a JASCO RMP-200 spectrophotometer. The absorption and CD spectra were measured in a 0.1-, 0.5-, 1.0-, or 10-mm quartz cell by a JASCO V-570 spectrophotometer and a JASCO J-725 or J-820 spectropolarimeter, respectively. The temperature (–10—100 °C) was controlled with a JASCO ETC 505T (for absorption spectral measurements) and a JASCO PTC-423L apparatus (for CD spectral measurements). The dynamic light scattering (DLS) measurements were performed by a Photal DLS-7070YN (Otsuka Electronics Co., Ltd., Osaka, Japan) equipped with a 10 mW He-Ne laser (632.8 nm) at 3 and 38 °C. The AFM measurements were performed using a Nanoscope IIIa microscope (Veeco Instruments, Santa Barbara, CA) in air at ambient temperature with standard silicon cantilevers (NCH, Nanoworld, Neuchâtel, Switzerland) in the tapping mode. The AFM images were measured at the resonance frequency of the tips with 125-μm-long cantilevers (200–300 Hz) and a spring constant of approximately 40 N/m. All the images were collected with the maximum available number of pixels (512) in each direction. The scanning speed was at a line frequency of 1.0 Hz. The effective silicon tip radii were estimated with Au colloids (5 nm; ICN Biomedicals, Inc., Aurora, OH) as imaging standards and were 5–10 nm.

CD measurements. The concentration of poly-**1** was calculated on the basis of monomer units and was 1.0 mg/mL (4.6 mM monomer units) unless otherwise stated. For the complexation of poly-**1** with optically active acids, poly-**1** (ca. 1 mg) and an appropriate amount of the chiral acid were dissolved in water in a 2-mL vessel equipped with a screwcap to keep the poly-**1** concentration at 1.0 mg/mL (4.6 mM), and the absorption and CD spectra were then taken.

Nonlinear effects of poly-1 with 2. The nonlinear effects between the intensities of the ICD and % ee of **2** during the complexation with poly-**1** were investigated in water. The molar ratio of **2** to the monomer units of poly-**1** ([**2**]/[poly-**1**]) was held constant at 4 (mol/mol). In the experiments, stock solutions of **2** were separately prepared for the large (2% ≤ ee ≤ 100%) and small (0.005% ≤ ee < 2%) ee values before the CD measurements.

Preparation of 2 solutions with large ee and CD measurements with poly-1. Stock solutions of (*S*)-**2** (18.6 mM, 10 mL) and (*R*)-**2** (18.6 mM, 10 mL) in acetone were prepared. Aliquots of the stock solutions of (*S*)- and (*R*)-**2** were placed into ten vessels so that the % ee of the mixtures (*S* rich) were 2, 3, 4, 5, 10, 20, 40, 60, 80, and 100, respectively. After the acetone was removed under reduced pressure from each vessel, 1.0 mg of poly-**1** was added to the vessels and they were dissolved in water to keep the poly-**1** concentration at 1.0 mg/mL (4.6 mM). The absorption and CD spectra were then taken for each vessel to determine the changes in the CD spectra.

Preparation of 2 solutions with small ee and CD measurements with poly-1. The stock solutions of **2** with small ee values (0.005% ≤ ee < 2%) were carefully prepared in a similar way as in the literature,[11a] and the experimental procedures are described below.

1.0 and 0.5 % ee of (*S*)-2 ((*S*):(*R*) = 50.5:49.5 and 50.25:49.75). Stock solutions of (*RS*)-**2** (37 mM) and (*S*)-**2** (0.37 mM) in acetone were first prepared; 61.1 mg of (*RS*)-**2** and 15.4 mg of (*S*)-**2** were placed in 10- and 250-mL flasks equipped with stopcocks, respectively.

To these was added acetone to the mark. Aliquots of the stock solutions of (*RS*)-**2** and (*S*)-**2** were transferred to two 2-mL vessels equipped with screwcaps so that the % ee of **2** ((*S*)-rich) was 0.5 and 1.0, respectively. After the acetone was removed under reduced pressure, 1.0 mg of poly-**1** was added to the vessels and they were dissolved in water to keep the poly-**1** concentration at 1.0 mg/mL (4.6 mM). The absorption and CD spectra were then taken for each vessel.

0.1 and 0.05 % ee of (*S*)-2 ((*S*):(*R*) = 50.05:49.95 and 50.025:49.975). A stock solution of (*S*)-**2** (0.037 mM) was first prepared as follows; 0.50 mL of the stock solution of (*S*)-**2** (0.37 mM) prepared above was transferred to a 5-mL flask equipped with a stopcock and the solution was diluted with acetone to the mark to produce the stock solution of (*S*)-**2** (0.037 mM) in acetone. Aliquots of the stock solutions of (*RS*)-**2** (37 mM) and (*S*)-**2** (0.037 mM) were transferred to two 2-mL vessels equipped with screwcaps so that the % ee of **2** ((*S*)-rich) was 0.1 and 0.05, respectively. After the acetone was removed under reduced pressure, 1.0 mg of poly-**1** was added to the vessels and they were dissolved in water to keep the poly-**1** concentration at 1.0 mg/mL (4.6 mM). The absorption and CD spectra were then taken for each vessel.

0.01 and 0.005 % ee of (*S*)-2 ((*S*):(*R*) = 50.005:49.995 and (*S*):(*R*) = 50.0025:49.9975). A stock solution of (*S*)-**2** (0.0037 mM) was first prepared as follows; 0.50 mL of the stock solution of (*S*)-**2** (0.37 mM) prepared above was transferred to a 50-mL flask equipped with a stopcock and the solution was diluted with acetone to the mark to produce the stock solution of (*S*)-**2** (0.0037 mM) in acetone. Aliquots of the stock solutions of (*RS*)-**2** (37 mM) and (*S*)-**2** (0.0037 mM) were transferred to two 2-mL vessels equipped with screwcaps so that the % ee of **2** ((*S*)-rich) was 0.01 and 0.005, respectively. After the acetone was removed under reduced pressure, 1.0 mg of poly-**1** was added to the vessels and they were dissolved in water to keep the poly-**1** concentration at 1.0 mg/mL (4.6 mM). The absorption and CD spectra were then taken.

DLS measurements. A stock solution of poly-**1** (1.0 mg/mL, 4.6 mM) complexed with (*S*)-**2** ([(*S*)-**2**]/[poly-**1**] = 4) was prepared in a 5-mL flask equipped with a stopcock in water. The solution was filtered using a 0.45 μm syringe filter (Toyo Roshi Co., Ltd., Japan) below 10 °C and then the DLS measurements of the sample were performed at a fixed scattering angle of 90° at 3 and 38 °C. The obtained autocorrelation functions were analyzed by the method of cumulants to give the translational diffusion coefficients (D_s). The corresponding hydrodynamic radius (R_h) was calculated using the Stokes-Einstein equation: $R_h = k_B T/(6\pi h D)$, where k_B, h, and T are the Boltzmann constant, the solvent viscosity, and the absolute temperature, respectively. The estimated R_h values for the poly-**1** in water at 3 and 38 °C were 43 nm and 2.35 μm, respectively, supporting that the formation of aggregates of the polymer main chains at high temperature.

AFM measurements. A stock solution of poly-**1** (0.01 mg/mL) in a 0.019 M (*S*)-**2** aqueous solution was prepared. A 20 μL aliquot of the stock solution was dropped on a freshly cleaved mica, the solution was simultaneously blown off with a stream of argon, then the mica substrate was dried *in vacuo* overnight to measure the AFM images in the tapping-mode (Figure 3-6).

References and Notes

(1) Reviews: (a) Okamoto, Y.; Nakano, T. *Chem. Rev.* **1994**, *94*, 349–372. (b) Nolte, R. J. M. *Chem. Soc. Rev.* **1994**, *23*, 11–19. (c) Green, M. M.; Peterson, N. C.; Sato, T.; Teramoto, A.; Cook, R.; Lifson, S. *Science* **1995**, *268*, 1860–1866. (d) Pu, L. *Acta. Polym.* **1997**, *48*, 116–141. (e) Srinivasarao, M. *Curr. Opin. Colloid Interface Sci.* **1999**, *4*, 370–376. (f) Green, M. M.; Park, J.-W.; Sato, T.; Teramoto, A.; Lifson, S.; Selinger, R. L. B.; Selinger, J. V. *Angew. Chem., Int. Ed.* **1999**, *38*, 3138–3154. (g) Nakano, T.; Okamoto, Y. *Chem. Rev.* **2001**, *101*, 4013–4038. (h) Cornelissen, J. J. L. M.; Rowan A. E.; Nolte, R. J. M.; Sommerdijk, N. A. J. M. *Chem. Rev.* **2001**, *101*, 4039–4070. (i) Fujiki, M. *Macromol. Rapid Commun.* **2001**, *22*, 539–563. (j) Nomura, R.; Nakako, H.; Masuda, T. *J. Mol. Catal. A: Chem.* **2002**, *190*, 197–205. (k) Fujiki, M.; Koe, J. R.; Terao, K.; Sato, T.; Teramoto, A.; Watanabe, J. *Polym. J.* **2003**, *35*, 297–344. (l) Yashima, E.; Maeda, K.; Nishimura, T. *Chem. –Eur. J.* **2004**, *10*, 43–51. (m) Lockman, J. W.; Paul, N. M.; Parquette, J. R. *Prog. Polym. Sci.* **2005**, *30*, 423–452. (n) Lam, J. W. Y.; Tang, B. Z. *Acc. Chem. Res.* **2005**, *38*, 745–754. (o) Aoki, T.; Kaneko, T. *Polym. J.* **2005**, *37*, 717–735. (p) Maeda, K.; Yashima, E. *Top. Curr. Chem.* **2006**, *265*, 47–88.

(2) Reviews: (a) Gellman, S. H. *Acc. Chem. Res.* **1998**, *31*, 173–180. (b) Hill, D. J.; Mio, M. J.; Prince, R. B.; Hughes, T. S.; Moore, J. S. *Chem. Rev.* **2001**, *101*, 3893–4011. (c) Sanford, A. R.; Gong, B. *Curr. Org. Chem.* **2003**, *7*, 1649–1659. (d) Huc, I. *Eur. J. Org. Chem.* **2004**, 17–29.

(3) Reviews: (a) Rowan, A. E.; Nolte, R. J. M. *Angew. Chem., Int. Ed.* **1998**, *37*, 63–68. (b) Brunsveld, L.; Folmer, B. J. B.; Meijer, E. W.; Sijbesma, R. P. *Chem. Rev.* **2001**, *101*, 4071–4097. (c) Elemans, J. A. A. W.; Rowan, A. E.; Nolte, R. J. M. *J. Mater. Chem.* **2003**, *13*, 2661–2670. (d) Mateos-Timoneda, M. A.; Crego-Calama, M.; Reinhoudt, D. N. *Chem. Soc. Rev.* **2004**, *33*, 363–372. (e) Zhang, J.; Albelda, M. T.; Liu, Y.; Canary, J. W. *Chirality* **2005**, *17*, 404–420. (f) Hoeben, F. J. M.; Jonkheijm, P.; Meijer, E. W.;

Schenning, A. P. H. J. *Chem. Rev.* **2005**, *105*, 1491–1546. (g) Keizer, H. M.; Sijbesma, R. P. *Chem. Soc. Rev.* **2005**, *34*, 226–234.

(4) Reviews: (a) Okamoto, Y.; Yashima, E. *Angew. Chem., Int. Ed.* **1998**, *37*, 1021–1043. (b) Yashima, E.; Yamamoto, C.; Okamoto, Y. *Synlett* **1998**, 344–360. (c) Kubo, Y. *Synlett* **1999**, 161–174. (d) Yashima, E. *J. Chromatogr. A* **2001**, *906*, 105–125. (e) Nakano, T. *J. Chromatogr. A* **2001**, *906*, 205–225. (f) Reggelin, M.; Doerr, S.; Klussmann, M.; Schultz, M.; Holbach, M. *Proc. Natl. Acad. Sci. U. S. A.* **2004**, *101*, 5461–5466.

(5) (a) Yashima, E.; Matsushima, T.; Okamoto, Y. *J. Am. Chem. Soc.* **1995**, *117*, 11596–11597. (b) Yashima, E.; Matsushima, T.; Okamoto, Y. *J. Am. Chem. Soc.* **1997**, *119*, 6345–6359. (c) Yashima, E.; Maeda, K.; Okamoto, Y. *Nature* **1999**, *399,* 449–451. (d) Goto, H.; Zhang, H. Q.; Yashima, E. *J. Am. Chem. Soc.* **2003**, *125*, 2516–2523. (e) Ashida, Y.; Sato, T.; Morino, K.; Maeda, K.; Okamoto, Y.; Yashima, E. *Macromolecules* **2003**, *36*, 3345–3350. (f) Maeda, K.; Morino, K.; Okamoto, Y.; Sato, T.; Yashima, E. *J. Am. Chem. Soc.* **2004**, *126*, 4329–4342. (g) Maeda, K.; Hatanaka, K.; Yashima, E. *Mendeleeve Commun.* **2004**, *14*, 231–233. (h) Morino, K.; Watase, N.; Maeda, K.; Yashima, E. *Chem. –Eur. J.* **2004**, *10*, 4703–4707. (i) Hasegawa, T.; Morino, K.; Tanaka, Y.; Katagiri, H.; Furusho, Y.; Yashima, E. *Macromolecules* **2006**, *39*, 482–488.

(6) (a) Onouchi, H.; Kashiwagi, D.; Hayashi, K.; Maeda, K.; Yashima, E. *Macromolecules* **2004**, *37*, 5495–5503. (b) Kamikawa, Y.; Kato, T.; Onouchi, H.; Kashiwagi, D.; Maeda, K.; Yashima, E. *J. Polym. Sci., Part A: Polym. Chem.* **2004**, *42*, 4580–4586. (c) Nishimura, T.; Tsuchiya, K.; Ohsawa, S.; Maeda, K.; Yashima, E.; Nakamura, Y.; Nishimura, J. *J. Am. Chem. Soc.* **2004**, *126*, 11711–11717. (d) Onouchi, H.; Miyagawa, T.; Furuko, A.; Maeda, K.; Yashima, E. *J. Am. Chem. Soc.* **2005**, *127*, 2960–2965. (e) Miyagawa, T.; Furuko, A.; Maeda, K.; Katagiri, H.; Furusho, Y.; Yashima, E. *J. Am. Chem. Soc.* **2005**, *127*, 5018–5019.

(7) (a) Yashima, E.; Nimura, T.; Matsushima, T.; Okamoto, Y. *J. Am. Chem. Soc.* **1996**, *118*, 9800–9801. (b) Kawamura, H.; Maeda, K.; Okamoto, Y.; Yashima, E. *Chem. Lett.* **2001**, 58–59.

(8) Hasegawa, T.; Maeda, K.; Ishiguro, H.; Yashima, E. *Polym. J.* **2006**, *38*, 912–919.

(9) (a) Yashima, E.; Maeda, Y.; Okamoto, Y. *Chem. Lett.* **1996**, 955–956. (b) Yashima, E.; Maeda, Y.; Matsushima, T.; Okamoto, Y. *Chirality* **1997**, *9*, 593–600. (c) Maeda, K.; Okada, S.; Yashima, E.; Okamoto, Y. *J. Polym. Sci., Part A: Polym. Chem.* **2001**, *39*, 3180–3189.

(10) (a) Maeda, K.; Takeyama, Y.; Sakajiri, K.; Yashima, E. *J. Am. Chem. Soc.* **2004**, *126*, 16284–16285. (b) Nagai, K.; Maeda, K.; Takeyama, Y.; Sakajiri, K.; Yashima, E. *Macromolecules* **2005**, *38*, 5444–5451. (c) Nagai, K.; Sakajiri, K.; Maeda, K.; Okoshi, K.; Sato, T.; Yashima, E. *Macromolecules* **2006**, *39*, 5371–5380.

(11) (a) Nonokawa, R.; Yashima, E. *J. Am. Chem. Soc.* **2003**, *125*, 1278–1283. (b) Nonokawa, R.; Oobo, M.; Yashima, E. *Macromolecules* **2003**, *36*, 6599–6606. (c) Nishimura, T.; Ohsawa, S.; Maeda, K.; Yashima, E. *Chem. Commun.* **2004**, 646–647. (d) Morino, K.; Oobo, M.; Yashima, E. *Macromolecules* **2005**, *38*, 3461–3468. (e) Morino, K.; Kaptein, B.; Yashima, E. *Chirality* **2006**, *18*, 717–722.

(12) (a) Saito, M. A.; Maeda, K.; Onouchi, H.; Yashima, E. *Macromolecules* **2000**, *33*, 4616–4618. (b) Onouchi, H.; Maeda, K.; Yashima, E. *J. Am. Chem. Soc.* **2001**, *123*, 7441–7442. (c) Nonokawa, R.; Yashima, E. *J. Polym. Sci., Part A: Polym. Chem.* **2003**, *41*, 1004–1013. (d) Onouchi, H.; Hasegawa, T.; Kashiwagi, D.; Ishiguro, H.; Maeda, K.; Yashima, E. *Macromolecules* **2005**, *38*, 8625–8633. (e) Onouchi, H.; Hasegawa, T.; Kashiwagi, D.; Ishiguro, H.; Maeda, K.; Yashima, E. *J. Polym. Sci., Part A: Polym. Chem.* **2006**, *44*, 5039–5048. (f) Miyagawa, T.; Yamamoto, M.; Muraki, R.; Onouchi, H.; Yashima, E. *J. Am. Chem. Soc.* **2007**, *129*, 3676–3682.

(13) Yashima, E., *Anal. Sci.* **2002**, *18*, 3–6.

(14) Onouchi, H.; Miyagawa, T.; Morino, K.; Yashima, E. *Angew. Chem., Int. Ed.* **2006**, *45*, 2381–2384.

(15) (a) Simionescu, C.; Percec, V.; Dumitrescu, S. *J. Polym. Sci.: Polym. Chem. Ed.* **1977**, *15*, 2497–2509. (b) Simionescu, C.; Percec, V. *Prog. Polym. Sci.* **1982**, *8*, 133–214. (c) Furlani, A.; Napoletano, C. V.; Russo, M. V.; Feast, W. J. *Polym. Bull.* **1986**, *16*, 311–317. (d) Kishimoto, Y.; Eckerle, P.; Miyatake, T.; Kainosho, M.; Ono, A.; Ikariya, T.; Noyori, R. *J. Am. Chem. Soc.* **1999**, *121*, 12035–12044. (e) Percec, V.; Rudick, J. G. *Macromolecules* **2005**, *38*, 7241–7250.

(16) For examples, see: (a) Deng, J.; Tabei, J.; Shiotsuki, M.; Sanda, F.; Masuda, T. *Macromolecules* **2004**, *37*, 1891–1896. (b) Deng, J.; Tabei, J.; Shiotsuki, M.; Sanda, F.; Masuda, T. *Macromol. Chem. Phys.* **2004**, *205*, 1103–1107. (c) Deng, J.; Zhao, W.; Wang, J.; Zhang, Z.; Yang, W. *Macromol. Chem. Phys.* **2007**, *208*, 218–223.

(17) Maeda, K.; Mochizuki, H.; Watanabe, M.; Yashima, E. *J. Am. Chem. Soc.* **2006**, *128*, 7639–7650.

(18) For reviews, see refs 1c,f–l,p. See also: (a) Okamoto, Y.; Nishikawa, M.; Nakano, T.; Yashima, E.; Hatada, K. *Macromolecules* **1995**, *28*, 5135–5138. (b) Takei, F.; Onitsuka, K.; Takahashi, S. *Polym. J.* **1999**, *31*, 1029–1032. (c) Tabei, J.; Nomura, R.; Masuda, T. *Macromolecules* **2002**, *35*, 5405–5409.

(19) (a) Green, M. M.; Garetz, B. A.; Munoz, B.; Chang, H.; Hoke, S.; Cooks, R. G. *J. Am. Chem. Soc.* **1995**, *117*, 4181–4182. (b) Selinger, J. V.; Selinger, R. L. B. *Phys. Rev. Lett.* **1996**, *76*, 58–61. (c) Li, J.; Schuster, G. B.; Cheon, K.-S.; Green, M. M.; Selinger, J. V. *J. Am. Chem. Soc.* **2000**, *122*, 2603–2612. (d) Green, M. M.; Cheon, K.-S.; Yang, S.-Y.; Park, J.-W.; Swansburg, S.; Liu, W. *Acc. Chem. Res.* **2001**, *34*, 672–680.

(20) Saxena, A.; Guo, G.; Fujiki, M.; Yang, Y.; Ohira, A.; Okoshi, K.; Naito, M. *Macromolecules* **2004**, *37*, 3081–3083.

(21) Pohl, F. M.; Jovin, T. M. *J. Mol. Biol.* **1972**, *67*, 375–396.

(22) (a) Toriumi, H.; Saso, N.; Yasumoto, Y.; Sasaki, S.; Uematsu, I. *Polym. J.* **1979**, *11*, 977–981, (b) Watanabe, J.; Okamoto, S.; Satoh, K.; Sakajiri, K.; Furuya, H. Abe, A. *Macromolecules* **1996**, *29,* 7084–7088.

(23) For leading references, see: (a) Hino, K.; Maeda, K.; Okamoto, Y. *J. Phys. Org. Chem.* **2000**, *13*, 361–367. (b) Cheon K. S., Selinger, J. V.; Green, M. M. *Angew. Chem., Int. Ed.* **2000**, *39*, 1482–1485. (c) Fujiki, M. *J. Am. Chem. Soc.* **2000**, *122*, 3336–3343. (d) Ohira, A.; Kunitake, M.; Fujiki, M.; Naito, M.; Saxena, A. *Chem. Mater.* **2004**, *16*, 3919–3923. (e) Tabei, J.; Nomura, R.; Sanda, F.; Masuda, T. *Macromolecules* **2004**, *37*, 1175–1179.

(24) (a) Fujiki, M.; Koe J. R.; Motonaga, M.; Nakashima, H.; Terao, K.; Teramoto, A. *J. Am. Chem. Soc.* **2001**, *123*, 6253–6261. (b) Morino, K.; Maeda, K.; Yashima, E. *Macromolecules* **2003**, *36*, 1480–1486. (c) Tabei, J.; Nomura, R.; Shiotsuki, M.; Sanda, F.; Masuda, T. *Macromol. Chem. Phys.* **2005**, *206*, 323–332.

(25) For leading references, see: (a) Okamoto, Y.; Nakano, T.; Ono, E.; Hatada, K. *Chem. Lett.* **1991**, 525–528. (b) Langeveld-Voss, B. M. W.; Christiaans, M. P. T.; Janssen, R. A. J.; Meijer, E. W. *Macromolecules* **1998**, *31*, 6702–6704. (c) Cheuk, K. K. L.; Lam, J. W. Y.; Chen, J.; Lai, L. M.; Tang, B. Z. *Macromolecules* **2003**, *36*, 5947–5959. (d) Cheuk, K. K. L.; Lam, J. W. Y.; Lai, L. M.; Dong, Y.; Tang, B. Z. *Macromolecules* **2003**, *36*, 9752–9762. (e) Maeda, K.; Morino, K.; Yashima, E. *J. Polym. Sci., Part A: Polym. Chem.* **2003**, *41*, 3625–3631. (f) Maeda, K.; Kamiya, N.; Yashima, E. *Chem. –Eur. J.* **2004**, *10*, 4000–4010. (g) Sanda, F.; Terada, K.; Masuda, T. *Macromolecules* **2005**, *38*, 8149–8154. Recently, Yashima et al. found that a helical poly(phenylacetylene) bearing the L- or D-alanine residue as the pendants with a long alkyl chain changed their main-chain stiffness in polar and nonpolar solvents, accompanied by inversion of the macromolecular helicity, see: (h) Okoshi, K.; Sakurai, S-i.; Ohsawa, S.; Kumaki, J.; Yashima, E. *Angew. Chem., Int. Ed.* **2006**, *45*, 8173–8176.

(26) Yashima, E.; Maeda, Y.; Okamoto, Y. *J. Am. Chem. Soc.* **1998**, *120*, 8895–8896.

(27) (a) Ishikawa, M.; Maeda, K.; Mitsutsuji, Y.; Yashima, E. *J. Am. Chem. Soc.* **2004**, *126*, 732–733. (b) Hase, Y.; Ishikawa, M.; Muraki, R.; Maeda, K.; Yashima, E. *Macromolecules* **2006**, *39*, 6003–6008.

(28) (a) Tang, K.; Green, M. M.; Cheon, K. S.; Selinger, J. V.; Garetz, B. A. *J. Am. Chem. Soc.* **2003**, *125*, 7313–7323. See also: (b) Zhao, H.; Sanda, F.; Masuda, T. *Macromolecules* **2004**, *37*, 8888–8892.

Chapter 4

Mechanism of Helicity Induction and Memory of the Macromolecular Helicity in Poly(phenyl isocyanide) Derivatives Based on Their Structural Analyses

Abstract: An optically inactive poly(4-carboxyphenyl isocyanide) (poly-**1**–**H**) changed its structure into the prevailing, one-handed helical structure upon complexation with optically active amines in DMSO and water, and the complexes show a characteristic induced circular dichroism (ICD) in the polymer backbone region. Moreover, the macromolecular helicity induced in water and aqueous organic solutions containing more than 50 vol% water could be "memorized" even after complete removal of the chiral amines (***h***-poly-**1b**–**H**), while that induced in DMSO and DMSO–water mixtures containing less than 30 vol% water could not maintain the optical activity after removing the chiral amines (poly-**1a**–**H**). In order to elucidate the mechanism of the helix induction with chiral amines and the memory of the macromolecular helicity in water and DMSO–water mixture, various spectroscopic measurements and theoretical calculations were performed. From the spectroscopic results such as circular dichroism (CD), absorption, IR, vibrational CD (VCD), and NMR of poly-**1a**–**H**, ***h***-poly-**1b**–**H**, and original poly-**1**–**H**, it was revealed that the specific configurational isomerization around the C=N double bonds occurs in the helicity induction process in each solvent. However, the spectroscopic results could not solve the questions what different helical structures the polyisocyanide can form in DMSO and water in the presence of chiral amines, respectively, and why the helical structure induced in DMSO cannot be memorized after removal of the chiral amines. In order to solve the questions, the author measured X-ray diffraction (XRD) of the uniaxially oriented films of the corresponding methyl esters (poly-**1**–**Me**, poly-**1a**–**Me**, and ***h***-poly-**1b**–**Me**) prepared from their liquid

crystalline polymer solutions together with the persistence lengths of the polymers. On the basis of the XRD analyses, the most plausible helical structure of poly-**1a**–**Me** was proposed to be an 18 unit / 5 turn helix and that of ***h***-poly-**1b**–**Me** was a 10 unit / 3 turn helix. In addition, the persistence length measurements revealed that these structural changes accompany the significant change in their main-chain stiffness. On the basis of these results, the mechanism of helix induction in poly-**1**–**H** and the memory of the macromolecular helicity are discussed.

Introduction

Polyisocyanides are among the most extensively studied helical polymers since the pioneering research by Millich, Drenth, and Nolte.[1,2] Millich proposed a 4 unit / turn (4/1) helical structure for polyisocyanides when they have a bulky side group[1c] by means of X-ray analysis.[1b] Nolte et al. succeeded in the direct chromatographic resolution of poly(*t*-butyl isocyanide) into enantiomeric helices, which clearly evidenced the stable helical structure of polyisocyanides.[3] The resolved polymer with a positive rotation was postulated to have a left-handed helical conformation based on a circular dichroism (CD) spectral analysis.[3b] The stable helical conformation of the polyisocyanides in solution was further supported by the helix-sense selective polymerization of achiral bulky isocyanides by Nolte[4] and Novak.[5] Since then, wide varieties of helical polyisocyanides with functional pendant groups have been synthesized and some of them were applied for optoelectronic and liquid crystalline materials.[1,6]

However, Green[7] and Salvadori[8] appealed that polyisocyanides bearing less bulky aliphatic and aromatic groups might not have a regular 4/1 helical conformation because of possible configurational isomerism (*syn–anti* isomerization) around the C=N double bond and *s-cis* and *s-trans* conformational isomerism around the C–C bond of the main-chain (Chart 4-1). Later, Euler and Rosen[9] experimentally proved such a slow interconversion of poly(phenyl isocyanide) from an "as-prepared" 4/1 helical conformation to a more extended *s-trans*, zigzag conformation; an analogous *s-trans* structure as one of the most stable structures was also proposed theoretically by Clericuzio and Salvadori.[10] Therefore, helical polyisocyanides, in particular, helical poly(phenyl isocyanide)s lack an unquestionable direct evidence for their helical structures.[11]

Recently, Yashima et al. reported that a helical polyisocyanide with a controlled helical sense could be produced based on the noncovalent "*helicity induction and chiral memory effect*".[12] An achiral poly(4-carboxyphenyl isocyanide) (poly-**1**–**H**) and its sodium salt (poly-**1**–**Na**) were found to form a preferred-handed helical conformation upon noncovalent

complexation with chiral amines in water.[13] The induced helix remained after complete removal of the chiral amines and further modifications of the pendant groups to esters and amide residues were possible without loss of the macromolecular helicity memory.[14] However, the helical structures of poly-**1**–**H** induced by chiral amines in water and aqueous organic solutions containing more than 50 vol% water could be effectively memorized after complete removal of the chiral amines (***h***-poly-**1b**–**H**; Figure 4-1), while the helical poly-**1**–**H** induced by chiral amines in DMSO[15] and DMSO–water mixtures containing less than 30 vol% water could not maintain the helicity after removing the chiral amines (poly-**1a**–**H**; Figure 4-1).[16] These results raise the questions what different helical structures the polyisocyanide can form in DMSO and water in the presence of chiral amines, respectively, and why the helical structure induced in DMSO cannot be memorized after removal of the chiral amines.

To address these questions, a series of isotopically labeled poly-**1**–**H**s and their methyl esters (poly-**1**–**Me**s) with deuterium (D), ^{13}C, and ^{15}N and non-labeled poly-**1**–**H** and poly-**1**–**Me**, and their structures before and after the helicity induction with chiral amines in water and organic solvent–water mixtures and subsequent memory were thoroughly investigated by means of absorption, CD, IR, vibrational CD (VCD), and NMR spectroscopies.[17] These spectroscopic measurement results revealed the specific configurational isomerization around the C=N double bonds that indeed took place during the helicity induction process in each solvent.

In this study, the author prepared the methyl esters of high-molecular-weight poly-**1**–**H**, poly-**1a**–**H**, and ***h***-poly-**1b**–**H** (HMW-poly-**1**–**Me**, HMW-poly-**1a**–**Me**, and HMW-***h***-poly-**1b**–**Me**, respectively), and measured X-ray diffraction (XRD) of the uniaxially oriented films prepared from their liquid crystalline (LC) polymer solutions together with the persistence lengths of the polymers. On the basis of the results, the most plausible helical structures of poly-**1a**–**Me** and ***h***-poly-**1b**–**Me** are proposed and the mechanism of helix induction in poly-**1**–**H** and the memory of the macromolecular helicity are discussed.

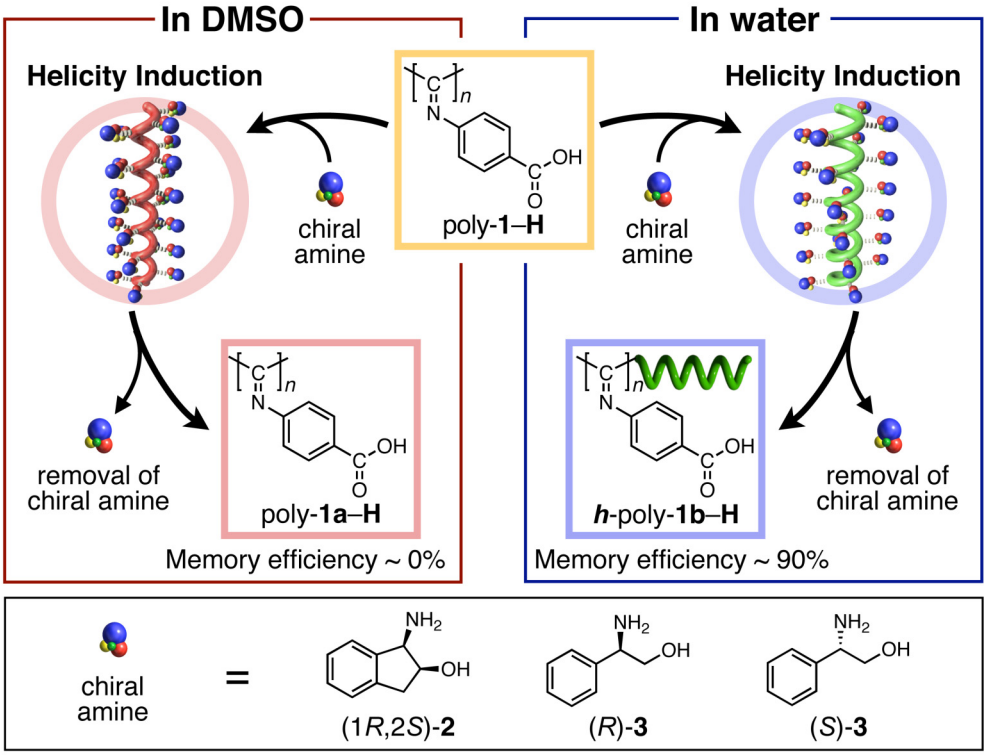

Figure 4-1. Schematic illustration of helicity induction in poly-**1**–**H** in DMSO and water with chiral amines (**2** or **3**) and subsequent removal of the chiral amines. The macromolecular helicity induced in water is memorized after complete removal of the chiral amines (***h***-poly-**1b**–**H**), whereas that induced in DMSO cannot be memorized (poly-**1a**–**H**).

Chart 4-1. Possible Triad Structures of Polyisocyanides (A), *s-Cis* and *s-Trans* Conformations (B), and Configurational *Syn-anti* Isomerization of Polyisocyanide Dyad (C)

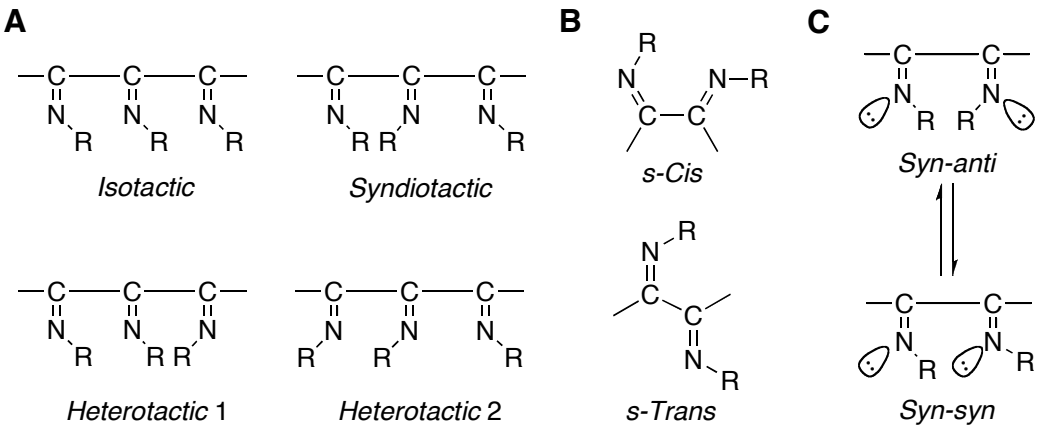

Results and Discussion

Synthesis of HMW-Poly-1-H and Macromolecular Helicity Induction with Chiral Amines and Isolation of the Polymers. HMW-poly-**1**-**H** was prepared by the polymerization of 4-(ethoxycarbonyl)phenyl isocyanide (**1**-**Et**) in dry tetrahydrofuran (THF) containing a small amount of alcohols such as methanol (MeOH) (THF–MeOH = 99:1, v/v) with the $NiCl_2 \cdot 6H_2O$ catalyst, affording a relatively high molecular weight poly-**1**–**Et** (HMW-poly-**1**–**Et**; M_n = 8.6 × 10^4) in 88% yield (Scheme 4-1).[18] The number-average molecular weights (M_n) was determined by size exclusion chromatography (SEC) with polystyrene standards using chloroform ($CHCl_3$) as the eluent. The obtained HMW-poly-**1**–**Et** was further alkaline hydrolyzed, followed by esterification with CH_2N_2 to give HMW-poly-**1**–**H** and HMW-poly-**1**–**Me**, respectively (Scheme 4-1).

HMW-poly-**1**–**H** was then annealed with (1*R*,2*S*)-**2** in DMSO–water (4:1, v/v) and (*R*)-**3** in 2-propanol–water (1:1, v/v) at 50 °C for 5 and 72 days in a similar way as reported previously.[16] The HMW-poly-**1**–**H**—(1*R*,2*S*)-**2** complex in DMSO–water (4:1, v/v) and the HMW-poly-**1**–**H**—(*R*)-**3** complex in 2-propanol–water (1:1, v/v) formed a predominantly one-handed helix and exhibited an induced CD (ICD) in the imino chromophore region of the polymer backbones (300—450 nm) and their CD spectral patterns and λ_{max} of the Cotton effects were similar to each other.

As reported previously, the helical HMW-poly-**1**–**H** (HMW-***h***-poly-**1b**–**H**) induced by (*R*)-**3** in aqueous organic solutions containing more than 50 vol% water was automatically memorized during the helicity induction process, thus showing an intense ICD after complete removal of the chiral amine, whereas the optical activity induced in HMW-poly-**1**–**H** by (1*R*,2*S*)-**2** in DMSO–water (4:1, v/v) almost completely disappeared after removing the chiral amine (HMW-poly-**1a**–**H**) (Table 4-1).[16] HMW-***h***-poly-**1b**–**H**s can be converted to the corresponding methyl esters (***h***-poly-**1b**–**Me**s) without the loss of the macromolecular helicity (run 2 in Table 4-1). On the other hand, HMW-poly-**1**–**H** could not retain the optical activity

induced in DMSO-water (4:1, v/v) with (1*R*, 2*S*)-**2** after removal of the chiral amine (run 1 in Table 4-1).

Scheme 4-1. Synthetic Scheme of HMW Poly(phenyl isocyanide) Derivatives

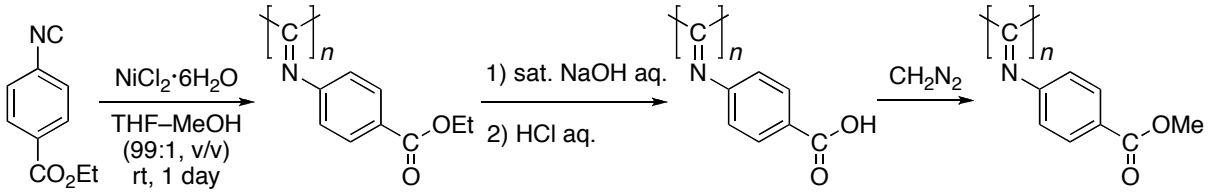

1–Et HMW-poly-**1–Et** HMW-poly-**1–H** HMW-poly-**1–Me**

88% yield
M_n = 8.6 x 10^5
M_w/M_n = 5.0

Table 4-1. CD Spectral Data of Helical HMW-poly-**1–H**s Induced by (1*R*,2*S*)-**2** in DMSO–Water (4:1, v/v) and by (*R*)-**3** in 2-Propanol–Water (1:1, v/v) and Isolated Polymers and Their Methyl Esters after Removal of Chiral Amines[a]

				after removal of chiral amines			HMW-poly-**1–Me**
run	chiral amine	solvent (v/v)	$\Delta\varepsilon$ (λ, time)[b]		$\Delta\varepsilon$ (λ)[c]	memory efficiency (%)[d]	$\Delta\varepsilon$ (λ)[e]
1	(1*R*, 2*S*)-**2**	DMSO-water (4/1)	+7.21 (362, 5)	HMW-poly-**1a–H**	+0.12 (362)	1.6	+0.04 (360)
2	(*R*)-**3**	2-propanol-water (1/1)	–17.9 (357, 72)[f]	HMW-***h***-poly-**1b–H**	–15.2 (360)	85	–14.9 (359)

[a] The concentration of polymers is 1.0 mg/mL. [b] Measured at ambient temperature (20–25 °C) after the samples had been allowed to stand at 50 °C for days; molar ratio of an amine to monomeric units of HMW-poly-**1–H**s is 10; $\Delta\varepsilon$ (M^{-1} cm^{-1}), λ (nm), and time (days). [c] Measured in alkaline water ([NaOH]/[polymer] = 1 and [polymer] = 1.0 mg/mL); $\Delta\varepsilon$ (M^{-1} cm^{-1}) and λ (nm). [d] Estimated on the basis of the ICD values of HMW-poly-**1**–amine complexes before isolation. [e] Measured in $CHCl_3$ ([polymer] = 1.0 mg/mL); $\Delta\varepsilon$ (M^{-1} cm^{-1}) and λ (nm). [f] Molar ratio of an amine to monomeric units of HMW-poly-**1**–**H** is 20.

Persistence Length Measurements. The backbone stiffness (persistence length (q)) of HMW-poly-**1**–**Me**, HMW-poly-**1a**–**Me**, and HMW-***h***-poly-**1b**–**Me** in $CHCl_3$ was then measured.[19] The q values of these polymers were estimated using SEC equipped with multi-angle laser light scattering (MALS) and refractive index detectors in series in conjunction with the wormlike chain model.[20] This model can be described as an analytical function of the molecular weight (M_w) and the radius of gyration (S) if the q values and the molar mass per unit contour length (M_L), which eventually leads to the monomer unit height (h), are given. In this way, the dependences of the M_w on the radii of gyration of these polymers were explored by using an SEC-MALS system using $CHCl_3$ as the eluent (Figure 4-2). The solid curves in the plots were calculated using the parameters determined from the fits of the unperturbed wormlike chain model over the entire M_w studied range, and are represented by the theoretical values of $<S^2>^{0.5}$.

The calculated q value of the "as-prepared" HMW-poly-**1**–**Me** is 59 nm, which is a little smaller than that of a helical polyisocyanopeptide (76 nm).[19j] Interestingly, HMW-***h***-poly-**1b**–**Me** with a macromolecular helicity memory exhibited a significantly larger q value of 88 nm. In contrast, HMW-poly-**1a**–**Me** which lost optically activity after helicity induction showed a dramatic decrease in its q value to 43 nm, leading to a rather semi-rigid polymer. These changes in the q values clearly demonstrate the specific configurational isomerization around the C=N double bonds (*syn–anti* isomerization) that likely takes place during the helicity induction process, resulting in the changes of the main-chain stiffness of HMW-poly-**1**–**Me**.

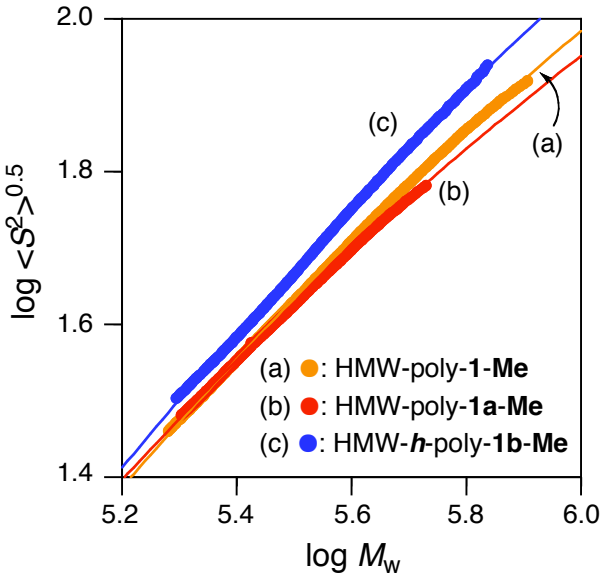

Figure 4-2. Double-logarithmic plots of the radius of gyration versus the molecular weight of HMW-poly-**1**–**Me** (a), HMW-poly-**1a**–**Me** (b), and HMW-***h***-poly-**1b**–**Me** (c) in $CHCl_3$ obtained by SEC-MALS measurements at 25 °C. Solid curves were obtained on the basis of the wormlike chain theory and fit well with the experimental data. The evaluated parameters are as follows: HMW-poly-**1**–**Me**, q = 59 nm, M_L = 1618 nm^{-1}, h = 0.10 nm; HMW-poly-**1a**–**Me**, q = 43 nm, M_L = 1483 nm^{-1}, h = 0.11 nm; HMW-***h***-poly-**1b**–**Me**, q = 88 nm, M_L = 1592 nm^{-1}, h = 0.10 nm.

Helical Structures. Although the helical structure of polyisocyanides has been postulated to be a 4 unit / turn (4/1) helical conformation on the basis of an X-ray analysis of poly(α-phenylethyl isocyanide) (PPEI),[1b,d,2a] because of the use of unoriented samples, the exact helical structure was difficult to determine by their X-ray diffractions. Nolte et al. successfully synthesized a series of rigid-rod helical polyisocyanopeptides with a controlled helicity, some of which showed cholesteric LC phases.[6a,b,e,f] Nevertheless, they measured X-ray diffraction of their unoriented cast films, and therefore, only an orthorhombic arrangement of the polymers in the solid could be proposed.[6b]

Recently, Yashima et al. found that some helical poly(phenyl isocyanide)s derived from low molecular weight ***h***-poly-**1b**–**H** (M_n = 3.3 × 10^4) after modification of the carboxy pendant groups with bulky primary and secondary amines or primary amines with a long

ethylene oxide trimer or a pyridylmethyl group formed lyotropic LC phases in concentrated solutions due to their main-chain stiffness, thus showing a fingerprint texture.[14] In contrast, the original ***h***-poly-**1b–H** and ***h***-poly-**1b–Me** did not show LC phases in concentrated solutions. However, as anticipated, HMW-poly-**1–H** was found to form a nematic LC phase in concentrated alkaline water solution (15–20 wt%). Its methyl ester (HMW-poly-**1–Me**) also showed a nematic LC phase in $CHCl_3$. Furthermore, the corresponding helical polymers, HMW-***h***-poly-**1b–H** and HMW-***h***-poly-**1b–Me** exhibited cholesteric LC phases in alkaline water (15 wt%) and 1,1,2,2-tetrachloroethane (20 wt%), respectively, showing a fingerprint texture. This finding of nematic and cholesteric LC formations of the polyisocyanides before and after the helicity induction and memory will make it possible to investigate the helical structure by XRD measurements of the shear-oriented films prepared from the LC samples. In fact, Yashima et al. recently succeeded in determining the helical structures of LC polyacetylenes and polyisocyanides by the X-ray analyses of the corresponding oriented films.[6h,21]

Figures 4-3A and B show the wide angle X-ray diffraction (WAXD) patterns of the uniaxially oriented HMW-poly-**1–Me** and HMW-***h***-poly-**1b–Me** films prepared from concentrated nematic and cholesteric LC $CHCl_3$ solutions, respectively. X-ray photographs were taken from the edge-view position with a beam parallel to the film surface at ambient temperature (20—25 °C).

The X-ray diffractions of an oriented optically inactive HMW-poly-**1–Me** and an optically active HMW-***h***-poly-**1b–Me** showed the diffuse, but similar pattern except for the intensity of the meridian reflection in the smallest angle region of nearly 4.0 Å as shown in Figures 4-3A and B and Table 4-2. The reflection intensity of nearly 4.0 Å is apparently weak for HMW-***h***-poly-**1b–Me**, while strong for HMW-poly-**1–Me**, suggesting that the regularity of the helical backbone of HMW-***h***-poly-**1b–Me** is still imperfect; the reflection will disappear when the regularity of the helical backbone increases. This speculation is supported by the NMR and IR measurement results; namely, the reflection of nearly 4.0 Å may not be

derived from the periodicity of the regular helical structure, but arise from the average helical pitch of imperfect helices without long range orders as described below for HMW-poly-**1**–**Me**.

The X-ray diffraction pattern with different ranges of sensitivities of the oriented HMW-***h***-poly-**1b**–**Me** film (Figure 4-3B) showed the broad, but apparent equatorial and near-meridional reflections. The four equatorial reflections, 14.19, 10.56, 6.46, and 5.13 Å can be indexed with a simple two-dimensional tetragonal lattice of a = 14.37 Å (Table 4-2). Next, the author determined the fiber periods to be 10.30 Å (= c) from the layer lines (1/10.30 $Å^{-1}$ apart) attributed to the helical structure, where the meridional reflections of 4.02 and 1.98 Å were excluded from this analysis because the reflections cannot be assumed for the regular helical structure of HMW-***h***-poly-**1b**–**Me** as described below for HMW-poly-**1**–**Me**. The near-meridian reflections observed around 2 Å are attributed to lateral reflections judging from WAXD measurements of the same polymer film using a flat imaging plate. The observed density (1.259 g/cm^3) indicates that this unit cell includes 10 monomer units / 1 chain along the c-axis, being in agreement with the calculated density (1.258 g/cm^3).[22] Although the author could not observe a meridian reflection on the 10th layer line (1.030 Å) (see Table 4-2) corresponding to the unit height (h) of the helical structure even when the X-ray measurements were performed using a cylindrical camera with the samples tilted ca. 48° normal to the beam, the most plausible helical structure of the HMW-***h***-poly-**1b**–**Me** can be proposed to be a 10 unit / 3 turn helix (10/3) on the basis of the strong reflection on the 3rd layer line (3.41 Å) and the reflection on the 4th layer line (2.59 Å) which correspond to the first- or second-order Bessel functions, respectively (Table 4-2), being consistent with the helical diffraction theory.[23] The plausible helical structure of ***h***-poly-**1b**–**Me** postulated by X-ray analysis is shown in Figure 4-4A.

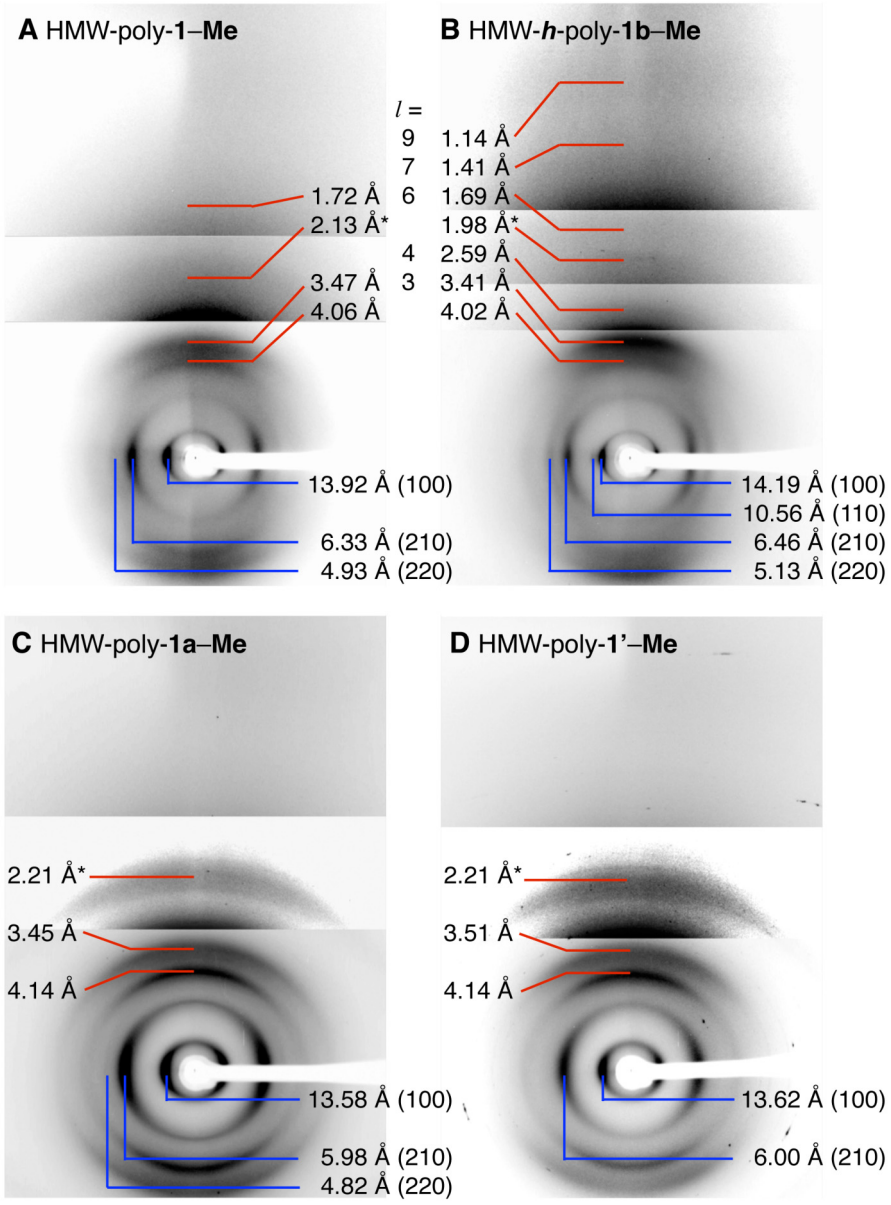

Figure 4-3. X-ray diffraction patterns of oriented films obtained from optically inactive HMW-poly-**1**–**Me** (A), optically active HMW-***h***-poly-**1b**–**Me** with helicity memory (B), optically inactive HMW-poly-**1a**–**Me** (C), and HMW-poly-**1'**–**Me** (D) with different ranges of sensitivities taken from the edge-view position with a beam parallel to the film surface; the vertical direction is nearly corresponding to the helical axis. HMW-poly-**1'**–**Me** was obtained from HMW-poly-**1**–**Me** after standing its $CHCl_3$ solution at room temperature for 3 months. The representative layer lines and the main reflections are labeled. The meridian reflections around 2 Å indicated by asterisks are found to be lateral reflections based on WAXD measurements of the same polymer film using a flat imaging plate.

Table 4-2. X-ray Diffraction Data of Optically Inactive HMW-poly-**1–Me**, Optically Active HMW-***h***-poly-**1b–Me**, Optically Inactive HMW-poly-**1a–Me**, and Optically Inactive HMW-poly-**1'–Me** Oriented Films

HMW-poly-**1–Me**						HMW-***h***-poly-**1b–Me**					
layer line *l*	d_{obs} (Å)[a]	d_{cal} (Å)[b]	*h k*[b]	I_{obs}[c]		layer line *l*	d_{obs} (Å)[a]	d_{cal} (Å)[d]	*h k*[d]	I_{obs}[c]	*n*[e]
0	13.92	13.96	1 0	s		0	14.19	14.37	1 0	vs	
							10.56	10.16	1 1	w	
	6.33	6.24	2 1	s			6.46	6.43	2 1	s	
	4.93	4.94	2 2	w			5.13	5.08	2 2	m	
	2.13	—	—	vw			1.98	—	—	w	
[h]	4.06	—	—	s		[h]	4.02	—	—	w	
[h]	3.47	—	—	s		3	3.41	3.43	nm[i]	vs	1
						4	2.59	2.58	nm[i]	vw	–2
[h]	1.72	—	—	vw		6	1.69	1.72	nm[i]	vw	2
						7	1.41	1.46	nm[i]	vw	–1
						9	1.14	1.14	nm[i]	vw	3
						10	[j]	1.03	0 0		0

HMW-poly-**1a–Me**						HMW-poly-**1'–Me**					
layer line *l*	d_{obs} (Å)[a]	d_{cal} (Å)[f]	*h k*[f]	I_{obs}[c]	*n*[g]	layer line *l*	d_{obs} (Å)[a]	d_{cal} (Å)[f]	*h k*[f]	I_{obs}[c]	*n*[g]
0	13.58	13.56	1 0	vs		0	13.62	13.56	1 0	vs	
	5.98	6.06	2 1	s			6.00	6.06	2 1	s	
	4.82	4.79	2 2	vw							
	2.21	—	—	w			2.21	—	—	w	
5	4.14	4.14	nm[i]	vs	1	5	4.14	4.14	nm[i]	vs	–1
6	3.45	3.45	nm[i]	s	–6	6	3.51	3.45	nm[i]	s	–6
18	[j]	1.15	0 0		0	18	[j]	1.15	0 0		0

[a] Spacings observed in X-ray diffraction patterns. [b] Spacings calculated and indexed on the basis of a tetragonal unit cell with parameters, a = 13.96 Å. It was difficult to determine the fiber period because HMW-poly-**1–Me** chains most likely compose of the mixture of a nearly 10/3 helix of HMW-***h***-poly-**1b–Me** and a nearly 18/5 helix of HMW-poly-**1a–Me** (see text). [c] Observed intensities; vs = very strong, s = strong, m = medium, w = weak, and vw = very weak. [d] Spacings calculated and indexed on the basis of a tetragonal unit cell with parameters, a = 14.37 and c = 10.30 Å. [e] Bessel function order based on a 10/3 helix. [f] Spacings calculated and indexed on the basis of a tetragonal unit cell with parameters a = 13.56 and c = 20.70 Å. [g] Bessel function order based on an 18/5 helix. [h] Unindexed reflection, which may be derived from imperfect helices. [i] Near meridional reflections. These reflections may be indexed as 10*l*, which should be split across the meridian. However, the imperfect orientation of the films may result in such arc-like reflections linked at the meridian, and their calculated d values were estimated as the 00*l* reflections because these reflections were read along the meridian. [j] Not observed.

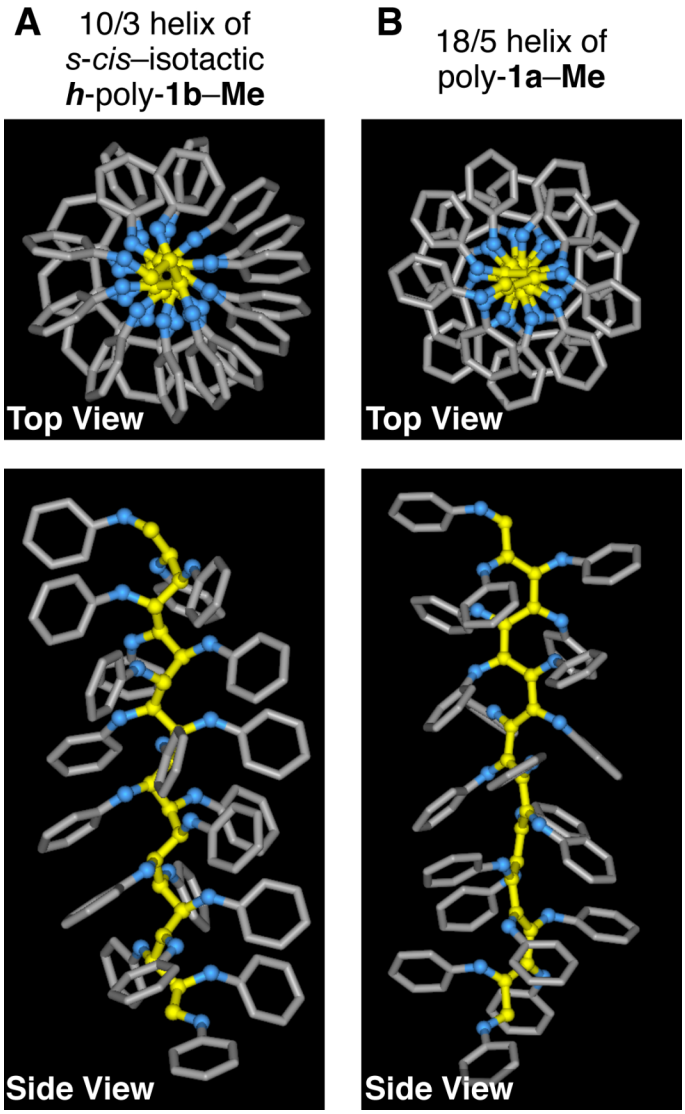

Figure 4-4. Top and side view of a possible 10/3 right-handed helical structure of *s-cis*—isotactic ***h***-poly-**1b**–**Me** (20-mer) (A) and a possible 18/5 helical structure of poly-**1a**–**Me** (20-mer) (B). The main-chain carbon and nitrogen atoms are shown in yellow and blue, respectively, using the ball and stick model for clarity. The phenyl groups of the side chains are shown in grey using the cylinder model, and hydrogen atoms and the methyl ester groups are omitted for clarity.

The structural determination for the HMW-poly-**1**–**Me** was also attempted by the same strategy using for the HMW-***h***-poly-**1b**–**Me**. The diffraction data indicates that the HMW-poly-**1**–**Me** chains are packed with a little smaller tetragonal lattice of a = 13.96 (Table 4-2). However, the author could not detect the reflection nearly 2.6 Å corresponding to the 4th layer line of the 10/3 helical structure as observed for HMW-***h***-poly-**1b**–**Me**, which suggests that there is not a correlation with the long range order as observed for HMW-***h***-poly-**1b**–**Me**. The remaining 3rd layer line of 10/3 helix indicates that some poly-**1**–**Me** segments may form nearly 10/3 helices having the average helical pitch of 3.47 Å, but it is supposed that other HMW-poly-**1**–**Me** segments form a nearly 18/5 helical structure because the diffuse and strong meridional reflection nearly 4.1 Å which may correspond to the 5th layer line of 18/5 helix as observed for HMW-poly-**1a**–**Me** (see below). The intensity of this reflection is clearly strong for the stereoirregular HMW-poly-**1**–**Me** structure, but weak for the regular HMW-***h***-poly-**1b**–**Me** (Figure 4-3B). These observations are well consistent with the IR and NMR results, which indicate that the HMW-***h***-poly-**1b**–**Me** has a more regular main-chain structure than HMW-poly-**1**–**Me**. The local structure of each unit seems to largely influence the regularity of the helical structure.

Next, the author tried to elucidate the structures of HMW-poly-**1a**–**Me** and HMW-poly-**1'**–**Me**, which were anticipated to have the same structure based on their essentially identical NMR and IR spectra, by XRD in the same way in order to address the questions concerning a difference in the helical structures of the polyisocyanides induced in DMSO and water in the presence of chiral amines, and why the preferred-handed helical structure induced in DMSO cannot be memorized after removal of the chiral amines.

The oriented optically inactive HMW-poly-**1a**–**Me** films showed the diffuse, but clearly strong and characteristic reflection of 4.14 Å, which could not be observed in the HMW-poly-**1**–**Me** and HMW-***h***-poly-**1b**–**Me** films, suggesting that the HMW-poly-**1a**–**Me** may have another regular helical structure being different from the 10/3 helical structure proposed for HMW-***h***-poly-**1b**–**Me**. As expected, thermodynamically most stable

HMW-poly-**1'–Me** showed an almost identical X-ray diffraction pattern to that of HMW-poly-**1a–Me**. Although the number of meridian reflections is limited, the structure of poly-**1a–Me** and poly-**1'–Me** could be proposed to be an 18 unit / 5 turn helix (18/5) on the basis of the strong reflections on the 5th layer line (4.14 Å) and the 6th layer line (3.45 Å) (Table 4-2 and see below). The calculated density based on an 18/5 helix (1.266 g/cm^3) is in good agreement with the observed density (1.255 g/cm^3).[22] Poly-**1a–Me** and poly-**1'–Me** most likely take the thermodynamically most stable structures. The author then performed the molecular mechanics (MM) calculations (see the Experimental Section) in order to obtain the optimized helical structure for poly-**1a–Me** and poly-**1'–Me** that satisfies the 18/5 helix; the optimized 18/5 helical structure was found to possess an *s-cis* and *s-trans* alternating structure as shown in Figure 4-4B. A similar helical structure was proposed theoretically by Clericuzio and Salvadori.[10]

Consequently, the ***h***-poly-**1b–Me** backbone with a preferred-handed helical conformation consists of the regular 10/3 helix as the major structural element and the poly-**1a–Me** and poly-**1'–Me** chains have 18/5 helices with different main-chain conformation and configuration from those of the ***h***-poly-**1b–Me**. The poly-**1–Me** chains may mainly compose of the mixture of a nearly 10/3 helix, a nearly 18/5 helix, and some other disordered segments.

Mechanism of Helicity Induction and Memory. Combining the previous spectroscopic observations and theoretical calculations and the present XRD and persistence length measurement results allowed the author to propose the mechanism of helix induction in poly-**1–H** with chiral amines in DMSO and water and the subsequent memory of the macromolecular helicity in water, and possible structures of relevant polyisocyanides (Figure 4-5).

The "as-prepared" poly-**1–H** may compose of the mixture of a nearly 10/3 helix and a nearly 18/5 helix as well as disordered segments arising from *syn* and *anti* states of each

monomer unit indicated by the previous IR and NMR results,[17] and lacks the long range order in its structure. In the presence of chiral amines in water or aqueous organic solutions containing more than 50 vol% water, the poly-**1**–**H** folds into a rigid preferred-handed 10/3 helical structure accompanied by transformation of an imino configurational mixture of *syn* and *anti* of poly-**1**–**H** to one of a single configuration, and this selective configurational isomerization assisted by hydrophobic and chiral ionic interactions in water forces a helical conformation on the polymer backbone to take an excess helical sense. Therefore, the induced helix is supposed to be controlled kinetically and remains after removal of the chiral amines at ambient temperature, while at high temperature, the helical conformation unravels due to the *syn–anti* configurational isomerization of the C=N double bonds, going back to an analogous structure of poly-**1**–**H**.

The poly-**1**–**H** also folds into a preferred-handed rather semi-rigid 18/5 helical conformation with an excess helical sense upon complexation with chiral amines in organic solutions and aqueous organic solutions containing less than 30 vol% water as evidenced by the appearance of an ICD similar to that of ***h***-poly-**1b**–**H**,[15] arising from the similar *syn–anti* configurational isomerization. In sharp contrast to ***h***-poly-**1b**–**H**, however, the resulting helical conformation is dynamic in nature, different from that of ***h***-poly-**1b**–**H**, and may spontaneously racemize after removing the chiral amines as observed for dynamically racemic polyacetylenes.[12a-l,n] Therefore, the induced helix in poly-**1a**–**H** is controlled by predominantly thermodynamics.[15] At high temperature, the poly-**1a**–**H** favorably changes to a structure similar to the original poly-**1**–**H** via configurational isomerization of the main-chain. The poly-**1a**–**H** structure may be among the thermodynamically most stable structures, since the "as-prepared" poly-**1**–**H** and kinetically produced ***h***-poly-**1b**–**H** also change their structures into a similar structure after standing in solution for an extremely long time, and this was confirmed by following the changes in its ^{13}C NMR spectrum with time without heat treatment. In addition, upon complexation with chiral amines in water, a preferred-handed helix with macromolecular helicity memory can also be induced in poly-**1a**–**H**.

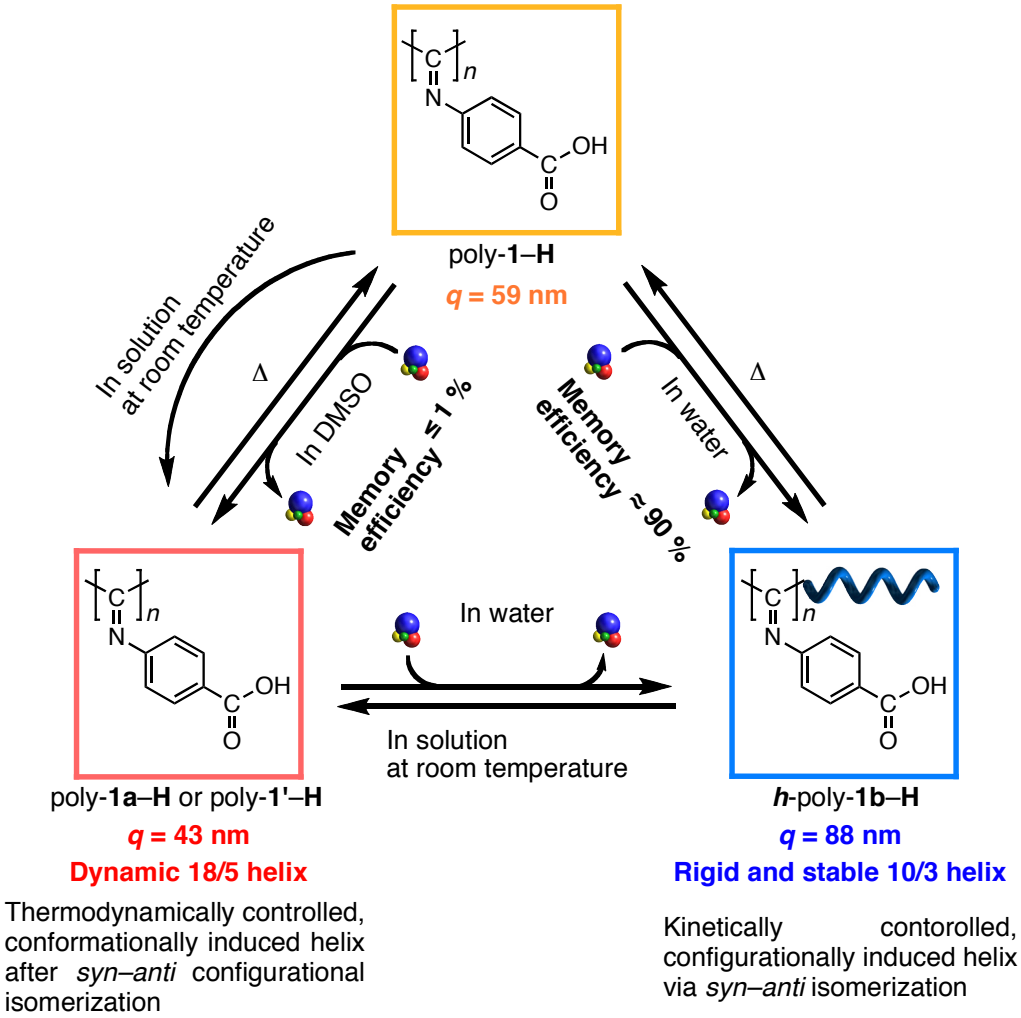

Figure 4-5. Possible structures of poly-**1**–**H**, poly-**1a**–**H**, poly-**1'**–**H**, and ***h***-poly-**1b**–**H** and their mutual interconversions.

Experimental Section

Materials. Chloroform ($CHCl_3$) was dried over calcium hydride, distilled, and stored under nitrogen. Anhydrous acetonitrile (CH_3CN), tetrahydrofuran (THF), toluene, 2-propanol, and methanol (water content < 0.005%) were purchased from Wako (Osaka, Japan) and stored under nitrogen. Ethyl 4-aminobenzoate was obtained from Wako. $NiCl_2 \cdot 6H_2O$ was purchased from Kishida (Osaka, Japan). Diphosgene was obtained from Merck. (1*R*,2*S*)-*cis*-1-amino-2-indanol ((1*R*,2*S*)-**2**) and (*R*)-phenylglycinol ((*R*)-**3**) were purchased from Aldrich and TCI, respectively. D_2O (99.9 atom %D, Isotec Inc.), NaOD in D_2O (40 wt%) (Cambridge Isotope Laboratories, Inc.), and DMSO-d_6 (99.9 atom %D, Isotec Inc.) were stored under nitrogen. $CDCl_3$ (99.8 atom %D, Merck) was dried over molecular sieves 4Å (Nacalai Tesque, Kyoto, Japan) and stored under nitrogen. Deionized, distilled water was degassed with nitrogen before use for all experiments. All solvents used for measurements of CD and NMR spectra and optical rotation were purged with nitrogen prior to use. 4-(Ethoxycarbonyl)phenyl isocyanide (**1**–**Et**) and sodium 4-isocyanobenzoate (**1**–**Na**) were prepared according to the reported methods.[13,24]

Instruments. The solution pH was measured with a B-211 pH meter (Horiba, Japan). NMR spectra were taken on a Varian Mercury 300 operating at 300 MHz for ^1H, a Varian VXR-500S operating at 500 MHz for ^1H and 125 MHz for ^{13}C, or a Varian Inova 700 spectrometer operating at 700 MHz for ^1H and 175 MHz for ^{13}C. Chemical shifts are reported in parts per million (δ) downfield from tetramethylsilane (TMS) as the internal standard in $CDCl_3$. In NMR measurements in D_2O and DMSO-d_6, CH_3CN (for D_2O), or a solvent residual peak (for DMSO-d_6) were used as the internal standards. Elemental analyses were performed by the Nagoya University Analytical Laboratory in School of Agriculture. SEC measurements were performed using a JASCO PU-980 liquid chromatograph (JASCO, Hachioji, Japan) equipped with a UV (254 nm; JASCO UV-970) detector. An SEC column, Tosoh (Tokyo, Japan) TSKgel MultiporeH_{XL}-M (30 cm) (for low molecular weight polymers) or TSKgel GMH_{HR}-H(S) (30 cm) and TSKgel GMH_{HR}-M(S) (30 cm) connected in series (for high

molecular weight polymers) were used. $CHCl_3$ was used as the eluent at a flow rate of 1.0 mL/min and the molecular weight calibration curves were obtained with polystyrene standards (Tosoh). IR spectra were recorded using a JASCO Fourier Transform IR-620 spectrophotometer. Absorption and CD spectra were measured in a 0.2- or 1.0-mm quartz cell on a JASCO V-560 spectrophotometer and a JASCO J-820 spectropolarimeter, respectively. The polymer concentration was calculated on the basis of the monomer units and was 1 mg/mL unless otherwise stated. Optical rotation was measured in a 5-cm quartz cell equipped with a temperature controller (EYELA NCB-2100) on a JASCO P-1030 polarimeter. X-ray measurements were performed with a Rigaku ultraX18 X-ray generator system with graphite monochromated CuKα radiation (0.15418 nm) focused through a 0.3-mm pinhole collimator, which was supplied at 45 kV voltage and 60 mA current, equipped with a curved imaging plate of specimen-to-plate distance 120.0 mm. The SEC-MALS measurements were performed using an HLC-8220 GPC system (Tosoh) equipped with a differential refractometer coupled to a DAWN-HELEOS MALS device equipped with a semiconductor laser (λ = 690 nm) (Wyatt Technology, Santa Barbara, CA) operated at 25 °C using two TSKgel MultiporeH_{XL}-M columns (Tosoh) in series. The scattered light intensities were measured by eighteen light scattering detectors at different angles. The differential refractive index increment, *dn*/*dc*, of the polymer with respect to the mobile phase at 25 °C was also measured by an Optilab rEX interferometric refractometer (Wyatt Technology).

Polymerization. Polymerization was carried out in a dry glass ampule using $NiCl_2{\cdot}6H_2O$ as a catalyst in a similar way previously reported (Scheme 1).[13] High molecular weight HMW-poly-**1**–**H** was prepared by the polymerization of 4-(ethoxycarbonyl)phenyl isocyanide (**1**–**Et**) with $NiCl_2{\cdot}6H_2O$ in THF–MeOH (99:1, v/v) at room temperature for 1 day ([**1**–**Et**]/[$NiCl_2{\cdot}6H_2O$] = 100, [**1**–**Et**] = 0.1 M) followed by hydrolysis of the ester groups in THF containing aqueous 10 N NaOH. HMW-Poly-**1**–**Et** was obtained in 88% yield and its M_n and M_w/M_n values were 8.6×10^4 and 5.0, respectively, as determined by SEC with polystyrene standards in $CHCl_3$ as the eluent (Scheme 4-1).

Spectroscopic data of high molecular weight HMW-poly-**1**–**Et**. IR (KBr, cm^{-1}): 1718 ($\nu_{C=O}$), 1649 ($\nu_{C=N}$). ^1H NMR ($CDCl_3$, 30 °C, 500 MHz): δ 1.5-1.7 (br, CH_3, 3H), 3.4-4.7 (br, CH_2, 2H), 5.0-8.0 (br, aromatic, 4H).

HMW-poly-**1**–**Et** was further hydrolyzed to HMW-poly-**1**–**H** with saturated aqueous NaOH in THF according to the previously reported method.[15]

Spectroscopic data of HMW-poly-**1**–**H**. IR (KBr, cm^{-1}): 1702 ($\nu_{C=O}$), 1655 ($\nu_{C=N}$). ^1H NMR (D_2O containing NaOD ([NaOD]/[HMW-poly-**1**–**H**] = 1), 30 °C, 500 MHz): δ 5.0-7.8 (br, aromatic, 4H). The resulting high molecular weight HMW-poly-**1**–**H** was further converted into the methyl ester with CH_2N_2 in ether solution according to the method reported previously.[13]

Spectroscopic data of HMW-poly-**1**–**Me**. IR ($CHCl_3$, cm^{-1}): 1723 ($\nu_{C=O}$), 1654 ($\nu_{C=N}$). ^1H NMR ($CDCl_3$, 30 °C, 500 MHz): δ 3.2-4.2 (br, CH_3, 3H), 4.9-7.9 (br, aromatic, 4H).

Helicity Induction in HMW-Poly-1–H in DMSO–Water Mixture and Isolation of Poly-1a–H. Helicity induction of HMW-poly-**1**–**H** in DMSO–water (4:1, v/v) and isolation of HMW-poly-**1a**–**H**s were performed in the same way as previously reported.[16] A typical experimental procedure is described below. A stock solution of HMW-poly-**1**–**H** (2 mg/mL) in DMSO was prepared in a 10-mL flask equipped with a stopcock. A 5 mL aliquot of the stock solution of HMW-poly-**1**–**H** was transferred to a 10-mL flask equipped with a stopcock, and (1*R*,2*S*)-**2** (101 mg) was added to the flask ([(1*R*,2*S*)-**2**]/[HMW-poly-**1**–**H**] = 10). The solution was diluted with DMSO and water (DMSO–water = 4:1, v/v) to keep the polymer concentration at 1.0 mg/mL and the initial absorption and CD spectra were measured. The solution was transferred to an ampule, which was then degassed with nitrogen and sealed. The ampule was thermostated at 50 °C on an oil bath under shielded light. A 0.3 mL aliquot of the solution was withdrawn with a pipette at appropriate time intervals and the UV–visible and CD spectra were taken at ambient temperature (ca. 20–25 ˚C). After the solution of HMW-poly-**1**–**H** with (1*R*,2*S*)-**2** in the DMSO–water mixture had been allowed to stand at 50 ˚C for 5 days, 1 N NaOH in methanol was added to the solution ([NaOH]/[monomeric units

of HMW-poly-**1**–**H**] = 10). The solution was then poured into a large amount of methanol to remove (1*R*,2*S*)-**2**. The precipitated HMW-poly-**1a**–**Na** was collected by centrifugation, and the recovered polymer was dissolved in a small amount of water to maintain the HMW-poly-**1a**–**Na** concentration of 0.5 mg/mL. The solution was then acidified with aqueous 1 N HCl and the precipitated HMW-poly-**1a**–**H** was collected by centrifugation, washed with methanol, and dried in vacuo at room temperature overnight. The conversion of HMW-poly-**1a**–**H** to HMW-poly-**1a**–**Me** was carried out in the same way as reported.[13]

Spectroscopic data of HMW-poly-**1a**–**H**. IR (KBr, cm^{-1}): 1702 ($\nu_{C=O}$), 1656 ($\nu_{C=N}$). ^1H NMR (D_2O containing NaOD ([NaOD]/[HMW-poly-**1a**–**H**] = 1), 30 ˚C, 500 MHz): δ 5.1-7.8 (br, aromatic, 4H).

Spectroscopic data of HMW-poly-**1a**–**Me**. IR (KBr, cm^{-1}): 1722 ($\nu_{C=O}$), 1655 ($\nu_{C=N}$). ^1H NMR ($CDCl_3$, 30 °C, 500 MHz): δ 3.2-4.2 (br, CH_3, 3H), 5.0-7.8 (br, aromatic, 4H).

Helicity Induction in 2-Propanol–Water Mixture and Isolation of HMW-*h*-Poly-1b–H. A typical experimental procedure is described below.[16] HMW-poly-**1**–**H** (100 mg) and (*R*)-**3** (1.86 g) were placed in a 100-mL flask equipped with a stopcock ([(*R*)-**3**]/[HMW-poly-**1**–**H**] = 20) and water (50 mL) was added with a syringe to dissolve HMW-poly-**1**–**H** and (*R*)-**3** completely. The solution was diluted with 2-propanol (2-propanol–water = 1:1, v/v) to keep the polymer concentration at 1.0 mg/mL and the initial absorption and CD spectra were measured. The solution was transferred to an ampule, which was then degassed with nitrogen and sealed. The ampule was thermostated at 50 °C on an oil bath under shielded light. A 0.3 mL aliquot of the solution was withdrawn with a pipette at appropriate time intervals and the UV–visible and CD spectra were taken at ambient temperature (ca. 20–25 °C). The CD intensity increased with time and reached an almost constant value after 40 days.[16] After the sample had been allowed to stand at 50 °C for 72 days, the 2-propanol was removed by evaporation and then the aqueous solution was lyophilized. The recovered polymer complexed with (*R*)-**3** was dissolved in a small amount of water and then aqueous 1 N NaOH (6.80 mL) was added ([NaOH]/[monomeric units of

HMW-poly-**1**–**H**] = 10) to the solution. The solution was poured into a large amount of THF to remove (*R*)-**3**. The aqueous layer was separated and acidified with aqueous 1 N HCl. The precipitated HMW-***h***-poly-**1b**–**H** was then collected by centrifugation, washed with methanol, and dried in vacuo at room temperature overnight. The conversion of HMW-***h***-poly-**1b**–**H** to HMW-***h***-poly-**1b**–**Me** was carried out in the same way as reported.[13]

Spectroscopic data of HMW-***h***-poly-**1b**–**H**. IR (KBr, cm^{-1}): 1703 ($\nu_{C=O}$), 1655 ($\nu_{C=N}$). ^1H NMR (D_2O containing NaOD ([NaOD]/[HMW-***h***-poly-**1b**–**H**] = 1), 30 °C, 500 MHz): δ 5.2-7.8 (br, aromatic, 4H).

Spectroscopic data of HMW-***h***-poly-**1b**–**Me**. IR ($CHCl_3$, cm^{-1}): 1718 ($\nu_{C=O}$), 1647 ($\nu_{C=N}$). ^1H NMR ($CDCl_3$, 30 °C, 500 MHz): δ 3.2–4.2 (br, CH_3, 3H), 5.0–7.8 (br, aromatic, 4H).

SEC-MALS Measurements. The SEC-MALS measurements were carried out with $CHCl_3$ used as the eluent at the flow rate of 0.5 mL/min. A standard polystyrene (M_w = 30500 (Polymer Laboratories, Shropshire, U.K.)) was used to calculate the device constants, such as the inter-detector delay, inter-detector band broadening, and light scattering detector normalization. HMW-poly-**1**–**Me**, HMW-poly-**1a**–**Me**, and HMW-***h***-poly-**1b**–**Me** were completely dissolved in $CHCl_3$ at the concentration of 0.1–0.2% (wt/vol) under gentle stirring for 1–2 h before injection. The evaluations of the molecular weights and radii of gyration were accomplished using ASTRA V software (version 5.1.3.5). The *dn*/*dc* values of HMW-poly-**1**–**Me**, HMW-poly-**1a**–**Me**, and HMW-***h***-poly-**1b**–**Me** in the eluent used for the evaluations were 0.1597, 0.1536, and 0.1612 mL/g, respectively.

Persistence Length Estimation from the Molecular Weight Dependence of the Radius of Gyration. The molecular weight dependence of the obtained radii of gyration of HMW-poly-**1**–**Me**, HMW-poly-**1a**–**Me**, and HMW-***h***-poly-**1b**–**Me** was used to estimate the persistence length (*q*) based on the wormlike-chain model. It was over the range of the elution volume where both the concentration and the scattering intensities are greater than 10% of the peak value. The unperturbed mean-square radius of gyration $\langle S^2 \rangle_0$ is given by[25]

$$< S^2 >_0 = (2q)^2 \left[\frac{1}{6} N - \frac{1}{4} + \frac{1}{4N} - \frac{1}{8N^2} (1 - \exp(-2N)) \right] \qquad (1)$$

where N is the Kuhn statistical segment number defined by $N = M_w/(2q \cdot M_L)$, and M_L denotes the molar mass per unit contour length of the polymer. The radius expansion factor α_s [$\equiv (<S^2>/<S^2>_0)^{0.5}$] for the excluded-volume effect was negligible because it is close to unity in the case of $N < 50$.[26] Equation (1) indicates that $<S^2>_0$ is characterized by q and M_L, so that a fitting procedure was employed to estimate q and M_L.

X-ray Measurements. Oriented HMW-poly-**1**–**Me**, HMW-***h***-poly-**1b**–**Me**, HMW-poly-**1a**–**Me**, and HMW-poly-**1'**–**Me** films were prepared for the X-ray analyses by shearing uniaxially LC nematic or cholesteric $CHCl_3$ solutions of the polymers, respectively, cast on a glass plate. HMW-poly-**1'**–**Me** was obtained from HMW-poly-**1**–**Me** after standing its $CHCl_3$ solution at room temperature for 3 months. After drying in air, the oriented polymer films were floated off from the glass substrates onto a water surface, carefully collected, and then dried. Several uniaxially oriented thin and rectangle-shaped polymer films of ca. 10 mm length, 1.0 mm width, and 0.02 mm thickness were prepared and piled up parallel to each other for the X-ray measurements. X-ray photographs were taken at ambient temperature (20–25 °C) from the edge-view position with a beam parallel to the film surface.

Molecular Modeling of *h*-Poly-1b–Me (Figure 4-4A). On the basis of the X-ray diffraction analysis, the most plausible helical structure of ***h***-poly-**1b**–**Me** is considered to be a 10 unit / 3 turn (10/3) helix, whose helical structure is resemble to that of poly(phenyl isocyanide) (PPI) determined by the DFT calculations (7/2 helix).[17] Then, the geometrical parameters (r, ϕ, and τ) of an ***h***-poly-**1b**–**Me** molecule were calculated so as to satisfy the X-ray results (10/3 helix).

Chart 4-2

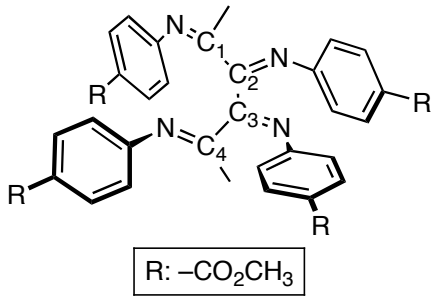

bond length: r (C_1–C_2)
bond angle: ϕ (C_1–C_2–C_3)
dihdral angle: τ (C_1–C_2–C_3–C_4)

Molecular modeling and molecular mechanics (MM) calculations were conducted using the Compass force field[27] as implemented in the MS Modeling software (version 4.2, Accelrys Inc., San Diego, CA) operated using a PC running under Windows® XP. The polymer model of the ***h***-poly-**1b**–**Me** (60 repeating monomer units) was constructed by a Polymer Builder module in MS Modeling software. The initial structure of ***h***-poly-**1b**–**Me** was constructed on the basis of the calculated structure of the helical PPI determined by the calculations at the B3LYP/MIX level.[17] First, a repeating unit of ***h***-poly-**1b**–**Me** was obtained by replacement of the hydrogen of the central part of the optimized helical PPI with methoxycarbonyl at the 4-position on the phenyl group. The side chain at the 4-position was then stabilized using the force field calculations. The monomer unit was then allowed to construct a 60-mer based on the X-ray analysis results combined with Miyazawa's equations (equations 2 and 3).[28]

$$\cos(\theta/2) = \cos(\tau/2)\sin(\phi/2) \qquad (2)$$

$$d\sin(\theta/2) = r\sin(\tau/2)\sin(\phi/2) \qquad (3)$$

where θ is the unit twist angle and d is the unit height.

According to Miyazawa, helical conformations of infinite (periodic) polymer chains such as ***h***-poly-**1b**–**Me** can be described by the helical parameters including the unit height (d), the unit twist angle (θ), and the backbone dihedral angle (τ) if the internal coordinates, the bond

length (r) and the bond angle (ϕ) are given. The unit height (d = 1.03 Å) and the unit twist angle (θ = 108˚) for ***h***-poly-**1b**–**Me** determined by the X-ray analysis were fixed, and the dihedral angle (τ) was varied from 75 to 105° at 0.5° intervals, since the dihedral angle (τ) of the 7/2 helical PPI was determined to be 85.2° by the DFT calculations. The geometrical parameters (r and ϕ) and energy profile were then calculated for each 60-mer defined as a function of τ according to Miyazawa's equations, which allows geometrically possible 10/3 helical structures of ***h***-poly-**1b**–**Me** 60-mers. The geometrical parameters for the helical ***h***-poly-**1b**–**Me** backbone structure were fixed during the following force field optimization. The dielectric constant was set to 1.0. The calculation was used with setup parameters that include a 10.0 kcal mol^{-1} $Å^{-1}$ final convergence for minimization. Geometry optimizations were carried out without any cutoff by the smart minimizer in three steps. First, the starting conformation was subject to the steepest decent optimization in order to eliminate the worse steric conflicts. Second, subsequent optimization until the convergence using a conjugate gradient algorithm was performed. The fully-optimized ***h***-poly-**1b**–**Me** model was obtained by the further energy minimization using the Newton method with the 0.1 kcal/mol/Å convergence criterion. The energy profile (Figure 4-6) revealed the lowest energy of a 10/3 helical ***h***-poly-**1b**–**Me** model with the bond length r (C_1–C_2: 1.455 Å), the bond angle ϕ (C_1–C_2–C_3: 110.3˚), and the dihedral angle τ (C_1–C_2–C_3–C_4: 88.5˚), respectively, as shown in Figure 4-4A.

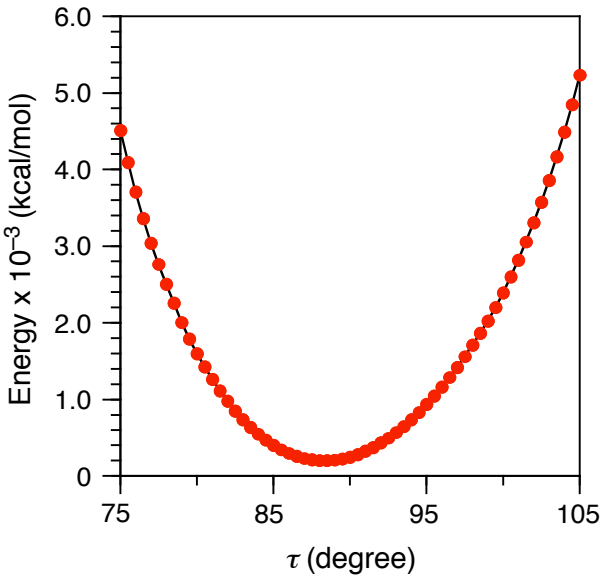

Figure 4-6. Total energy profile for the backbone dihedral angle (τ) of 60-mers of an ***h***-poly-**1b**–**Me** as calculated by force field optimization.

Molecular Modeling of Poly-1a–Me (Figure 4-4B). Figure 4-7 shows the flow charts for the determination processes of the helical structure of poly-**1a**–**Me** on the basis of the X-ray diffraction patterns (Figure 4-3C) together with the density measurement results. Although the most plausible helical structure of poly-**1a**–**Me** was considered to be an 18/5 helix, the author assumed the structure of poly-**1a**–**Me** may be different from an *s-cis*–isotactic structure like ***h***-poly-**1b**–**Me** (Figure 4-4A) because of essentially different IR and NMR spectral patterns from those of ***h***-poly-**1b**–**Me**.[17] The author then attempted to construct a molecular model for an 18/5 helical poly-**1a**–**Me** using MM calculations because poly-**1a**–**Me** was anticipated to be thermodynamically the most stable judging from the previous NMR measurements.[17]

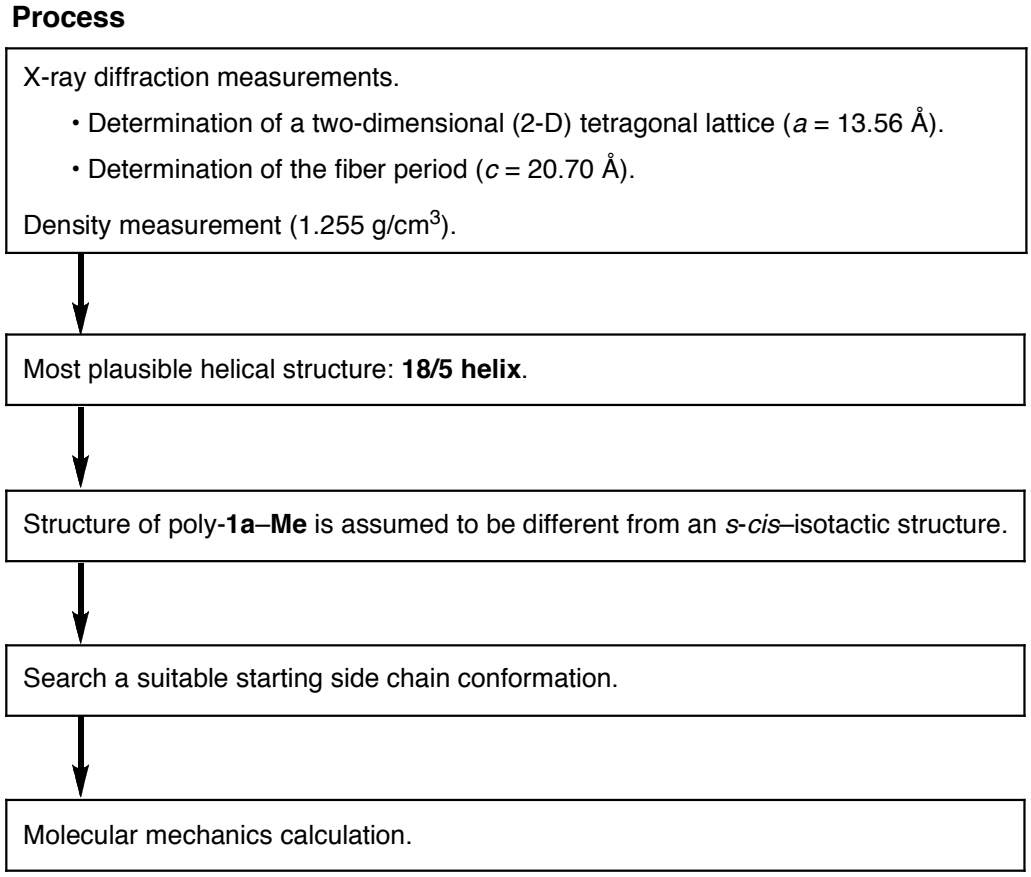

Figure 4-7. The determination processes of the helical structure of poly-**1a**–**Me**.

First, the author constructed an *s-cis*–isotactic 18/5 helical structure of poly-**1a**–**Me** with a repeating structure unit (1-mer) for the periodicity like ***h***-poly-**1b**–**Me** (Chart 4-2), then the MM calculation was conducted. However, the energy minimized conformation had a much higher energy than that of the 10/3 helical ***h***-poly-**1b**–**Me** (Figure 4-6), indicating that the helical structure of poly-**1a**–**Me** may be different from an *s-cis*–isotactic structure like ***h***-poly-**1b**–**Me**.

Chart 4-3

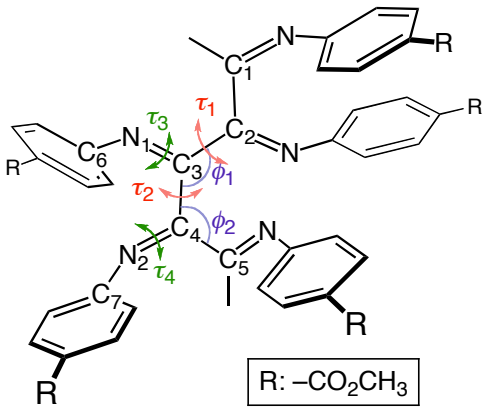

bond length: r_1 (C_2–C_3)
bond length: r_2 (C_3–C_4)

bond angle: ϕ_1 (C_2–C_3–C_4)
bond angle: ϕ_2 (C_3–C_4–C_5)

dihedral angle: τ_1 (C_1–C_2–C_3–C_4)
dihedral angle: τ_2 (C_2–C_3–C_4–C_5)
dihedral angle: τ_3 (C_4–C_3–N_1–C_6)
dihedral angle: τ_4 (C_3–C_4–N_2–C_7)

The author then considered the plausible helical structure of poly-**1a**–**Me** that has a repeating structure unit (2-mer) for the periodicity (Chart 4-3). The repeating monomer unit of 2-mer was then allowed to construct a 60-mer based on the X-ray analysis results combined with Miyazawa's equations (equations 4 and 5).[28]

$$\cos(\theta/2) = \cos(\tau_1/2 + \tau_2/2)\sin(\phi_1/2)\sin(\phi_2/2) - \cos(\tau_1/2 - \tau_2/2)\cos(\phi_1/2)\cos(\phi_2/2) \quad (4)$$

$$d\sin(\theta/2) = (r_1 + r_2)\sin(\tau_1/2 + \tau_2/2)\sin(\phi_1/2)\sin(\phi_2/2) - (r_1 - r_2)\cos(\tau_1/2 - \tau_2/2)\cos(\phi_1/2)\cos(\phi_2/2) \quad (5)$$

where θ is the unit twist angle and d is the unit height.

The bond lengths were set to $r_1 = r_2 = 1.527$ Å on the basis of the calculated structure for a helical PPI determined by the calculations at the B3LYP/MIX level. The bond angles (ϕ_1 and ϕ_2) were assumed to be identical. The other internal coordinate combinations were calculated by Miyazawa's equation[28] so as to satisfy the helical parameters ($d = 2.30$ Å and $\theta = 200°$) obtained by the X-ray analysis.

In order to search for a suitable starting side chain conformation for the 18/5 helical structure of poly-**1a**–**Me**, the author first constructed a 60-mer of poly-**1a**–**Me** having various

dihedral angles of C_4–C_3–N_1–C_6 (τ_3) and C_3–C_4–N_2–C_7 (τ_4); τ_3 and τ_4 were individually rotated at 10° intervals, then each initial structure was energy minimized to obtain energy profiles (Figure 4-8). The geometrical parameters of the monomer unit of the optimized polymer models with the lowest total potential energy were τ_3 = 240° and τ_4 = 300°; these values were used as a starting side chain conformation for further structural optimization of the polymer main-chain.

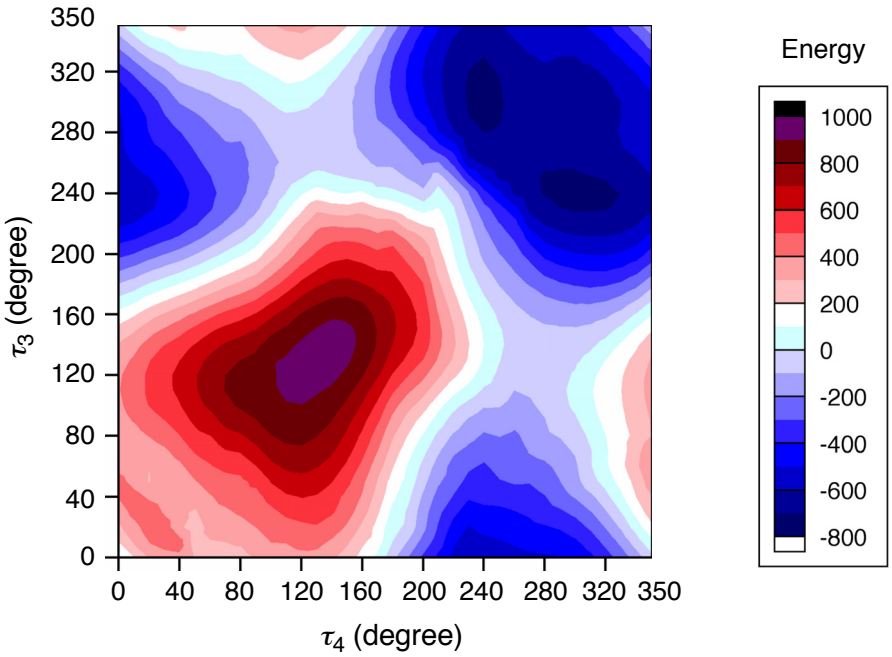

Figure 4-8. Two dimensional energy profiles of the 60-mers of an 18/5 helical poly-**1a**–**Me**; dihedral angles (τ_3 and τ_4) are individually varied from 0 to 350° at 10° intervals.

The polymer model (60-mer) of poly-**1a**–**Me** with the optimized side chain conformation was then constructed based on the internal coordinate combinations calculated by Miyazawa's equation. Here, τ_1 was set to 0–180°, then ϕ_1 (= ϕ_2) and τ_2 were calculated accordingly. The energy profiles (Figure 4-9) revealed the lowest energy of an 18/5 helical poly-**1a**–**Me** model with the bond angle ϕ_1 (= ϕ_2) (122.2°), the dihedral angle τ_1 (C_1–C_2–C_3–C_4: 10.0°), and τ_2 (C_2–C_3–C_4–C_5: 199.0°), respectively. The optimized helical structure of poly-**1a**–**Me** that satisfies the 18/5 helix was found to have an alternate arrangement of *s-cis* and *s-trans* conformations (Figure 4-4B).

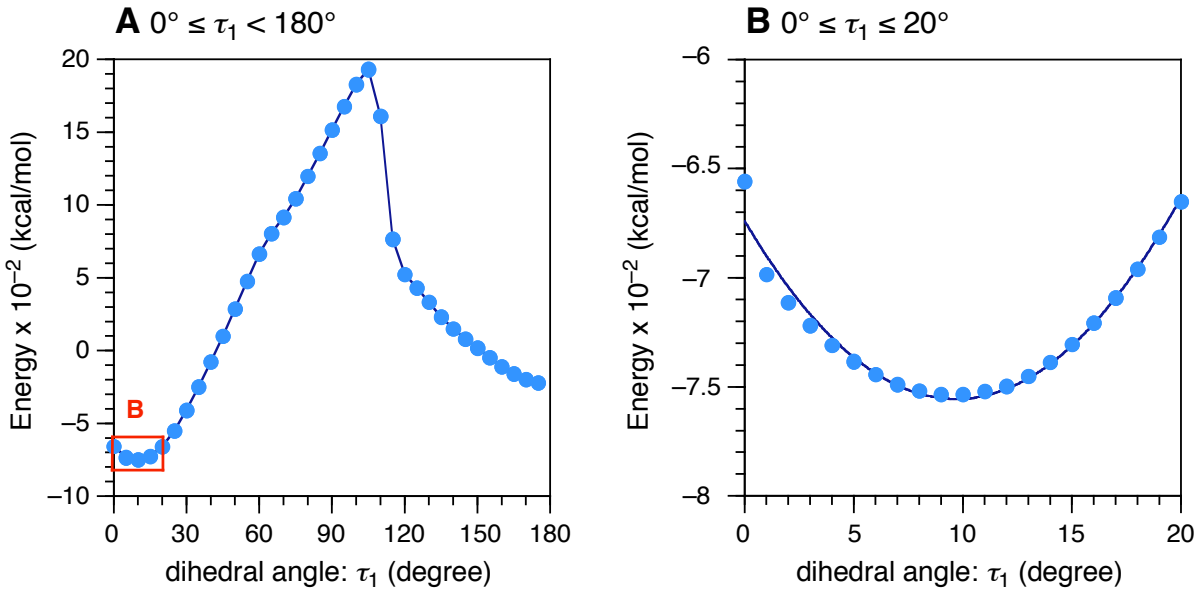

Figure 4-9. (A) Total energy profile for the backbone dihedral angle (τ_1) of the 60-mers of an 18/5 helical poly-**1a**–**Me**. Detailed energy profiles corresponding to the areas indicated by the square in A is shown in B.

References and Notes

(1) Reviews: (a) Millich, F. *Chem. Rev.* **1972**, *72*, 101–113. (b) Millich, F. *Adv. Polym. Sci.* **1975**, *19,* 117–141. (c) Drenth, W.; Nolte, R. J. M. *Acc. Chem. Res.* **1979**, *12,* 30–35. (d) Millich, F. *J. Polym. Sci. Macromol. Rev.* **1980**, *15*, 207–253. (e) Nolte, R. J. M. *Chem. Soc. Rev.* **1994**, *23*, 11–19. (f) Takahashi, S.; Onitsuka, K.; Takei, F. *Proc. Japan Acad. Ser. B* **1998**, *74*, 25-30. (g) Cornelissen, J. J. L. M.; Rowan, A. E.; Nolte, R. J. M.; Sommerdijk, N. A. J. M. *Chem. Rev.* **2001**, *101*, 4039–4070. (h) Suginome, M.; Ito, Y. *Adv. Polym. Sci.* **2004**, *171*, 77-136. (i) Amabilino, D. B.; Serrano, J.-L.; Sierra, T.; Veciana, J. *J. Polym. Sci., Part A: Polym. Chem.* **2006**, *44*, 3161-3174.

(2) (a) Millich, F.; Sinclair, R. G., II. *J. Polym. Sci., Part C* **1968**, *22*, 33–43. (c) Nolte, R. J. M.; Zwikker, J. W.; Reedijk, J.; Drenth, W. *J. Mol. Catal.* **1978**, *4*, 423–426. (d) van Beijnen, A. J. M.; Nolte, R. J. M.; Zwikker, J. W.; Drenth, W. *J. Mol. Catal.* **1978**, *4*, 427–432.

(3) (a) Nolte, R. J. M.; van Beijnen, A. J. M.; Drenth, W. *J. Am. Chem. Soc.* **1974**, *96*, 5932–5933. (b) van Beijnen, A. J. M.; Nolte, R. J. M.; Drenth, W. Hezemans, A. M. F. *Tetrahedron* **1976**, *32*, 2017–2019.

(4) (a) Kamer, P. C. J.; Nolte, R. J. M.; Drenth, W. *J. Chem. Soc., Chem. Commun.* **1986**, 1789-1791. (b) Kamer, P. C. J.; Nolte, R. J. M.; Drenth, W. *J. Am. Chem. Soc.* **1988**, *110*, 6818–6825.

(5) Deming, T. J.; Novak, B. M. *J. Am. Chem. Soc.* **1992**, *114*, 7926–7927.

(6) For liquid crystalline polyisocyanides: (a) Cornelissen, J. J. L. M.; Donners, J. J. J. M.; de Gelder, R.; Graswinckel, W. S.; Metselaar, G. A.; Rowan, A. E.; Sommerdijk, N. A. J. M.; Nolte, R. J. M. *Science* **2001**, *293,* 676–680. (b) Cornelissen, J. J. L. M.; Granswinckel, W. S.; Rowan, A. E.; Sommerdijk, N. A. J. M.; Nolte, R. J. M. *J. Polym. Sci. Part A: Polym. Chem.* **2003**, *41*, 1725–1736. (c) Tian, Y.; Kamata, K.; Yoshida, H.; Iyoda, T. *Chem. –Eur. J.* **2006**, *12*, 584-591. (d) Kajitani, T.; Okoshi, K.; Sakurai, S.-i.; Kumaki, J.; Yashima, E. *J. Am. Chem. Soc.* **2006**, *128*, 708–709. (e) Wezenberg, S. J.;

Metselaar, G. A.; Rowan, A. E.; Cornelissen, J. J. L. M.; Seebach, D.; Nolte, R. J. M. *Chem. –Eur. J.* **2006**, *12*, 2778–2786. (f) Metselaar, G. A.; Adams, P. J. H. M.; Nolte, R. J. M.; Cornelissen, J. J. L. M. Rowan, A. E. *Chem. –Eur. J.* **2007**, *13*, 950–960. (g) Metselaar, G. A.; Wezenberg, S. J.; Cornelissen, J. J. L. M.; Nolte, R. J. M.; Rowan, A. E. *J. Polym. Sci. Part A: Polym. Chem.* **2007**, *45*, 981–988. (h) Onouchi, H.; Okoshi, K.; Kajitani, T.; Sakurai, S.-i.; Nagai, K.; Kumaki, J.; Onitsuka, K.; Yashima, E. *J. Am. Chem. Soc.* **2008**, *130*, 229–236. (i) Kajitani, T.; Lin, H.; Nagai, K.; Okoshi, K.; Onouchi, H.; Yashima, E. *Macromolecules, in press* (DOI:10.1021/ma802345g). For optoelectronic polyisocyanides, see: (j) Kauranen, K.; Verbiest, T.; Boutton, C.; Teerenstra, M. N.; Schouten, A. J.; Nolte, R. J. M.; Persoons, A. *Science* **1995**, *270*, 966–969. (k) Hida, N.; Takei, F.; Onitsuka, K.; Shiga, K.; Asaoka, S.; Iyoda, T.; Takahashi, S. *Angew. Chem., Int. Ed.* **2003**, *42*, 4349–4352. For other leading references on helical polyisocyanides prepared by the polymerization of the corresponding optically active monomers, see: (l) Cornelissen, J. J. L. M.; Fischer, M.; Sommerdijk, N. A. J. M.; Nolte, R. J. M. *Science* **1998**, *280*, 1427-1430. (m) Amabilino, D. B.; Ramos, E.; Serrano, J.-L.; Sierra, T.; Veciana, J. *J. Am. Chem. Soc.* **1998**, *120*, 9126–9134. (n) Amabilino, D. B.; Ramos, E.; Serrano, J.-L.; Veciana, J. *Adv. Mater.* **1998**, *10*, 1001-1005. (o) Hasegawa, T.; Kondoh, S.; Matsuura, K.; Kobayashi, K. *Macromolecules* **1999**, *32*, 6595–6603. (p) Takei, F.; Yanai, K.; Onitsuka, K.; Takahashi, S. *Chem. –Eur. J.* **2000**, *6,* 983–993. (q) Cornelissen, J. J. L. M.; Graswinckel, W. S.; Adams, P. J. H. M.; Nachtegaal, G. H.; Kentgens, A. P. M.; Sommerdijk, N. A. J. M.; Nolte, R. J. M. *J. Polym. Sci., Part A: Polym. Chem.* **2001**, *39*, 4255–4264. (r) Yamada, Y.; Kawai, T.; Abe, J.; Iyoda, T. *J. Polym. Sci., Part A: Polym. Chem.* **2002**, *40*, 399–408. (s) Takei, F.; Onitsuka, K.; Takahashi, S. *Macromolecules* **2005**, *38*, 1513-1516. (t) Kajitani, T.; Okoshi, K.; Yashima, E. *Macromolecules* **2008**, *41*, 1601–1611.

(7) Green, M. M.; Gross, R. A.; Schilling, F. C.; Zero, K.; Crosby, C. *Macromolecules* **1988**, *21*, 1839–1846.

(8) Pini, D.; Iuliano, A.; Salvadori, P. *Macromolecules* **1992**, *25*, 6059–6062.

(9) (a) Spencer, L.; Kim, M.; Euler, W. B.; Rosen, W. *J. Am. Chem. Soc.* **1997**, *119*, 8129–8130. (b) Euler, W. B.; Huang, J-.T.; Kim, M.; Spencer, L.; Rosen, W. *Chem. Commun.* **1997**, 257–258. (c) Huang, J.-T.; Sun, J.; Euler, W. B.; Rosen, W. *J. Polym. Sci., Part A, Polym. Chem.* **1997**, *35*, 439–446. (d) Spencer, L.; Euler, W. B.; Traficante, D. D.; Kim, M.; Rosen, W. *Magn. Reson. Chem.* **1998**, *36*, 398–402.

(10) Clericuzio, M.; Alagona, G.; Ghio, C.; Salvadori, P. *J. Am. Chem. Soc.* **1997**, *119*, 1059–1071.

(11) Recently, Yashima et al. reported the helix-sense-selective living polymerization of an optically active phenyl isocyanide bearing an L-alanine pendant with a long decyl chain with the achiral μ-ethynediyl Pt–Pd catalyst that unprecedentedly produced both right- and left-handed helical, rigid-rod polyisocyanides at once with a different molecular weight and a narrow molecular weight distribution, which could be separated into each helix in a facile fractionation with acetone. The structures of both right- and left-handed helical polyisocyanides were proposed to be a 15 unit / 4 turn (15/4) helix based on the X-ray analyses of the corresponding oriented films.[6h] However, the detailed structural analysis such as configurational and conformational isomerism of the main-chain has never been investigated.

(12) (a) Yashima, E.; Maeda, K.; Okamoto, Y. *Nature* **1999**, *399,* 449–451. (b) Yashima, E.; Maeda, K.; Nishimura, T. *Chem. –Eur. J.* **2004**, *10*, 42-51. (c) Maeda, K.; Morino, K.; Okamoto, Y.; Sato, T.; Yashima, E. *J. Am. Chem. Soc.* **2004**, *126*, 4329–4342. (d) Morino, K.; Watase, N.; Maeda, K.; Yashima, E. *Chem. –Eur. J.* **2004**, *10*, 4703–4707. (e) Onouchi, H.; Kashiwagi, D.; Hayashi, K.; Maeda, K.; Yashima, E. *Macromolecules* **2004**, *37*, 5495–5503. (f) Onouchi, H.; Miyagawa, T.; Furuko, A.; Maeda, K.; Yashima, E. *J. Am. Chem. Soc.* **2005**, *127*, 2960–2965. (g) Miyagawa, T.; Furuko, A.; Maeda, K.;

Katagiri, H.; Furusho, Y.; Yashima, E. *J. Am. Chem. Soc.* **2005**, *127*, 5018–5019. (h) Onouchi, H.; Hasegawa, T.; Kashiwagi, D.; Ishiguro, H.; Maeda, K.; Yashima, E. *Macromolecules* **2005**, *38*, 8625–8633. (i) Hasegawa, T.; Morino, K.; Tanaka, Y.; Katagiri, H.; Furusho, Y.; Yashima, E. *Macromolecules* **2006**, *39*, 482–488. (j) Hasegawa, T.; Maeda, K.; Ishiguro, H.; Yashima, E. *Polym. J.* **2006**, *38*, 912–919. (k) Maeda, K.; Yashima, E. *Top. Curr. Chem.* **2006**, *265*, 47-88. (l) Yashima, E.; Maeda, K. *Macromolecules* **2008**, *41*, 3-12. (m) Kawauchi, T.; Kumaki, J.; Kitaura, A.; Okoshi, K.; Kusanagi, H.; Kobayashi, K.; Sugai, T.; Shinohara, H.; Yashima, E. *Angew. Chem., Int. Ed.* **2008**, *47*, 515-519. (n) Yashima, E.; Maeda, K.; Furusho, Y. *Acc. Chem. Res.* **2008**, *41*, 1166-1180. (o) Kawauchi, T.; Kitaura, A.; Kumaki, J.; Kusanagi, H.; Yashima, E. *J. Am. Chem. Soc.* **2008**, *130*, 11889-11891. For chiral memory effect of other macromolecular and supramolecular systems, see: (p) Furusho, Y.; Kimura, T.; Mizuno, Y.; Aida, T. *J. Am. Chem. Soc.* **1997**, *119*, 5267-5268. (q) Mizuno, T.; Takeuchi, M.; Hamachi, I.; Nakashima, K.; Shinkai, S. *J. Chem. Soc., Perkin Trans. 2* **1998**, 2281-2288. (r) Bellacchio, E.; Lauceri, R.; Gurrieri, S.; Scolaro, L. M.; Romeo, A.; Purrello, R. *J. Am. Chem. Soc.* **1998**, *120*, 12353-12354. (s) Prins, L. J.; Jong, F. D.; Timmerman, P.; Reinhoudt, D. N. *Nature* **2000**, *408*, 181-184. (t) Kubo, Y.; Ohno, T.; Yamanaka, J.-i.; Tokita, S.; Iida, T.; Ishimaru, Y. *J. Am. Chem. Soc.* **2001**, *123*, 12700-12701. (u) Lauceri, R.; Raudino, A.; Scolaro, L. M.; Micali, N.; Purrello, R. *J. Am. Chem. Soc.* **2002**, *124*, 894-895. (v) Mammana, A.; D'Urso, A.; Lauceri, R.; Purrello, R. *J. Am. Chem. Soc.* **2007**, *129*, 8062-8063. (w) Rosaria, L.; D'Urso, A.; Mammana, A.; Purrello, R. *Chirality* **2008**, *20*, 411-419. (x) Ousaka, N.; Inai, Y.; Kuroda, R. *J. Am. Chem. Soc.* **2008**, *130*, 12266-12267.

(13) Ishikawa, M.; Maeda, K.; Mitsutsuji, Y.; Yashima, E. *J. Am. Chem. Soc.* **2004**, *126*, 732–733.

(14) (a) Hase, Y.; Mitsutsuji, Y.; Ishikawa, M.; Maeda, K.; Okoshi, K.; Yashima, E. *Chem. Asian J.* **2007**, *2*, 755–763. (b) Miyabe, T.; Hase, Y.; Iida, H.; Maeda, K.; Yashima, E. *Chirality* **2009**, *21,* 44–50.

(15) Ishikawa, M.; Maeda, K.; Yashima, E. *J. Am. Chem. Soc.* **2002**, *124*, 7448–7458.

(16) Hase, Y.; Ishikawa, M.; Muraki, R.; Maeda, K.; Yashima, E. *Macromolecules* **2006**, *39*, 6003–6008.

(17) Hase, Y. Ph. D Thesis, Graduate School of Engineering, Nagoya University (2007).

(18) The effect of MeOH on the polymerization of **1**-**Et** with $NiCl_2 \cdot 6H_2O$ remains obscure, but this method may be useful to obtain high molecular weight polyisocyanides.

(19) The persistence length (q) is a useful measure to evaluate the stiffness of rodlike polymers, but only a limited number of q values have been determined for synthetic helical polymers. See: (a) Sato, T.; Teramoto, A. *Adv. Polym. Sci.* **1996**, *126*, 85–161. (b) Nieh, M.-P.; Goodwin, A. A.; Stewart, J. R.; Novak, B. M.; Hoagland, D. A. *Macromolecules* **1998**, *31*, 3151–3154. (c) Gu, H.; Nakamura, Y.; Sato, T.; Teramoto, A.; Green, M. M.; Andreola, C. *Polymer* **1999**, *40*, 849–856. (d) Teramoto, A.; Terao, K.; Terao, Y.; Nakamura, N.; Sato, T.; Fujiki, M. *J. Am. Chem. Soc.* **2001**, *123*, 12303–12310. (e) Nomura, R.; Tabei, J.; Nishiura, S.; Masuda, T. *Macromolecules* **2003**, *36*, 561–564. (f) Ashida, Y.; Sato, T.; Morino, K.; Maeda, K.; Okamoto, Y.; Yashima, E. *Macromolecules* **2003**, *36*, 3345-3350. (g) Okoshi, K.; Sakajiri, K.; Kumaki, J.; Yashima, E. *Macromolecules* **2005**, *38*, 4061–4064. (h) Okoshi, K.; Sakurai, S.-i.; Ohsawa, S.; Kumaki, J.; Yashima, E. *Angew. Chem., Int. Ed.* **2006**, *45*, 8173–8176. Persistence length values of certain polyisocyanide derivatives have been measured, see ref 7 and: (i) Bieglé, A.; Mathis, A.; Galin, J.-C. *Macromol. Chem. Phys.* **2000**, *201*, 113-125. (j) Samorí, P.; Ecker, C.; Gössl, I.; de Witte, P. A. J.; Cornelissen, J. J. L. M.; Metselaar, G. A.; Otten, M. B. J.; Rowan, A. E.; Nolte, R. J. M.; Rabe, J. P. *Macromolecules* **2002**, *35*, 5290-5294. (k) Okoshi, K.; Nagai, K.; Kajitani, T.; Sakurai, S.-i.; Yashima, E. *Macromolecules*, **2008**, *41*, 7752–7754.

(20) (a) Yamakawa, H.; Fujii, M. *Macromolecules* **1974**, *7*, 128–135. (b) Yamakawa, H.; Yoshizaki, T. *Macromolecules* **1980**, *13*, 633–643.

(21) (a) Nagai, K.; Sakajiri, K.; Maeda, K.; Okoshi, K.; Sato, T.; Yashima, E. *Macromolecules* **2006**, *39*, 5371–5380. (b) Sakurai, S.-i.; Okoshi, K.; Kumaki, J.; Yashima, E. *Angew. Chem., Int. Ed.* **2006**, *45*, 1245–1248. (c) Sakurai, S.-i.; Ohsawa, S.; Nagai, K.; Okoshi, K.; Kumaki, J.; Yashima, E. *Angew. Chem., Int. Ed.* **2007**, *46*, 7605-7608.

(22) The densities of the HMW-poly-**1**–**Me**, HMW-poly-**1a**–**Me**, and HMW-***h***-poly-**1b**–**Me** films were measured by the standard flotation method in a KBr saturated aqueous solution—water mixture at ambient temperature (20–25 °C).

(23) Cochran, W.; Crick, F. H. C.; Vand, V. *Acta Crystallogr.* **1956**, *5*, 581–586.

(24) Skorna, G.; Ugi, I. *Angew. Chem., Int. Ed. Engl.* **1977,** *16*, 259–260.

(25) Benoit, H.; Doty, P. *J. Phys. Chem.* **1953**, *57*, 958–963.

(26) Yamakawa, H. *Helical Wormlike Chains in Polymer Solutions*, Springer, Berlin, 1997, p. 278.

(27) Sun, H. *J. Phys. Chem. B* **1998**, *102*, 7338–7364.

(28) Miyazawa, T. *J. Polym. Sci.* **1961**, *55*, 215–231.

Chapter 5

Anomalous Stiff Backbones of Helical Poly(phenyl isocyanide) Derivatives

Abstract: The persistence lengths of a series of optically active helical poly(phenyl isocyanide)s bearing different optically active functional groups, such as L-alanine, L-lactic acid, L-phenylalanine, and L-alaninol residues, with a long *n*-decyl chain as the pendants were estimated by a size exclusion chromatography system equipped with multi-angle laser light scattering and refractive index detectors in conjunction with the wormlike chain model. The persistence lengths of the polymers significantly depended on their chiral pendant structures involving the hydrogen-bonding ability and bulkiness, and the poly(phenyl isocyanide) with L-alanine *n*-decyl esters as the pendants was found to possess an unprecedented long persistence length of 220 nm. This value is the highest among all synthetic helical polymers reported so far and is comparable to those of biological, multi-stranded helical polymers, such as the triple-stranded helical collagen and schizophyllan.

Introduction

Fully synthetic helical polymers with an excess one-handed helical sense have recently drawn much attention because of implications for biological helices and functions as well as their possible applications as chiral materials.[1] Rodlike synthetic helical polymers are particularly interesting, since they often form chiral liquid crystals (LCs) in concentrated solutions or in a melt,[2] as observed in biological polymers, such as DNA,[3] polysaccharides,[4] and polypeptides,[5] which adopt a stiff rodlike structure with a controlled helix-sense stabilized by intra- and/or inter-molecular hydrogen-bonding networks. Such intramolecular hydrogen bonds have been utilized in constructing biomimetic helical polymers, such as polyisocyanopeptides,[1d,2c,6] amino acid-bound polyacetylenes,[7,8] and foldamers.[9]

Recently, Yashima et al. reported a unique polyisocyanide (poly-**1** in Chart 5-1) prepared by the polymerization of an enantiomerically pure phenyl isocyanide bearing an L- or D-alanine pendant with a long *n*-decyl chain with an achiral $NiCl_2$ catalyst, whose helical sense (right- or left-handed helix) could be controlled by the polymerization solvent and temperature. The resulting diastereomeric poly-**1**s showing intense first Cotton effects ($\Delta\varepsilon_{1st}$ = –11.0—+8.14) at the imino chromophore regions of the polymer backbones (ca. 360 nm) formed lyotropic cholesteric LCs with opposite twist senses in concentrated solutions due to their main-chain stiffness arising from the intramolecular hydrogen-bonding between the pendant amide groups.[10]

Chart 5-1. Structures of Helical Polyisocyanides

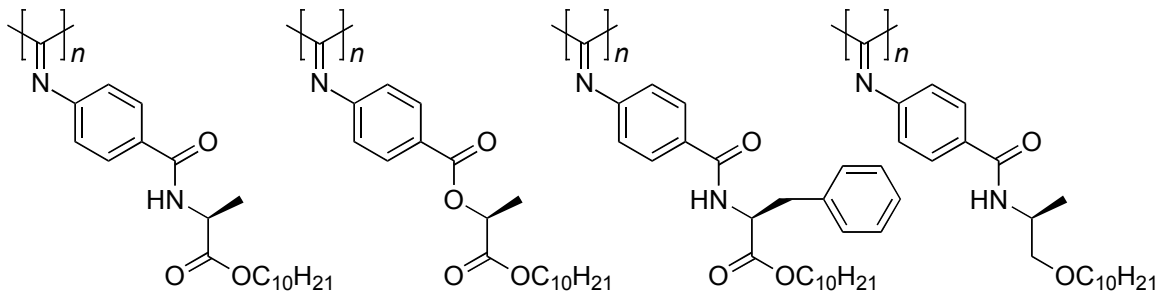

In order to explore the effect of the chiral pendant structure on the chiroptical properties of the polyisocyanide, a series of optically active polyisocyanides bearing different optically active functional groups, such as L-lactic acid (poly-**2**), L-phenylalanine (poly-**3**), and L-alaninol (poly-**4**) residues, with the same *n*-decyl chain as the pendants were prepared in various solvents at different temperatures.[11] In sharp contrast to poly-**1**, poly-**2** and poly-**4** exhibited weak Cotton effects, while poly-**3** showed rather intense positive Cotton effects, independent of the polymerization conditions. Yashima et al. then concluded that the helical senses and the excess of one helical sense of the polyisocyanides were governed by specific interactions (intermolecular hydrogen-bonding and steric effect) occurring between the pendant residues of the growing chain end and monomers during the propagation reaction, which might be influenced by the solvent polarity and temperature of the polymerization process.

Although the fact that poly-**1** formed a cholesteric LC in concentrated solutions, which indicated its rigid rodlike feature of the main-chain, the persistence length *q*, a useful measure to evaluate the stiffness of rodlike polymers, has not been estimated. We now show the persistence lengths of a series of helical polyisocyanides bearing different optically active pendant groups (poly-**1**—poly-**4**) and describe the effect of the chiral pendant structures on their main-chain stiffness. We found that poly-**1** possesses an extremely long *q* value of 220 nm, which is the highest among all synthetic helical polymers reported so far. Although a number of rodlike helical polymers have been prepared, only a limited number of *q* values has been determined for helical polymers. The reported high *q* values for synthetic helical polymers are 13.5 nm (poly(*N*-propargylamide)),[7b] 20–40 nm (poly(*n*-hexyl isocyanate)),[12] 42 nm (poly(*N*-(1-phenylethyl)-*N'*-methylcarbodiimide)),[13] 76 nm (polyisocyanopeptides),[6b] 103 nm (poly(((*R*)-3,7-dimethyloctyl)-((*S*)-3-methylpentyl)-silylene)),[14] and 135 nm (poly(4-ethynylbenzoyl-L-alanine *n*-decyl ester).[8d]

Results and Discussion

Poly-**1**—poly-**4** were prepared according to previously reported methods by the polymerization of the corresponding monomers with an achiral $NiCl_2$ catalyst under the experimental conditions that yielded helical polyisocyanides with high molecular weights (M_n = 17.3—20.8 × 10^4) showing almost the highest Cotton effect intensities (Table 5-1),[10,11] although the $\Delta\varepsilon_{1st}$ values reflecting the excess of one helical sense were different from each other.[11]

The q values of poly-**1**—poly-**4** were then estimated on the basis of the wormlike chain model,[15] which can be described as an analytical function of the molecular weight (M_w) and the radius of gyration (S) if the q values and the molar mass per unit contour length (M_L), which eventually leads to the monomer unit height (h), are given. The radii of gyration (S) of (poly-**1**—poly-**4**) in tetrahydrofuran (THF) containing 0.1 wt % tetra-*n*-butyl ammonium bromide (TBAB) were measured as a function of M_w using size exclusion chromatography (SEC) equipped with multi-angle laser light scattering (MALS) and refractive index detectors in series (Figure 5-1).

The solid curves in the plots were calculated using the parameters determined from the fits of the unperturbed wormlike chain model over the entire M_w studied range, and are represented by the theoretical values of $<S^2>^{0.5}$. The calculated h values of poly-**1**—poly-**4** are in agreement with the reported value (0.087 nm) of poly-**1** determined by X-ray structural analysis,[16] indicating that these polymers appear to take a similar helical conformation irrespective of the structures of the chiral pendant groups.

Table 5-1. Chiroptical Properties of Helical Polyisocyanides[a]

polymer	$M_n \times 10^{-4}$ [b]	M_w/M_n [b]	$[\alpha]^{25}_D$ [c]	$\Delta\varepsilon_{1st}$ [c]	q (nm)[d]
poly-**1**[e]	19.0	1.92	–814	–11.0	220
poly-**2**	17.3	2.17	–243	–3.21	30.8
poly-**3**	19.8	2.08	+688	+8.94	103
poly-**4**	20.8	1.53	–273	–1.28	81.8

[a] Obtained by polymerization with $NiCl_2 \cdot 6H_2O$ in toluene at 100 °C (cited from ref 11). [b] Determined by SEC-MALS measurements with THF containing TBAB (0.1 wt %) as the eluent. [c] Measured in chloroform at 25 °C. [d] Estimated by SEC-MALS measurements with the wormlike chain model. [e] Obtained by annealing a toluene solution of the polymer at 100 °C for 6 days.[10]

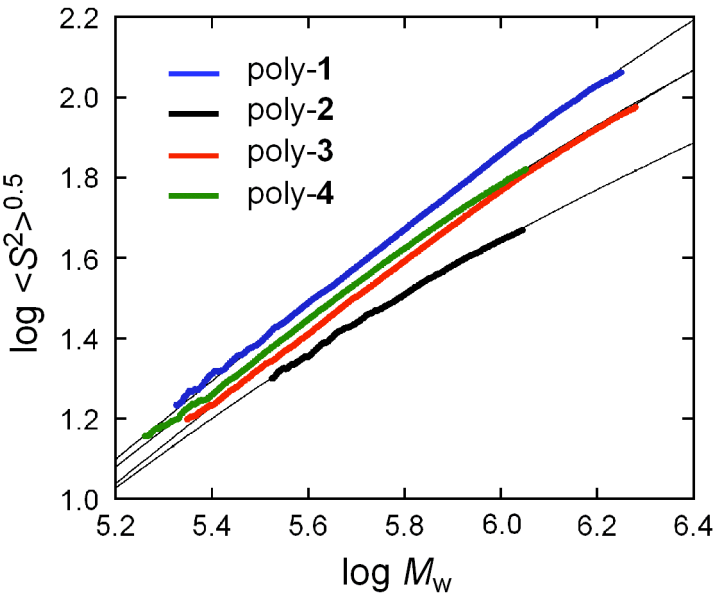

Figure 5-1. Double-logarithmic plots of the radius of gyration versus the molecular weight of poly-**1** (blue points), poly-**2** (black points), poly-**3** (red points), and poly-**4** (green points) in THF containing TBAB (0.1 wt %) obtained by SEC-MALS measurements at 40 °C. Solid curves (black lines) were obtained on the basis of the wormlike chain theory and fit well with the experimental data. The evaluated parameters are as follows: q = 220 nm, M_L = 3577, h = 0.10 nm for poly-**1**; q = 30.8 nm, M_L = 3796, h = 0.094 nm for poly-**2**; q = 103 nm, M_L = 4041, h = 0.11 nm for poly-**3**; q = 81.8 nm, M_L = 3625, h = 0.095 nm for poly-**4**.

The calculated q value of poly-**1** is 220 nm, which is unprecedentedly long and the highest value among all synthetic helical polymers reported so far,[17] including polyisocyanates,[12] polyguanidines,[13] polyisocyanides,[6b] polysilanes,[14] and polyacetylenes[8d] and is comparable to those of biological, multi-stranded helical polymers, such as the triple-stranded helical collagen (160–180 nm)[18] and schizophyllan (150–200 nm),[19] and even stiffer than the double-stranded helical DNA (60 nm)[20] and xanthan (120 nm).[21] In contrast, poly-**2** in which the amide linkage of poly-**1** was replaced by an ester showed a dramatic decrease in its persistence length to 30.8 nm, indicating a rather semi-rigid polymer. This change in the q value clearly demonstrates that the main-chain stiffness of poly-**1** can be dictated by intramolecular hydrogen-bonding networks of the pendant amide groups (Figure 5-2).[16]

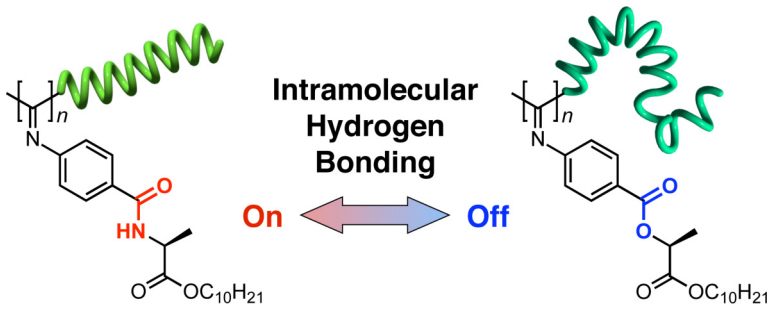

Figure 5-2. Schematic illustration of the extremely different main-chain stiffness of poly-**1** and poly-**2** resulting from the "on and off" of the intramolecular hydrogen-bonding networks.

Atomic force microscopy (AFM) images of the isolated poly-**1** and poly-**2** chains were then measured on mica modified with trimethoxypropylsilane, which also support the change in their main-chain stiffness (A and B in Figure 5-3, respectively). Individual polymer chains with extended and tangled structures for poly-**1** and poly-**2**, respectively, can be directly visualized on the mica, indicating the stiff and flexible main-chain conformations, respectively. Helical poly(isocyanopeptide)s developed by Nolte, Rowan, and coworkers are also stabilized by well-defined arrays of intramolecular hydrogen bonds as supported by their characteristic IR spectra, thus showing a relatively high q value of 76 nm,[6b] being shorter than

that of poly-**1**. Therefore, an extremely long q value (220 nm) of an analogous helical polyisocyanide poly-**1** may be ascribed to the phenyl substituents as the pendant groups, which may contribute more or less to its rigidity of the poly-**1** main-chain.

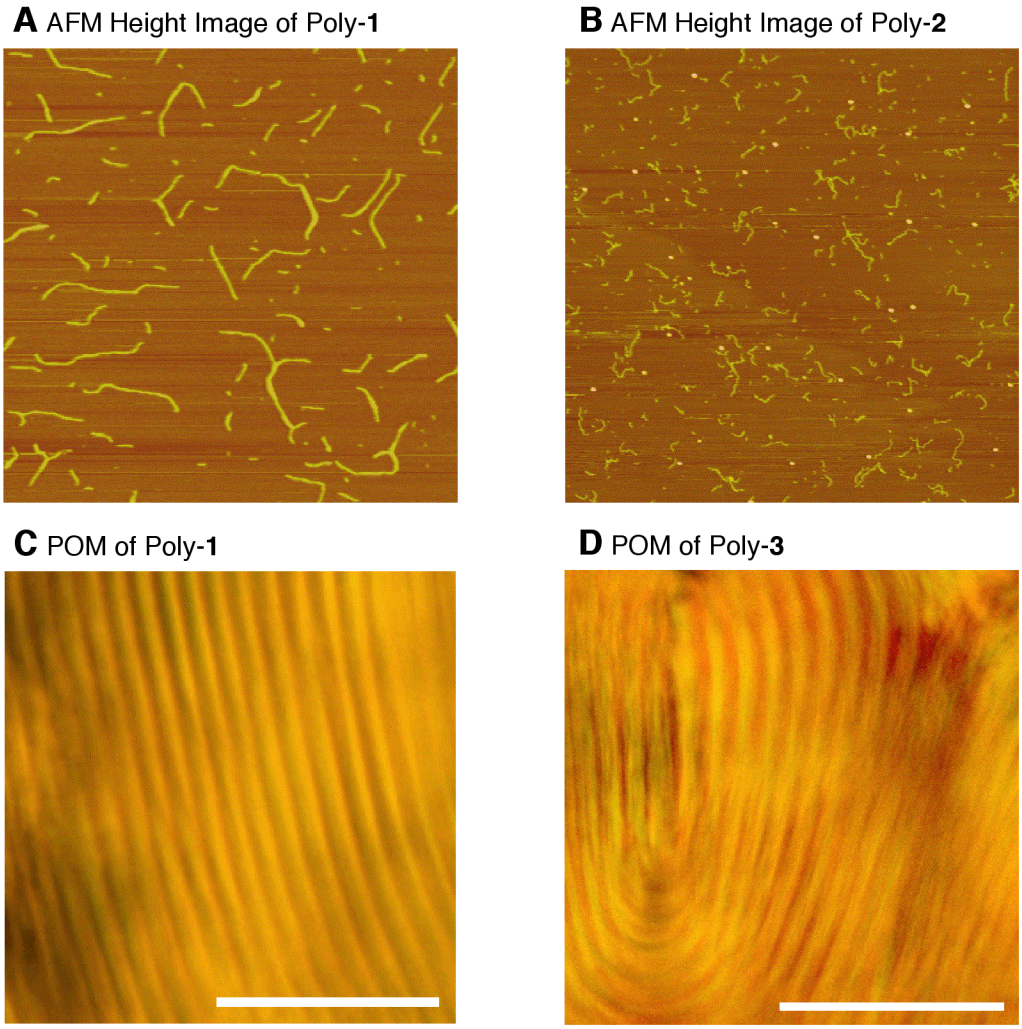

Figure 5-3. AFM height images (2 × 2 μm^2) of poly-**1** (A) and poly-**2** (B) cast from a dilute solution of chloroform (2.5 μg/mL) on mica modified with trimethoxypropylsilane. Polarized optical micrographs (POM) of poly-**1** (C) and poly-**3** (D) in 15 wt % chloroform solutions in glass capillary tubes taken at ambient temperature (20–25 °C). Scale bars: 50 μm.

The author notes that the persistence length of poly-**1** was measured by an SEC-MALS system using THF containing 0.1 wt % TBAB as the eluent due to the strong adsorption on the SEC columns in THF and chloroform, which does not diminish the intramolecular hydrogen bonds of poly-**1** as observed in the IR and CD spectra (Figure 5-4).

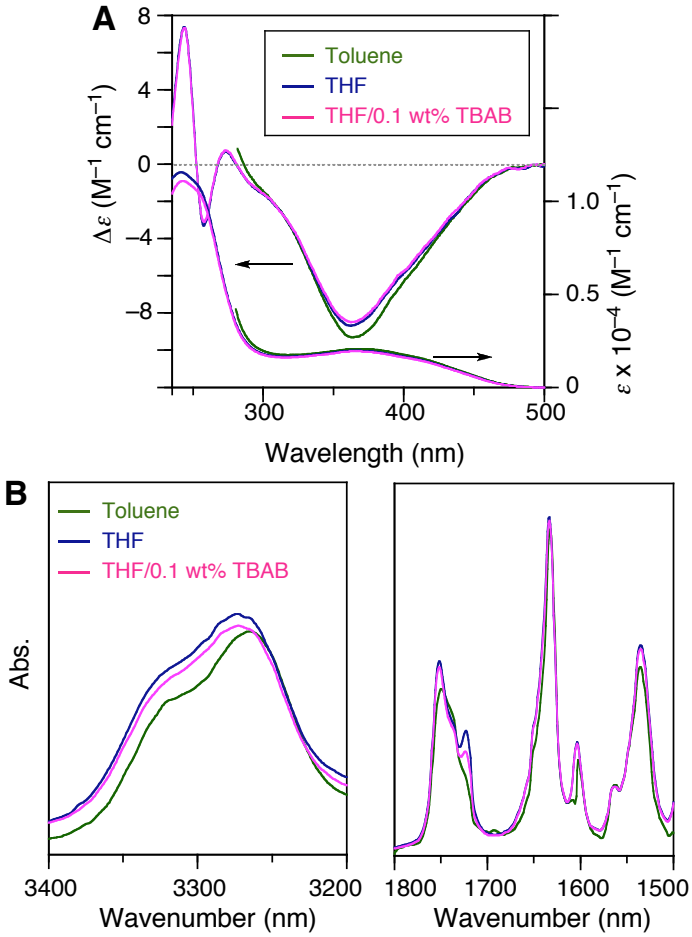

Figure 5-4. CD and absorption (A) and FT-IR spectra (B) of poly-**1** in toluene (green lines), THF (blue lines), and THF containing TBAB (0.1 wt %) (pink lines) at room temperature. FT-IR spectra were measured in a 0.1-mm CaF_2 cell.

Poly-**3**, whose structural characteristic is similar to that of poly-**1** except for its bulky phenylalanine residue, and poly-**4** in which the ester linkage of poly-**1** was replaced by an ether also maintained the main-chain stiffness, but exhibited relatively shorter persistence lengths of 103 and 81.8 nm, respectively. These results indicated that the appropriate bulkiness as well as the ester carbonyl groups at the pendant groups plays some roles in the stiffness of the polymer main-chain. In other words, the pendant groups of the polyisocyanides require an appropriate bulkiness to be packed in the preferable helical structure so that the amide groups as well as the ester carbonyl groups can participate in the formation of the intramolecular hydrogen-bonding networks,[11] resulting in stiff, rodlike polyisocyanides. A poly-**1** with similar molecular weight (M_n = 22.2 × 10^4) but lower optical activity ($\Delta\varepsilon_{1st}$ = –1.28 and $[\alpha]^{25}_D$ = –59) prepared in different polymerization conditions[11] also showed a large q value (175 nm), indicating that the excess of one-helical sense of poly-**1** may not influence its main-chain stiffness, although the reason for the apparent difference in their q values of the poly-**1**s is not clear at the present.

As expected from the rodlike features of poly-**1** and poly-**3** together with their optical activity derived from a preferred-handed helical structure, these polymers formed lyotropic cholesteric LCs in a concentrated chloroform solution, thus showing a fingerprint texture (C and D in Figure 4-3, respectively). Poly-**2** and poly-**4** appear to be stiff enough to show a liquid crystallinity. However, they exhibited a nematic-like birefringence due to their low optical activity, that is, low one-handedness excesses on the basis of their $\Delta\varepsilon_{1st}$ values (Table 5-1).

Conclusions

In summary, the author has estimated the persistence lengths of a series of optically active helical poly(phenyl isocyanide)s and investigated the effect of the chiral pendant structures on their stiffness. A helical poly(phenyl isocyanide) bearing L-alanine *n*-decyl esters as the pendants was found to possess an unprecedentedly long persistence length of 220 nm stabilized by intramolecular hydrogen-bonding networks. This may be the highest persistence length among the synthetic helical polymers prepared so far. The present results may contribute to the design and synthesis of new rodlike helical polyisocyanides with a controlled helical sense. In addition, helical polyisocyanides with an extremely stiff polymer backbone together with a large electric dipole moment of the pendant amide residues[8e,16] may be used as a novel scaffold to build up uniformly aligned, supramolecular helical arrays, which will be further applicable to optoelectrical devices due to its polar structure.

Experimental Section

Materials. Anhydrous chloroform (water content < 30 ppm) was purchased from Wako (Osaka, Japan) and used for the AFM measurements and polarized optical microscopic observations. Tetrahydrofuran (THF) was used for the size exclusion chromatography-multi-angle light scattering (SEC-MALS) measurements, and was of HPLC grade (Wako). Tetra-*n*-butylammonium bromide (TBAB) was purchased from Tokyo Kasei (TCI, Tokyo, Japan), and trimethoxypropylsilane was from Aldrich and used without further purification. The optically active polyisocyanides (poly-**1**—poly-**4**) were prepared according to the previously reported methods using a $NiCl_2$ catalyst in toluene.[11]

Instruments. The SEC-MALS measurements were performed at 40 °C using an HLC-8220 GPC system (Tosoh, Tokyo, Japan) equipped with a differential refractometer coupled to a DAWN-HELEOS MALS device equipped with a solid state laser (λ = 684 nm) (Wyatt Technologies, Santa Barbara, CA) using two TSKgel Multipore H_{XL}-M columns (Tosoh) in series. The scattered light intensities were measured by eighteen light scattering detectors with different angles. The differential refractive index increments, *dn*/*dc*, of the polymers with respect to the mobile phase (THF containing 0.1 wt % TBAB) were also measured by an Optilab rEX interferometric refractometer (Wyatt Technology Corp.). The IR spectra were recorded using a JASCO FT/IR-680 spectrophotometer. The polymer concentration was 5.0 mg/mL for the IR measurements. The polarizing optical microscopic observations were carried out using an E600POL polarizing optical microscope (Nikon, Tokyo, Japan) equipped with a DS-5M CCD camera (Nikon) connected to a DS-L1 control unit (Nikon).

SEC-MALS Measurements. The SEC-MALS measurements were carried out in THF containing TBAB (0.1 wt %) at the flow rate of 0.5 mL/min. A standard polystyrene (M_w = 30500 (Polymer Laboratories, Shropshire, U.K.)) was used to calculate the device constants, such as the inter-detector delay, inter-detector band broadening, and light scattering detector normalization. Poly-**1**—poly-**4** were completely dissolved in the eluent at the concentration of

0.1–0.2 % (wt/vol) under gentle stirring for 1–2 h before injection. Poly-**1** of $M_w = 19.0 \times 10^4$ and $M_w/M_n = 1.92$, poly-**2** of $M_w = 17.3 \times 10^4$ and $M_w/M_n = 2.17$, poly-**3** of $M_w = 19.8 \times 10^4$ and $M_w/M_n = 2.08$, and poly-**4** of $M_w = 20.8 \times 10^4$ and $M_w/M_n = 1.53$ were used for the SEC-MALS measurements. The evaluations of the molecular weights and the radii of gyration of poly-**1**—poly-**4** were accomplished using ASTRA V software (version 5.1.3.0). The *dn*/*dc* values of poly-**1**—poly-**4** in the eluent used for the evaluations were 0.118, 0.092, 0.142, and 0.119 mL/g, respectively (the uncertainties were ±0.0019, ±0.0015, ±0.0024, and ±0.0001 mL/g, respectively), on the assumption that the *dn*/*dc* values were independent of the molecular weight.

Persistence Length Estimation from the Molecular Weight Dependence of the Radius of Gyration. The molecular weight dependences of the obtained radii of gyration of poly-**1**—poly-**4** were used to estimate the persistence length q based on the wormlike chain model. It was over the range of the elution volume where both the concentration and the scattering intensities are greater than 10% of the peak value. The unperturbed mean-square radius of gyration $\langle S^2 \rangle_0$ is given by[22]

$$\langle S^2 \rangle_0 = (2q)^2 \left[\frac{1}{6} N - \frac{1}{4} + \frac{1}{4N} - \frac{1}{8N^2} (1 - \exp(-2N)) \right] \quad (1)$$

where N is the Kuhn statistical segment number defined by $N = M_w/(2q \cdot M_L)$, and M_L denotes the molar mass per unit contour length of the polymer. The radius expansion factor α_s [$\equiv (\langle S^2 \rangle / \langle S^2 \rangle_0)^{0.5}$] for the excluded-volume effect was negligible because it is close to unity for $N < 50$.[23] Equation (1) indicates that $\langle S^2 \rangle_0$ is characterized by q and M_L, therefore a fitting procedure was used to estimate q and M_L.

AFM Measurements. Stock solutions of poly-**1** and poly-**2** in chloroform (2.5 μg/mL) were prepared. Samples for the AFM measurements of poly-**1** and poly-**2** were prepared by spin casting (1800 rpm) 10 μL aliquots of the stock solutions of the polymers on mica

modified with trimethoxypropylsilane,[8d] and then the substrates were dried under vacuum for 2 h. The AFM measurements were performed using a Nanoscope IIIa microscope (Veeco Instruments, Santa Barbara, CA) in air at ambient temperature with standard silicon cantilevers (NCH, NanoWorld, Neuchâtel, Switzerland) in the tapping mode. The scanning speed was at a line frequency of 1.5 Hz. The Nanoscope image processing software was used for the image analyses.

References and Notes

(1) (a) Green, M. M.; Peterson, N. C.; Sato, T.; Teramoto, A.; Cook, R.; Lifson, S. *Science* **1995**, *268*, 1860–1865. (b) Okamoto, Y.; Yashima, E. *Angew. Chem., Int. Ed.* **1998**, *37*, 1020–1043. (c) Nakano, T.; Okamoto, Y. *Chem. Rev.* **2001**, *101*, 4013–4038. (d) Cornelissen, J. J. L. M.; Rowan, A. E.; Nolte, R. J. M.; Sommerdijk, N. A. J. M. *Chem. Rev.* **2001**, *101*, 4039–4070. (e) Fujiki, M.; Koe, J. R.; Terao, K.; Sato, T.; Teramoto, A.; Watanabe, J. *Polym. J.* **2003**, *35*, 297–344. (f) Reggelin, M.; Doerr, S.; Klussmann, M.; Schultz, M.; Holbach, M. *Proc. Natl. Acad. Sci. U. S. A.* **2004**, *101*, 5461–5466. (g) Yashima, E.; Maeda, K.; Nishimura, T. *Chem. –Eur. J.* **2004**, *10*, 42–51. (h) Amabilino, D. B.; Serrano, J.-L.; Sierra, T.; Veciana, J. *J. Polym. Sci. Part A: Polym. Chem.* **2006**, *44*, 3161–3174. (i) Maeda, K.; Yashima, E. *Top. Curr. Chem.* **2006**, *265*, 47–88. (j) Yashima, E; Maeda, K. *Macromolecules* **2008**, *41*, 3–12.

(2) (a) Sato, T.; Sato, Y.; Umemura, Y.; Teramoto, A.; Nagamura, Y.; Wagner, J.; Weng, D.; Okamoto, Y.; Hatada, K.; Green, M. M. *Macromolecules* **1993**, *26*, 4551–4559. (b) Okoshi, K.; Kamee, H.; Suzaki, G.; Tokita, M.; Fujiki, M.; Watanabe, J. *Macromolecules* **2002**, *35*, 4556–4559. (c) Cornelissen, J. J. L. M.; Granswinckel, W. S.; Rowan, A. E.; Sommerdijk, N. A. J. M.; Nolte, R. J. M. *J. Polym. Sci. Part A: Polym. Chem.* **2003**, *41*, 1725–1736. (d) Kim, J.; Novak, B. M.; Wadden, A. J. *Macromolecules* **2004**, *37*, 8286–8292.

(3) (a) Strzelecka, T. E.; Davidson, M. W.; Rill, R. L. *Nature* **1988**, *331*, 457–460. (b) Livolant, F.; Levelut, A. M.; Doucet, J.; Benoit, J. P. *Nature* **1989**, *339*, 724–726.

(4) (a) Fortin, S.; Charlet, G. *Macromolecules* **1989**, *22*, 2286–2292. (b) Inatomi, S.-i.; Jinbo, Y.; Sato, T.; Teramoto, A. *Macromolecules* **1992**, *25*, 5013–5019.

(5) (a) Robinson, C.; Ward, J. C. *Nature* **1957**, *180*, 1183–1184. (b) Tsujita, Y.; Yamanaka, I.; Takizawa, A. *Polym. J.* **1979**, *11*, 749–754. (c) Yu, S. M.; Conticello, V. P.; Zhang, G.; Kayser, C.; Fournier, M. J.; Mason, T. L.; Tirrel, D. A. *Nature* **1997**, *389*, 167–170.

(6) (a) Cornelissen, J. J. L. M.; Donners, J. J. J. M.; de Gelder, R.; Graswinckel, W. S.; Metselaar, G. A.; Rowan, A. E.; Sommerdijk, N. A. J. M.; Nolte, R. J. M. *Science* **2001**, *293*, 676–680. (b) Samorí, P.; Ecker, C.; Gösell, I.; de Witte, P. A. J.; Cornelissen, J. J. L. M.; Metselaar, G. A.; Otten, M. B. J.; Rowan, A. E.; Nolte, R. J. M.; Rabe, J. P. *Macromolecules* **2002**, *35*, 5290–5294. (c) Metselaar, G. A.; Adams, P. J. H. M.; Nolte, R. J. M.; Cornelissen, J. J. L. M. Rowan, A. E. *Chem. –Eur. J.* **2007**, *13*, 950–960. (d) Metselaar, G. A.; Wezenberg, S. J.; Cornelissen, J. J. L. M.; Nolte, R. J. M.; Rowan, A. E. *J. Polym. Sci. Part A: Polym. Chem.* **2007**, *45*, 981–988.

(7) (a) Nomura, R.; Tabei, J.; Masuda, T. *J. Am. Chem. Soc.* **2001**, *123*, 8430–8431. (b) Nomura, R.; Tabei, J.; Nishiura, S.; Masuda, T. *Macromolecules* **2003**, *36*, 561–564. (c) Cheuk, K. L.; Lam, J. W. Y.; Tang, B. Z. *Macromolecules* **2003**, *36*, 9752–9762. (d) Lam, J. W. Y.; Tang, B. Z. *Acc. Chem. Res.* **2005**, *38*, 745–754.

(8) (a) Okoshi, K.; Sakajiri, K.; Kumaki, J.; Yashima, E. *Macromolecules* **2005**, *38*, 4061–4064. (b) Sakurai, S.-i.; Okoshi, K.; Kumaki, J.; Yashima, E. *Angew. Chem., Int. Ed.* **2006**, *45*, 1245–1248. (c) Sakurai, S.-i.; Okoshi, K.; Kumaki, J.; Yashima, E. *J. Am. Chem. Soc.* **2006**, *128*, 5650–5651. (d) Okoshi, K.; Sakurai, S.-i.; Ohsawa, S.; Kumaki, J.; Yashima, E. *Angew. Chem., Int. Ed.* **2006**, *45*, 8173–8176. (e) Okoshi, K.; Kajitani, T.; Nagai, K.; Yashima, E. *Macromolecules* **2008**, *41*, 258–261.

(9) *Foldamers: Structure, Properties, and Applications*; Hecht, S., Huc, I., Eds.; Wiley-VCH: Weinheim, 2007.

(10) Kajitani, T.; Okoshi, K.; Sakurai, S.-i.; Kumaki, J.; Yashima, E. *J. Am. Chem. Soc.* **2006**, *128*, 708–709.

(11) Kajitani, T.; Okoshi, K.; Yashima, E. *Macromolecules* **2008**, *41*, 1601–1611.

(12) Gu, H.; Nakamura, Y.; Sato, T.; Teramoto, A.; Green, M. M.; Andreola, C. *Polymer* **1999**, *40*, 849–856.

(13) Nieh, M.-P.; Goodwin, A. A.; Stewart, J. R.; Novak, B. M.; Hoagland, D. A. *Macromolecules* **1998**, *31*, 3151–3154.

(14) Teramoto, A.; Terao, K.; Terao, Y.; Nakamura, N.; Sato, T.; Fujiki, M. *J. Am. Chem. Soc.* **2001**, *123*, 12303–12310.

(15) (a) Yamakawa, H.; Fujii, M. *Macromolecules* **1974**, *7*, 128–135. (b) Yamakawa, H.; Yoshizaki, T. *Macromolecules* **1980**, *13*, 633–643.

(16) Onouchi, H.; Okoshi, K.; Kajitani, T.; Sakurai, S.-i.; Nagai, K.; Kumaki, J.; Onitsuka, K.; Yashima, E. *J. Am. Chem. Soc.* **2008**, *130*, 229–236.

(17) Sato, T.; Teramoto, A. *Adv. Polym. Sci.* **1996**, *126*, 85–161.

(18) Saito, T.; Iso, N.; Mizuno, H,; Onda, N.; Yamato, H.; Odashima, H. *Biopolymers* **1982**, *21*, 715–728.

(19) (a) Yanai, T.; Norisuye, T.; Fujita, H. *Macromolecules* **1980**, *13*, 1462–1466. (b) Kashiwagi, Y.; Norisuye, T.; Fujita, H. *Macromolecules* **1981**, *14*, 1220–1225.

(20) Godfrey, J. E.; Einsenberg, H. *Biophys. Chem.* **1976**, *5*, 301–318.

(21) Sato, T.; Norisuye, T.; Fujita,H. *Polym. J.* **1984**, *16*, 341–350.

(22) Benoit, H.; Doty, P. *J. Chem. Phys.* **1953**, *57*, 958–963.

(23) Yamakawa, H. In *Helical Wormlike Chains in Polymer Solutions*; Springer: Berlin, 1997; p. 278.

Chapter 6

Helical Structure of Liquid Crystalline Poly(*N*-((4-butylphenyl)diphenylmethyl) methacrylamide)

Abstract: The optically active and inactive poly(*N*-((4-butylphenyl)diphenylmethyl) methacrylamide)s were prepared by radical polymerization in the presence and absence of (+)-menthol (***h***-poly-**1** and poly-**1**), respectively. The obtained polymethacrylamides were highly isotactic and exhibited lyotropic liquid crystalline (LC) phases in concentrated chloroform solutions, indicating their rigid-rod helical characteristics as evidenced by the long persistence lengths of 53 nm (***h***-poly-**1**) and 57 nm (poly-**1**). X-ray diffraction of the shear-oriented ***h***-poly-**1** and poly-**1** films showed almost the same diffraction pattern, suggesting that both polymers may have the same helical structure despite the difference in their optical activity. On the basis of the X-ray analyses, the most plausible helical structure of the polymethacrylamides is proposed to be a 4 unit / 1 turn or 6 unit / 1 turn helix. The high-resolution atomic force microscopy observations of the polymers provided more detailed molecular structures including molecular length and helical pitch.

Introduction

Biological polymers, such as proteins and nucleic acids, possess a characteristic single-handed helical structure, which links to their sophisticated functions in living systems.[1] Inspired by biological helices, the synthesis and structures of artificial helical polymers with controlled helicity have attracted considerable attention. Okamoto et al. prepared the first helical vinyl polymer by polymerization of an achiral bulky methacrylate, triphenylmethyl methacrylate (TrMA), using chiral anionic initiators, which produced a single-handed, fully isotactic helical polymer with a large optical rotation (PTrMA).[2] Since then, a number of synthetic helical polymers that fold into a one-handed helical conformation have been prepared to develop helical polymers with a controlled helical sense and functions.[3] Later, Okamoto et al. discovered that the one-handed helical PTrMA showed a remarkable chiral recognition for a variety of stereochemically interesting racemic compounds, when the helical PTrMA was used as a chiral stationary phase (CSP) for high-performance liquid chromatography (HPLC),[4] through which many optically active polymers have been prepared and applied to CSPs in HPLC.[3a,d,5] In addition, Reggelin et al. recently found that analogous helical poly(triarylmethyl methacrylate)s bearing pyridyl residues could be used as an efficient polymeric ligand for catalytic asymmetric C–C bond forming reactions.[6]

Although a series of helical poly(triarylmethyl methacrylate)s with optical activity have been prepared to apply them to CSPs and asymmetric polymeric catalysts, their helical structures have not yet been elucidated experimentally because high-molecular weight polymers suitable for X-ray diffraction (XRD) studies are insoluble in common organic solvents. Computational studies based on molecular mechanics calculations suggested a 3.6 monomer unit per turn (3.6 / 1) helix with 2.0 Å pitch per monomer unit for an isotactic PTrMA.[7]

Okamoto et al. recently found that the radical polymerization of *n*-butyl-substituted *N*-triphenylmethyl methacrylamides in toluene or tetrahydrofuran (THF) produced high molecular weight polymethacrylamides with a nearly 100% isotacticity being soluble in

common organic solvents, such as chloroform. When chiral additives such as (+)-menthol were used as a polymerization solvent, the optically active polymers due to a preferred-handed helicity were obtained.[8] Moreover, a few poly(*n*-butyl-substituted *N*-triphenylmethyl methacrylamide)s were found to exhibit a lyotropic liquid crystalline (LC) phase in concentrated chloroform solution,[8c] which enabled us to investigate the helical structure of the polymethacrylamides by XRD measurements of the shear-oriented films prepared from the LC samples. In fact, Yashima et al. recently succeeded in determining the helical structures of LC polyacetylenes and polyisocyanides by the X-ray analyses of the corresponding oriented films.[9] These polymers possess a stiff rodlike helical main-chain with a large persistence length (q), which is a useful measure to evaluate the stiffness of rodlike polymers.[10] In this study, the author investigated the helical structure of optically active and inactive poly(*N*-((4-butylphenyl)diphenylmethyl) methacrylamide)s (***h***-poly-**1** and poly-**1**, respectively) by means of XRD measurements together with high-resolution atomic force microscopy (AFM) observations. The backbone stiffness of poly-**1** and ***h***-poly-**1** was also estimated by a size exclusion chromatography (SEC) system equipped with multi-angle laser light scattering (MALS) and refractive index detectors in conjunction with the wormlike chain model.

Results and Discussion

Poly-**1** and ***h***-poly-**1** were prepared according to the previously reported method[8b] by the radical polymerization of the corresponding monomer with α,α'-azobisisobutyronitrile (AIBN) in toluene and (+)-menthol, respectively, under UV irradiation at 0 °C. The number-average molecular weight (M_n) and the molecular weight distribution (M_w/M_n) of poly-**1** and ***h***-poly-**1** were $M_n = 3.1 \times 10^5$ and $M_w/M_n = 2.6$ and $M_n = 7.5 \times 10^5$ and $M_w/M_n = 1.8$, respectively, as determined by SEC-MALS measurements using chloroform as the eluent. The ***h***-poly-**1** prepared in (+)-menthol was optically active and its specific rotation ($[\alpha]_{365}^{25}$) was –20.0 (*c* 0.4, chloroform); this value is considerably lower than that of a one-handed helical PTrMA prepared by the screw-sense-selective anionic polymerization ($[\alpha]_{365}^{25}$ = ca. 1400) (*c* 0.5, THF).[3a,11] The tacticities of the poly-**1**s were nearly 100% isotactic (*mm*) as estimated by their ^{1}H NMR spectra of the corresponding polymethacrylamide derived from poly-**1**s in D_2SO_4.[8b]

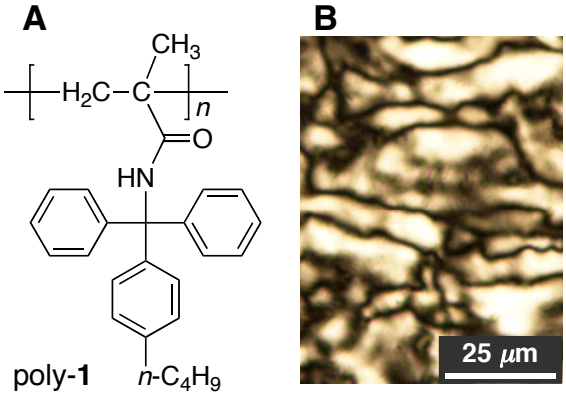

Figure 6-1. (A) Structure of poly-**1**. (B) Polarized optical micrograph of a nematic LC phase of optically inactive poly-**1** in ca. 25 wt% chloroform solution taken at ambient temperature (ca. 25 °C).

Figure 6-1B shows the polarized optical micrograph of a concentrated chloroform solution of poly-**1**. Poly-**1** formed a lyotropic nematic LC phase as observed previously for analogous poly(*N*-di(4-butylphenyl)phenylmethyl methacrylamide),[8c] indicating the rigid rodlike main-chain structure of the polymer. The author first anticipated that optically active ***h***-poly-**1** might form a chiral nematic (cholesteric) LC phase. However, ***h***-poly-**1** also showed a similar nematic-like LC phase due to the low optical activity, that is, the one handedness of the ***h***-poly-**1** may not be high.

The q values of poly-**1** and ***h***-poly-**1** were then estimated on the basis of the wormlike chain model,[12] which can be described as an analytical function of the molecular weight (M_w) and the radius of gyration (S) if the q values and the molar mass per unit contour length (M_L), which eventually leads to the monomer unit height (h), are given. The radii of gyration (S) of poly-**1**s in chloroform were measured as a function of M_w using SEC equipped with MALS and refractive index detectors in series (Figure 6-2). The solid and dotted curves in the plots were calculated using the parameters determined from the fits of the unperturbed wormlike chain model over the entire M_w studied range, and are represented by the theoretical values of $<S^2>^{0.5}$. The calculated q values of poly-**1** and ***h***-poly-**1** are 57.4 ± 3.8 and 52.6 ± 2.0 nm, respectively. In general, the persistence length of polyolefins is small. The reported q values for polyolefins are ~ 1 nm (atactic polystyrene),[13] ~ 2 nm (isotactic poly(methyl methacrylate)),[14] and 2–3 nm (atactic poly(methyl methacrylate)).[14] The author notes that the q values are almost the same for both the optically inactive and active poly-**1**s; the latter value is slightly smaller than the former one. The fact that both the polymers are highly isotactic independent of the polymerization solvent, i.e., toluene for poly-**1** and (+)-menthol for ***h***-poly-**1**, suggests that the difference in optical activity that corresponds to the difference in their helical sense excess may more or less influence the rigidity of the polymers. These large q values indicate that both the poly-**1**s are rigid and their LC formations are definitely based on their main-chain stiffness. Such stiff helical polymethacrylamides are expected to form a

regular helical structure over long distance so that the author anticipated that their helical conformations could be determined from the X-ray analysis.

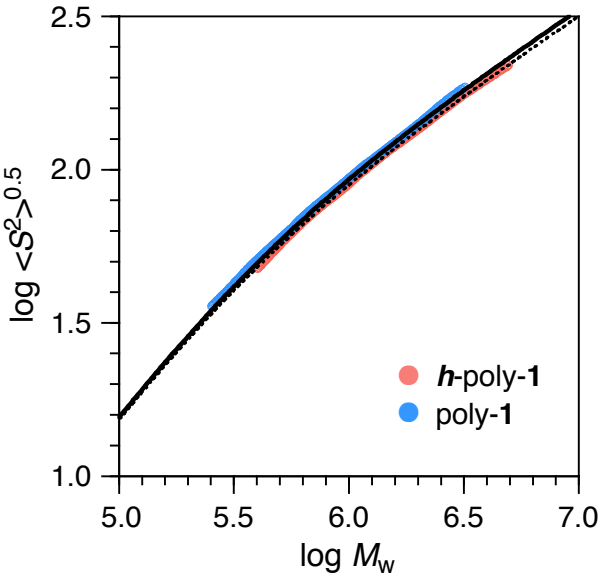

Figure 6-2. Double-logarithmic plots of the radius of gyration versus the molecular weight of optically inactive poly-**1** (●) and optically active ***h***-poly-**1** (●) in chloroform obtained by SEC-MALS measurements at 25 °C. Solid and dotted curves (solid curve for poly-**1** and dotted curve for ***h***-poly-**1**) were obtained on the basis of the wormlike chain theory and fit well with the experimental data. The evaluation parameters are as follows: q = 57.4 nm, M_L = 1678 nm^{-1}, h = 0.23 nm for poly-**1**; q = 52.6 nm, M_L = 1686 nm^{-1}, h = 0.23 nm for ***h***-poly-**1**.

Figures 6-3A and 6-3B show the wide-angle X-ray diffraction (WAXD) patterns of the uniaxially oriented optically inactive poly-**1** and optically active ***h***-poly-**1** films prepared from concentrated LC chloroform solutions, respectively. X-ray photographs were taken from the edge-view position with a beam parallel to the film surface at ambient temperature (20–25 °C). The X-ray diffractions of oriented poly-**1** and ***h***-poly-**1** films showed essentially the same pattern, exhibiting diffuse, but apparent equatorial and near- and off-meridional reflections. The three equatorial reflections, 15.68, 8.82, and 5.41 Å for poly-**1** and 15.66, 8.80, and 5.38 Å for ***h***-poly-**1**, can be indexed with a two-dimensional orthogonal lattice of *a*

= 17.80 and *b* = 15.68 Å for poly-**1** and *a* = 17.60 and *b* = 15.66 Å for ***h***-poly-**1**, respectively, and the observed *d*-spacings are listed in Table 6-1. The author then determined the fiber periods to be 10.30 Å for poly-**1** and 10.25 Å for ***h***-poly-**1** (= *c*) from the layer lines and attempted to index the reflections based on the orthogonal unit cell (Table 6-1). Although, due to the limited number of reflections, an unambiguous helical structure of poly-**1**s could not be determined at the present, the author assumes that poly-**1**s may have a 4/1 or 6/1 helix on the basis of the reflection on the 3rd layer line (~ 3.3 Å) and on the 4th layer line (~ 2.5 Å), respectively. The comparison of the two helical structures is summarized in Table 6-2. The author could not unambiguously determine the helical structure of poly-**1**s at the present.

The plausible 6/1 helical structure based on the X-ray diffraction studies is shown in Figure 6-3C. The present X-ray results together with the fact that both polymers have almost the same persistence length support that poly-**1** and ***h***-poly-**1** have a stiff 4/1 or 6/1 helical structure independent of their helical sense ratio. However, as mentioned above, the helical structure of poly-**1**s may need a further minor revision due to the limited resolution and number of X-ray reflections.

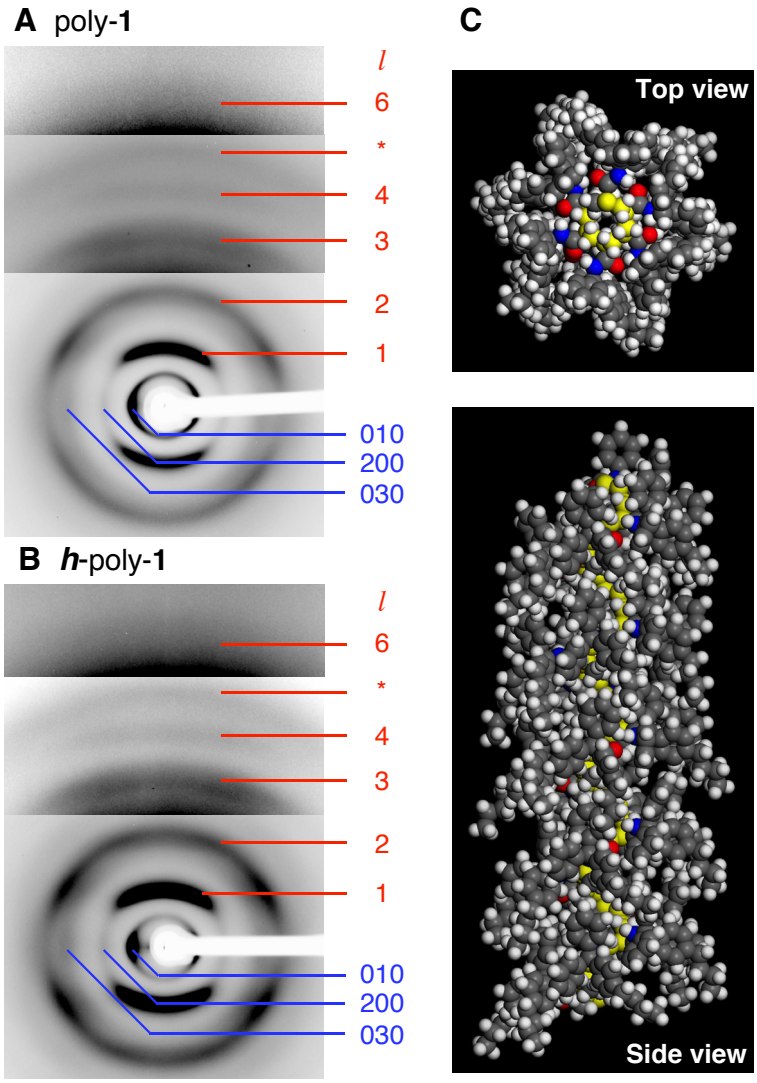

Figure 6-3. WAXD patterns of oriented optically inactive poly-**1** (A) and optically active ***h***-poly-**1** (B) films with different ranges of sensitivities; the representative layer lines are labeled. The vertical direction is nearly corresponding to the helix axis. The meridian reflections around 2.1 Å indicated by asterisks were assigned to lateral reflections judging from WAXD data of the same polymer films using a flat imaging plate. The uniaxially oriented films were prepared from concentrated LC chloroform solutions. (C) Top and side view of a possible 6/1 helical structure of isotactic poly-**1** (30-mer) on the basis of the X-ray structural analysis followed by molecular mechanics calculations (see the Experimental Section). The main-chain carbon atoms are shown in yellow color.

Table 6-1. X-ray Diffraction Data of Oriented Optically Inactive Poly-**1** and Optically Active ***h***-Poly-**1** Films Prepared from Concentrated Chloroform Solutions

layer line l	optically inactive poly-**1**				optically active ***h***-poly-**1**				
	d_{obs} (Å)[a]	d_{cal} (Å)[b]	I_{obs}[c]	hk[b]	d_{obs} (Å)[a]	d_{cal} (Å)[d]	I_{obs}[c]	hk[d]	n[e]
0	15.68	15.68	vs	01	15.66	15.66	vs	01	0
	8.82	8.90	w	20	8.80	8.80	w	20	
	5.41	5.23	w	03	5.38	5.22	vw	03	
1	8.88	8.91	vs	10	8.84	8.85	vs	10	1
	4.69	4.66	s	31	4.63	4.65	s	31	
2	4.68	4.72	s	11	4.62	4.69	m	11	2
	3.63	3.67	vw	03	3.64	3.66	vw	03	
3	3.34	3.43	w	streak	3.33	3.42	m	streak	3
4	2.54	2.58	vw	streak	2.50	2.56	m	streak	–2
6	1.72	1.72	vw	streak	1.76	1.71	vw	streak	0

[a] Spacings observed in X-ray diffraction patterns. [b] Spacings calculated and indexed on the basis of an orthorhombic unit cell with parameters, a = 17.80, b = 15.68, and c = 10.30 Å. [c] Observed intensities; vs = very strong, s = strong, m = medium, w = weak, and vw = very weak. [d] Spacings calculated and indexed on the basis of an orthorhombic unit cell with parameters, a = 17.60, b = 15.66, and c = 10.25 Å. [e] Bessel function order based on a 6/1 helix. The average intensity of the layer line is stronger with smaller n.

Table 6-2. Comparison of the Two Helical Structures

		density (g/cm^3)	unit height (h) (nm)	number-average molecular length (L_n) (nm)
observed values	poly-**1**	1.07[a]	0.23[b]	161[c]
candidate structures	4/1 helix	0.89[d]	0.26[e]	210[f]
	6/1 helix	1.30[d]	0.17[e]	137[f]

[a] Measured by the standard flotation method in a KBr saturated aqueous solution—water mixture at ambient temperature (20–25 °C). [b] Estimated by SEC-MALS measurements (Figure 6-2). [c] Estimated by AFM observations of the individual chain (Figure 6-6). [d] Calculated on the basis of an orthorhombic unit cell with parameters, a = 17.80, b = 15.68, and c = 10.30 Å obtained from the WAXD measurement. [e] Estimated based on the WAXD measurement (Table 6-1). [f] Calculated from the equation, $L_n = (M_n/M_0) \times h$, where M_n, M_0, and h represent the absolute molecular weight (3.1×10^5) estimated from SEC-MALS measurements, the molecular weight (383.53) of the repeating unit of poly-**1**, and the unit height, respectively.

The helical structure of poly-**1**s was further investigated by AFM. Figure 6-4 shows typical high-resolution AFM height (A) and phase (B) images of poly-**1** deposited from a dilute chloroform solution (0.01 mg/mL) on highly oriented pyrolytic graphite (HOPG) followed by chloroform vapor exposure at ca. 25 °C for 12 h. This method is very useful for constructing highly ordered two-dimensional (2D) helix-bundles with a controlled helicity for helical polyacetylenes, polyisocyanides, and complementary double-stranded helical polymers on HOPG, and their helical structures were visualized by AFM.[9b-d,15] The poly-**1** self-assembled into well-defined 2D helix-bundles with a constant height of ~1.8 nm (Figure 6-5). The bundle structures were resolved into individual poly-**1** chains packed parallel to each other with a chain–chain spacing of ca. 1.5 nm. Although a number of periodic oblique stripes with a pitch of ca. 1.0 nm (see also Figure 6-4C) were observed along the main-chain (yellow lines), which may originate from a helical array of the pendants, it was difficult to identify the helical sense (right- or left-handed helix). However, the helical pitch and the

chain-to-chain distance of poly-**1** by high-resolution AFM images were in good agreement with those observed by X-ray diffraction measurements (1.0 nm and 1.6–1.8 nm, respectively). ***h***-Poly-**1** also formed similar 2D helix-bundle structures with a helical pitch of ca. 1.0 nm on HOPG. However, the helical sense of the ***h***-poly-**1** with an excess handedness could not be identified by AFM.

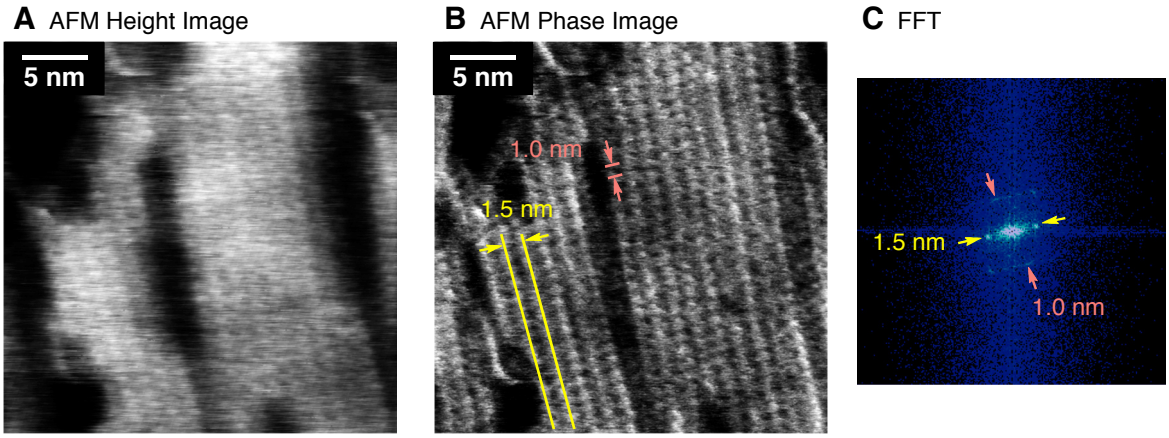

Figure 6-4. High-resolution AFM height (A) and phase (B) images of 2D self-assembled poly-**1** prepared by casting a dilute chloroform solution (0.01 mg/mL) on HOPG. Yellow lines represent the main-chain axes of poly-**1**; pink lines indicate the helical pitch of poly-**1** helices. Scale 30 × 30 nm. (C) Typical 2D fast Fourier transform (FFT) of the image in (B).

Conclusions

In summary, the author investigated the helical structure of poly(*N*-((4-butylphenyl)diphenylmethyl) methacrylamide) (poly-**1**) by means of X-ray diffraction measurements of the oriented films prepared from the LC state together with high-resolution AFM observations. This may be the first example of helical structures (4/1 or 6/1 helix) proposed experimentally for poly(triarylmethyl methacrylamide)s on the basis of the X-ray measurements. Moreover, persistence length measurements unambiguously revealed that the poly-**1** chain is rigid-rod as to form an LC phase due to the main-chain stiffness. The present results will contribute to a better understanding of the mechanism of the screw-sense-selective polymerization of triarylmethyl methacrylamides and analogous triarylmethyl methacrylates and also developing a more efficient CSP and asymmetric polymer catalysts.

Experimental Section

Instruments. NMR spectra were measured using a Varian AS 500 spectrometer (Varian, Palo Alto, CA) operating at 500 MHz for ^{1}H and 125 MHz for ^{13}C using TMS as the internal standard. The IR spectra were recorded using a JASCO FT/IR-680 spectrometer (JASCO, Tokyo, Japan). The SEC-MALS measurements were performed using an HLC-8220 GPC system (Tosoh, Tokyo, Japan) equipped with a differential refractometer coupled to a DAWN-HELEOS MALS device equipped with a semiconductor laser (λ = 690 nm) (Wyatt Technology, Santa Barbara, CA) operated at 25 °C using two TSKgel GMH_{HR}-H(S) columns (Tosoh) in series. The scattered light intensities were measured by eighteen light scattering detectors at different angles. The differential refractive index increment, dn/dc, of the polymer with respect to the mobile phase at 25 °C was also measured by an Optilab rEX interferometric refractometer (Wyatt Technology). The optical rotations were measured in a 5-cm quartz cell on a JASCO P-1030 polarimeter. The AFM measurements were performed using a Nanoscope IIIa or Nanoscope IV microscope (Veeco Instruments, Santa Barbara, CA) in air at ambient temperature with standard silicon cantilevers (NCH, Nanoworld, Neuchâtel, Switzerland) in the tapping mode. The WAXD measurements were carried out using a Rigaku RINT RAPID-R X-ray diffractometer (Rigaku, Tokyo, Japan) with a rotating-anode generator and graphite monochromated CuKα radiation (0.15418 nm) focused through a 0.3 mm pinhole collimator, which was supplied at a 45 kV voltage and a 60 mA current, equipped with a curved imaging plate having a specimen-to-plate distance of 120.0 mm. The X-ray photographs were taken at ambient temperature (20–25 °C) from the edge-view position with a beam parallel to the film surface. The polarizing optical microscopic observations were carried out with an E600POL polarizing optical microscope (Nikon, Tokyo, Japan) equipped with a DS-5M CCD camera (Nikon) connected to a DS-L1 control unit (Nikon). The sample solution was placed on a glass plate with a cover glass to develop the planar structure before observation of the microscopic texture at ambient temperature (20–25 °C).

Materials. Anhydrous chloroform (water content < 50 ppm) was purchased from Wako and stored under dry nitrogen. Poly(*N*-((4-butylphenyl)diphenylmethyl) methacrylamide)s (poly-**1**s) were prepared according to the previously reported method by radical polymerization of the corresponding monomer using AIBN as an initiator in toluene or (+)-menthol.[8b] The number-average molecular weight (M_n) and the molecular weight distribution (M_w/M_n) of optically inactive poly-**1** and optically active ***h***-poly-**1** were $M_n = 3.1 \times 10^5$ and $M_w/M_n = 2.6$ and $M_n = 7.5 \times 10^5$ and $M_w/M_n = 1.8$, respectively, as determined by SEC-MALS measurements using chloroform as the eluent. The tacticities of poly-**1**s were highly isotactic as estimated by their ^{1}H NMR spectra of the corresponding polymethacrylamides derived from poly-**1**s in D_2SO_4.[8b]

Wide-Angle X-ray Diffraction (WAXD) Measurements. The oriented poly-**1** and ***h***-poly-**1** films for the X-ray analyses were prepared by shearing uniaxially LC solutions of poly-**1**s in chloroform cast on a glass plate. Although the solubility of the polymers in chloroform was poor at room temperature, they were completely dissolved after cooling the solutions to –60 °C for 1 h. After drying the films in air, the oriented poly-**1** films were floated off from the glass substrates onto a water surface, carefully collected, and then dried. Several uniaxially oriented thin and rectangle-shaped poly-**1** films of ca. 10 mm length, 1.5 mm width, and 0.02 mm thickness were prepared and piled up parallel to each other for the X-ray measurements. In the same way, the oriented ***h***-poly-**1** films were prepared from a concentrated chloroform LC solution of ***h***-poly-**1** in chloroform. X-ray photographs were taken at ambient temperature (20–25 °C) from the edge-view position with a beam parallel to the film surface. The reflections in the diffraction patterns of poly-**1** and ***h***-poly-**1** can be properly indexed with orthorhombic lattices; $a = 17.80$ Å, $b = 15.68$ Å, $c = 10.30$ Å, and $a = 17.60$ Å, $b = 15.66$ Å, $c = 10.25$ Å, respectively. The spacings and mirror indices of the reflections are listed in Table 6-1.

SEC-MALS Measurements. The SEC-MALS measurements were carried out according to a previously reported method using chloroform as the eluent at a flow rate of 0.5 mL/min.[9c,10i,j] A standard polystyrene (M_w = 30500 (Polymer Laboratories, Shropshire, U.K.)) was used to calculate the device constants, such as the inter-detector delay, inter-detector band broadening, and light scattering detector normalization. Poly-**1** and ***h***-poly-**1** were completely dissolved in chloroform at the concentration of 0.1–0.2 % (wt/vol) under gentle stirring at –60 °C for 1–2 h before injection. The evaluations of the molecular weights and the radii of gyration of poly-**1**s were accomplished using ASTRA V software (version 5.1.3.5). The *dn*/*dc* values of poly-**1** and ***h***-poly-**1** in the eluent used for the evaluations were 0.1439 and 0.1456 mL/g, respectively (the uncertains were ± 0.0038 and ± 0.0054 mL/g, respectively) on the assumption that the *dn*/*dc* value was independent of the molecular weight.

Persistence Length Estimation from the Molecular Weight Dependence of the Radius of Gyration. The molecular weight dependence of the obtained radii of gyration of poly-**1** and ***h***-poly-**1** was used to estimate the persistence length (q) based on the wormlike-chain model. It was over the range of the elution volume where both the concentration and the scattering intensities are greater than 10% of the peak value. The unperturbed mean-square radius of gyration $\langle S^2 \rangle_0$ is given by[16]

$$\langle S^2 \rangle_0 = (2q)^2 \left[\frac{1}{6}N - \frac{1}{4} + \frac{1}{4N} - \frac{1}{8N^2}(1 - \exp(-2N)) \right] \quad (1)$$

where N is the Kuhn statistical segment number defined by $N = M_w/(2q \cdot M_L)$, and M_L denotes the molar mass per unit contour length of the polymer. The radius expansion factor α_s [$\equiv (\langle S^2 \rangle / \langle S^2 \rangle_0)^{0.5}$] for the excluded-volume effect was negligible because it is close to unity in the case of $N < 50$.[17] Equation (1) indicates that $\langle S^2 \rangle_0$ is characterized by q and M_L, so that a fitting procedure was employed to estimate q and M_L.

Molecular Modeling and Calculations (Figure 6-3C). The helical conformation of isotactic poly-**1** (6/1 helix) was explored using Miyazawa's equation.[18] According to Miyazawa, the helical parameters (unit height (*h*) and number of repeating units (*n*) per one helical turn) of infinite (periodic) polymer chains can be described by internal coordinates, such as the bond lengths (C_1–C_2 (r_1) and C_2–C_3 (r_2)), the bond angles (C_1–C_2–C_3 (ϕ_1) and C_2–C_3–C_4 (ϕ_2)), and the internal rotation angles (C_1–C_2–C_3–C_4 (τ_1) and C_2–C_3–C_4–C_5 (τ_2)). The atomic connectivities and dihedral angles of poly-**1** are depicted in Chart 6-1.

Chart 6-1

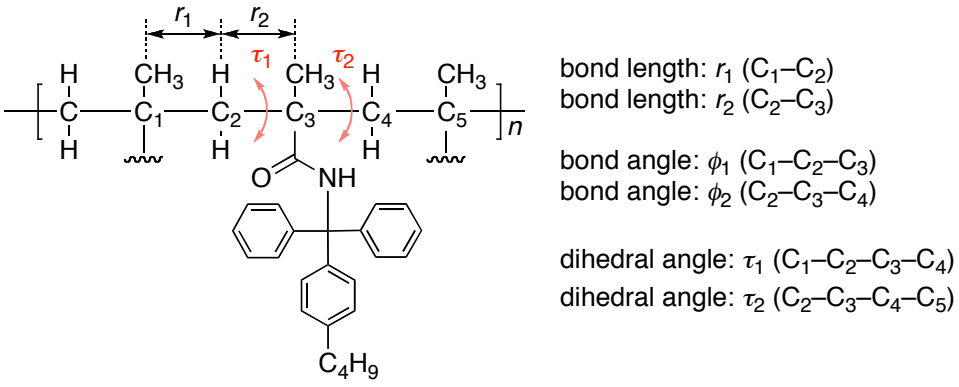

The bond lengths and bond angles were set to $r_1 = r_2 = 1.53$ Å and $\phi_1 = \phi_2 = 124°$, respectively on the basis of the reported value.[7] The other internal coordinate combinations, that is τ_1 and τ_2, were calculated by Miyazawa's equation so as to satisfy the helical parameters (*h*; 1.72 Å, and *n*; 6.00) obtained by the X-ray diffractions, respectively ($\tau_1 = 152°$, $\tau_2 = -108°$). The molecular modeling and molecular mechanics (MM) calculations were conducted with the Compass force field[19] as contained in the MS Modeling software (version 4.0, Accelrys, Inc., San Diego, CA) operated using a PC running under Windows® XP.

The polymer models (50 repeating monomer units) of poly-**1** with a side chain conformation optimized by MM calculations of the corresponding monomer unit were constructed using the Polymer Builder module in the MS Modeling software. The geometrical parameters for the poly-**1** backbone were fixed during the following force field optimization.

The dielectric constant was set to 1.0. Geometry optimizations were carried out without any cutoff by the smart minimizer in three steps. First, the starting conformation was subject to the steepest decent optimization in order to eliminate the worse steric conflicts. Second, subsequent optimization until the convergence using a conjugate gradient algorithm was performed. The fully-optimized poly-**1** model was obtained by the further energy minimization using the Newton method with the 0.1 kcal/mol/Å convergence criterion. The final right-handed helical poly-**1** is shown in Figure 6-3C.

AFM Measurements of 2D Poly-1 Assemblies (Figures 6-4 and 6-5). A stock solution of optically inactive poly-**1** in dry chloroform (0.01 mg/mL) was prepared after cooling the solution at –60 °C for 30 min. Samples for the AFM measurements were prepared by casting a 40-μL aliquot of the stock solution of the polymer. The casting was done at room temperature on freshly cleaved HOPG under chloroform vapor atmospheres. After the polymers had been deposited on the HOPG, the HOPG substrates were further exposed to a chloroform vapor for 12 h, and then the substrates were dried under vacuum for 2 h according to the reported procedure.[9b-d,15] The chloroform vapor was prepared by putting 1 mL of chloroform into a 2-mL flask that was inside a 50-mL flask, and the HOPG substrates were then placed in the 50-mL flask. The typical settings of the AFM for the high-magnification observations were as follows: amplitude 1.0–1.5 V; set point 0.9–1.4 V; scan rate 2.5 Hz. The Nanoscope image processing software was used for the image analysis.

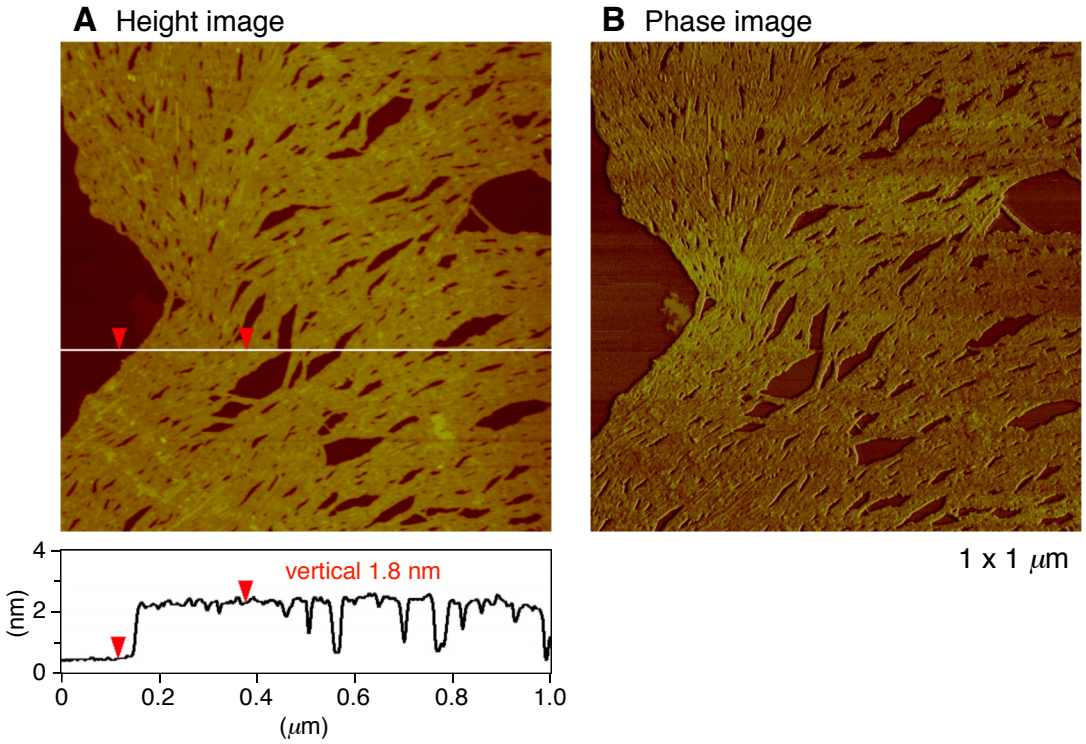

Figure 6-5. (A) AFM height and phase images of self-assembled optically inactive poly-**1** on HOPG. The polymer was dissolved in chloroform (0.01 mg/mL) at –60 °C for 30 min, and then the solution was allowed to warm to room temperature and used to prepare the 2D self-assemblies of poly-**1** by casting the dilute chloroform solution on HOPG for AFM measurements. The height profile obtained along the white line is also shown.

AFM Measurement of Individual Poly-1 Chains (Figure 6-6). Mica substrates were modified with trimethoxypropylsilane according to a literature procedure.[20] Trimethoxypropylsilane was dissolved in methanol (0.1 vol%), and freshly cleaved mica substrates were immersed in the solution for 5 min. The mica substrates were taken out, washed three times with methanol, and then dried *in vacuo*. A stock solution of poly-**1** in chloroform (3.0 μg/mL) was prepared in the same way for the AFM measurements on HOPG. Samples for the AFM measurements of poly-**1** were prepared by spin casting (1000 rpm) 10-μL aliquots of the stock solution on the mica substrates, and the substrates were then dried under vacuum for 2 h. The AFM measurements were performed using a Nanoscope IIIa

microscope in air at ambient temperature with standard silicon cantilevers (NCH) in the tapping mode. The scanning speed was at a line frequency of 2.0 Hz. Figure 6-6 shows the typical tapping-mode AFM height image of poly-**1** on the modified mica. Under a dilute condition, single molecules of poly-**1** could be observed, and such a molecular resolution allowed direct measurements of the average molecular length of poly-**1**.[9c, 21] On the basis of an evaluation of 370 molecules in the AFM images including the image in Figure 6-6A, the number-average molecular length (L_n = 161 nm), the weight-average molecular length (L_w = 234 nm), and the length distribution (L_w/L_n = 1.45) of poly-**1** were estimated (Figure 6-6B). These values were measured without compensation for the tip radius of curvature (ca. 10 nm), so that the measured values were overestimated because of the broadening effect of the tip. However, the tip broadening played a minor role in the determination of the contour length of the rod-like species.[22] Polymer lengths were measured using the Image J program, developed at the National Institutes of Health (available on the Internet at http://rsb.info.nih.gov/nih-image/). The number-average molecular weight was then calculated to be 3.59×10^5 from the equation, $M_n = (L_n/h) \times M_0$, where h and M_0 represent the unit height (0.172 nm) estimated from the X-ray analysis of poly-**1** (6/1 helix) and the molecular weight (383.53) of the repeating unit of poly-**1**, respectively.

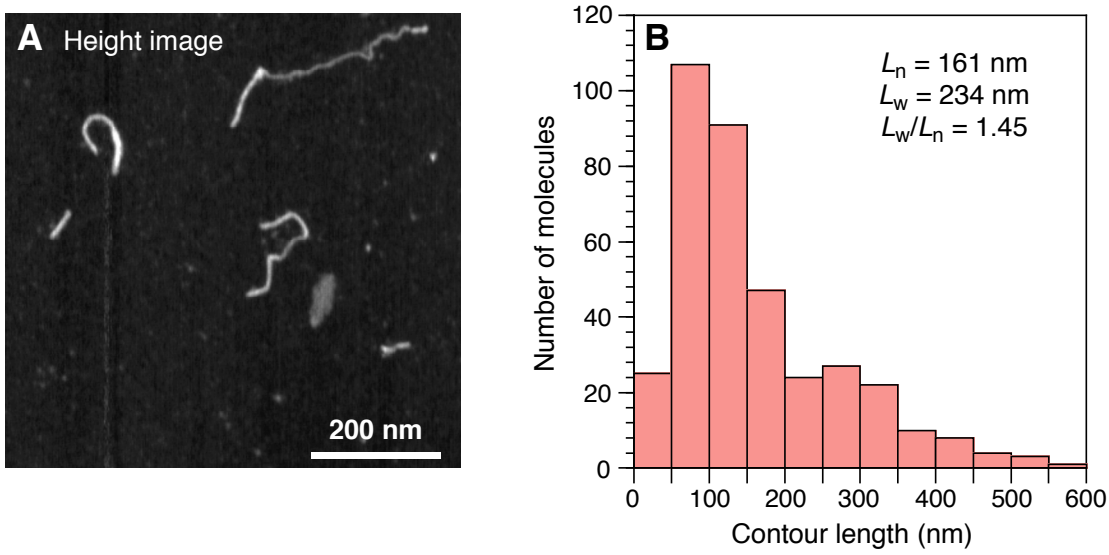

Figure 6-6. (A) AFM height image of the optically inactive poly-**1** on mica modified with trimethoxypropylsilane. (B) Histogram of the molecular length distribution of poly-**1** obtained from the AFM images including (A). Based on an evaluation of 370 molecules, the number-average molecular length (L_n), the weight-average molecular length (L_w), and the length distribution (L_w/L_n) were estimated.

References and Notes

(1) (a) Schulz, G. E.; Schirmer, R. H. *Principles of Protein Structure*; Springer-Verlag: New York, 1979. (b) Saenger, W. *Principles of Nucleic Acid Structure*; Springer-Verlag: New York, 1984.

(2) Okamoto, Y.; Suzuki, K.; Ohta, K.; Hatada, K.; Yuki, H. *J. Am. Chem. Soc.* **1979**, *101*, 4763-4765.

(3) For reviews on helical polymers, see: (a) Okamoto, Y.; Nakano, T. *Chem. Rev.* **1994**, *94*, 349–372. (b) Nolte, R. J. M. *Chem. Soc. Rev.* **1994**, *23*, 11–19. (c) Green, M. M.; Park, J.-W.; Sato, T.; Teramoto, A.; Lifson, S.; Selinger, R. L. B.; Selinger, V. B.; Selinger, J. V. *Angew. Chem., Int. Ed.* **1999**, *38*, 3138–3154. (d) Nakano, T.; Okamoto, Y. *Chem. Rev.* **2001**, *101*, 4013–4038. (e) Cornelissen, J. J. L. M.; Rowan, A. E.; Nolte, R. J. M.; Sommerdijk, N. A. J. M. *Chem. Rev.* **2001**, *101*, 4039–4070. (f) Nomura, R.; Nakako, H.; Masuda, T. *J. Mol. Catal. A: Chem.* **2002**, *190*, 197–205. (g) Fujiki, M.; Koe, J. R.; Terao, K.; Sato, T.; Teramoto, A.; Watanabe, J. *Polym. J.* **2003**, *35*, 297–344. (h) Yashima, E.; Maeda, K.; Nishimura, T. *Chem. –Eur. J.* **2004**, *10*, 42–51. (i) Suginome, M.; Ito, Y. *Adv. Polym. Sci.* **2004**, *17*, 77–136. (j) Lam, J. W. Y.; Tang, B. Z. *Acc. Chem. Res.* **2005**, *38*, 745–754. (k) Aoki, T.; Kaneko, T.; Teraguchi, M. *Polymer* **2006**, 37, 717–735. (l) Maeda, K.; Yashima, E. *Top. Curr. Chem.* **2006**, *265*, 47–88. (m) Yashima, E. Maeda, K. *Macromolecules* **2008**, *41*, 3–12. (n) Pijper, D.; Feringa, B. L. *Soft Matter* **2008**, *4*, 1349–1372. (o) Yashima, E.; Maeda, K.; Furusho, Y. *Acc. Chem. Res.* **2008**, *41*, 1166-1180.

(4) Yuki, H.; Okamoto, Y.; Okamoto, I. *J. Am. Chem. Soc.* **1980**, *102*, 6356-6358.

(5) (a) Nakano, T. *J. Chromatogr. A* **2001**, *906*, 205-225. (b) Yamamoto, C.; Okamoto, Y. *Bull. Chem. Soc. Jpn.* **2004**, *77*, 227-257. (c) Okamoto, Y.; Ikai, T. *Chem. Soc. Rev.* **2008**, *37*, 2593-2608.

(6) (a) Reggelin, M.; Schultz, M.; Holbach, M. *Angew. Chem., Int. Ed.* **2002**, *41*, 1614-1617. (b) Reggelin, M.; Doerr, S.; Klussmann, M.; Schultz, M.; Holbach, M. *Proc. Natl.*

Acad. Sci. U. S. A. **2004**, *101*, 5461-5466.

(7) Cavallo, L.; Corradini, P.; Vacatello, M. *Polym. Commun.* **1989**, *30*, 236–238.

(8) (a) Hoshikawa, N.; Hotta, Y.; Okamoto, Y. *J. Am. Chem. Soc.* **2003**, *125*, 12380-12381. (b) Azam, A. K. M. F.; Kamigaito, M.; Okamoto, Y. *Polym. J.* **2006**, *38*, 1035–1042. (c) Hoshikawa, N.; Yamamoto, C.; Hotta, Y.; Okamoto, Y. *Polym. J.* **2006**, *38*, 1258–1266.

(9) (a) Nagai, K.; Sakajiri, K.; Maeda, K.; Okoshi, K.; Sato, T.; Yashima, E. *Macromolecules* **2006**, *39*, 5371-5380. (b) Sakurai, S.-i.; Okoshi, K.; Kumaki, J.; Yashima, E. *Angew. Chem., Int. Ed.* **2006**, *45*, 1245-1248. (c) Sakurai, S.-i.; Ohsawa, S.; Nagai, K.; Okoshi, K.; Kumaki, J.; Yashima, E. *Angew. Chem., Int. Ed.* **2007**, *46*, 7605-7608. (d) Onouchi, H.; Okoshi, K.; Kajitani, T.; Sakurai, S.-i.; Nagai, K.; Kumaki, J.; Onitsuka, K.; Yashima, E. *J. Am. Chem. Soc.* **2008**, *130*, 229-236.

(10) The persistence length (q) is a useful measure to evaluate the stiffness of rodlike polymers, but only a limited number of q values have been determined for synthetic helical polymers, see refs 9a and c. See also: (a) Sato, T.; Teramoto, A. *Adv. Polym. Sci.* **1996**, *126*, 85–161. (b) Nieh, M.-P.; Goodwin, A. A.; Stewart, J. R.; Novak, B. M.; Hoagland, D. A. *Macromolecules* **1998**, *31*, 3151–3154. (c) Gu, H.; Nakamura, Y.; Sato, T.; Teramoto, A.; Green, M. M.; Andreola, C. *Polymer* **1999**, *40*, 849–856. (d) Teramoto, A.; Terao, K.; Terao, Y.; Nakamura, N.; Sato, T.; Fujiki, M. *J. Am. Chem. Soc.* **2001**, *123*, 12303–12310. (e) Samorí, P.; Ecker, C.; Gössl, I.; de Witte, P. A. J.; Cornelissen, J. J. L. M.; Metselaar, G. A.; Otten, M. B. J.; Rowan, A. E.; Nolte, R. J. M.; Rabe, J. P. *Macromolecules* **2002**, *35*, 5290-5294. (f) Nomura, R.; Tabei, J.; Nishiura, S.; Masuda, T. *Macromolecules* **2003**, *36*, 561–564. (g) Ashida, Y.; Sato, T.; Morino, K.; Maeda, K.; Okamoto, Y.; Yashima, E. *Macromolecules* **2003**, *36*, 3345-3350. (h) Okoshi, K.; Sakajiri, K.; Kumaki, J.; Yashima, E. *Macromolecules* **2005**, *38*, 4061–4064. (i) Okoshi, K.; Sakurai, S.-i.; Ohsawa, S.; Kumaki, J.; Yashima, E. *Angew.*

Chem., Int. Ed. **2006**, *45*, 8173–8176. (j) Okoshi, K.; Nagai, K.; Kajitani, T.; Sakurai, S.-i.; Yashima, E. *Macromolecules*, **2008**, *41*, 7752–7754.

(11) Nakano, T.; Okamoto, Y.; Hatada, K. *J. Am. Chem. Soc.* **1992**, *114*, 1318-1329.

(12) (a) Yamakawa, H.; Fujii, M. *Macromolecules* **1974**, *7*, 128–135. (b) Yamakawa, H.; Yoshizaki, T. *Macromolecules* **1980**, *13*, 633–643.

(13) Konishi, T.; Yoshizaki, T.; Saito, T.; Einaga, Y.; Yamakawa, H. *Macromolecules* **1990**, *23*, 290-297.

(14) Arai, T.; Sawatari, N.; Yoshizaki, T.; Einaga, Y.; Yamakawa, H. *Macromolecules* **1996**, *29*, 2309-2314.

(15) (a) Kajitani, T.; Okoshi, K.; Sakurai, S.-i.; Kumaki, J.; Yashima, E. *J. Am. Chem. Soc.* **2006**, *128*, 708-709. (b) Maeda, T.; Furusho, Y.; Sakurai, S.-i.; Kumaki, J.; Okoshi, K.; Yashima, E. *J. Am. Chem. Soc.* **2008**, *130*, 7938-7945.

(16) Benoit, H.; Doty, P. *J. Chem. Phys.* **1953**, *57*, 958–963.

(17) Yamakawa, H. *Helical Wormlike Chains in Polymer Solutions*, Springer, Berlin, 1997, p. 278.

(18) Miyazawa, T. *J. Polym. Sci.* **1961**, *55*, 215-231.

(19) Sun, H. *J. Phys. Chem. B* **1998**, *102*, 7338–7364.

(20) Hu, J.; Wang, M.; Weier, H.-U. G.; Frantz, P.; Kolbe, W.; Ogletree, D. F.; Salmeron, M. *Langmuir* **1996**, *12*, 1697–1700.

(21) (a) Prokhorova, S. A.; Sheiko, S. S.; Möller, M.; Ahn C.-H.; Percec, V. *Macromol. Rapid Commun.* **1998**, *19*, 359–366. (b) Börner, H. G.; Beers K.; Matyjaszewski, K.; Sheiko, S. S.; Möller, M. *Macromolecules* **2001**, *34*, 4375–4383. (c) Cornellissen, J. J. L. M.; Graswinckel, W. S.; Adams, P. J. H. M.; Nachtegaal, G. H.; Kentgens, A. P. M.; Sommerdijk, N. A. J. M.; Nolte, R. J. M. *J. Polym. Sci., Part A: Polym. Chem.* **2001**, *39*, 4255–4264. (d) Sakurai, S.-i.; Kuroyanagi, K.; Nonokawa, R.; Yashima, E. *J. Polym. Sci., Part A: Polym. Chem.* **2004**, *42*, 5838–5844.

(22) Samorí, P.; Francke, V.; Müllen, K.; Rabe, J. P. *Chem. –Eur. J.* **1999**, *5*, 2312–2317.

List of Publications

Papers

1) "Helicity Induction and Chiral Amplification in a Poly(phenylacetylene) Bearing *N*,*N*-Diisopropylaminomethyl Groups with Chiral Acids in Water"
Kanji Nagai, Katsuhiro Maeda, Yoshihisa Takeyama, Koichi Sakajiri, and Eiji Yashima
Macromolecules **2005**, *38*, 5444–5451.

2) "Hierarchical Amplification of Macromolecular Helicity in a Lyotropic Liquid Crystalline Charged Poly(phenylacetylene) by Nonracemic Dopants in Water and Its Helical Structure"
Kanji Nagai, Koichi Sakajiri, Katsuhiro Maeda, Kento Okoshi, Takahiro Sato, and Eiji Yashima
Macromolecules **2006**, *39*, 5371–5380.

3) "Temperature-Induced Chiroptical Changes in a Helical Poly(phenylacetylene) Bearing *N*,*N*-Diisopropylaminomethyl Groups with Chiral Acids in Water"
Kanji Nagai, Katsuhiro Maeda, Yoshihisa Takeyama, Takahiro Sato, and Eiji Yashima
Chem. Asian J. **2007**, *2*, 1314–1321.

4) "Anomalous Stiff Backbones of Helical Poly(phenyl isocyanide) Derivatives"
Kento Okoshi, Kanji Nagai, Takashi Kajitani, Shin-ichiro Sakurai, and Eiji Yashima
Macromolecules **2008**, *41*, 7752–7754.

5) "Helical Structure of Liquid Crystalline Poly(*N*-((4-butylphenyl)diphenylmethyl) methacrylamide)"
Kanji Nagai, Kento Okoshi, Shin-ichiro Sakurai, Motonori Banno, A. K. M. Fakhrul Azam, Masami Kamigaito, Yoshio Okamoto, and Eiji Yashima
in preparation.

Other Related Papers

1) "Two-Dimensional Helix-Bundle Formation of a Dynamic Helical Poly(phenylacetylene) with Achiral Pendant Groups on Graphite"
Shin-ichiro Sakurai, Sousuke Ohsawa, Kanji Nagai, Kento Okoshi, Jiro Kumaki, and Eiji Yashima
Angew. Chem., Int. Ed. **2007**, *46*, 7605–7608.

2) "Uniaxial Orientation of a Rodlike Helical Poly(phenylacetylene) in an Electric Field"
Kento Okoshi, Takashi Kajitani, Kanji Nagai, and Eiji Yashima
Macromolecules **2008**, *41*, 258–261.

3) "Two- and Three-Dimensional Smectic Ordering of Single-Handed Helical Polymers"
Hisanari Onouchi, Kento Okoshi, Takashi Kajitani, Shin-ichiro Sakurai, Kanji Nagai, Jiro Kumaki, Kiyotaka Onitsuka, and Eiji Yashima
J. Am. Chem. Soc. **2008**, *130*, 229–236.

4) "Helical Polyisocyanides with Fan-Shaped Pendants"
Takashi Kajitani, Hongzhen Lin, Kanji Nagai, Kento Okoshi, Hisanari Onouchi, and Eiji Yashima
Macromolecules, *in press* (DOI: 10.1021/ma802345g).

5) "Enantiomer-Selective and Helix-Sense-Selective Living Block Copolymerization of Isocyanide Enantiomers Initiated by Single-Handed Helical Poly(phenyl isocyanide)s"
Zong-Quan Wu, Kanji Nagai, Motonori Banno, Kento Okoshi, Kiyotaka Onitsuka, and Eiji Yashima
submitted.

6) "Lattice-Like Smectic Liquid Crystal Phase in a Rigid-Rod Helical Polyisocyanide with Mesogenic Pendants"
Takashi Kajitani, Hisanari Onouchi, Shin-ichiro Sakurai, Kanji Nagai, Kento Okoshi, Kiyotaka Onitsuka, and Eiji Yashima
submitted.

7) "Mechanism of Helix Induction in Poly(4-carboxyphenyl isocyanide) with Chiral Amines and Memory of the Macromolecular Helicity and Its Helical Structures"
Yoko Hase, Kanji Nagai, Hiroki Iida, Katsuhiro Maeda, Noriaki Ochi, Kyoichi Sawabe, Koichi Sakajiri, Kento Okoshi, and Eiji Yashima
in preparation.

8) "Two-Dimensional Bilayer Smectic Ordering of Rigid-Rod Helical Diblock Copoly(isocyanides) on Graphite"
Zong-Quan Wu, Kanji Nagai, Shin-ichiro Sakurai, Kento Okoshi, and Eiji Yashima
in preparation.

9) "Effect of the Pendant Alkyl Chain Length of L-Alanine-Bound Poly(phenylacetylene)s on Macromolecular Helicity and Stiffness"
Kento Okoshi, Kanji Nagai, Zong-Quan Wu, and Eiji Yashima
in preparation.

10) "Electric-Field-Induced Alignment of Helical Polyisocyanides with a Large Dipole Moment along Their Long Axis"
Takashi Kajitani, Kento Okoshi, Kanji Nagai, Hisanari Onouchi, and Eiji Yashima
in preparation.

Reviews

1) "Recent Development in Structural Determination of Synthetic Helical Polymers"
Kanji Nagai and Eiji Yashima
Kobunshi **2009**, *58*, 33–38.

2) "Helical Polymers: Synthesis, Structures, and Functions"
Eiji Yashima, Katsuhiro Maeda, Hiroki Iida, and Kanji Nagai
Chem. Rev. in preparation.

Acknowledgment

The present study was carried out at the Department of Molecular Design and Engineering, Graduate School of Engineering, Nagoya University, during 2004—2009.

The author wishes to express his grateful acknowledgment to Professor Eiji Yashima whose encouragement and helpful suggestions have been indispensable to the completion of the present thesis. He would also like to acknowledge Professor Takahiro Sato of Osaka University for pertinent and tolerant advice and helpful discussion. He is deeply grateful to Professors Yoshio Okamoto and Masami Kamigaito and Dr. A. K. M. Fakhrul Azam for their generous supply of the polymethacrylamide derivatives. The author is deeply indebted to Drs. Kento Okoshi, Koichi Sakajiri, Katsuhiro Maeda, Jiro Kumaki, Shin-ichiro Sakurai, Takashi Kajitani, Hisanari Onouchi, Zong-Quan Wu, Toshiaki Kamachi, Yoshio Furusho, Kazuhide Morino, and Hiroki Iida for practical guidance and fruitful discussion.

It is pleasure to express his appreciation to the colleagues of Professor Yashima Laboratory for their encouragement and friendship, especially to Drs. Yoko Hase, Sousuke Ohsawa, and Takashi Hasegawa, and Messrs. Yoshihisa Takeyama, Mitsuo Muto, Oh Seong Dae, Masao Morimoto, Atsushi Kitaura, Shinzo Kobayashi, Kazumi Tamura, Kazuhiro Miwa, Motonori Banno, and Toshitaka Miyabe.

The author also thanks Professors Takashi Yamane, Atsuo Suzuki, and Tatsuo Hikage for their help in the X-ray diffraction measurements.

He is very grateful to the Research Fellowship of the Japan Society for the Promotion of Science for Young Scientists during 2006—2009.

Finally, he would like to give his special thanks to Professors Takahiro Seki and Yoshihito Watanabe for serving on his dissertation committee.

January, 2009

Kanji Nagai